Correlation of the Elastic Properties of Stretch Film on Unit Load Containment

James V. Bisha

Dissertation submitted to the faculty of the Virginia Polytechnic Institute and State University in partial fulfillment of the requirements for the degree of:

Doctor of Philosophy

In

Forest Products

D. Earl Kline, Chair

Marshall S. White

Young Tek Kim

Kimberly P. Ellis

Laszlo Horvath

May 24, 2012

Blacksburg, Virginia

Keywords: Stretch Film, Stiffness, Containment Force, Unit Load, Material Handling, Pallet, Stretch Wrapping

Correlation of the Elastic Properties of Stretch Film on Unit Load Containment

James V. Bisha

ABSTRACT

The purpose of this research was to correlate the applied material properties of stretch film with its elastic properties measured in a laboratory setting. There are currently no tools available for a packaging engineer to make a scientific decision on how one stretch film performs against another without applying the film. The system for stretch wrap comparison is mostly based on trial and error which can lead to a significant loss of product when testing a new film or shipping a new product for the first time. If the properties of applied stretch film could be predicted using a tensile test method, many different films could be compared at once without actually applying the film, saving time and money while reducing risk.

The current method for evaluating the tensile properties of stretch film advises the user apply a hysteresis test to a standard sample size and calculate several standard engineering values. This test does not represent how the material is actually used. Therefore, a new tensile testing method was developed that considers the film gauge (thickness) and its prestretch. The results of this testing method allowed for the calculation of the material stiffness (Bisha Stiffness) and were used to predict its performance in unit load containment.

Applied stretch film is currently compared measuring containment force, which current standards define as the amount of force required to pull out a 15.2cm diameter plate, 10.1cm out, located 25.4cm down from the top and 45.7cm over from the side of a standard 121.9cm width unit load. Given this definition, increasing the amount of force required to pull the plate out can be achieved by manipulating two different stretch film properties, either increasing the stiffness of the film or increasing the tension of the film across the face of the unit load during the application process. Therefore, for this research, the traditional definition of containment force has been broken down into two components. Applied film stiffness was defined as the amount of force required to pull the film a given distance off the unit load. Containment force was defined as the amount of force that an applied film exerts on the corner of the unit load.

The applied stretch film was evaluated using two different methods. The first method used the standard 10.1cm pull plate (same plate as ASTM D 4649) to measure the force required to pull the film out at different increments from the center on the face of the unit load. This measurement force was transformed into a material stiffness and film tension (which were subsequently resolved into containment force). The second newly developed method involved wrapping a bar under the film, on the corner of the unit load, and pulling out on the bar with a tensile testing machine. This method allowed for the direct measurement of the containment force and material stiffness. The results indicated that while some statistically significant differences were found for certain films, the material stiffness and containment were relatively consistent and comparable using either method.

The use of the Bisha Stiffness to predict the applied stiffness and containment force yielded a statistically significant correlation and with a coefficient of determination of approximately 0.4. These results suggest that while film thickness and prestretch are key variables that can predict applied stiffness and containment force, more research should be conducted to study other variables that may allow for a better prediction. High variability of the predictions observed were caused by the differences in film morphology between the different method of elongation (tensile vs application).

This study was the first that attempted to define and correlate the tensile properties of stretch film and the applied properties of stretch film. From this research many terms have been clarified, myths have been dispelled, formulas have been derived and applied to the data collected and a clear path forward has been laid out for future researchers to be able to predict applied stiffness and containment force from the elastic properties of stretch film.

Acknowledgements

This research would not have been possible without the support of Prof. Dr. Kline, Prof. em. Dr. White, and Mr. Ralph Rupert. I am eternally indebted for your continuous encouragement, guidance and knowledge that you offered during my seven years of post graduate work. Thank you.

Thanks to Rick Caudill and David Jones at the Brooks Forest Products Center for helping me assemble the nuts and bolts of every experiment. Without you, none of this research could have been completed.

Thanks to Millwood Inc. for supplying the stretch wrap machine and stretch film that made this research possible.

Finally, I would like to thank my wife, Jen, who has been there for me through the many up and downs of this education process. What a Ride.

This dissertation is dedicated to every packaging engineer that struggles with stretch film. May this start to bring you answers.

All Photographs by author 2012.

Contents

Contents v
Figures ix
Tables xiii
1 Introduction 1
1.1 Problem Statement 3
1.2 Research Questions 4
1.3 Purpose and Objectives 4
1.4 Research Contributions 5
1.5 Practical Contributions 6
1.6 Assumptions and Limitations 6
2 Literature review 8
2.1 Unit load Stabilization 8
2.1.1 History of the stretch wrapper 8
2.1.2 History of stretch film 8
2.1.3 Prominent LLDPE resin suppliers and film converters 9
2.1.4 Other methods of unit load stabilization 10
2.2 Manufacturing and Application Methods of Stretch Film 11
2.2.1 Manufacturing Methods 11
2.2.2 Application Methods 11
2.2.3 Wrapping a four sided object 12
2.2.4 Prestretching 12
2.2.5 Stretch Wrapping Patterns 13
2.3 Stretch Film Properties 13
2.3.1 Chemical Composition Stretch Film 14
2.3.2 Material Behavior Under Strain 14
2.3.3 Crystallinity 17
2.3.4 Material Properties of Stretch Film 18
2.3.5 Temperature 20
2.4 Stretch Film Evaluation Methods 20
2.4.1 ASTM D 4649-03 20

2.4.2 ASTM D 5459–01 21
2.4.3 ASTM D 5458-95 21
2.4.4 ASTM D 882 -09a 22
2.4.5 Evaluating containment force using non-ASTM methods 22
2.4.6 The Center for Unit Load Design 23
2.5 Summary 23
3 Materials and Methods 25
3.1 Measuring tensile film stiffness s_b 25
3.1.1 Theoretical interaction of test methods 25
3.1.2 Measuring s_b & f_i 27
3.1.3 Limitations of s_b & f_i 30
3.2 Modeling Stiffness of the Applied Film 31
3.2.1 Theoretical Interaction of Testing Methods for s_a 34
3.2.2 Building of the test frame that simulates a unit load 41
3.2.3 Stretch wrapper description and operation 42
3.2.4 Measuring f_{af} with a pull plate 48
3.2.5 Limitations to the f_{af} measurement system 50
3.2.6 Measuring f_{ac} with a bar 50
3.2.7 Limitations to the f_{ac} measurement system 52
3.3 Correlation of s_a and s_b 53
3.4 Comparison of results 53
4 Evaluating tensile properties of stretch film beyond its yield stress 55
4.1.1 Experimental Design 59
4.1.2 Materials & Methods 59
4.1.3 Results & Discussion 61
4.1.4 Conclusion & Summary 70
5 Evaluating the stiffness of applied film, containment force and the layering effect 72
5.1 Evaluating the applied stiffness and containment force of applied stretch film 74
5.1.1 Experimental Design 74
5.1.2 Materials and Methods 75
5.1.3 Results & Discussion 77
5.1.4 Conclusions & Summary 83

5.2 Evaluating the layering effect on the applied stiffness and containment force of the film 85
5.2.1 Experimental Design 86
5.2.2 Materials and Methods 86
5.2.3 Results & Discussion 87
5.2.4 Conclusion & Summary 92
5.3 Summary of stiffness and containment force of applied film 93
6 Predicting applied stretch film stiffness and load containment using modified ASTM tensile testing. 96
6.1 Using Bisha Stiffness to predict the applied stiffness of stretch film 99
6.2 Using the initial force from the Bisha Stiffness to predict the applied containment force of stretch film 101
6.3 Summary 103
7 Conclusions 105
7.1.1 Characterize elastic properties of stretch film through tensile testing. 105
7.1.2 Evaluate film behavior in terms of stiffness and containment force performance when applied to a unit load. 106
7.1.3 Investigate the correlation between the elastic tensile properties and the applied stiffness and containment force of stretch film. 106
7.2 Limitations of Research 107
7.3 Future Research 107
7.3.1 Improvement of corner evaluation method 107
7.3.2 Quantification of slack in application of films 107
7.3.3 Comparison between s_a and s_b of a single film. 108
7.3.4 Evaluating how corner slippage effects stiffness and containment force 108
7.3.5 Evaluating prestretch, length, thickness and width interactions 108
7.3.6 Extrapolation of layering data with regard to wrap pattern 108
7.3.7 Extrapolation of layering data with regard to stretch roping 109
7.3.8 Observed functional adjustments to Bisha Stiffness data 110
7.3.9 Use of actual stress and strain in evaluating the Bisha Stiffness 111
7.3.10 Investigation of potential errors with evaluating applied stretch film properties 112
7.3.11 Improvement of the test frame 112
7.3.12 Energy absorbed by stretch wrap 112
7.3.13 Prestretch roller surface and stretch film interaction 112

7.3.14 Improved application of ASTM D 5459 112
7.3.15 Other research options not directly related to this dissertation 113
Literature Cited 114
8 Appendix A 117
8.1 Appendix A1: Thesaurus of Stretch film terms 117
8.2 Appendix A2: Determining prestretch variability of the stretch wrap machine 117
8.2.1 Experimental Design 118
8.2.2 Materials and Methods 119
8.2.3 Results & Discussion 120
8.2.4 Conclusion & Summary 121
8.3 Appendix A3: Comparing the Bisha Stiffness of films using different sample preparations methods 122
8.3.1 Experimental Design 124
8.3.2 Materials & Methods 124
8.3.3 Results & Discussion 129
8.3.4 Conclusions & Discussion 131
8.4 Appendix A4: Comparing the time dependent elastic properties of stretch film using the s_{af} and the s_{br} methods 131
8.4.1 Measuring how s_{br} changes over time 133
8.4.2 Measuring how s_{af} changes over time 137
8.4.3 Predicting applied stiffness and film tension from the Bisha Stiffness 141
8.4.4 Conclusions & Summary 142
8.5 Appendix A5: The Effect of Stretch Wrap Containment Force on Unit Load Stability 143
8.5.1 Experimental Design 143
8.5.2 Materials & Methods 143
8.5.3 Results & Discussion 151
8.5.4 Conclusion & Summary 156
9 Appendix B1: Raw Data Tables 163

Figures

Figure 1 Flow chart of research tasks 5
Figure 2 Diagram of critical load/deflection regions and points 15
Figure 3 Crystalline alignment with a film under strain 16
Figure 4 Where prestretching occurs in the application process 19
Figure 5 Different segments of the proposed tensile test profile identified 26
Figure 6 Materials used to cut a s_{b1} sample 28
Figure 7 Testing set up for s_{b20} 29
Figure 8 Grips used to evaluate s_{b1} 30
Figure 9 Spring diagrams identifying the general theory of evaluating the film stiffness of a given wrap pattern (s_w) 32
Figure 10 The different methods of evaluating f_a and their respective film extensions during the test are compared. 34
Figure 11 Top view of the component breakdown of forces associated with modeling f_{ac} 35
Figure 12 Top view of the component break down with forces associated with modeling f_{af} 39
Figure 13 Test frame used to simulate a unit load 42
Figure 14 Pull plate sitting flush under the stretch film before f_{af} test 42
Figure 15 Constricting the movement of the prestretch carriage 44
Figure 16 Alignment marks for turntable 45
Figure 17 Mark allowing visibility of rotational speed of roller 45
Figure 18 Diagram showing diameter options for the test frame 46
Figure 19 Rotational speed of turn table versus output prestretch rollers 47
Figure 20 Simulation of s_{af} with ruler against backing 49
Figure 21 Side view of s_{af} evaluation at maximum extension 50
Figure 22 Evolution of force vectors when evaluating f_{af} 50
Figure 23 Components of f_{ac} Testing Setup 52
Figure 24 Data output from f_{ac} testing identifying how s_{ac} and f_c is calculated and how the initial separation between the test frame and the bar did not affects results 53
Figure 25 Results of comparing the percent stretch of different film on the same stretch wrapper 56
Figure 26 The change in s_{br} of Berry Plastics 11.4 µ over a 2 hour period. The s_{br} initially increased over the first hour of testing but did not significantly change after that. 57
Figure 27 The change in the initial f_i when evaluating the s_{br} over a two hour period. Note that as time progresses the amount of f_i reduces. 58
Figure 28 Materials used to cut a s_{b1} sample 60
Figure 29 The s_{b1} results are plotted against the original material thickness 62
Figure 30 The s_{b20} results are plotted against the original material thickness 63
Figure 31 The force from the s_{b1} test was multiplied times 20 to calculate s_{b1}`. This figure shows a comparison between the $s_{b1}$` and the s_{b20} results where the trend lines are forced through the origin... 64

Figure 32 Graphical comparisons of how the means from the sb1`(N/cm) and the sb20(N/cm) compare 64
Figure 33 Slopes compared using the ANCOVA analysis. Note that the origin was not forced so an ANCOVA could be conducted. 65
Figure 34 The f_{i1} results are plotted against the original material thickness..... 66
Figure 35 The f_{i20} results are plotted against the original material thickness 67
Figure 36 The f_{i1} was multiplied by 20 to calculate the f_{i1}`. This figure shows a comparison between the $s_{b1}$` and the s_{b20} results..... 68
Figure 37 Graphical comparisons of how the means from the f_{i1}`(N) and the f_{i20} (N)compare 68
Figure 38 Slopes compared using the ANCOVA analysis. Note that the origin was not forced so an ANCOVA could be conducted. 69
Figure 39 The change in s_a of Berry Plastics 11.4µ over an hour. While there was no discernible layer effect of the film, in every test the s_a increased over time and eventually leveled off in one hour. 73
Figure 40 The change in f_t of Berry Plastics 11.4µ over an hour. While there was no discernible layering effect of the film, in every test the f_t decreased over time and eventually leveled off in one hour. 73
Figure 41 Correlation of s_{ac} and s_{af} results, note that s_{ac} is consistently lower than either s_{af}. The s_{ac} is the stiffness of the film measured via the corner test while the s_{af} is the stiffness of the film measured with the face test. Note that the trend lines are forced to fit the origin..... 78
Figure 42 Graphical comparisons of how the means from the s_a (N/cm) testing compare 78
Figure 43 Comparison of regressions for s_{af1}, s_{af2} and s_{ac}. Note that the origin in not forced within the ANCOVA analysis..... 79
Figure 44 Correlation of f_{cf} and f_{cc} results. The f_{cf} is much more linear than the f_{cc} results due to the AEP 22.8µ film producing lower than anticipated results. Note that the trend lines are forced to fit the origin. 81
Figure 45 Graphical comparisons of how the means from the f_c (N) testing compare 81
Figure 46 Comparison of regressions for f_{cf} and f_{cc}. Note that the origin is not forced within the ANCOVA analysis..... 82
Figure 47 Roll of AEP 22.8µ film used in testing with irregular profile..... 84
Figure 48 Roll of Intertape 12.7µ film used with irregular profile..... 84
Figure 49 s_{ac} per layer of film applied to the test frame..... 88
Figure 50 Plot of the increase in s_{ac}/layer applied to the test frame per thickness of film. 88
Figure 51 The additive s_{ac} effect of each film is shown. This is a very powerful comparison which may prove that thinner films can behave like thicker films. 89
Figure 52 f_{cc} per layer of film applied to the test frame 90
Figure 53 Plot of the increase in f_{cc}/layer applied to the test frame per thickness of film..... 91
Figure 54 The f_{cc} effect of each film is shown. This comparison provides knowledge as to the layering forces the film applies to the corner of the test frame. 92
Figure 55 Different segments of the proposed tensile test profile identified..... 96
Figure 56 Crystalline alignment with a film under strain..... 97
Figure 57 Spring diagrams identifying the general theory of evaluating the film stiffness of a given wrap pattern (sw)..... 99
Figure 58 Comparison of $s_{b1,}$ s_{ac} and s_{af1} results plotted against original material thickness..... 100

Figure 59 The s_{b1} data was used to predict the s_{ac} and the s_{af1} data. Note that the overall trend was consistent but not very linear and that the s_{ac} prediction was consistently lower than the s_{af1} prediction. 101
Figure 60 Comparison of $f_{i1,}$ f_{cc} and f_{cf} results plotted against original material thickness. 102
Figure 61 The f_{i1} data was used to predict the f_{cc} and the f_{cf} data. Note that the overall trend was inconsistent. 103
Figure 62 Raw data plot comparing s_{b1}``, s_{af1}, and s_{ac} across original µ 111
Figure 63 Results of comparing the percent stretch of different films on the stretch wrapper 120
Figure 64 Round unit load recommended for wrapping during prestretching evaluation 122
Figure 65 Different segments of the proposed tensile test profile identified 123
Figure 66 Top view of the component break down with forces associated with modeling f_{af}. 124
Figure 67 Visual representation of creating the s_{br} samples 126
Figure 68 s_{bp} Stretch film rewind station 126
Figure 69 Layers of the rewind pipe when creating S_{BP} samples 127
Figure 70 The separation of stretch wrap and foam 127
Figure 71 s_{bp} tensile testing setup 128
Figure 72 Complete view of s_{bp} tensile testing setup 129
Figure 73 Dual necking phenomena when evaluating the S_{BR} samples 131
Figure 74 Different segments of the proposed tensile test profile identified 133
Figure 75 Berry 16µ s_{br} results over time 134
Figure 76 Berry 11.4µ s_{br} results over time 135
Figure 77 Berry 16µ f_i results over time 135
Figure 78 Berry 11.4µ f_i results over time 136
Figure 79 Dual necking phenomena when evaluating the s_{br} samples 137
Figure 80 Berry Plastics 16µ s_{af} change over time. Note that the second layer variant was not completed due to lack of film resources. 139
Figure 81 Berry Plastics 16µ f_t change over time. Note that the second layer variant was not completed due to lack of film resources. 139
Figure 82 Berry Plastics 11.4µ s_{af} change over time. 140
Figure 83 Berry Plastics 11.4µ f_t change over time. 140
Figure 84 Stacking Pattern of One Layer of 2x4's in Test Containers 144
Figure 85 Photograph of the Standard Test Unit 144
Figure 86 Photograph of the Wulftech Stretch Wrap Machine used to Apply 145
Figure 87 Photograph of the LAB vibration tale used. The stanchions used are seen on the table. 147
Figure 88 Photograph of the Incline impact tester used in testing with the steel leveling table in place 148
Figure 89 Photograph of the Pallet Stop fabricated into the steel leveling table 148
Figure 90 Top View of Pallet Indicating Where Tape Lines Were Placed On 149
Figure 91 Photograph of the Side View of the Pallet Indicating Where the 5 Measurements were taken 150
Figure 92 Visual Column Sign Inversion Explanation 151
Figure 93 CAD in Vibration Testing 152
Figure 94 CAMD in vibration testing 153

Figure 95 CAD in impact testing 154
Figure 96 CMAD in impact testing 154
Figure 97 CAD for impact testing without bottom layer data 155
Figure 98 CMAD for impact testing without bottom layer data 156

Tables

Table 1 Largest suppliers of raw LLDPE 9
Table 2 Top dollar producers of stretch film 10
Table 3 The differential between the two sides of evaluation for the methods of evaluating f_a 34
Table 4 Experimental design for Section 4 59
Table 5 Films and their respective prestretched used in evaluating the s_b and f_i 60
Table 6 Average and COV results for s_b evaluation in tensile testing 61
Table 7 ANCOVA t-ratio results for all interactions concerning s_b 65
Table 8 Average and COV results for f_i in s_b evaluation during tensile testing 65
Table 9 ANCOVA t ratio results for all interactions concerning f_i 69
Table 10 Experimental design for evaluating the s_a and f_c of the applied stretch film 75
Table 11 Films and their respective prestretched used in evaluating the f_{af} and f_{ac} 75
Table 12 Average results for s_{af} and s_{ac} 77
Table 13 COV of s_a results. 79
Table 14 ANCOVA t ratio results for all interactions concerning s_a 79
Table 15 Average f_c results 80
Table 16 COV of f_c results 82
Table 17 ANCOVA t ratio results for the interaction between f_{cc} and f_{cf} 82
Table 18 Experimental design for evaluating the s_{ac} and the f_{cc} of the different layers of applied film 86
Table 19 Average results of s_{ac} for layer evaluation 87
Table 20 COV of the s_{ac} results for layer evaluation 87
Table 21 Average results of f_{cc} for layer evaluation 89
Table 22 COV of the f_{cc} results for layer evaluation 90
Table 23 Average results of s_{af1}, s_{ac} and s_{b1} 100
Table 24 Results of least squares regression using the s_{b1} results to predict the s_{af1} and s_{ac} 100
Table 25 Average results of f_{cf}, f_{cc} and f_{i1} 101
Table 26 Results of least squares regression using the f_{i1} results to predict the f_{cc} and f_{cf} 102
Table 27 Results of the ANCOVA comparing the s_{b1}`` and the s_a test 111
Table 28 Films used in evaluating prestretch by the stretch wrapper 119
Table 29 Visual representation of the experimental design for comparing s_b preparation methods 124
Table 30 Description of materials and respective extensions used 125
Table 31 Range of Bisha Stiffness evaluations 125
Table 32 Bisha Stiffness results for of s_{b1}, s_{br}, s_{bt} 130
Table 33 Visual representation of the experimental design for Section 8.4.1 134
Table 34 Visual representation of the experimental design for Section 8.4.1 138
Table 35 Average results of the 16µ Bisha Stiffness, applied stiffness, tension force and initial force of Bisha Stiffness 142

Table 36 Average results of the 11.4µ Bisha Stiffness, applied stiffness, tension force and initial force of Bisha Stiffness 142
Table 37 Experimental Design for measuring the effect of standard containment force on load stability 143
Table 38 f_{c-s} pretest 145
Table 39 f_{c-s} for actual testing 146
Table 40 Impact Testing Forces 148
Table 41 Average Transmisibility 152
Table 42 Data table of Stiffness 163
Table 43 Data table of initial force and containment force 164
Table 44 Data table of layering results 165

1 Introduction

The international dry goods shipment industry moved $7.6x10^{12}$ kg (8.4 billion tons) of goods in 2009 (UNCTAD, 2011). Domestically, according to the 2009 US Census, goods were shipped 121,040 Million km (75,211 million miles) (U.S.-Census-Bureau, 2009). This movement of goods around the planet is a huge business with tentacles that reach from developing countries to the most consumer rich, first world countries. Globalization has made the world today a single market place. A major challenge in creating and sustaining this marketplace is making sure that goods can get from one location to another undamaged.

When transporting consumer goods between two distribution points in which the cost of an average laborer is very high (North America, Europe), goods can be bundled together as a shipping unit and placed on a pallet, at which point that single entity is designated a unit load. The unit load may have hundreds of different characteristics depending on the method of transport, the goods transported, and the supply chain utilized. They can be comprised of homogenous loads or have a variety of different stock keeping units within the unit load depending on the request from the customer. Sixty five percent of these unit loads are held together, or "stabilized" with stretch film as they are moved throughout their respective supply chains (Wainer, 2002).

Stretch film is an elastic film (Linear Low Density Polyethylene, LLDPE, based) that is unwrapped from a roll, often stretched (either manually or mechanically), and wrapped around a unit load to maintain load stability and provide product protection during transport and storage. The film acts like a compression bandage around the entire unit load, creating a "hugging" force to keep everything together and stable. In 2003, 628 Million kg (1.385 Billion pounds) of stretch film was produced in North America (Gardner-Publications, 2003).

Current methods an end user has available to determine what stretch film will perform best on their unit loads are limited. Stretch wrap is often specified by the manufacturer for sale by one of the following five film specifications (for definitions see Section 2.3)

1. Roll weight per gauge: The weight of each roll (lbs)
2. Micron (µ): The thickness of the film, also called gauge (3.937µ = 1 gauge)
3. Length of film: The length of the film as it arrives from the supplier (ft.)
4. Length of prestretched film: The Length of film after it has been prestretched
5. Prestretch (also called Yield or Percent Elongation): The amount of stretch that is recommended a user apply in the prestretching process

None of these methods consider the performance of the film as applied to a unit load. Roll weight addresses shipping costs from the film supplier to the end user. Length of the film coupled with prestretch percentage addresses how many loads can be wrapped per roll. Thickness is the closest performance predictor; however, it alone is not sufficient due to the wide array of stretch film manufacturing processes, additives and post manufacturing treatments. Note that none of these methods allow for performance comparisons of the films as applied to a unit load. The development of

a method to evaluate stretch film whereby a user could assess and compare applied film effectiveness against the cost of the film would enable end-users a powerful tool in assembling and optimizing their supply chains.

When a company is looking to switch to stretch film or switch stretch film suppliers, they are generally looking to lower handling costs, reduce labor and transportation costs, increase product protection, modify inventory control (Wainer, 2002), reduce exposure to weather and/or mitigating pilferage in transit (German, 1998). Over the years, there have been many different tests that use a wide variety of films available in the market place. They are paired to a specific set of stretch wrap machine settings (per film) and applied to a single unit load. The results of these tests are typically measured in containment force (pounds, via ASTM D 4649). An example of one of these tests and reported information can be found in the *Inside Scoop Archive* by Bill Jackson on 3/20/2007 (Jackson, 2006-2007).

Evaluating stretch film in the field using ASTM D 4649 (ASTM, 2003a) for scientific comparisons has inherent uncontrolled variables in the system. Box to box interaction (coefficient of friction, density of boxes packed, etc.), overlap and under hang of the boxes over the pallet, and the compression of box walls when a tight film is applied are all uncontrollable variables of the unit load that should be controlled and reported or eliminated. In addition, the exact stretch wrapper machine settings / behavior should be evaluated and reported.

ASTM D 4649 Standard Guide for Selection and Use of Stretch Wrap Films and its Annex "A1 Test Method for General Evaluation of Stretch Wrap Materials Under Non-Laboratory Conditions" is the only official way to compare one film to another making it a critical reference point for determining how to wrap a unit load before shipping. The only testing that may reflect the containment force of a unit load is a non-laboratory test requiring the user to pull a plate that is placed behind the film outward. Once it has been applied to a unit load it may be adequate enough to compare two films, but this process becomes more difficult when testing a wide variety of films from multiple suppliers. The amount of time and money required to test 10 different film types per unit load to determine which allows for the highest performance value per the cost is not economical, especially when the decaying force of the films over time is currently not accounted for in the testing protocol.

The decay of polymeric based material under load is not a new phenomenon. This phenomenon has been studied for decades by scientists (Peacock, 2000) and (Brown, 1999) via tensile testing. Most of this testing has been conducted in the initial linear region of the stress strain graph. Beyond this region there has been very little research conducted and testing methods developed to understand and quantify the behavior of stretch film as applied to a unit load.

The current standard to evaluate stretch film is ASTM D 5459 in which the film is evaluated using a hysteresis test from traditional engineering philosophy. The test involves the extension and relaxation of the film in repetition to calculate the permanent deformation, elastic recovery and stress retention. All of these values do not offer any significant information with regard to how the film will perform when it is applied to a unit load.

Despite the inadequate testing standards and purchasing methods that do not help identify the effectiveness of a given film, there has been no push for a quantitative comparison standard for the films. Creating a new test method would help the film users directly compare different films while giving manufacturers an appropriate standard with which to design their film.

1.1 Problem Statement

Stretch wrap has been used to hold together unit loads for almost 40 years. During that time there have been many technological advances in stretch film. Some have allowed for increased performance though most of them allowed for increased profitability for the stretch film producers. With regard to film performance, there has been heavy focus on creating a stiffer, thinner gauge that can be stretched to a higher percent elongation during application allowing for a higher containment force value when the film is evaluated using the current ASTM standard. This performance increase has mostly been done through advances in polymer technology and cast film extrusion processes that allowed for more layering (Jackson, 2006-2007).

ASTM D 4649 is the current standard that evaluates the amount of containment force a stretch film posses when applied to a unit load (ASTM, 2003a). The standard measures the force that is required to pull the film off the unit load a set distance in a set location. The problem with this measurement is that the force value can be achieved through a combination of machine settings and film properties and is not necessarily a good predictor of the actual performance of the film in the distribution environment. In contrast, it is hypothesized that the containment force, as defined by ASTM D 4649, can be broken down into applied stiffness, defined as the slope of the force/displacement curve as the film is pulled from the unit load, and containment force, defined as the amount of force the film exerts on the corner of the unit load.

ASTM D 5459 is the current standard for evaluating the tensile properties of stretch film. However, the testing profile specified is a standard hysteresis test that does not represent the film in application. The test calls for the extension of the film to a given percentage and then a relaxation of the film back to a zero point. When film is applied to a unit load, the film is stretched and then held at that extension because it is applied to a unit load. A new testing method that would properly emulate the film in its use may be able to produce useful values with regard to applied film performance.

The current ASTM standards that are used to evaluate stretch film are a starting point for evaluating film properties. These standards give no indication about how the film will respond when applied to a unit load. There is no method for comparing stretch films before application. This leaves stretch film manufacturers responsible for making performance specifications based on non-universal methods. End users for these stretch film products are forced to complete their own film comparisons based on each end user's equipment. Because of the variability of this machinery, the comparisons will not only be inconsistent between end users, but unreliable in each individual manufacturing facility.

This study attempts to address the need for research by creating a new tensile test method to evaluate film stiffness using different sample preparation methods. In addition, the research will breakdown the traditional definition of containment force into applied film stiffness and containment force and then

use two different methods to quantify the values of the applied film. Finally, a correlation of tensile properties and applied film properties will be attempted.

1.2 Research Questions

It is proposed that there is a link between how stretch film is applied and behaves on a unit load and how the film can be evaluated in a laboratory setting. If this link is identified, film users will be able to compare film properties before it is applied to a unit load, and manufacturers will understand how to optimize their individual films for their customers. Based on this hypothesized link and the needs identified in the problem statement, the following questions guided this research:

- How can the applied film stiffness and containment force be predicted by emulating the prestretching and application of stretch film with a particular thickness through tensile testing? This question will be answered by moving away from the traditional stretch film tensile testing methods to an evaluation method that simulates how stretch film is treated during application to a unit load. Force and displacement measurements from the new testing method will be used to calculate material stiffness values.

- When stretch film is applied to a unit load, what is its stiffness and containment force and can the values be confirmed using multiple methods of evaluation? Answering this question will require dissection of the traditional containment force definition and evaluation method. It will be divided into applied film stiffness (force required to pull out on the film a set distance) and containment force (force exerted on the corner of the unit load).

- How can the stiffness and force results from tensile testing (first question) be used to calculate the stiffness and containment force results from the second question (for the same film)? The stiffness and force results from tensile testing will be used to create a model to predict the stiffness and containment force results from the applied film (second question).

1.3 Purpose and Objectives

The purpose of this research was to establish a link between the applied stiffness and containment force of stretch film and tensile stiffness properties measured in a laboratory setting. A flow chart of the research tasks is shown in Figure 1. Specifically, the objectives of the study were to:

- Characterize elastic properties of stretch film through tensile testing.
- Evaluate film behavior in terms of stiffness and containment force performance when applied to a unit load.
- Investigate the correlation between the elastic tensile properties and the applied stiffness and containment force of stretch film.

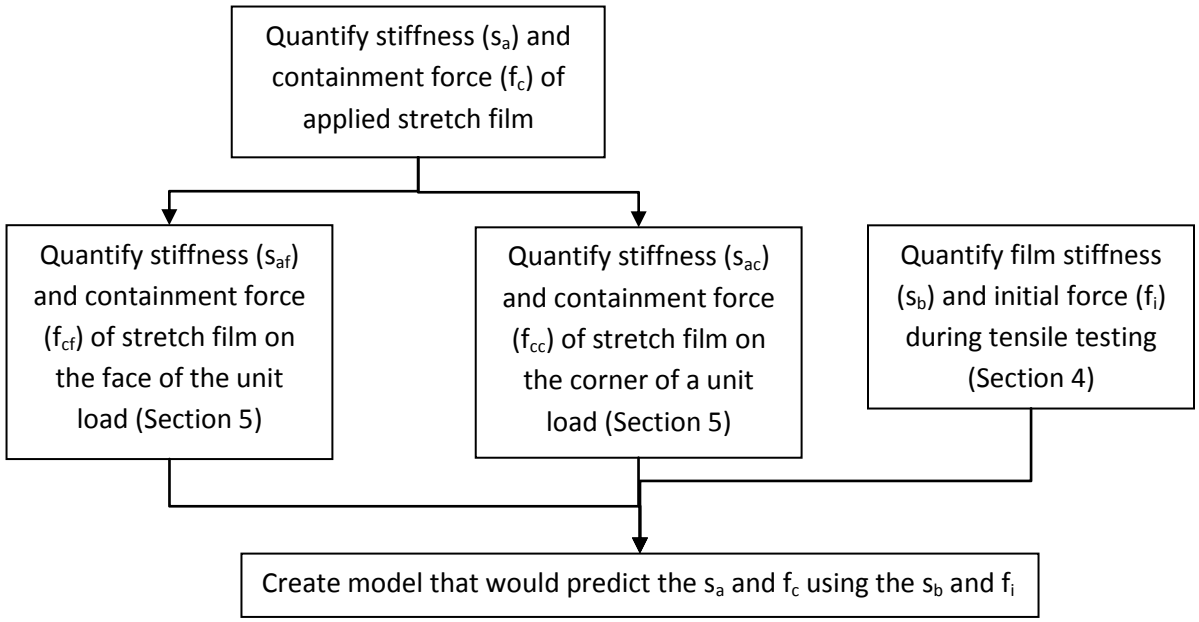

Figure 1 Flow chart of research tasks

1.4 Research Contributions

The results of this research contribute to the body of knowledge in the fields of unit load design, polymer material science and supply chain execution.

Contributions to the field of unit load design: This study enhances the knowledge of load stabilizers as applied to a unit load, a field that has received very little attention in any packaging literature or text. Stretch film application will be described in detail along with how the application process manipulates film properties.

- Create a new tensile evaluation method that will allow for the quantification of film stiffness.
- Define how the stretch film and stretch wrapper interaction can be broken down to better understand the components of the system which will enable the prediction of applied film properties.
- Evaluate applied stretch film stiffness and containment force
- Determine if the tensile properties can be used to predict applied film stiffness and containment force.

Contributions to the Field of Polymer Science: There has been very little research conducted with stretch films' properties beyond their yield point. This research will investigate the behavior of film

beyond the linear elastic region and how this behavior can impact a film's performance when applied to a unit load.

Contributions to the field of supply chain execution: This research will help supply chain material optimizers choose the most effective stretch film for their individual supply chains. They will be able to conduct a direct cost/benefit analysis between film effectiveness and cost. If their current film is not performing at a desired level then the critical properties of that film can be analyzed and compared to potential new films. This direct comparison is not currently available. The analysis will save companies time and effort as the ability to compare a wide range of films from multiple suppliers is currently not easily feasible. Once a user has a test method that can be used in comparison studies, they could then, more precisely define their requirements to help film manufacturers design more effective stretch film formulations as their supply chain changes and evolves.

1.5 Practical Contributions

There are several practical applications for this research, as follow:

- Users of stretch film will be able to compare stretch film properties before they are applied to a unit load. This will allow for a cost/performance analysis to be conducted on a variety of films.
- Users will be able to optimize their stretch film usage per SKU. This optimization will be of great benefit if a user has unit loads with varying weight that all go to the same stretch wrapper. This optimization will also benefit users who ship to a variety of different supply chains that vary in length, allowing for short term films to be applied in short term situations.
- Manufacturers will have a well defined testing method to evaluate their films

1.6 Assumptions and Limitations

This study makes several critical assumptions when evaluating film stiffness on a unit load. They are as follows:

- The film is not able to slip around the vertical edges of the unit load. This assumption is important because when evaluating the film stiffness on one side of the unit load, the volume of material evaluated will not change throughout the test. If the material were to pull around the corner of the unit load then the measured stiffness would be artificially low.
- The film is able to slip over the top and bottom edges of the unit load. The amount of film overlap over the top of the unit load is not consistent. Some companies only wrap to the top edge, others wrap with up to or over 6 inches of film overlap over the top edge. With this much variation in the wrapping pattern, an assumption has to be made that the interactions between the top edges of the unit load and the film is insignificant. In addition, there is no force pulling the film across the top of the unit load. All of the force from the film is assumed to be solely in the film's machine direction.
- The chemistry of all the films will be treated as if they are the same. Much of the stretch film literature is based on proprietary formulations and mixtures of films. To ensure that each film is treated the same and to ensure that one particular formulation is not touted as the best

(possible conflict of interest), the formulation of the films will be ignored. See Section 2.3.1 for details.

- The tack of the films is high enough to allow multiple layers of film to act as a single layer of film when applied to a unit load and the film stiffness is evaluated. If a film under investigation was not tacky enough to stick together, then it would slip between layers. Such slippage introduces variability that is more complicated to model and evaluate.
- Evaluating how film stiffness correlates with unit load stability is beyond the scope of this study. The stability of a unit load is dependent on much more than just stretch film. Pallets, stacking pattern and load density characteristics also play a large role. It will be up to the individual user to determine how each film helps to stabilize their unit loads.
- When evaluating the stiffness of the film using the Corner f_{ac} method (see chapter 3), the stiffness of the film is constant through the first 2.54 cm of evaluation. The irregularities in this range, using this evaluation method, are due to the weight of the bar and the interaction between the bar and the test frame, both of which are assumed to not significantly affect the evaluation of material stiffness. See Section 3.0 for details.
- Selecting the optimum temperature and relative humidity for the best film performance is outside the scope of this study. The facilities used in this research did not allow for film evaluation under different temperature environments.
- The speed of the tensile tester available cannot match the speed of the prestretching process. This could reduce the measured tensile stiffness of the film.
- The time required for a film to stabilize under these testing conditions depends on the amount of film tested, the sample preparation method and the sample size. No matter what combinations were used, trends of these results should be relatively consistent due to the polymeric nature of the stretch film as discussed in Section 2.3.

2 Literature review

The following section provides a discussion of the current stretch film market and its origination, creation, application and evaluation as applied to a unit load and in a laboratory setting.

2.1 Unit load Stabilization

An assumption is made that when a product leaves the manufacturing facility it will not be damaged. Yet, domestically, the Grocery Manufacturers of America (GMA) estimate that about 1% of grocery items shipped in the United States are damaged or unsellable by the time they arrive at their destination grocery store (GMA-Wipro, 2010). If that percentage is applied to the 1.8 x10^12 kg (20 billion tons) of products shipped in the United Sates, that leaves approximately 181 trillion kg (200 million tons) of goods damaged in shipping each year (BTS, 2002). To put a dollar figure on this value, the GDP non durable goods for 2012 is estimated to be 1,997 billion dollars, if 1% of that value is unsellable, that is 19 billion dollars lost due to product damage(U.S., 2012).

One of the strategies used to reduce the amount of goods damaged in transit is to bundle a series of goods together and place them upon a shipping platform. This bundling is typically done with stretch film. Stretch film is an elastic film that is stretched and wrapped around a group of items to keep them bundled together during handling. This film is most commonly applied to boxed items that have been set upon a pallet to form a unit load. Once the film has been applied to this system, the single unit is called a “unit load”.

2.1.1 History of the stretch wrapper

The stretch wrapping machine initially applied stretch film to a unit load that was 152.4cm (60”) wide in multiple layers as the unit load turned on a turn table with limited prestretching of the film. As the market for stretch film broadened, the variety of web widths increased. With cost being a major driver of the market, a solution that could be applied to a wide range of unit loads was able to bring down cost. Eventually the market settled on 50.8cm (20”) as a standard minimum web width that could be applied to almost any unit load. However, multiple film widths are still available (Jackson, 2006-2007). The larger stretch wrap machine manufacturers include Lantech, Highlight Industries and Wulftech.

There have been many different technological advances with regard to prestretching and application. Most have revolved around the issues involved in wrapping a square object (see Section 2.2) and issues around consistent percent and variable percent prestretch. The current trend is to roll stretch film, called “roping”, during the film application process. If a film is roped, a portion or all of the film is rolled into a “rope” as it is applied to the unit load.

2.1.2 History of stretch film

Metal strapping was the first step beyond rope for combining smaller boxes or crates together for transport. It easily damaged product (point loading), rusted and caused many physical injuries during application and removal. Stretch wrap originally solved all of those problems. The application of stretch

film to a unit load was first proposed in 1973 by Pat Lancaster (of Lantech). Films were constructed of Low Density Polyethylene (LDPE) and Polyvinyl chloride (PVC) in the 70's. They were 1 layer cast film that was around 24.5µ (100ga)("Mobilrap C" stretch film). At this stage the PVC was able to stretch farther than the LDPE (50% vs 30%). As the industry evolved, the use of PVC quickly went by the wayside. It easily tore and zippered off unit loads. In addition, the ability of LDPE to stretch beyond 50% grew, identifying PVC as the inferior product (Jackson, 2006-2007).

The chemical composition of the LDPE has changed significantly over the years. The original LDPE film gave way to Linear Low Density Polyethylene (LLDPE) film created in the late 1970's and produced by Mobil under the market name "X". This film was vastly superior to anything on the market. The short branches off the primary polymer chains of the LLDPE allowed for vastly superior stretch and greater puncture resistance. With the market acceptance of LLDPE, various film formulations with these polymers flourished (Jackson, 2006-2007).

Throughout the years layering has been a big selling point of stretch film. The original single layer film transformed into three layer film in the early 1980's, 5 layer films in the early 1990's and then skyrocketed to 7 and 9 layer films quickly after that. Each layer contained a different chemical that would increase the desirable properties of the stretch film (Jackson, 2006-2007)

According to Jackson's *Inside Scoop Archive* (Jackson, 2006-2007) the industry has been continually down gauging since its inception. Starting in 1995, the average performance film sold had a thickness of 18µ, while in 2010, the average thickness of performance films had dropped to 13µ. The average down gauging that occurs every couple of years coincides with different technological advances in film formulation or manufacturing method.

2.1.3 Prominent LLDPE resin suppliers and film converters

According to Kathy Hall (4/8/11) of Petro-Chem Wire, the companies listed in Table 1 are some of the largest suppliers of raw LLDPE. The companies that convert raw resin to stretch film are shown in Table 2 and are arranged by sheet sales (Crain, 2011).

Table 1 Largest suppliers of raw LLDPE

Company	Annual Output (Billions of pounds)
Chevron Phillips	0.525
Dow	2.205
ExxonMobil	1.145
Formosa	0.65
LyondellBasell	1.13
Westlake	0.88

Table 2 Top dollar producers of stretch film

Company	Film & sheet sales
	(millions $)
Bemis Co. Inc. (P) a	3,300.00
Neenah, WI	
Sigma Plastics Group	2,450.00
Lyndhurst, NJ	
Berry Plastics Corp. b	1,700.00
Evansville, IN	
Inteplast Group c	1,090.00
Livingston, NJ	
AEP Industries Inc. (P)	800.57
South Hackensack, NJ	
Intertape Polymer Group Inc. (P)	290
Bradenton, FL	

2.1.4 Other methods of unit load stabilization

There are many different load stabilizers that compete with stretch film. The most closely related is stretch hooding. Stretch hooding is a large tube of film that is heat sealed on top, stretched open, pulled down over the unit load and released. When the hood is released it applies force on 5 sides of the unit load (all except the bottom). Stretch hooding has its place in the load stabilization market. However, it is currently limited by the cost of machinery and film and the complexity of the machine compared to the simplicity of the stretch wrap machine (Bisha, 2008).

Another film applied to a unit load is shrink film. Shrink film can either come in roll or hood form. After the film has been applied, the film is heated at which point the film significantly shrinks. This shrinking action causes the film to become taut over the surface of the unit load. Once cooled, the film does not cause a great amount of inward force on the unit load. Shrink film is very stiff after it has been heated, reducing the amount of movement the unit load can experience. The disadvantage is the vast amount of energy required to shrink the film properly. In addition, the heat can sometimes affect the contents of the unit load (Bisha, 2008).

Strapping, the traditional load stabilizer has gone from steel to polyester (green) to polypropylene (black). In each case the strapping is wrapped around the unit load and fastened with either a buckle or a friction weld. Strapping is extremely strong but can cause point damage to the unit load when it is tightened too much. In addition, unless the strapping is touching every component of the unit load, the load is more likely to come undone in transit. These issues can be slightly mitigated by the use of corner protectors underneath the strapping. These protectors can be made of paper or plastic and help apply the force of the straps over a larger area (Bisha, 2008).

2.2 Manufacturing and Application Methods of Stretch Film

This section discusses the process of manufacturing stretch film and how the stretch film is applied to the unit load.

2.2.1 Manufacturing Methods

There are two different methods of manufacturing stretch wrap. One is a blown process and the other is a cast process. The blown process starts by extruding molten resin through a circular die. It is then pulled to a desired height while being inflated, usually from 20' to over 100'. The balloon is then flattened, cut into the desired widths and rolled. Blown films are typically hand wrap films (see hand wrapping below). Cast film is produced when molten resin is sent through an extruder and forced out as a thin sheet. The sheet is then rolled over a cooling drum, cut to width and rolled (German, 1998). More film types can be constructed using the cast process than in the blown process due to the ability to add more layers with better quality control. Cast films are typically machine grade films (see automatic and semiautomatic below).

The blown films are typically bi-actually oriented (it has more desirable properties in both the machine and cross machine direction). In contrast, the cast films are typically uni-axially oriented and only have desirable properties in the machine direction. Each of these processes possess their benefits and drawbacks and are discussed at length in many other publications (Osborn , et al., 1992).

2.2.2 Application Methods

The method for applying stretch film to a unit load affects film performance. In general, there are three methods of application, the hand reel, the semi-automatic machine, and the fully automatic machine. Note that each process (and each individual machine) can prestretch films differently. The Stretchability of a film is the consistency of which a stretch wrap machine can stretch any given film (Patrick Lancaster, 1993).

Hand held application is when the employee walks around the load with the reel of film, wrapping as he/she goes in a predetermined pattern (simple turn tables can also be used allowing the employee to stand still). Hand wrapping rolls are often lighter than machine rolls for better ergonomics and can be from 12.7cm (5") to 50.8cm (20") in roll width.

The semiautomatic rotary systems are fixed position units. Stretch films for semiautomatic and automatic stretch systems are predominantly sold on a 50.8cm (20") roll. There are two methods of wrap with many variations, turn table and ring. Both of these methods require less labor than hand wrap. The only employee involvement includes initially putting the unit load in place, attaching the wrap, starting the machine, cutting the wrap and then removing the unit load (Collins).

For a turn table wrapper, the unit load is placed on a turn table (hand truck or fork truck), next to which there is a vertical mast that has a lift with a wrap dispenser attached (prestretch carriage). The film is then affixed to the unit load, the turn table is started and the lift moves up and down corresponding to the desired wrap pattern. When complete, the film is cut and the unit load is manually removed from the turn table.

For a ring wrapper (also called rotary tower), the unit load is positioned underneath the wrap dispenser which travels around the unit load on a ring or halo like track, dispensing as it moves in a predetermined pattern. This is typically used when the load to be wrapped will become unstable if a rotary machine is used (such as empty bottles)(Collins).

Either of these semiautomatic systems can become fully automatic with the addition of automatic feeding conveyors, machine features and software. It is also possible to program a split pattern, allowing for the wrapping of multiple unit loads stacked on one another in one cycle.

Vertical load wrappers are built around conveyor systems and are therefore inherently automatic systems. They allow unit loads to slowly pass through a stretch wrapping tunnel, being wrapped along the way (long vinyl siding).

2.2.3 Wrapping a four sided object

When a unit load is wrapped in stretch film, the corners travel faster than the faces even though the overall rotation speed has not changed. This has been illustrated by Kurt Riemenschneider at Highlight Industries in his presentation at the AMI Stretch & Shrink Conference 2011 (Riemenschneider, 2011). Kurt's research has shown that if a unit load is rotating at 12 rpm then the face of the unit load would travel at speeds between 39.6 m and 45.7 m (130 and 150 ft.)/ minute while the corners would travel at 60.9 m (200 ft.) /minute (Riemenschneider, 2011). This phenomenon makes the tension bar (dancer bar) necessary. The farther this bar is held open the faster the prestretching will occur to try and compensate for this problem. Therefore the prestretching process is not held to a consistent rate wile wrapping a unit load. For more detail on stretch wrapper operation see Section 2.1

2.2.4 Prestretching

There are several different methods of prestretching films on the market. Most involve an initial roller that pulls the film off the roll and holds the film while a second sticky roller has an outside surface that moves much faster causing the film to stretch between the two sticky rollers.

Downey conducted a specific investigation into the effectiveness of prestretching. They found that as a film was stretched to its yield point, the thickness and cross-sectional area reduced consistently. After the yield point, the thickness and width of the films started to reduce at inconsistent rates. The thickness of the film slowly reduced to almost half, while the width of the film was reduced, or necked down, at infrequent rates depending on the yield points of the different portions of the specimen. However, there was a general relationship determined between the original thickness, the stretched thickness and the percent extension after the yield point (assuming that the density does not change significantly during elongation) This relationship is outlined in Equation 2-1 (Downey , et al., 2001).

$$t_n = \frac{t_0}{n^{.5}}$$ **Equation 2-1**

Where:

t_n= Thickness after stretching

t_0= Thickness before stretching

n= how many times its original length

With regard to tack, it was also found that prestretching stretch film reduced the effectiveness of the tack by over half. However, the level of tack seen at 300% elongation was observed to still form an adequate bond for the loose end of the film to adhere to the load (Downey, et al., 2001).

Evaluating the amount of prestretch imparted on a film as applied to a unit load can be done with ruler or a star wheel (Jackson, 2006-2007). To use the ruler method, ink marks are applied on the film at known distance interval before the film was prestretched. The film is then prestretched using the desired prestretch carriage and the average distance between marks was recorded. Measurements could be taken at any point across the web width to evaluate for consistency of stretch.

The star wheel applies a mark on the unstretched film at known distance intervals while the machine is running. The distance from each mark can then be measured once the film has been applied and stretched to determine the actual prestretch amount. This method can be used to evaluate the initial prestretch applied to the film from the prestretch carriage in addition to the stretch imparted on the film from a high tension to load (see Section 2.4). As with the ruler method, measurements could be taken at any point across the web width to evaluate for consistency of stretch.

To evaluate the amount of stretch due to tension to load, the amount of stretch from the prestretch carriage must first be quantified. The difference between the percent stretch of the carriage and the percent stretch due to tension to load is the amount of additional stretch imparted on the film.

2.2.5 Stretch Wrapping Patterns

Any of the previously mentioned application techniques can be used to apply stretch film in any pattern the user desires. There are three predominant wrap patterns used, one building on the other. First, a spiral wrap can be started anywhere on the unit load, typically on the bottom or the top. From there the machine will make a single spiral pass over the unit load. If more wrapping is required, a cross spiral pattern can be added, wrapping the unit load in a mirrored pattern in the opposite direction. The amount of overlap between spirals is up to the individual user to determine, however 40% to 80% is common (Collins) If additional stability is required, multiple horizontal wraps are utilized (typically three) at the top and bottom of the unit load as specified in the UPS Airfreight Packaging Pointers (UPS, 2005), the Home Depot Shipping Platform Standards (G. Panagopoulos, 1991) and the Pennsylvania DGS Supplier Shipping and Receiving Guidelines (Riemenschneider, 2011).

When discussing wrap pattern, the top overlap (top wrap, over wrap) is the amount of film that covers the top of the unit load when wrapped. The bottom wrap is the amount of film that covers the pallet at the bottom of the unit load.

2.3 Stretch Film Properties

The physical properties of polyethylene can generally be described as the polymer characteristics that involve the reorganization of their base structure or the deformation of their original structure based on a force exerted onto the substance. The following review and subsequent research will focus on the

effect of how high strain properties affect physical film characteristics. Specifically, there will be a focus on how the dimensions and stiffness of the film can change.

2.3.1 Chemical Composition Stretch Film

Commercial application of LLDPE started in the 1950's. When stretch film application started to become a major film market in the 1970's, the film companies started to look into how different polyolefins affect stretch film in application. This industrial growth harbored the creation of many different additives that offered a variety of attributes to the stretch film industry. All of the additives below are very short chain resins that are essentially considered linear (Peacock, 2000). Note that over 80% of the cost of stretch film has to do with the raw materials that comprise an individual film. The rest of the cost has to do with Maintenance, Labor, Energy etc.

Polypropylene (PP), Ethylene Vinylacetate (EVA) and High Molecular Weight High Density Polyethylene (HMWHDPE) were all used at different points along the evolution of stretch film but have mostly been phased out due to the development of new and better polymers (Jackson, 2006-2007).

Butene and Hexene were invented by Union Carbide. Butene did not have any properties that were particularly useful in stretch film application. As a consequence, it is typically used as an inexpensive filler instead of LLDPE in some modern stretch films, but primarily in bags and sheeting (Jackson, 2006-2007). Hexene was invented to compete directly with Octene and had similar properties as Butene but offered better cling and puncture resistance (Jackson, 2006-2007). Octene LLDPE was invented by Dow Chemical and had physical properties that were similar to Butene and Hexene.

The term Metallocene is used to describe a family of catylists that were invented by W. Kaminsky in the early 1980's that allow for the control of activation sites for the polymerization of film. The industry found, through trial and error, that blending in a variety of Metallocene catalysts did offer some benefit, though, not as much as when the material was layered next to LDPE. When done properly, the desirable properties were increased dramatically. These catalysts offered twice the puncture and tear resistance as straight LLDPE (Jackson, 2006-2007).

2.3.2 Material Behavior Under Strain

Hooke's law states that the extension of a spring is in direct proportion to the load added as long as the spring does not pass its elastic limit. This law is expressed as Equation 2-2. Once past its elastic limit Hooke's law starts to break down because the material structure begins to change. The polymer chains will start to realign in the direction of the exerted force. This realignment phenomenon is discussed in greater detail in this section below.

$$F = Kx \qquad \text{Equation 2-2}$$

Where:

F = Force vector (Newton)

x = distance (cm)

K = Spring Constant

According to Peacock, Polyethylene does not behave in a truly Hookean manor (Peacock, 2000). However, the descriptive terms from Hooke's law and further investigation by Cauchy are still used to describe the different phases of polyethylene under constant increasing load. Figure 2 is an example of an elastic, single direction, load-deflection curve with definitions of critical regions labeled (Mal , et al., 1991).

For non-polymeric based materials, a true stress-strain curve is the most common way to graphically display and compare material properties data. While true stress is easily measured in force (Newtons), the true strain (area of sample) dynamically changes during tensile testing beyond the proportional limit. The change in cross sectional area (necking) is due to the increased alignment of the polymeric chains (crystalinity). The changing width of the material requires special equipment to measure the cross sectional area change during the test. This equipment is necessary to calculate the actual strain of the material. If this equipment is not available, the results should be displayed via a load-deflection curve (a.k.a. stress & engineering strain) (Peacock, 2000).

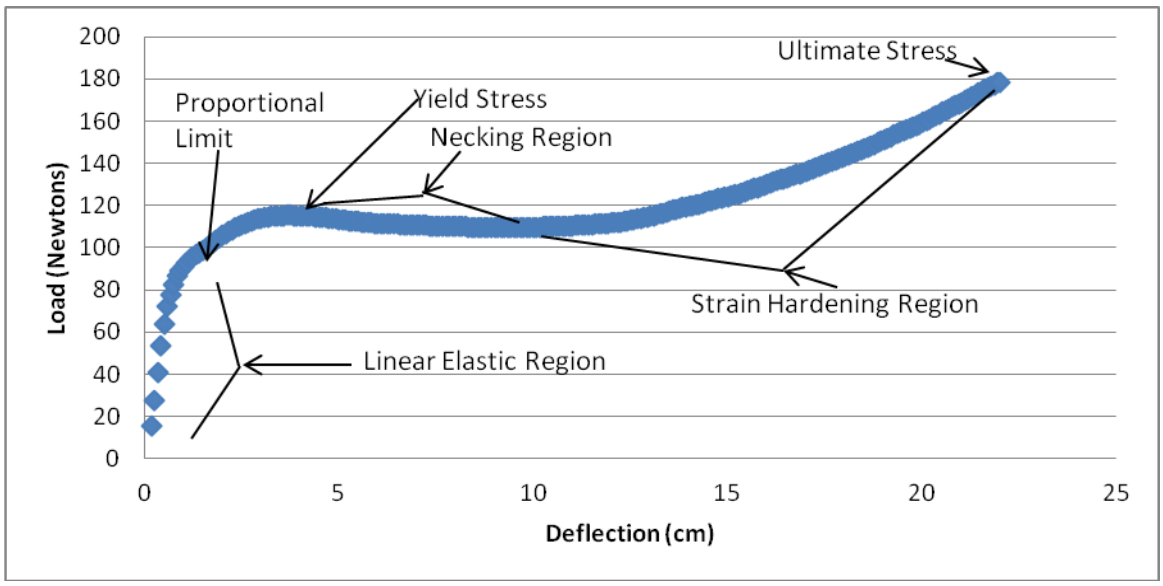

Figure 2 Diagram of critical load/deflection regions and points

The ability of a film to elongate when a pulling force is applied and then relax (retract) once the pulling force is removed is known as a films Elasticity (elasticity (n.d.)). Tensile Strength is the amount of force required to hold the film at a certain percent elongation (Soroka, 1999). The slope of the line before the proportional limit is known as the Elastic Modulus, after which the slope is no longer linear but the film is still in an elastic state(Hernandez , et al., 2000). After the Yield Stress occurs the material will continue to strain (elongate) without additional stress (increase in force requirement). Once the yield stress is reached, the film will experience permanent deformation with the continuous application of strain. This deformation is non recoverable (German, 1998) and is the general region in which stretch wrap is designed to perform.

The force required to pull beyond the yield stress actually causes the film to start to change on the microscopic level. Strain hardening and necking coincide after the yield point and before the Breaking Point in the inelastic region (Peacock, 2000).

The strain hardening function is generally considered a positive attribute for stretch film. This is where the percentage of crystallinity within the stretch film continues to grow as the film is elongated (attributes of crystallinity will be discussed later). A desired percent crystallinity is determined by different film manufacturers. This aligning and eventual break down (after the ultimate stress) of the molecules causes the film to decrease in width called necking (Hernandez, et al., 2000);(ITW Mima Packaging Systems, 2009). A graphical display of the necking phenomena is displayed in Figure 3. The decreasing force to elongate the film after the yield point indicates that there is more necking than strain hardening occurring. Once this force starts to increase again, necking diminishes and the strain hardening function has taken hold.

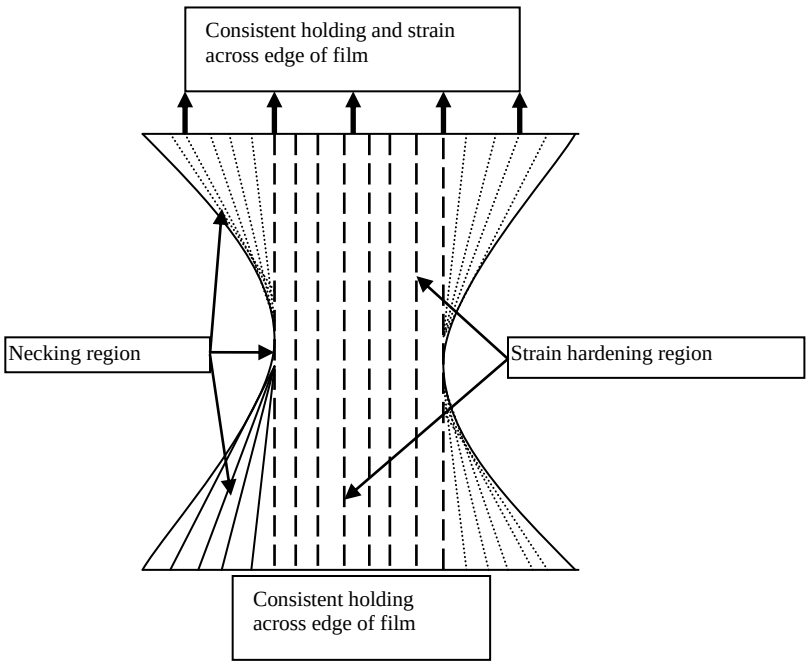

Figure 3 Crystalline alignment with a film under strain

The proportion between the necking region and the strain hardening region is important in understanding the shape of the stress-strain curve in the inelastic region. Every film has a specific necking characteristic that will occur depending on the width of film and the distance pulled. If the distance of pull is kept consistent, narrower films will be consumed by the pure necking phenomena. As the films get wider, strain hardening becomes the predominant tensile characteristic. Eventually the force per unit distance to pull the entire width of film starts to stabilize indicating an accurate testing width and force per inch reading.

The rate of sample elongation greatly effects how the material responds to the test. Faster draw of polyethylene may increase the amount of necking that may occur and lower yield stresses among other

properties (Peacock, 2000). Brown confirms this in his discussion about test piece geometry. The discussion revolves around how the results of a test can be influenced by the shape and size of a test sample (Brown, 1999). Therefore, during testing the sample sizes and extension rates should mimic the behavior of the film on the stretch wrapper (Section2.2.2) and be held constant across all evaluations to eliminate uncontrollable error.

The Poisson Ratio of film (applied to many materials beyond polymeric materials) is the ratio of the elongation strain to the contraction strain when a tensile force is applied. The range for all normal materials is from -1 to .5. In the case of PE and specifically LLDPE the values will range from .4 to .5. This means that as the film elongates it will shrink in width and thickness with this proportion. The problem with these values is that they are a gross over simplification of the actual material behavior. Everything from the room temperature, to the film cure time, to the time allowed to conduct the test, will affect the exact Poisson ratio of a film.

2.3.3 Crystallinity

According to Brown (1999), crystallinity is not commonly examined in polymer based materials (Brown, 1999), however, it is critical in the polymers that make up stretch film. There are a few polymers with many different additives and treatments that comprise stretch film, some allowing for a higher crystalline percentage than others (see next section). When these polymers are stretched (either in the factory or just before use) the individual chains within the film try to align into the lowest energy state possible forming spontaneous crystalline sections throughout the film (Hernandez, et al., 2000). This process is called cold drawing. This morphological change can be utilized to increase desirable properties within the film. Large amounts of cold drawing can make the material bidirectional due to the large amount of crystallinity imparted into the specific direction of the film (Campbell, 2004). The increase in crystallinity in a single direction is what aids stretch film in becoming so effective at holding together a unit load (further discussion in next section). The more crystalline the original film, the sharper the summit of the yield point of the material on a load-deflection graph (Peacock, 2000).

One of the most important morphological changes that stretch film undergoes during its application and utilization is the increased amount of stiffness. The stiffness of a film is increased any time the film is pulled beyond its yield point, whether continually pulled, pulled and held or pulled and let go. The film stiffness is an indication of the amount alignment that the polymeric chains underwent during the film augmentation. The process of increasing stiffness can repeat itself time and time again until the ultimate failure of the film occurs. This increase in stiffness allows stretch film to perform as it does when applied to a unit load. According to Hernandez, as crystallinity increases the density and tensile strength will increase while the tear resistance, impact strength, recovery and many other material properties will decrease because the film is becoming harder (Hernandez, et al., 2000).

After the film has been produced using either the cast or blown method described in Section 2.2. The film can then be stretched in the factory with a Machine Direction Orientation (MDO) system. A MDO system can stretch the film many times its original length. This process significantly increases the percent crystallinity within the film while significantly increasing the length of the film and decreasing the thickness. This decrease in thickness resulting from the MDO process has led to the creation of the

ultra thin films with an increased density and tensile strength leading to higher containment force when applied to a unit load (see Section 2.4 for containment force evaluation methods)(Smith, 2010).

2.3.4 Material Properties of Stretch Film

Stretch film will elongate when a pulling force is applied although how it elongates depends on its temperature, speed of elongation and the volume of material tested. The longer it is stretched in the machine direction (typically the direction of wrap) the more the film loses its thickness and width (necking). As a material, stretch wrap is bidirectional due to the chemical makeup and the manufacturing process of the material. The direction parallel to the film's web (a.k.a. the direction of unroll) is known as the Machine Direction (MD), where as the perpendicular direction, across the machine web, is known as the Cross Machine Direction (CD) or Transverse Direction (Osborn, et al., 1992). There are many different properties of stretch film. Some of the critical properties will be discussed in the following section. McNally found that stretch films are generally strongest at break in the MD (McNally , et al., 2005). Billham found that films allowed for more ultimate elongation in the CD, but have a lower break strength (Billham , et al., 2001).

Puncture resistance is the film's ability to resist the act of piercing (Downey, et al., 2001). This resistance property is typically tested by using the dart drop method (Provincial Paper & Packaging Ltd., 2008)

Tear resistance refers to the resistance to tear that has been started by a rough edge or puncture while the film is under tension. If the film tears easily in the CD, the film can quickly remove itself from the unit load. Conversely, if the film tears easily in the MD, the integrity of the unit load is mostly maintained (Downey, et al., 2001). An Elmendorf Tear Tester is the testing devise typically used to measure the amount of force it takes to propagate an initiated tear in a film (Provincial Paper & Packaging Ltd., 2008). There are three different ASTM standards that can be used to evaluate the tear resistance, ASTM D1004, D1922 and D1938 (Osborn, et al., 1992).

Prestretch is the percent elongation that is imparted on the film just prior to application in the prestretch carriage (see Section2.2). This stretching is done by running the film through two sets of rollers that are rubberized and sized differently, the second having a circumference that is proportionally larger that the first. The center axis of the rollers is turning at different rates causing the outer surface of the larger roller to turn faster than the smaller roller, thus stretching the film (see Figure 3). If a film's new length is stretched to 3 times its original length, it has a prestretch of 300%. (For a mathematical explanation of prestretch see Equation 2-3).

Tension-to-load can be used in tandem with prestretching to force the film to prestretch to an ever higher percentage. Tension-to-load occurs when the film is pulled out of the carriage due to the speed of the turntable being higher than the speed of the output prestretch roller (see Section 2.2 for explanation of machine parts and processes). Note that the higher the tension to load, the more likely necking will occur (Provincial Paper & Packaging Ltd., 2008) meaning there will be more film required to wrap the unit load with the same desired overlap. The methods to quantify the amount of stretch imparted on the film are described in Section 2.2.

$$Percent\ Stretch = \frac{\Delta\ell - \ell}{\ell}$$ **Equation 2-3**

Where:

Percent Stretch = The percent that the films is stretched during the application process

$\Delta\ell$ = Legnth of film after stretching

ℓ = Legnth of film before Stretching

Figure 4 Where prestretching occurs in the application process

Elastic Recovery is one of the basic material properties that makes stretch wrap effective for unit load containment. Once the film is stretched it will try to return to its lowest energy state. In doing so, this increases the amount of crystallinity within the film, over time, as the polymer chains start to align. Higher percent stretch (therefore crystallinity) will make the film a more rigid material and be less likely to recover its lost form. It is this property that allows a stretch film to retain its holding force during load shifting and settling during transport (Downey, et al., 2001). Recovery of the film starts as soon as a constant load is applied to a sample and can continue from hours to years and will be more pronounced in less crystalline structures (Peacock, 2000).

Containment force of a given film is based on its elastic recovery. Containment force is described as the "hugging" force of a film when applied to the unit load. This value is measured in pounds or Newtons (N). Higher elastic recovery leads to a higher containment force. To increase the force beyond one layer of film, an infinite number of wrap patterns could be applied to double and triple the properties of the film. Containment force is a function of wrap pattern, MD retainment force, CD retainment force, elasticity, holding force and elastic recovery in both CD and MD and possibly tack. ASTM 4649-03 refers to this value as film force. In this paper, the term used will be Containment Force (ASTM, 2003a). The

surface tension of the film is closely tied to containment force and is defined as the amount of tautness, across the surface of the film, from one edge of the unit load to the other.

Cling is the ability of a film to stick to itself (ITW Mima Packaging Systems, 2009). This is the property that prevents the film from peeling off the unit load (Tailing). This can be a problem when a unit load is traveling down a conveyor belt in a warehouse (film can get stuck) or traveling down the road in the back of a truck during transit (unit load can fall apart). Adding tackifiers (a.k.a. cling bonding agent) will make the film smooth and glossy, allowing for a greater film to film contact area (Downey, et al., 2001). It is this property that allows multiple layers of wrap to act as a single entity when applied to a unit load.

The tackifier most commonly used is Polyisobutylene (PIB). This polymer is injected into the raw stock and extruded with the film creation. The PIB will not migrate to the surface until the film is heat cured for a certain amount of time. There are three general applications of cling in stretch film, none, one sided and two sided. Each name explains where the cling is located on the film surface. However, PIB does have some problems with enabling the bloom of the tackifier onto the surface of the film which can be further complicated in high temperature environments (Jackson, 2006-2007).

There are many other material properties that can be added or changed depending on customer request including ultraviolet inhibitors and vapor corrosion inhibitors (Wainer, 2002). ASTM D 4649-03 (ASTM, 2003b)lists further details about stretch wrap and key properties influencing its performance.

2.3.5 Temperature

The tensile properties of polyethylene are temperature dependant. In general, as the temperature increases, the chains become more fluid as the polymer matrix starts to become more fluid. Conversely, the chains become more rigid in colder temperatures. An in-depth explanation of temperature effects can be found in Brown's Handbook of Polymer Testing (Brown, 1999) and Peacock's Handbook of Polyethylene (Peacock, 2000).

2.4 Stretch Film Evaluation Methods

This section describes the different methods to evaluate how stretch film has been applied to a unit load.

2.4.1 ASTM D 4649-03

The primary section entitled ASTM D 4649-03 (ASTM, 2003b) *Standard guide for Selection and Use of Stretch Wrap Films* is a collection of terminology and test methods that are typical in the process of selecting a stretch wrap to use. Within its pages there is no method presented on how to predict containment force of applied film given specific film properties in a laboratory setting. Further research found no method to evaluate the film in a laboratory that resulted in a potential applied containment force value.

Section A1.10 of this testing procedure outlines two testing methods for measuring the containment force once the material has been applied to a unit load. The first procedure using a pull plate is outlined as follows:

1. Apply the desired film in the desired wrap pattern
2. Cut a 15.2cm (6”) hole 25.4cm (10”) from the top of the unit load and 45.7cm (18”) from the side of the unit load
3. Insert a 15.2cm (6”) diameter plate so that the plate sits completely under the film, flush against the unit load
4. Cut a 2.54cm (1”) hole and insert a ruler
5. Pull the plate 10.1cm (4”)
6. Record the observed force (pounds) required to pull 10.1cm (4”) (ASTM, 2003b)

The second method requires a unit load to be wrapped with the desired film in the desired pattern with a bathroom scale or strain gauge under the wrap. The center of the scale or gauge should be 25.4cm (10”) from the top and 45.7cm (18”) in from the side. The device should record more than just the max data as the amount of force a given film can exert changes over time. The data should be recorded in pounds (ASTM, 2003a).

2.4.2 ASTM D 5459–01

ASTM D 5459 – 01 *Standard Test Method for Machine Direction Elastic Recovery and Permanent Deformation and Stress Retention of Stretch Wrap Film* is the current standard to identify and measure the performance of stretch wrap. The test method calls for a sample long enough to provide for an initial grip separation of 5 inches and a sample width of 1 inch. The strain rate is 12.7cm (5”)/minute to a total extension of 15, 50, 100, 150, or 200%.

The method calls for an initial extension of one of the previously mentioned amounts to create an initial force deflection curve at which point the sample is held for 60 seconds or 24 hours to allow the film to recover. After the allotted time, the sample is then retracted to a zero force level. The sample is then given 180 seconds to rest and then the process is repeated. Using the force and extension displacements permanent deformation, elastic recovery and stress retention can be calculated (ASTM, 2007).

The testing profile described above is commonly known as a hysteresis test. These tests have been used in dynamic loading situations for structural application for many years on a wide variety of materials including wood, cement and steel I-beams (Jozef Bodig, 1993). How this testing procedure emulates the process of applying stretch film on a unit load and then put the unit load into a supply chain that exposes the load to a series of shocks and vibrations should be scientifically questioned. Future research could look at stretch film after it has been applied to a unit load, essentially modifying the testing procedure to properly emulate the use of stretch film.

2.4.3 ASTM D 5458-95

ASTM D 5458-95 Standard Test Method for Peel Cling of Stretch Wrap Film is the standard evaluation for how to quantify the cling between two layers of unstretched or prestretched film. The standard fixture requires a large piece of film to be applied to a flat surface. A smaller piece of film is then pressed onto the larger piece of film. The force required to pull the smaller piece of film is recorded as the cling

strength of the film. Prestretched film can be used in this process but ensuring the film is prestretched the same amount without relaxation between prestretching and testing is a challenge (ASTM, 2003b).

2.4.4 ASTM D 882 -09a

ASTM D882 -09a Standard Test Methods for Tensile Properties of Thin Plastic Sheeting is the current testing method to evaluate the tensile properties of all thin plastics. The test method calls for a test specimen of any length but that has a width between .5cm (.2") and 2.54cm (1"). The speed of the test is determined by multiplying the initial strain rate times the initial grip separation. The testing profile calls for a simple elongation of the specimen until all of the desired data has been collected (ASTM, 2009).

2.4.5 Evaluating containment force using non-ASTM methods

ASTM D 4649 (ASTM, 2003b) states that the containment force should be evaluated 45.7cm (18") down and 25.4cm (10") over from the top corner of the side of a unit load that is 121.9cm (48") across. However, the location for containment force evaluation changes depending on the sales person or company. Some follow the ASTM specification. Others have moved the evaluation location point to 25.4cm (10") down and 25.4cm (10") over or to the middle of the unit load. The distance pulled is also changed per user, some companies pull the film out between 2.54cm (1") to7.62cm (3").

The snap back measurement is an informal film evaluation method that is used to measure the amount of pressure a stretch film applies to a unit load. Once the film has been applied to the unit load, the film is cut off the unit load in one vertical swipe. The film is then pulled off the unit load by the evaluators and reapplied to the unit load. The distance between the edges of the film is measured and recorded. If one film has a larger snap back gap than the other, then that film was applying more inward force to the unit load (Jackson, 2006-2007).

The packaging broker Group O sells a patented device used to evaluate containment force. The device starts out at about 6 inches long and 1 inch wide. Once the device is under the film, a second arm is swiveled out from underneath the original arm to create a 25.4cm (10") long 2.54"(1") wide evaluation surface. This evaluation surface is then pulled out from the unit load four inches (GroupO, 2012).

Lantech (Lantech, 2011) has a different patented method of evaluating containment force. The CTF-5 is a measurement tool that uses a thin measurement chain attached to a force measurement device. This tool is employed by placing the chain at the corner of the unit load and positioning the hand held scale lever at the opposite end of the measuring chain. Once this has been accomplished, the "10 inch piercing finger" is placed behind the stretch film from the top edge of the unit load, leaving the "fulcrum finger" outside of the stretch film. The apparatus is then rotated to "kiss" the film so that the indicator foot is flat against the unit load and the indicator line is perpendicular to the unit load. The operator engages the scale when this is achieved and records the displayed containment force. (Lantech, 2011).

According to common industry practice, the tension to load (wrap force) that a stretch wrap machine applies the film can be used to calculate the total containment force by simply multiplying the tension to load times the number of wraps (Patrick Lancaster, 1993). The method of measuring the force can be applied to any point within the unit load. However, this method does not take into consideration any

material property and assumes that all stretch film has a uniform and constant spring coefficient when applied to the unit load.

2.4.6 The Center for Unit Load Design

The Center for Unit Load Design at Virginia Tech has been on the forefront of research on pallets and unit load behavior in the material handling stream for 40 years. The center employs systems based design approaches to solving unit load and material handling issues. They have a full testing laboratory where contract testing, pallet and unit load research, and students all work together to learn how to improve a given material handling system.

It was at the Center for Unit Load Design that research by White focused on whether or not stretch wrapping the pallet to the unit load had an effect on unit load stability. He determined that wrapping around the pallet provided a significant stability improvement compared to not overlapping the pallet (White, 2008).

In another study, Rotondo compared two different gauges of stretch wrap, two different unit load wrapping patterns and two corrugated stacking patterns. The results of this study indicated that 20.3µ (80ga) stretch wrap allowed less displacement than 15.2µ (60ga) during the horizontal impact test and that three 100% overlapping layers of stretch wrap are more effective than three 50% overlapping layers (Rotondo, 2006).

Bisha assessed the effectiveness of different unit load stabilizers given a standard unit load. He found that strapping was the most effective unit load stabilizer during vibration testing and that stretch hooding was the most effective load stabilizer during impact testing. During both of these tests he observed that displacement was generally larger in the top of the unit load than the bottom. He also noted that evaluating container displacement with either the average displacement or the average maximum displacement offered no advantage over the other (Bisha, 2008). Note that with conversation with many of the customers of the Center for Unit Load design, there is a common industry belief that the tighter a unit load was wrapped, the less load shift will occur.

2.5 Summary

Stretch film is manufactured in two methods, the cast and blown method. The film used for application by machine is primarily cast film. This is the process of extruding the desired formulation of a film sheeting die which can handle multiple layers of film. The sheet of film is then stretched using a Machine Direction Orientation process in which can be applied in either direction, however, mostly applied in the machine direction. The film is then cut down into the desired width (usually 50.7cm (20”)) and sold to individual customers for application.

Once the film reaches its end user, the film is used in a myriad of different stretch wrapping machines. All of these different machines conduct the same basic function which include, prestretching and applying the film to an object or series of objects that are to be transported as one unit. This unit can be put up in a storage rack or shipped around the world. The handling the unit will see during it’s life will determine how the unit is wrapped including how much film is used.

It is the stretching of the film beyond its yield point in multiple stages which helps to orient the polymer chains within the film. This stretching increases the crystallinity of the film, making the film stiffer. As with any matter, the polymer chains want to rest at its lowest energy state, therefore after stretching the film it will try to return to its original state. Due to the change in crystallinity and the film application to a unit, the film's lowest possible energy state has changed. It is the influence of this change on the film's material properties that this research will investigate. This change process means that when the film is first applied, it is applying the highest amount of inward containment force possible to the unit load. Over time this containment force will decrease as the amount of crystallinity in the film increases (hence increasing stiffness).

Understanding of a film's properties and how they change over time can be used to understand how stretch film responds to holding a unit together during shipping. After the film has been stretched and applied to a unit load the film starts to recover, increasing rigidity and decreasing inward force over time.

Therefore, a critical question is which property is more important, stiffness or inward force? The answer depends on the unit load system in question. An extremely stiff film can be thought of as a box that has been put over the unit. It will hold the unit in place but will exert no inward force onto the unit. The inward force will help to keep the unit very tightly together through the light shocks and vibrations but will do very little against the large shocks that are common within the global supply chain (speed bumps to rail car coupling). The purpose of this research is to gain knowledge about film material properties beyond their yield point to better understand their performance in applying containment forces to unit loads.

3 Materials and Methods

This section outlines the materials and methods used to achieve the objectives stated in Section 1.3. This Section includes discussion of the proposed methods to evaluate stretch film on a tensile testing machine in addition to a discussion of the methods used to assess film properties as applied to a test frame. The latter includes a discussion of the stretch wrap machine and the stretch film used, the experimental test frame used and the test methods used to evaluate the applied stretch film. A theoretical comparison of the different evaluation methods is found in Section 3.3. Note that all of the film evaluated during these experiments was kept at room temperature and out of the direct or indirect sun light.

As described in Section 2.1.1, stretch film is applied to a unit load to help keep it together during transit. The film has two properties that enable it to help maintain unit load stability. The first is its ability to apply a compressive force on the unit load, commonly known as containment force. Second is the films ability to resist movement once in motion. This property is the stiffness, which is relative to the amount of force the film can apply per the internal movement of the different components of the unit load.

Per the discussion in Section 2.4.1, these two film properties have often been combined and confused. This section outlines distinctive methodologies to quantify the applied film stiffness (s_a) and the containment force (c_f) that a film can apply to a unit load.

3.1 Measuring tensile film stiffness s_b

The objective was to characterize the elastic properties of stretch film through tensile testing. The film stiffness was measured on a tensile testing machine using two different sample preparation methods. One method represented the current ASTM standard and one that was a modified version of that standard. Due to the inherent nature of polymer based tensile testing discussed in Section 2, a functional difference was expected between the resultant stiffness values of the two sample preparation methods.

3.1.1 Theoretical interaction of test methods

The measured film stiffness (termed Bisha Stiffness, s_b) was developed for the purpose of predicting the pulling, or extension, of the film off the unit load as the film is being evaluated for s_a per ASTM D 4649. The testing profile that was used is shown in Figure 5. The initial extension was calculated from the actual prestretch of the film (denoted in blue in Figure 5) as applied to the test frame. The film was then held for one hour (green) allowing for the film to recover and stiffen per preliminary test findings (Section 8.4). The film was then extended again at the same speed (purple) to simulate the evaluation of s_a. The slope of this line is called the Bisha Stiffness (s_b), while the initial force of the s_b test is denoted by f_i. The f_i force is hypothesized to correlate with the amount of containment force (f_c) or film tension (f_t) that a film possesses after being wrapped around a unit load. For more on containment force and film tension see Section 3.2. Note that the longer the green line recovers (falls), the less film tension f_i is

theoretically available to be applied on to the unit load. On the other hand, the s_b value captures the film stiffness that is theoretically applied to the unit load.

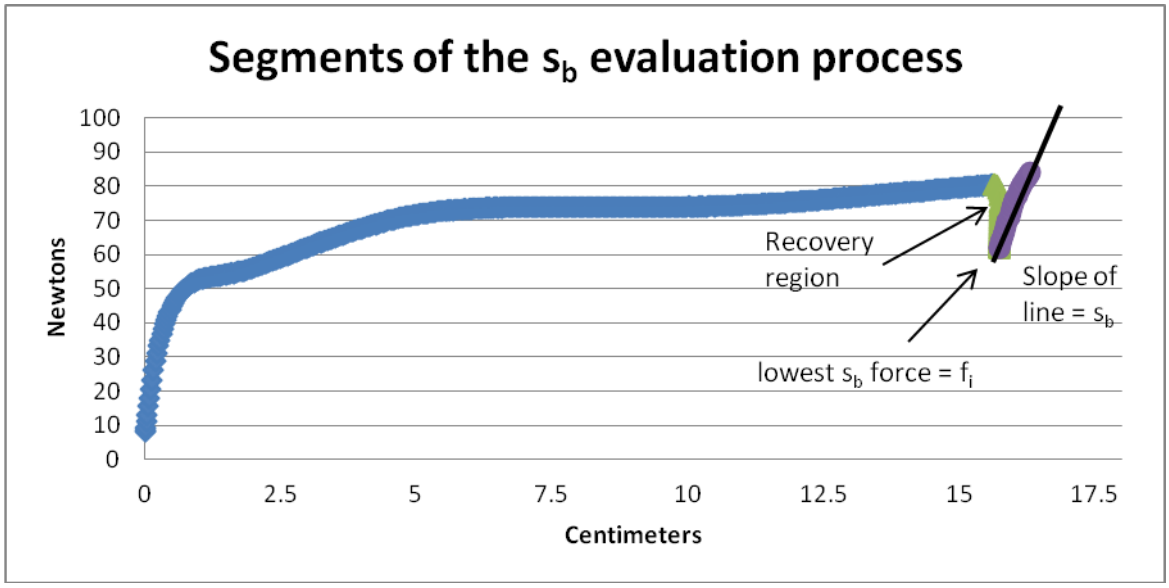

Figure 5 Different segments of the proposed tensile test profile identified

There are several observations that are made from the shape of this curve. First, it characterizes how the film behaves during the prestretching process. In Section 2.3.2 the critical points of this curve were discussed, including the identification of the yield stress, strain hardening and linear elastic region. The shape of the different regions indicates the initial properties (sample size, gauge, and stiffness ect.) and how those properties change as the film is extended (rate dependent). The recovery region of Figure 5 indicates how well the film can retain its tensile force overtime and its stiffness response. The shape of the curve, in general terms, can be influenced by many different variables, including film extrusion methodology, chemical formulation and post manufacturing treatment.

The two sample preparation methods used to evaluate the film are the 2.54cm (1") method and the 50.7cm (20") method. The respective s_b and f_i measurements from these tests were called s_{b1} & s_{b20} and f_{i1} & f_{i20}. Because 2.54cm samples are 20 times smaller in width than the 50.7cm samples, they are expected to correlate, however, the exact function of the relationship between the two may be more complex than a simple multiplication factor of 20 due to the other variables not considered in this research. For a further discussion of the differences in the geometry of the samples see Section 3.4. The functions are shown in Equation 3-1 and Equation 3-2.

$$\mathbf{s_{b20}} = f(\mathbf{s_{b1}}) + Error \qquad \textbf{Equation 3-1}$$

$$\mathbf{f_{i20}} = f(\mathbf{f_{i1}}) + Error \qquad \textbf{Equation 3-2}$$

Where:

s_{b20} = Bisha stiffness measured using the 50.7cm (20”) sample preparation technique

s_{b1} = Bisha stiffness measured using the 2.54cm (1”) sample preparation technique

f_{i20} = Initial force at the beginning of the s_{b20} evaluation

f_{i1} = Initial force at the beginning of the s_{b1} evaluation

3.1.2 Measuring s_b & f_i

ASTM D 5459-95 calls for a 2.5cm (1”) wide sample that is 12.7cm (5”) inches long, although, the film in its application is 43.1cm to 50.8cm (17” to 20”) wide and infinitely long. Note that the true application width of the film onto a unit load was observed to be between 43.5cm (17.128”) and 45cm (17.75”) wide due to necking during application. How film necking impacts the forces measured during the s_b tests is an important factor in explaining the additional functional adjustments and impacts on Equation 3-1 and Equation 3-2. The necking phenomena was discussed in Section 2.3.2 and will be further discussed in the results of Section 3.4.

The goal of the tensile testing procedure was to create a sample and testing method that allowed for an accurate and precise representation of what was occurring as the film was applied to the unit load. As such, four different sample preparation techniques were studied and compared, the ASTM 5459 standard 2.5 cm (1”) wide sample, a 50.8cm (20”) sample, a Tube sample and a Roll sample. These four sample preparations methods were investigated because preliminary results indicated the 2.5 cm (1”) samples did not convey any information that was transferable to how the film was applied to the unit load (despite the ASTM standard requiring the sample size). The creation and evaluation methods of the 2.5cm and 50.7cm samples will be discussed in the following section. The Tube and the Roll sample preparations were not used in the final experimental model. However, they are discussed in Section 8.3 (Appendix) as alternative sample preparation methods that may be useful for future research.

s_{b1} Sample Preparation

The film was pulled off of the roll and stuck to a piece of glass with no wrinkles and minimal bubbles under the film. One side of a small framing square was then held parallel to one side of the glass. A 2.5cm (1”) wide razor sample cutter was then used to cut a sample of the film in the machine direction by running the sample cutter along the side of the small framing square. A picture of the materials used is shown in Figure 6.

Figure 6 Materials used to cut a s_{b1} sample

s_{b20} Sample Preparation:

Wider grips than what are commercially available were created out of wood and hand stretch film to evaluate the stiffness of the film at a 50.7cm width. A single clamp consisted of two 55.8cm x 7.6cm x 2.5cm (22”x3”x1”) southern yellow pine boards that were wrapped in 20.3µ (80ga) Sigma hand wrap. The hand wrap prevented the test sample from ripping on the rough wood edge and the tackiness of the stretch film held the film sample in place.

A wooden jig was created that allowed the wooden clamps to be spaced 2.5cm (5”) apart (same as ASTM 5459-95). The film sample was taken off the film roll and placed over the half of the clamps that were in the jig. The sample was then aligned with no folds and the other half of the clamps were placed on top. To hold the clamps together during assembly two drywall screws held the clamps together on the ends of the clamps. At this point the sample was cut from the film web and four .63cm (.25”) bolts were then used to hold the sample together. They were spaced at 5.0cm (2”) and 20.3cm (8”) in from either end. The bolts went through each wooden clamp and were tightened to 542.3n/cm (4 foot/pounds) of torque. A picture of the test setup can be seen in Figure 7.

Figure 7 Testing set up for s_{b20}

The tensile testing machine used in evaluating all s_b samples was an MTS 10 G/L with a 225 pound load cell. In accordance with ASTM D5459 both the 2.5cm (1”) and the 50.7cm (20”) samples measured 12.7cm (5”) between grips when testing was started. The grips used in tensile testing the s_{b1} samples were MTS Advantage Grips shown in Figure 8.

The clamps used in the evaluation of the s_{b20} samples were then placed into the MTS machine via two stabilizing bolts in the bottom clamp and one stabilizing bolt in the top clamp. Two wedges were then used to solidify the top clamp in between the top of the clamp and the metal assembly that held the single bolt (see Figure 7).

Figure 8 Grips used to evaluate s_{b1}

The estimation of the Bisha Stiffness was calculated from the force/displacement data within 1st cm of the secondary extension of the film. This extension was 7.8% of the original sample size which was the same extension during the evaluation of the applied film on the test frame. For more on the calculation of the extension of the film on the test frame see Equation 3-33.

3.1.3 Limitations of s_b & f_i

There were several limitations to the grips used in evaluating the s_{b1} samples. The rubber grips that actually held the film sample were prone to slipping on the metal backing under high force or under moderate force over extended periods of time. The slipping can affect test results by reducing the measured force.

When clamping the samples together, the interaction of the rubber grips causes the film sample to be taken up with in the grips. When closing the first grip this interaction is not an issue. However, closing the second grip can impart an extra stretching force on the film which may affect test results. The grips themselves are held in by cotter pins that can rotate slightly. This rotation is not an issue when closing the first set of grips. When closing the second set of grips, the top of the jaws close first and the sample can be pulled up before the initiation of the test, possibly affecting test results.

All of these errors were mitigated by consistency in the testing process for each test. For each test the top jaws were closed first so that the sample could hang free, allowing for good alignment with the bottom jaws. Each sample was tightened as much as possible to reduce slipping of the samples. The forces during the s_{b1} tests were not high enough to force the pads on the grips to slide.

In the creation of the s_{b1} samples, it was possible that the edges of the samples were not perfectly straight or contained small nicks due to human error.

According to the load cell literature, the load cell used was outside of its useable range to evaluate the s_{b1} samples. This deviation from standard means that the values recorded may not be as accurate as values that were recorded inside the useable range. This may not be a critical point because the s_{b1} is a stiffness value and therefore a slope of a line. The exact values of the data points on the line are not critical to this research because how the values fit into a linear regression is the focus of the experiment. Even with an initial bias of the load cell, the stiffness of the film is still able to be assessed properly.

With regard to s_{b20} samples, the way the clamps were attached to the tensile testing machine could have been improved. The bottom jaw was not held in place, but instead could move, allowing for one side of the material to stretch more than the other. This movement never appeared to be a large issue because after one side had extended into its strain hardening region the other would be weaker and therefore more susceptible to stretch allowing for equal stretch by the time of full extension.

In addition, the top jaw was held level with two opposing wedges. It is possible that the top jaw was not perfectly level in each test. In future systems, optimum control of grip fixturing can help minimize testing variation.

3.2 Modeling Stiffness of the Applied Film

The objective of this section is to evaluate film behavior in terms of stiffness and containment force when applied to a unit load. Specifically, the stiffness (s_a) and the containment force (f_c) of applied film will be evaluated. As stated in Section 1, stretch film applies a compressive force to help hold loose items together as they are assembled for shipping. This compressive force will be evaluated as a Hookean Spring (Section 2.3.2) and the K value will be replaced with film stiffness(s) value (N/cm). A generalized visualization of the two methods to model applied film stiffness of a wrap pattern and their representative spring components are shown in Figure 9.

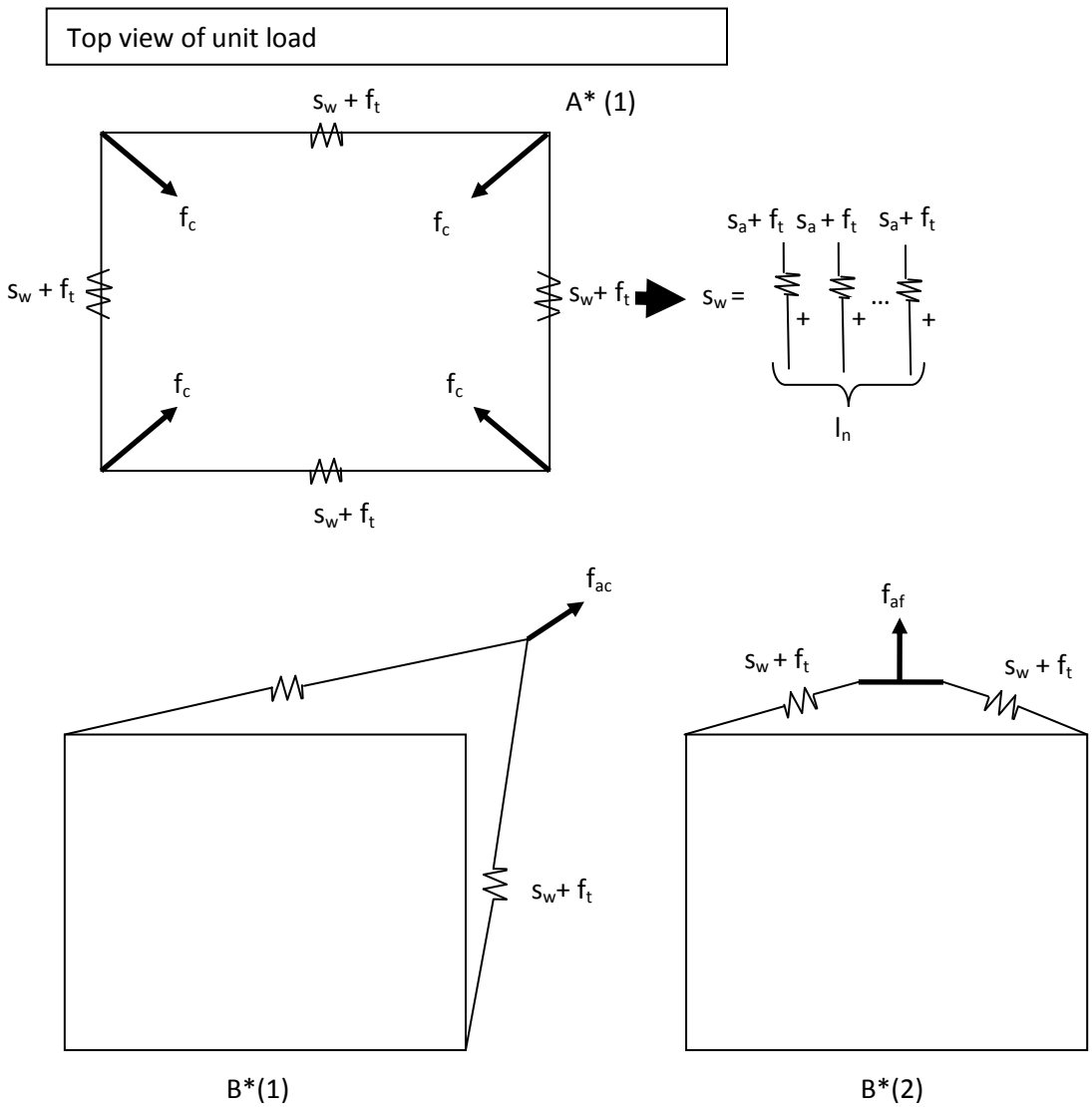

Figure 9 Spring diagrams identifying the general theory of evaluating the film stiffness of a given wrap pattern (s_w)

Where:

s_a = Stiffness of Applied film (N/cm). Describes the spring stiffness of any single layer of film applied to a unit load or test frame, calculated by dividing the f_{ac} by the x_{ac}

f_{af} = Force resisted by the applied film measured on the Face (N). Describes the resistance force of the film applied to a unit load or test frame that has been measured using the Pull Plate method described ASTM D 4649 and in Section 2.4.1

f_{ac} = Force resisted by the applied film measured on the Corner (N). Describes the resistance force of the film applied to a unit load or test frame that has been measured using the bar method (See Section 3.2.6 for methods)

f_c = Containment Force (N). Describes the amount of inward force that a film applies to a corner of a unit load or test frame

f_t = Tension Force (N). Describes the amount of tension in the film on a given side of the unit load or test frame

s_w = Stiffness of Wrap pattern (N/cm). Describes the measured stiffness of any wrap pattern on the corner of a unit load

l_n = Number of Layers (#). Describes the number of layers of film applied to a unit load or test frame

Therefore, the basic relationships identified in Figure 9 are:

$$\mathbf{f_{ac}} = f(\mathbf{s_w}, \mathbf{f_c}) \qquad \textbf{Equation 3-3}$$

$$\mathbf{f_{af}} = f(\mathbf{s_w}, \mathbf{f_c}) \qquad \textbf{Equation 3-4}$$

$$\mathbf{s_w} = \mathbf{s_a} * \mathbf{l_n} \qquad \textbf{Equation 3-5}$$

The lengths and extensions of the individual spring components during the f_a tests, labeled B*(1) and B*(2) in Figure 9, varied. When the film was pulled out 5.07cm (2”), the change in length of the spring components depended on the test method utilized. The differentiation between these rates is shown in Figure 10. The differential between the different rates of extension is shown in Table 3. These values were calculated assuming 86.3cm (34”) and 106.6cm (42”) for the sides of the test frame. These values are used because the film that is coming in contact with the 15.2cm (6”) pull pate is not being evaluated for stiffness (see Section 2.4.1 for more on the pull plate or 3.2.2 for the test frame).

Note that in Figure 10, the extension during the f_{ac} testing method is initially higher and increases at a significantly higher rate than for the f_{af} test method. In addition, the differentiation between the sides appears to be minimal. But when looking at the differential between each set of lines in Table 3, the sides of the f_{af} test method are dividing twice as fast as the sides in the f_{ac} test method. The divergence between the different extension rates and the different sides of the test frame were accounted for when comparing the calculated s_a of the material.

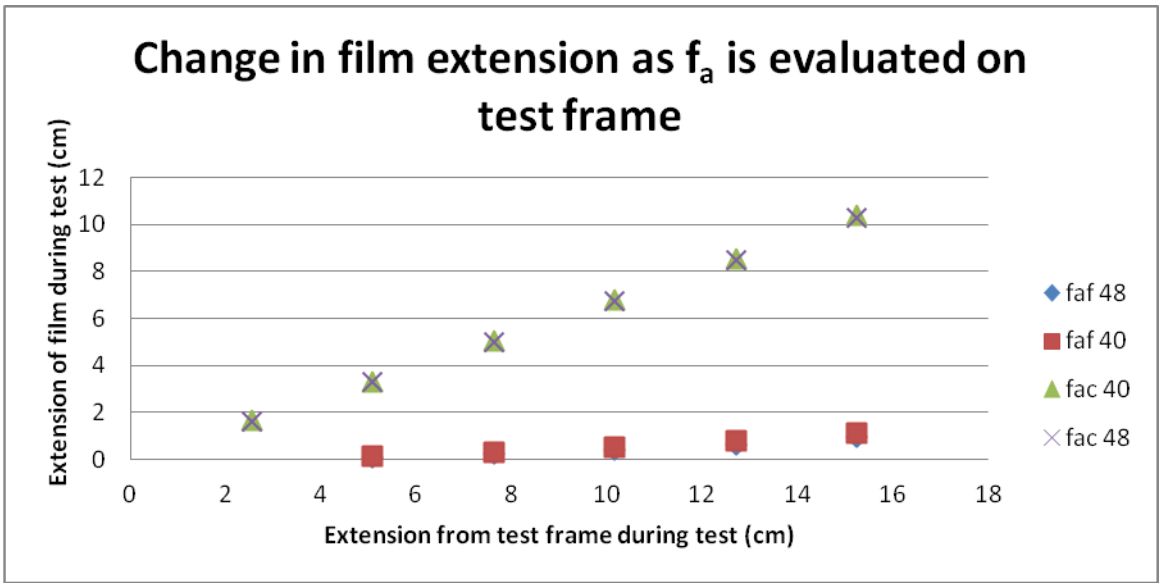

Figure 10 The different methods of evaluating f_a and their respective film extensions during the test are compared.

Table 3 The differential between the two sides of evaluation for the methods of evaluating f_a.

extension from test frame (cm)	f_{af}	f_{ac}
5.08	0.021	0.012
7.62	0.047	0.026
10.16	0.084	0.044
12.70	0.131	0.067
15.24	0.188	0.094

3.2.1 Theoretical Interaction of Testing Methods for s_a

The two methods used to model Stiffness of Applied film (s_a) and their theoretical interactions are described in this section. As stated in Section 1, stretch film helps to hold loose items together after they are assembled for shipping. The stretch film achieves this by utilizing two different applied film properties. The first is the amount of force the film applied on to a unit load, defined as Containment Force (f_c) measured in Newtons (N). The second is the amount of stiffness the applied (s_w for multiple wrap layers or s_a if $l_n = 1$) film possesses. The film stiffness is what prevents the assembled goods from shifting during transport. This stiffness is measured as a Hookean Spring (Section 2.3.2) where the K value was replaced with a film stiffness (s_a) value (N/cm).

The methods used to estimate s_a involve measuring resistance forces for vector f_{ac} and for the vector f_{af}. The vector f_{ac} was measured using the bar method described in Section 3.2.6 while the vector f_{af} was calculated using the method described in Section 3.2.4. The following formulations describe the theory and functional relationships for the two modeling methods. In these formulations it was assumed that one layer of film was applied ($l_n = 1$).

The vector f_{ac} was measured by applying 1 layer of parallel stretch film to a test frame and pulling the film off the corner of the test frame using a bar that was longer than the web was wide. A breakdown of the forces when evaluating the film using the s_a is shown in Figure 11. An assumption was made that the film was not able to creep around the corners of the test frame during the test.

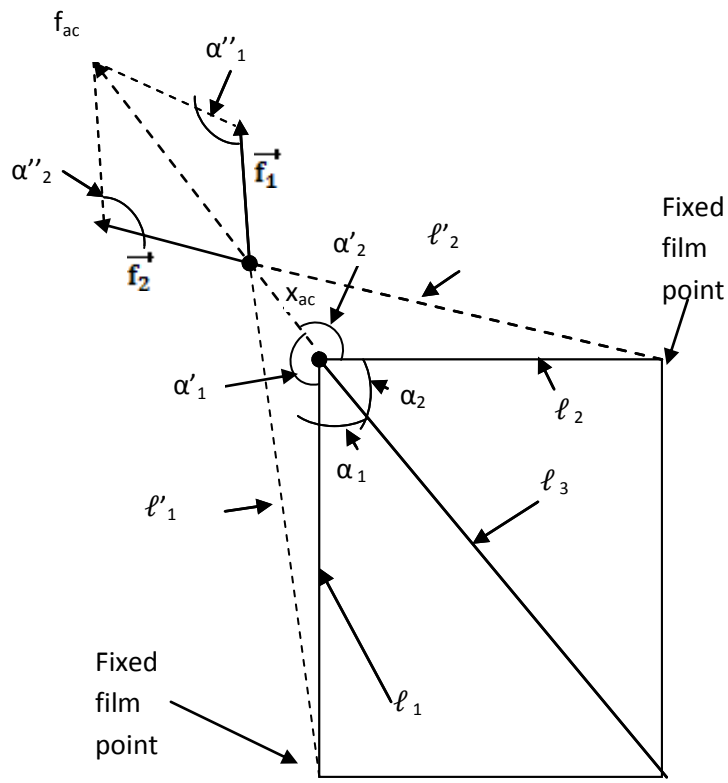

Figure 11 Top view of the component breakdown of forces associated with modeling f_{ac}

Figure 11 identifies vector f_{ac} as a resultant of vector f_1 and vector f_2 as shown in Equation 3-6, and assumes that vector f_1 is a function of its respective film stiffness and that assumes that it was pulled off the corner at the stated angle.

$$\vec{f_{ac}} = \vec{f_1} + \vec{f_2} \qquad \textbf{Equation 3-6}$$

Where:

f_1 = the force component of f_{ac} that corresponds to the long side of the test frame

f_2 = the force component of f_{ac} that corresponds to the short side of the test frame

Specifically the magnitude of vector f_{ac} was calculated by its Pythagorean relationship with vector f_1 and vector f_2 shown in Equation 3-7.

$$f_{ac} = \sqrt{f_1^2 + f_2^2} \qquad \textbf{Equation 3-7}$$

The magnitude of each of the forces was defined as either a relationship with their respective α or as a relationship between the s_{ac} and the change in ℓ during the evaluation. These relationships are defined in Equation 3-8 and Equation 3-9.

$$\mathbf{f_1 = \sin\alpha_1 * f_{ac} = s_a(\ell'_1 - \ell_1)} \qquad \textbf{Equation 3-8}$$

$$\mathbf{f_2 = \sin\alpha_2 * f_{ac} = s_a(\ell'_2 - \ell_2)} \qquad \textbf{Equation 3-9}$$

Where:

α_1 = the inside angle between the direction of pull for f_{ac} and the long side of the test frame

α_2 = the inside angle between the direction of pull for f_{ac} and the long side of the test frame

ℓ_1 = the length of the long side of the test frame

ℓ'_1 = the length of the film on the long side of the test frame at any given point during s_{ac} evaluation

ℓ_2 = the length of the short side of the test frame

ℓ'_2 = the length of the film on the short side of the test frame at any given point during s_{ac} evaluation

Note that the ℓ'_1 and ℓ'_2 components in Equation 3-8 and Equation 3-9 are calculated by using the following method which was based on the law of cosine.

$$\mathbf{\ell'_1 = \sqrt{\ell_1^2 + x_{ac}^2 - 2 * \ell_1 * x_{ac} * \cos(\alpha''_1)}} \qquad \textbf{Equation 3-10}$$

$$\mathbf{\ell'_2 = \sqrt{\ell_2^2 + x_{ac}^2 - 2 * \ell_2 * x_{ac} * \cos(\alpha''_2)}} \qquad \textbf{Equation 3-11}$$

Where:

x_{ac} = distance the applied film was pulled during the s_{ac} test method

α''_1 = the distorted angle between the direction of pull for f_{ac} and f_2 (note that $\alpha''_1 = 180-\alpha'_1$)

α''_2 = the transformed angle between the direction of pull for f_{ac} and f_2 (note that $\alpha''_2 = 180 - \alpha'_2$)

Per Figure 11, α''_1 and α''_2 are non-linear functions of x_{ac}. Since the corner stiffness s_{ac} is defined as the composite spring resistance the instant that x_{ac} is displaced, it was assumed that $\alpha''_1 \approx \alpha'_1$ and $\alpha''_2 \approx \alpha'_2$ for small changes in x_{ac}. Using this assumption, Equation 3-10 and Equation 3-11 can be simplified to:

$$\mathbf{\ell'_1 = \sqrt{\ell_1^2 + x_{ac}^2 - 2 * \ell_1 * x_{ac} * \cos(\alpha'_1)}} \qquad \textbf{Equation 3-12}$$

$$\ell_2' = \sqrt{\ell_2^2 + x_{ac}^2 - 2 * \ell_2 * x_{ac} * \cos(\alpha_2')}$$ **Equation 3-13**

Where:

α'_1 = the outside angle between the direction of pull for f_{ac} and the long side of the test frame (note that $\alpha'_1 = 180 - \alpha_1$)

α'_2 = the outside angle between the direction of pull for f_{ac} and the long side of the test frame (note that $\alpha'_2 = 180 - \alpha_2$)

The change in ℓ in Equation 3-8 and Equation 3-9 was replaced with the term $\Delta\ell$ to further simplify the equations into a simple Hookean form.

$$f_1 = s_a \Delta\ell_1$$ **Equation 3-14**

$$f_2 = s_a \Delta\ell_2$$ **Equation 3-15**

Therefore by substituting Equation 3-14 and Equation 3-15 into Equation 3-7 the resultant form is Equation 3-16 and further simplified into Equation 3-17.

$$f_{ac} = \sqrt{s_a^2 \Delta\ell_1^2 + s_a^2 \ \Delta\ell_2^2}$$ **Equation 3-16**

$$f_{ac} = \sqrt{s_a^2 (\Delta\ell_1^2 + \Delta\ell_2^2)}$$ **Equation 3-17**

The simplified term in Equation 3-17 is used to calculate the distance x_{ac} shown in Equation 3-18.

$$x_{ac} = \sqrt{\Delta\ell_1^2 + \Delta\ell_2^2}$$ **Equation 3-18**

Therefore x_{ac} was substituted into Equation 3-17 to yield a simple Hookean form for the prediction of f_{ac} shown in Equation 3-19.

$$f_{ac} = s_a x_{ac}$$ **Equation 3-19**

Per diagram A* in Figure 9 the force exerted on the corner of the unit load is termed vector f_c. To calculate the force required to pull out on the stretch film, the vector f_c is an adjustment as shown in Equation 3-20. The Containment Force (f_c) is the y intercept when f_{ac} is plotted against x_{ac}.

$$\mathbf{f_{ac} = (s_a * x_{ac} + f_c) + error} \qquad \textbf{Equation 3-20}$$

To estimate the stiffness of the applied film, s_a, the model in Equation 3-19 can be used from experimental load-displacement data in a corner test. (see Section 5). The final linear model, Equation 3-20, introduces the residual containment force f_c that exists on the test frame giving the total f_{ac} when the film is extended off the corner. This model implies that once the film stiffness, s_a, is known, then the amount of force that is applied to the corner of a unit load can be predicted when the contents are shifted x distance in either direction. A 95% confidence interval was used to describe the model error.

An additional benefit of using this method was that it allows for the direct quantification of containment force (f_c) on the corner of the test frame. When the data was collected during the f_{ac} test and was plotted against the x_{ac}, the y intercept was a representation of the force the single layer of film exerted on the test frame. This value has additive implications when building the performance of a wrap pattern as discussed in Equation 3-28.

Note that the simplified model in Equation 3-20 assumes that the stiffness of the applied film (s_a) is uniform around the entire unit load and that an orthogonal geometry exists at the instant the corner is pulled. However, in the actual experiment, x_{ac} had to be extended a distance of 3.8cm (1.5”) to estimate the stiffness. Therefore, this assumption was tested within the length range of the experimental corner testing and it was found that errors were less than 5 percent, very small relative to other errors dealing with the uniformity of film application to the unit load (discussed in Section 2.2.3). As such it was found that the simplified model was appropriate to determine s_a. Finally, it is important to note that in future research using Equation 3-20 above in modeling containment forces, the errors associated with large displacements x_{ac} may require more precise geometric effects.

The second method of evaluating the s_a was the f_{af} method which is very similar to the current ASTM D 4649 standard. This was used to measure film stiffness because it is a simple field test that only needs slight modification for testing. If the f_{af} method can be correlated to the f_{ac} method, the f_{af} method may still have some validity in measuring applied film properties. The f_{af} method was measured by applying 1 layer of parallel stretch film to a test frame and pulling the film off the face of the test frame utilizing the evaluation plate specified in ASTM D 4649. This breakdown of the f_{af} vector is using this method is explained from a vertical view point shown in Figure 12.

The assumption was made that when evaluating f_{af} any side of the unit load was an independent spring system from the other sides, as shown in Figure 9. This meant that the film was not able to slip around the corners of the test frame. Additionally, the film was not fixed on the top and bottom edges of the applied film, leading to the assumption that the f_{af} was not affected the forces that originated from the horizontal edges of the film.

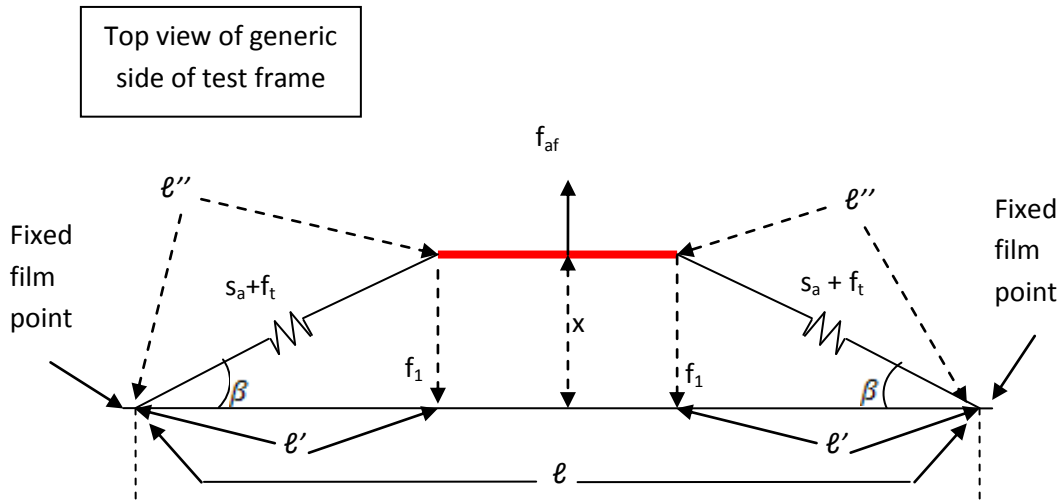

Figure 12 Top view of the component break down with forces associated with modeling f_{af}

The top view of the two dimensional diagram in Figure 12 identifies vector f_{af} as a function of 2x the vector f_1 as shown in Equation 3-21. Note that this diagram assumes that the film is being evaluated in the middle of the side of the test frame allowing for equal environments on either side of the pull plate. If vector f_{af} evaluation were to move to either side, the environment would change allowing for two different systems which would lead to an odd plate evaluation angle. This would make the calculation for f_{af} much more complicated. The environment also changed per the length of the side of the test frame. This will be addressed in Equation 3-22.

$$\mathbf{f_{af} = 2 * f_1 * \sin\beta + f_t}$$ **Equation 3-21**

Where:

f_1 = force component of f_{ac} that is experienced on one side of the pull plate

β = the inside angle between the face of the test frame and the film during f_{af} evaluation

The force f_1 is the primary force acting on the plate in Figure 12. This force is resultant of the s_a and the change in ℓ plus the f_t perpendicular to the evaluation f_{af}. These relationships are defined as Equation 3-22.

$$\mathbf{f_1 = s_a * \Delta\ell + f_t}$$ **Equation 3-22**

The change in length of the film during vector f_{af} test is defined as $\Delta\ell$ and is defined as Equation 3-23.

$$\Delta\ell = \sqrt{\ell'^2 + x^2} - \ell'$$ **Equation 3-23**

Where:

ℓ' = distance on the face of the test frame between the corner and the edge of the pull plate

x = distance the pull plate was pulled upon recording f_{af}

Due to standard trigonometry, α is defined as Equation 3-24.

$$\beta = \text{atan}\left(\frac{x}{\ell'}\right) \qquad \text{Equation 3-24}$$

Equation 3-21 is then rewritten as Equation 3-25

$$f_{af} = 2 * \sin(\beta) * (s_a * \Delta\ell + f_t) \qquad \text{Equation 3-25}$$

Note that Equation 3-25 has two unknowns, the stiffness (s_a) and the containment force (f_t). Therefore Equation 3-25 can be linearized into the form Equation 3-26.

$$\frac{f_{af}}{2 * \sin(\beta)} = (s_a * \Delta\ell + f_t) + \text{error} \qquad \text{Equation 3-26}$$

To estimate the stiffness of the applied film and the amount of initial tension in the film, s_a and f_t, the model in Equation 3-26 can be used from experimental load-displacement data in a pull plate test. This model implies that once s_a and f_t are known, the amount of force that is applied to the contents of the unit load after they have shifted x amount can be predicted. Confidence intervals were used to describe the model error.

Unlike the corner test (f_{ac}) that was previously discussed, the pull plate test (f_{af}) can not directly measure the f_c. However, once the f_t on the individual sides has been calculated, Pythagorean's theorem can be used to calculate the f_c on the corner of the unit load. This value has additive implications when building the performance of a wrap pattern as discussed in Equation 3-29.

It is important to note that in future research using Equation 3-26 in modeling s_a and f_t using the f_{af} method, significant error could be experienced by the deformation of the film as forces increase and the plate is extended from the unit load. If this effect is significant, a functional adjustment may be required to properly predict the s_a and f_c from the f_{af}. This phenomenon is further addressed Section 3.2.5.

In the previous discussions the film's s_a and f_c were calculated using two different methods, the f_{ac} and the f_{af} in Equation 3-20 and Equation 3-26. Both of these equations resulted in linear forms, therefore they are compared using ANCOVA. The general form of an ANCOVA is shown in Equation 3-27.

$$y_{ij} = \mu + \tau_i + \beta(x_{ij} - \bar{x}) + e_{ij} \qquad \text{Equation 3-27}$$

Where:

y_{ij} = Dependant variable

μ = Average of all data analyzed

τ_i = Treatment effect

β = Covariate effect

x_{ij}= Independent variable

x bar = Average for the entire data set

e_{ij} = error for data set

Once the s_a and f_c of a single layer of film has been determined, the stiffness and containment force of a wrap pattern (s_{wp} & f_{wp}) are derived by Equation 3-28 and Equation 3-29.

$$s_{wp} = (s_a * l_n) + \text{Error} \qquad \text{Equation 3-28}$$

$$f_{wp} = (f_c * l_n) + \text{Error} \qquad \text{Equation 3-29}$$

Where:

s_{wp} = stiffness of the wrap pattern

f_{wp} = the amount of force that a wrap patter exerts on the corner of the test frame

l_n = number of layers of stretch film

f_c = the amount of force a single layer of stretch film exerts on the corner of a test frame

s_a = the stiffness of the applied film as determined by either the f_{af} or the f_{ac} test method

Note that Equation 3-29 assumes that the angle of which the film was applied did not cause ℓ to change significantly when applied to a side of the unit load. The angle of the wrap pattern is determined by the speed of the carriage applying the stretch film and the diameter of the unit load being wrapped. If the ℓ did change, the calculations above would have to be recalculated.

The error stated in Equation 3-28 and Equation 3-29 has to do with the error associated with wrapping the test frame in a laboratory environment. An additional error source is the creation and behavior of the unit load being wrapped and its interaction with the stretch film. If during the wrapping of the unit load, the stretch film applies so much force that it compresses/shifts the unit load, changing the $\Delta\ell$, the s_a and f_c could vary drastically.

3.2.2 Building of the test frame that simulates a unit load

The test frame was made of 2x4 lumber and attached to a pallet for ease of movement. The frame had a length of 121.9 cm (48”) a depth of 101.6cm (40”) and a height of 152.4 cm(60”). A stabilization mass of 889.6 Newtons (200 Pounds) was added to the base to prevent the frame from moving during film application. This stabilization mass was centered on the turntable of the stretch wrap machine (details on stretch wrap machine in Section 3.2.3) allowing for similar wrapping conditions on all sides. The critical film contact points were covered in stretch film to prevent slippage of the film around corners

when evaluating the f_a. For a picture of the test frame set up a see Figure 13. The locations where f_{af} was evaluated had a recessed backing allowing the pull plate specified in the annex of ASTM D 4649 -03 to sit flat underneath the stretch film while not touching the film. This allowed for a true zero point when evaluating the film. For a picture of this testing setup see Figure 13. For a f_{af} test simulation see Figure 14.

Figure 13 Test frame used to simulate a unit load

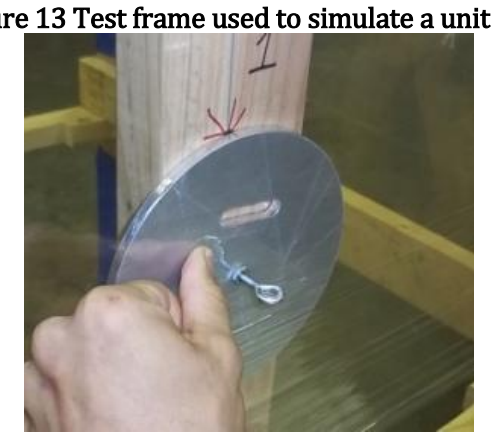

Figure 14 Pull plate sitting flush under the stretch film before f_{af} test

3.2.3 Stretch wrapper description and operation

The stretch wrap machine (Wulftec model number WSML-150-b) that was used in this experiment had two key variables with regard to film application and stiffness, turn table rotation speed and film tension between the unit load and the prestretch carriage. Determining each of these settings is an inexact science, as the knobs on the front of the machine are only labeled with 9 dots. These dots act as reference points for machine settings but do not inform the user exactly what settings are being used.

Rotation speed is adjusted by turning the knob to a specific dot which corresponds to a preset rotational speed that is not known unless properly measured. When the wrap sequence is initiated, the rotational

pull of the unit load that is sitting on the turntable will take up the film as it is forced out of the prestretch carriage.

Film tension is also adjusted on the control panel via the dot series. The two critical parts of film tension are the tension bar (dancer bar) and the output prestretch roller. The tension bar acts as an activation switch for the speed of the prestretch rollers. The farther open the bar is pulled, the faster the rollers will turn. The higher the setting of the film tension knob, the lower the speed of the output rollers.

If the prestretch rollers are rotating slower than the turntable, the film will be applied with additional stiffness (more stretching will occur). If the prestretch rollers are rotating faster than the turntable, the film will be applied with additional slack.

Ideally, the test frame (which is sitting on the turn table) and the output prestretch rollers should be turning at the same speed. This would allow for a constant tension on the film. However, this is difficult to achieve per the discussion in Section 2.2.3 and for three additional reasons. First, adjusting the speed of the turntable will change the amount of tension on the bar thereby changing the speed of the prestretch rollers. Second, adjusting the tension to load will change the range of speeds the prestretch rollers will operate in. Third, different films have different prestretch amounts; therefore, the tension bar will be in a different position for each film causing different speeds of the prestretch rollers.

When wrapping a unit load, particularly when using a semi-automatic stretch wrapper (Section 2.2.2) the machine has a set pattern to follow that is preset by the user. Within most wrap patterns the film is spirally wound around the unit load but the exact angle of the spiral can change drastically depending on user specification. Unfortunately, the effect of spirally winding film on the film's applied stiffness has not been scientifically quantified. Therefore, the spiral wrapping of the film should be eliminated as a variable to reduce the amount of independent error that could occur within the system.

When applying the stretch film, the prestretch carriage was restricted to allow for parallel passes around the test frame. A parallel pass was achieved by restricting the sensors on the stretch wrap machine. If both of the sensors are closed the prestretch carriage would not travel when the machine was started. For a picture of how the censors were constrained see Figure 15. The film was broken before the final slow wrap (auto programmed into the machine) could be applied as this was not the desired machine setting to apply and evaluate the film.

Figure 15 Constricting the movement of the prestretch carriage

The rotational speed of the turn table and the output prestretch roller were measured to understand how the two pieces of the stretch wrapper were interacting as a unit load was being wrapped. As discussed in Section 2.2.3, changing rotation speed of either component can affect how the stretch film is prestretched and applied to the unit load and, therefore, its performance as a load stabilizer.

The rotational speed of the stretch wrapper turn table and the output prestretch roller were evaluated using the same method. A slow motion camera was used to capture the speeds. Evaluating the performance of each component was done when the machine was running at full speed. When evaluating the speed of the output prestretch roller, an average of 10 rotations was used. This number was chosen because the rotational speed effects associated with wrapping a four sided object as discussed in Section 2.2.3. To review, the corners of the test frame will travel faster than the faces of the test frame. This variation will cause the tension bar to move when wrapping a unit load. As the tension bar moves the speed of the prestretch rollers will change. Evaluating the speed over an average of 10 rotations allows for an accurate representation of the average speed of the output roller. For a picture of how the turn table and the output roller were marked for timing see Figure 16 and Figure 17.

Figure 16 Alignment marks for turntable

Figure 17 Mark allowing visibility of rotational speed of roller

The rotational speed of the surface of the turn table and the output prestretch roller was calculated using Equation 3-30. The output prestretch roller had a radius of 4.4cm (1.75”) and the test frame used the radius of the turn table at 73.6cm (29”).

$$rs = \frac{2 * \pi * r}{t}$$ **Equation 3-30**

rs= rotational speed of the surface of the object

r = radius of the object in question

t= period of one rotation

The radius of the turn table was used because it allowed for a direct comparison between the two stretch wrap machine settings. However, using the radius of the turn table may not have been the best solution. As discussed in section 2.2.3, the corners of the test frame will rotate faster than the faces of the test frame. This makes choosing the correct radius to represent the test frame difficult.

The corners of the test frame or the faces of the test frame could be used to simulate the radius of the test frame, however, these options are extreme situations which would not make logical choices. Connecting the corners would make a circle so large that there would be too much slack in the system affecting stiffness and force readings. Using the faces of the unit load would allow for too much additional stretching due to tension to load (more below). For a visual representation of this issue see Figure 18. Therefore, a circumference that was in between the two outliers would allow for some tension to load was used. This is why the radius of the turn table was chosen.

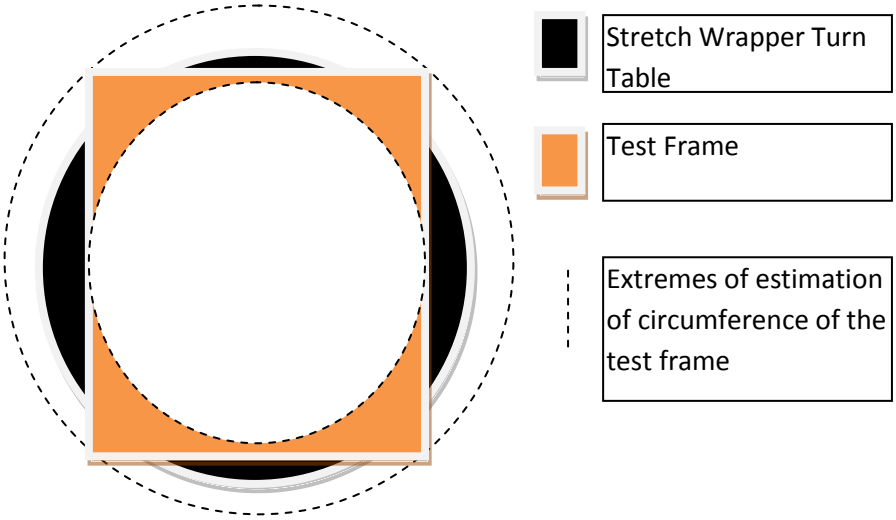

Figure 18 Diagram showing diameter options for the test frame

To study the impact of rotational speed on the test frame, the maximum and minimum speed of the output prestretch roller and the turn table were observed and graphed in Figure 19. At 7.7 dots and a speed of 75.7cm/sec (29.8”/sec) the lines crossed. This speed was chosen for the optimum machine performance. The turn table could not be slower than the output roller because extra slack in the system would lead to too much unpredictability with regard to film performance.

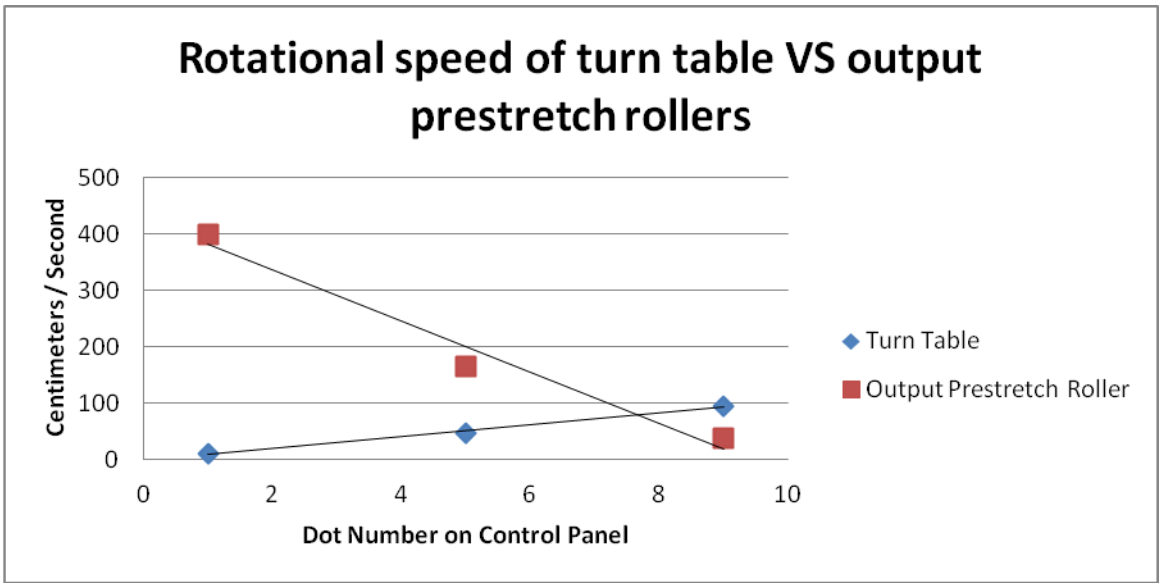

Figure 19 Rotational speed of turn table versus output prestretch rollers

As stated in Section 2.3.3, the amount of prestretch that is imparted on the film affects the amount of crystallinity that has been imparted into the film. The percent crystallinity in the film is what gives the film its stiffness. The stiffness of the film is what makes stretch film an effective load stabilizer.

There are two methods to evaluate the amount of prestretch that a stretch wrap machine will impart onto a film. Both of them were described in Section 2.2.4. The ruler method involved using a marker and a 12.7cm (5 in) piece of wire to mark evaluation intervals on the top and bottom of the unstretched film while still on the roll. Once the film was run through the prestretcher but before applied to the unit load test frame, the machine was stopped. Prestretch was measured, middle mark to middle mark, for 10 repetitions and a total of 20 readings taken. Data collection alternated taking top and bottom data first, every other reading, to ensure that any constricting of the film that occurred during the time to take the first data point was eliminated from the system. The ruler method of evaluating prestretch will be called p_r.

When the stretch wrap machine settings allow for the tension-to-load to increase causing additional film stretch, the amount of stretch imparted on the film (beyond the stretch of the pre-stretch carriage) was measured by a star wheel. (Section 2.2.4). The wheel had a circumference of 20.3cm (8”). The wheel was held against the unstretched film as the machine was wrapping the test frame. The star wheel applied a mark on the film every full rotation. After the film was applied to the test frame and the machine had finished its wrapping cycle, the distance between marks was measured. The final distance between marks was divided by the initial 8 inches to calculate the % stretch the system imparted on the film. The star wheel method of evaluating prestretch will be called p_s.

The difference between p_s and p_r would quantify the Post Prestretch (pp) film behavior. Mathematical representations are shown in Equation 3-31 and Equation 3-32. Pp will have larger affects on applied

film performance the farther from zero it becomes. A positive value would indicate that Tension to Load (pp_t) was able impart additional to stretch onto the film (turn table was turning faster than the output prestretch roller). A negative value could mean two things. In trying to return to its original form, the film might have reduced its length in the time that was taken to apply the film or the turn table was turning slower than the output prestretch roller. Either way, these scenarios allow for slack in the film when it is being applied to a unit load. This negative reading (Slack) will be called $+pp_s$.

$$-pp_s = p_s - p_r$$ **Equation 3-31**

$$+pp_t = p_s - p_r$$ **Equation 3-32**

For this experiment a $+pp_t$ was necessary because the effect of slack on stretch film application has not been quantified. Therefore, film tension should be constant throughout the application process to eliminate this independent variable.

3.2.4 Measuring f_{af} with a pull plate

When evaluating containment forces according to ASTM D 4649 Annex A1 a 15.2cm (6”) pull plate was placed behind the film. Note that ASTM D 4649 (ASTM, 2003b) requires the user to cut a hole in the film on the side of the unit load to place the plate under the film. In doing this the strength of the film is potentially compromised. For this experiment the plate is slid behind the film so that the only film rupture is from the ruler hole. For a further explanation see Section 2.4.1 and Figure 20.

The measurement of f_{af} used the same methods except force readings at 5.0cm, 7.6cm, 10.1cm, 12.7cm and 15.2cm (2”, 3”, 4”, 5” and 6”) were recorded. A ruler hole was cut into the pull plate to allow for the most accurate distance measurement possible. The plate was covered in a plastic material (box tape) to prevent slippage of the stretch film off of the plate when the f_{af} tests occurred. This slippage could skew the stiffness results of the test. The tape can be seen on the surface of the pull plate in Figure 20. A Shimpo digital force gauge (FGE-100) was used to measure the amount of force required to pull on the plate. The slope of the force readings versus their respective extensions were used to calculate the Face Stiffness of the Applied Film (s_{af})of a given film.

The percent of film extension of the film off the face of the test frame was calculated so that it could be correlated to the percent extension used in the Bisha Stiffness test (Section 3.1). To calculate the percent extension, half the diameter (p_d) of the pull plate was subtracted from half the length of the side of the test frame. Then, depending on the extension from the side of the test frame, Pythagoreans Theorem was used to calculate the length of the hypotenuse. The initial length was then subtracted from the hypotenuse, divided by the initial length and turned into a percent. The formula is shown in Equation 3-33.

$$\%\ \mathbf{ext.} = ((\sqrt{((\ell/2 - p_d d/2)^2 + (x)^2)}) - (\ell/2 - p_d d/2))/(\ell/2 - p_d d/2\ )) * 100$$ **Equation 3-33**

Figure 20 Simulation of s_{af} with ruler against backing

When the film is extended to a full 15.2cm (6”) using the f_{af} evaluation method the film looks like it does in Figure 21. The film that is just around the vertical edges of the plate is collapsing much less than the film on the horizontal edges of the plate. This helped to corroborate with the assumption in Section 3.2.1 where the horizontal edges of the plate are not evaluating the stiffness of the film because the film was not pinned to the top of the test frame.

Figure 21 Side view of s_{af} evaluation at maximum extension

3.2.5 Limitations to the f_{af} measurement system

The limitations of using this evaluation system include the inherent variability of the stretch wrapper applying the film to the test frame and the human error that could be introduced due to the angle of pull not being consistent during every test.

The major limitation of this test is the assumption that the force vectors are consistent on the pull plate when evaluating the f_{af}. In actuality they change as the plate is pulled from the face of the test frame as shown in Figure 22. The initial force vectors at small extensions are directly acting on the plate with similar amounts of force, but as the plate is extended further, the vectors start to bend and increase along the vertical edges of the plate leading to a disproportionally higher force vector. The deformation of the film over the extension range of this test is best to be modeled using Finite Element Analysis and is beyond the scope of this study.

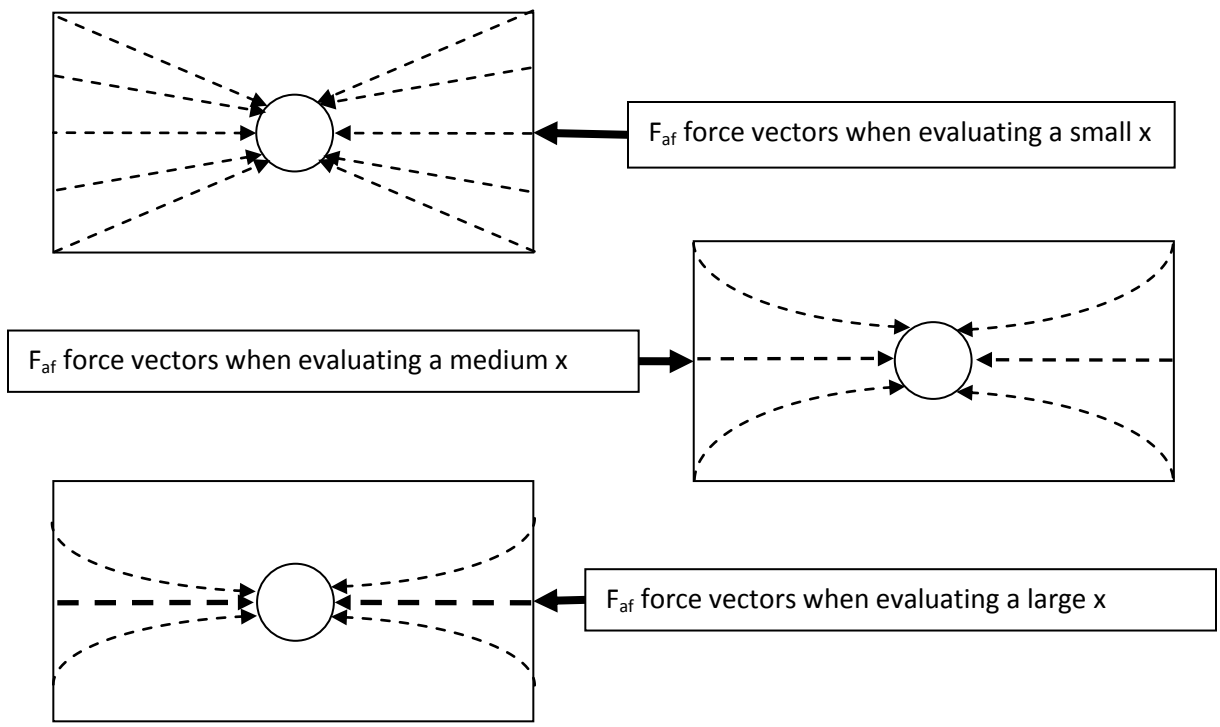

Figure 22 Evolution of force vectors when evaluating f_{af}

3.2.6 Measuring f_{ac} with a bar

The pull plate used to evaluate f_{af} originated at a time when the web width of stretch film was equal to the height of the unit load. Therefore, the pull plate could be used because there was one large layer wrapping the unit load. Modern films are 50.8cm (20”) or 76.2cm (30”) wide and require many more rotations of the unit load to achieve the same coverage. When the plate is slid behind the film and pulled out a desired amount it is possible to evaluate partial layers. Some layers do not come in contact with the plate but do come in contact with the film around the plate that is being evaluated. To complicate the issue further, depending on the level of tack in the film, these partial layers can

delaminate from the web while being evaluated, causing inconsistent measurements that represent actual containment force on a unit load.

These inconsistencies lead to the creation of a bar stiffness evaluation system. This system optimally works on films that have been applied on a test frame by a stretch wrap machine that has had its prestretch carriage restricted of movement as described in section 3.2.3 (could also work on an actual unit load). The film can be evaluated on either the face or the corner of the test frame, but for this experiment the film was evaluated on the corner of the test frame. When measuring the f_{ac} on the corner of the test frame, either the corner needs to be flattened in order to allow the bar to sit flat on a surface during wrapping or the bar needs to have a recessed side to sit on the corner.

In setting up the system for f_{ac} measurement, the bar was secured in place with a wire attached to one end. The test frame is then wrapped with the bar on the corner of the test frame. After the wrapping sequence, the wire was reattached at the other end. An additional benefit of this measurement system is that the Y intercept of the f_{ac} is the f_c the film imparts on the corner of the test frame.

For this experiment, a 2.5cm (1”) aluminum bar was used with 1.2cm (.5”) x 2.5 (1”) bolt in either end of the bar. The wire had a loop in each end and the bolt was placed in that loop as the bolt was screwed into either end. The wire was attached to an S-hook and a thicker cable which traveled through a wheel on an axle to change the direction of pull to vertical. The wire was then hooked to a 22,241.1N (5000 #) load cell attached to an hydraulic MTS machine (different machine than the one used for evaluating s_b) which moved at a speed of 12.7cm/min (5”/min). During preliminary testing a stretch film was applied with multiple wraps and the experiment was conducted beyond normal extensions. This allowed the test frame to rotate on the stretch wrapper turn table to a central point for evaluation. The machine was reset to this point before every test. A picture of the test set-up is shown in Figure 23.

The f_{ac} was evaluated between 4.4cm and 6.9cm (1.75” and 2.75”) from the corner of the test frame. This was done to ensure that the bar had no contact with the test frame and had stabilized after falling off the corner.

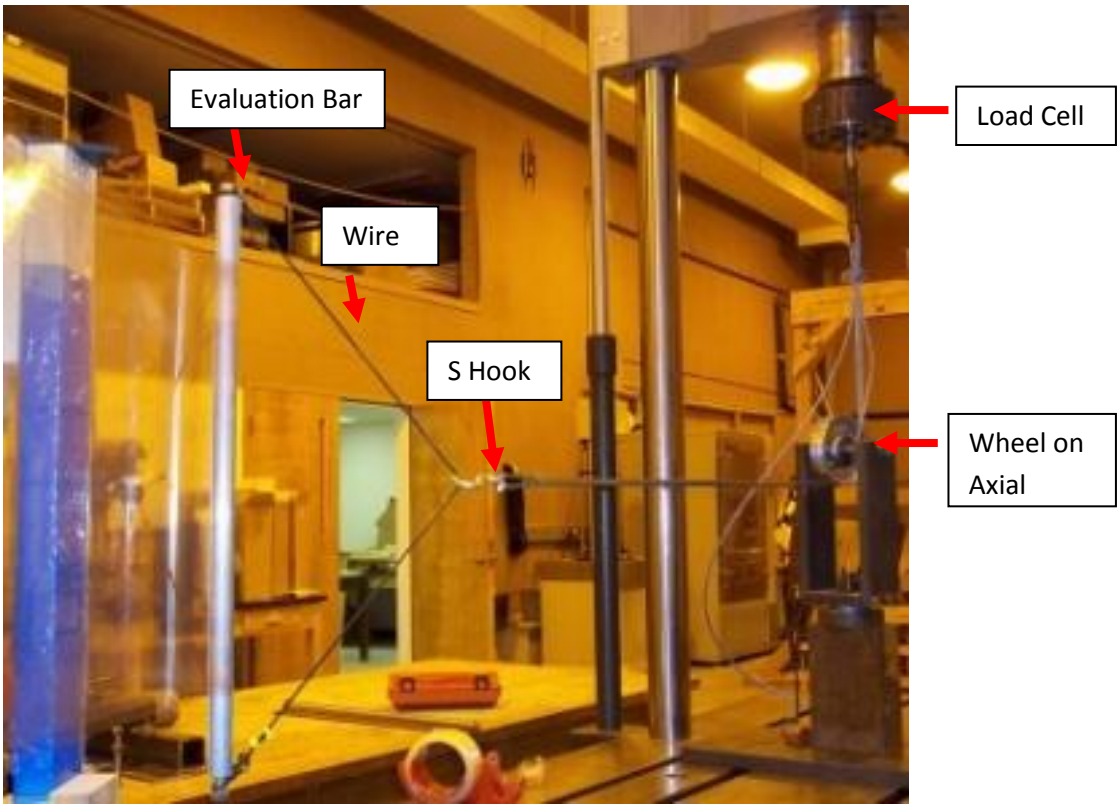

Figure 23 Components of f_{ac} Testing Setup

3.2.7 Limitations to the f_{ac} measurement system

There are several limitations that are of concern in evaluating the f_{ac}. The primary concern being that a stretch wrap machine is not a piece of machinery that is built for scientific accuracy and repeatability. The machine performs inconsistently if the amount of voltage to the machine changes over time. This inconsistent performance may happen if the heating or air conditioning of the building cycles on and off, affecting the available power to the machine. It was also noted during testing that the machine had to "warm up" before results were in line with data from the previous day. This warm up consisted of 3 complete wrapping cycles of the test frame.

The test frame was made out of wood and it is possible that when large forces were applied, deflections in the test frame could be significant enough to cause errors in the measurement results. While no significant deflections were observed visually, no precise deflection measurements were monitored to verify this observation.

During the evaluation of the f_{ac} the bar was slowly pulled off the corner of the test frame. At the point at which the stretch film could no longer hold the bar to the test frame, the bar fell, causing slight inconsistency in the data curve. However, these inconsistencies in the data set occurred before data for the s_{ac} was collected. Note that the aluminum bar was the lightest bar available that would not bend during the evaluation.

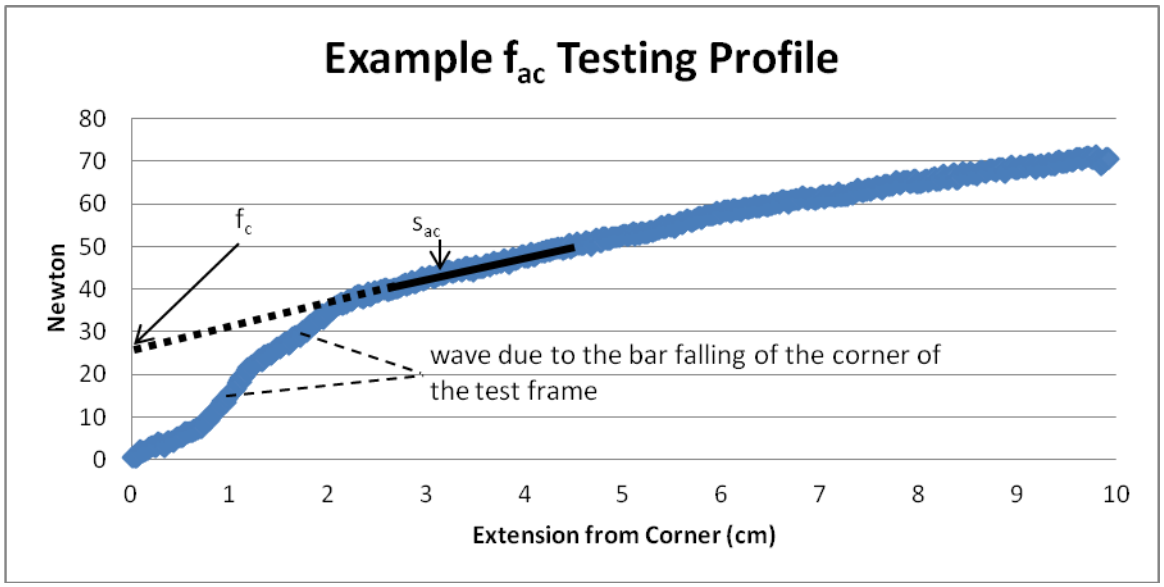

Figure 24 Data output from f_{ac} testing identifying how s_{ac} and f_c is calculated and how the initial separation between the test frame and the bar did not affects results

3.3 Correlation of s_a and s_b

The third objective of this research was to investigate the correlation between the elastic tensile properties and the applied stiffness and containment force of stretch film. Specifically, determine how s_b and f_i from Section 3.1 can be used to predict the s_a and f_c from Section 3.2. A linear regression was used to form the predictions, an F test was used to determine significance and the coefficient of determination was used to relay the proportion of variability in the data set. The results are discussed in Section 6.

$$\mathbf{s_a} = f(\mathbf{s_b}) + error$$

Equation 3-34

$$\mathbf{f_c} = f(\mathbf{f_i}) + error$$

Equation 3-35

3.4 Comparison of results

There were multiple statistical comparisons conducted throughout this research. T-Tests were used to test if data sets had dissimilar means. If multiple comparisons were to be conducted a Tukey's HSD was conducted. The formulas for the Tukey's HSD test are shown in Equation 3-36 and Equation 3-37.

$$W <= |\overline{y_{i\cdot}} - \overline{y_{j\cdot}}|$$

Equation 3-36

$$W = q_\alpha(t, v)\sqrt{\frac{s_w^2}{n}}$$

Equation 3-37

Where:

W = Difference in the means

y_i or y_j = means of the different data sets

s_w^2= mean square variance within samples based on *v* degrees of freedom

$q_\mu(t,v)$= upper-tail critical value of the studentized range for comparing t different population

n - Number of observations in each sample.

Linear comparisons of different data sets were conducted with an ANCOVA analysis. The ANCOVA analysis was chosen because in preliminary testing the stiffness and containment force values were generally linear when plotted against the thickness of the original film. The ANCOVA (based on an ANOVA) is a way of controlling the linear variables that are not desirable within the study. The undesirable variables are called covariates. The general formula for calculating an ANCOVA is summarized by allowing for the observed response to equal the overall mean, plus treatment effect, plus covariate effect, plus the error. The formula is shown in Equation 3-38.

$$y_{ij} = \ddot{u} + \tau_i + \beta(x_{ij} - \bar{x}) + e_{ij}$$

Equation 3-38

Where:

y_{ij} = Response of the model

ü = Average of all data analyzed

τ_i = Treatment effect

β = Covariate effect

x_{ij} = Input of the model

x bar = Average for the entire data set

e_{ij} = error for data set

4 Evaluating tensile properties of stretch film beyond its yield stress

As discussed in Section 2, stretch films are designed to be applied by a stretch wrapper well beyond their yield stress. The advertising literature for both the films and the stretch wrappers corroborates this extreme stretching design (Schwind, 1996). Such extreme stretching realigns the polymers within the film, increasing its stiffness and reducing its elasticity (Hernandez, et al., 2000).

The physical alteration of the molecular make-up of stretch film during the application process allows for the end user to select the correct balance between film stiffness and containment force that a given stretch film applies to a unit load. Once the film has been stretched beyond its yield point and applied to the unit load, the molecular chains try to return to their lowest energy state, allowing for the further increase in film stiffness and decrease in containment force. If stretch film was applied to a unit load and left long enough, it would essentially become a stiff dust shield that would apply no inward force to the unit load. However, as soon as the contents of the unit load are shifted, causing the film to stretch into a new position, the containment force is increased on the unit load contents that caused the stretching while the stiffness of that same film has been reduced only to reinitiate the settling of the molecular chains into their new lowest energy state. This phenomenon is what makes stretch film so effective at containing unit loads.

There are two components that introduce variability into the application of stretch film, which in turn affect its performance in the system described in the previous paragraph. The first component consists of the stretch film properties, including thickness, polymeric make up and post manufacturing treatments during the manufacturing process. As discussed in Section 2.3, these films are primarily LLDPE and include “layers” of additives, which are mixed into the film just before the extrusion process (Peacock, 2000). Once the film has been extruded, the film is stretched to align the polymer chains into the machine direction of the film. This stretching process enables some additives to bloom to the surface of the material (such as tackifiers). However, this is not an exact science, leading to variability in the amount of bloom across the film web (G. Panagopoulos, 1991).

The second component of variability consists of the application process including the speed of the turn table versus the speed of the output prestretch roller, percent stretch, the amount of material applied and the amount of time between application and evaluation. As described in Section 2.3, the speed and amount of elongation of any given polymeric sample can have significant implications on the final films material properties, especially when stretching beyond the yield stress (Brown, 1999). A slow extension of a film allows for the polymer chains to realign causing the creation of a larger, uniform, crystalline area within the film. During a rapid extension, the chains will form many smaller crystalline regions that are not linked with each other. This differentiation in crystallization can cause variability in the perceived material properties when the percent stretch is held constant.

The percent stretch that is imparted on a film via a prestretch carriage is easily quantified using the start wheel or ruler method described in Section 2.2.4. Preliminary research investigated the variability of the prestretch carriage (Section 3.2.3). The prestretch was measured using the ruler method and measurements were taken, center mark to center mark, after prestretching. Data collection procedure alternated top and bottom with respect to which was taken first. This was done in case the film was retracting enough to effect results during the time taken to evaluate the first measurement. There were 11 different films investigated ranging from 11.4µ to 23.1µ and each test was conducted 10 times. The

average results are shown in Figure 25 and the full report is found in Section 8.2. The advertised prestretch of the machine is 200%, however, it has been retro fitted to prestretch films 250%. The dotted line in Figure 25 represents the anticipated prestretch of the films.

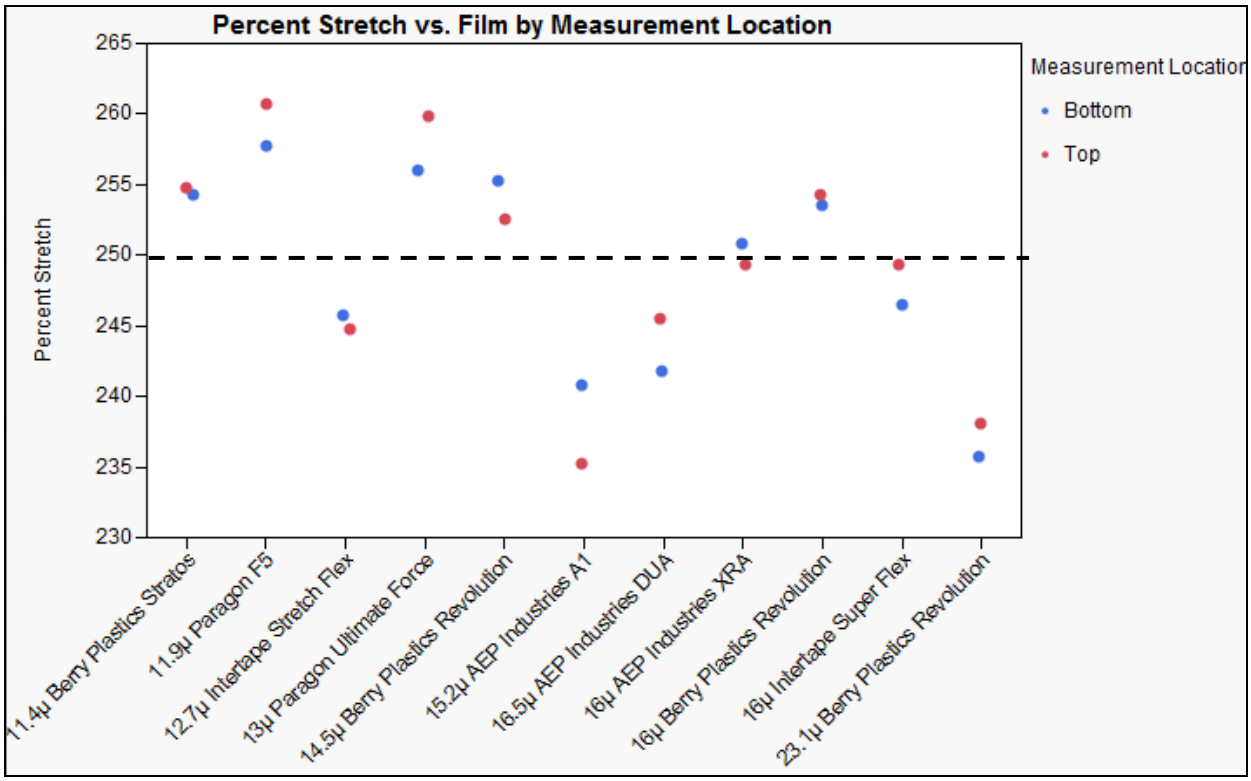

Figure 25 Results of comparing the percent stretch of different film on the same stretch wrapper

The results shown in Figure 25 indicate that there is a larger percent prestretching imparted on to the top of the film than the bottom. This bias may have been caused by a misaligned or improperly formed prestretch roller which allowed more stretch on the top of the film web than the bottom. The results were highly variable surrounding the anticipated prestretch of 250%, however there was a general trend of the thinner films prestretching more than the thicker films.

While the results of this exercise were revealing in terms of how much prestretch variability there can be in the application of stretch film, the implications of the results are inconclusive without determining the differences in applied film properties within the given range of extensions. There are too many possible variables to control within the stretch wrapping machine; therefore, more properly controlled testing is needed.

The high variability and the lack of implication of these results from measuring the prestretch imparted onto the film by the stretch wrapper indicate that the percent stretch for each film should be individually evaluated on the stretch wrap machine in use when determining the parameters for the tensile s_b evaluation.

The literature review in Section 2 and the preliminary research referenced above indicates that the application of stretch film to a unit load is relatively fast and not very controlled and the use of the

tensile testing machine is not optimum for estimating the applied stiffness of a film because of the natural errors that occur.

Recall from Section 2.4.2 that the ASTM testing standard (ASTM, 2007) suggests either a 60 second or a 24 hour time duration to evaluate material properties. To understand the behavior of stretch wrap and to verify the appropriate evaluation time interval, an additional preliminary test investigated how the s_b and f_i changed over time. The samples were prepared using the roll method and therefore the s_b for this test is called the s_{br}. For more details on the preparation of the roll sample see Section 8.3 (Appendix). Evaluations were conducted on a tensile testing machine using the testing profile described earlier in Figure 5. A minimum of three samples were used at each time increment. A sample of the results using Berry Plastics 11.4µ film is shown in Figure 26 and Figure 27. Note that it was previously determined in Figure 25 that the Berry 11.4µ film stretches to 253% on the stretch wrapper used therefore the samples were stretched to that amount before the s_{br} evaluation.

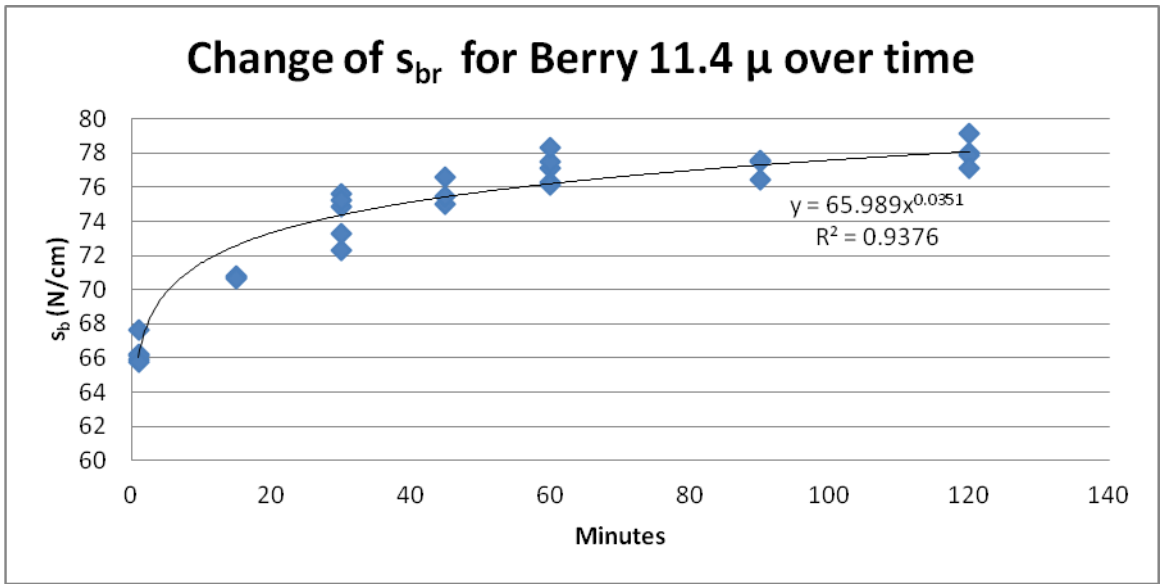

Figure 26 The change in s_{br} of Berry Plastics 11.4 µ over a 2 hour period. The s_{br} initially increased over the first hour of testing but did not significantly change after that.

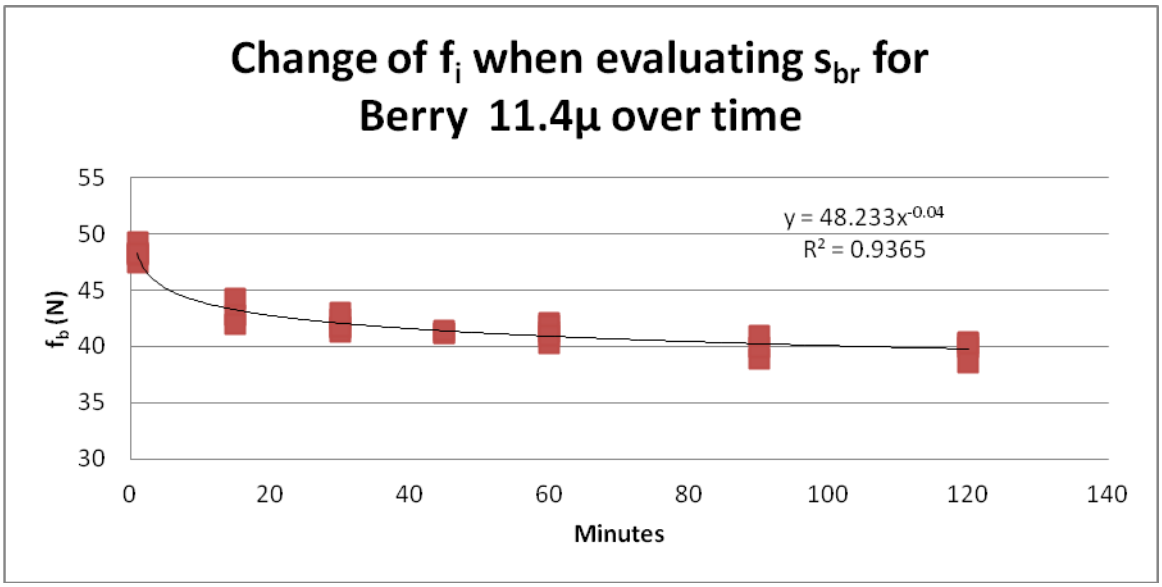

Figure 27 The change in the initial f_i when evaluating the s_{br} over a two hour period. Note that as time progresses the amount of f_i reduces.

The results of the s_{br} Berry Plastics 11.4µ evaluation show that the s_{br} increased over 13% within the first hour of evaluation, at which point the s_{br} leveled off into a more predictable, asymptotic trend. The f_i investigation found similar results with an inverse trend. The f_i decreased 14% within the first hour of the investigation at which point the data trended into an asymptotic form. The f_i may relate to the amount of f_c when the film is applied to a unit load using similar application and turn table speeds. This will be further investigated in Section 6.

The time required for a film to stabilize under these testing conditions depends on the amount of film tested, the sample preparation method and the sample size. No matter what combination used, trends of these results should be relatively consistent due to the polymeric nature of the stretch film as previously discussed in this section and in Section 2.3. For a formal discussion of the details of the testing methods and expanded results of the preliminary research shown in Figure 26 and Figure 27, see Section 8.4.

During the preliminary research of the percent stretch comparison and the s_{br} evaluation a comparative observation was made. When evaluating the stretch film on the stretch wrapper, the film that was stretched between the two prestretch rollers were two non-fixed points. In the case of evaluating the stretch film on the tensile testing machine, the film was stretched between two fixed points. This difference in non-fixed vs. fixed points causes the geometry of the samples to be different. The film necks down approximately 10% on the stretch wrapper during the prestretch process. When the film leaves the prestretch carriage the film is a constant width, implying that a relatively equal force was applied to the entire film width. However, when conducting the tensile test with the MTS machine, the sample forms an hour glass shape due to the alignment of the polymer chains and the focus of strain in the middle of the sample. This focus of strain causes an inconsistent stretch across the film sample, allowing for more stretch mid sample than stretch that occurs next to the jaws. This phenomenon will affect the results of the different samples widths when evaluating the s_b (Figure 3). It is hypothesized that the differentiation between sample behaviors/volumes will influence the testing results and will require functional adjustments to equate the two.

The preliminary observations and research outlined above indicate the need for a precise method to control stretch film prestretch and film load deflection response over time on a tensile testing device. Therefore, the Bisha testing profile (Figure 5) was used in conjunction with two different sample creation methods. As in the preliminary research, the Bisha Stiffness method allows for the extension of the film beyond the yield point, a holding period and then a final extension. The slope of the final extension is known as the Bisha Stiffness of the material. This consistent, easily replicated method simulated the prestretching, application and evaluation of applied stretch film.

The first sample preparation method emulated the sample preparation method outlined by ASTM D 5459 ((ASTM, 2007), while the second utilizes the full web width of the film. As outlined in Section 3.1, the Bisha stiffness is denoted as s_b and the initial force measured at the beginning of the s_b evaluation is denoted as f_i.

This experiment addressed the first objective of evaluating the desirable tensile properties of stretch film in a method that simulates the application of stretch film to a unit load. The results will be used to compare against actual stiffness and containment force values in Section 6.

4.1.1 Experimental Design

Six films were tested and each film was prepared using one of two methods as described in Section 4.1.2. Each experiment was replicated three times resulting in 36 tensile tests. This experiment investigated the influence of the testing method and film gauge on material properties (s_b and f_i) of film 1 hour after being stretched to the target prestretch. The purpose of this experimental design was to investigate if the ASTM D 5459 (ASTM, 2007) standard 2.54 cm (1”) sample testing procedure correctly emulated the 50.8cm (20”0 sample width when evaluating s_b and f_i. A visual representation of the experimental design is shown in Table 4.

Table 4 Experimental design for Section 4

Test Sample preparation➔	ASTM 2.54 cm	50.8 cm Full Width
Parameters Estimated➔	S_{b1} and F_{i1}	S_{b20} and F_{i20}
Film Thickness:	Number of test replicates	
10 µ	3	3
11.4 µ	3	3
12.7 µ	3	3
16 µ	3	3
22.8 µ	3	3
30.5 µ	3	3

4.1.2 Materials & Methods

The research in this section is a comparison between the s_b and f_i of samples prepared using the ASTM method (2.54 cm (1”) wide) and samples prepared using the full film width of 50.8cm (20”). The measured stiffness, s_b and tension f, for the 2.54cm (1”) wide samples and the 50.7cm (20”) samples were denoted by s_{b1} and f_{i1} and s_{b20} and f_{i20}, respectively. A photo of the materials used to make the 2.54cm samples is shown in Figure 28.

Figure 28 Materials used to cut a s_{b1} sample

The six films used were Paragon 10 Micron (µ) UF 100500, Berry Plastics 11.4µ Stratos, Intertape 12.7µ Stretch Flex, Intertape 16µ Super Flex, AEP 22.8µ A1 and AEP 30.5µ A1. The samples were prepared using the methods outlined in Section 3.2. A load deflection curve was generated for all the samples and the s_b and f_i were calculated for each sample and compared. The s_b is the slope of the force vs extension line created within the first centimeter after the film has been stretched, held for a specific time and then stretched again. The f_i is the initial force at the beginning of this slope. The test was conducted at a speed of 50.8cm/min (20”/min). The sample length was 12.7cm (5”). For more details see Section 3.1.

As discussed in Section 2.2, each film interacts with the stretch wrapper and test frame differently; therefore, each film was evaluated for its own percent prestretch. The different extensions are shown in Table 5. Note that because the rotational speeds of the stretch wrap turn table and prestretch output rollers are very similar, the corners of the test frame traveled faster than the output prestretch rollers while the faces of the test frame moved slower than the output rollers causing the tension to load to stretch the film. For more details see Section 3.1.4.

Table 5 Films and their respective prestretched used in evaluating the s_b and f_i

Film Type	% Stretch when Applied to the Test Frame
Paragon 10µ UF 100500	305%
Berry Plastics 11.4µ Stratos	310%
Intertape 12.7µ Stretch Flex	319%
Intertape 16µ Super Flex	300%
AEP 22.8µ A1	297%
AEP 30.5µ A1	297%

The s_b and f_i results were visually and statistically compared by forming a regression of the results against the original material thickness and using an ANCOVA to compare the results. Note that to

conduct this analysis, the 2.54cm wide samples were multiplied by 20 to determine if the results are significantly different than the 50.8cm samples. The standard form of an ANCOVA is shown in Equation 4-1.

$$y_{ij} = \ddot{u} + \tau_i + \beta(x_{ij} - \bar{x}) + e_{ij} \qquad \textbf{Equation 4-1}$$

The individual comparisons conducted are shown in Equation 4-2 and Equation 4-3:

$$\mathbf{s_{b20}} = \ddot{u} + \tau_i + \beta(\mathbf{s_{b1}}` - \overline{\mathbf{s_{b1}}`}) + e_{ij} \qquad \textbf{Equation 4-2}$$

$$\mathbf{f_{i20}} = \ddot{u} + \tau_i + \beta(\mathbf{f_{i1}}` - \overline{\mathbf{f_{i1}}`}) + e_{ij} \qquad \textbf{Equation 4-3}$$

Where:

s_{b1}` = Bisha stiffness of the 2.45cm sample that has been multiplied by 20

f_{i1}`= Initial force of the Bisha Stiffness of the 2.54cm samples that has been multiplied by 20

ü = Average of all data analyzed

τ_i = Treatment effect

β = Covariate effect

e_{ij} = error for data set

4.1.3 Results & Discussion

Table 6 Average and COV results for s_b evaluation in tensile testing

	Thickness (µ)	s_{b1} (N/cm)	s_{b20} (N/cm)	s_{b20}/s_{b1}	s_{b1} COV	s_{b20} COV
Paragon	10	1.03	27.36	26.56	5.1%	2.8%
Berry	11.4	1.87	45.97	24.58	6.8%	1.4%
Intertape	12.7	2.19	69.59	31.78	9.6%	3.2%
Intertape	16	2.36	62.79	26.61	7.1%	1.8%
AEP	22.8	1.62	51.93	32.06	11.6%	1.2%
AEP	30.5	2.46	69.90	28.41	9.0%	1.7%

The s_{b1} results in Table 6 have an average of 1.92 N/cm and a standard deviation of 0.54 N/cm. They had a range of 1.43 N/cm with a maximum s_{b1} of 2.46 N/cm from the AEP 30.5µ film and a minimum s_{b1} of 1.03 N/cm from the Paragon 10µ film. The two Intertape films and the Berry Plastics 11.4µ film resulted in higher than expected s_{b1} values providing significant variation from anticipated linear trend of s_{b1} vs µ.

A least squares linear regression was conducted to determine if there was a relationship between the s_{b1} and the µ. The R^2 (Coefficient of Determination) of the line was low at 0.23, indicating that very little of the change in s_b could be explained by the variation in film thickness. A graph with the results and the respective least squares fit is shown in Figure 29. The fit of the regression is poor due to the lower s_{b1} results of the Paragon 10µ and the AEP 22.8µ samples. However, there is a statistically significant positive slope indicating a higher s_{b1} as the thickness of the material increases.

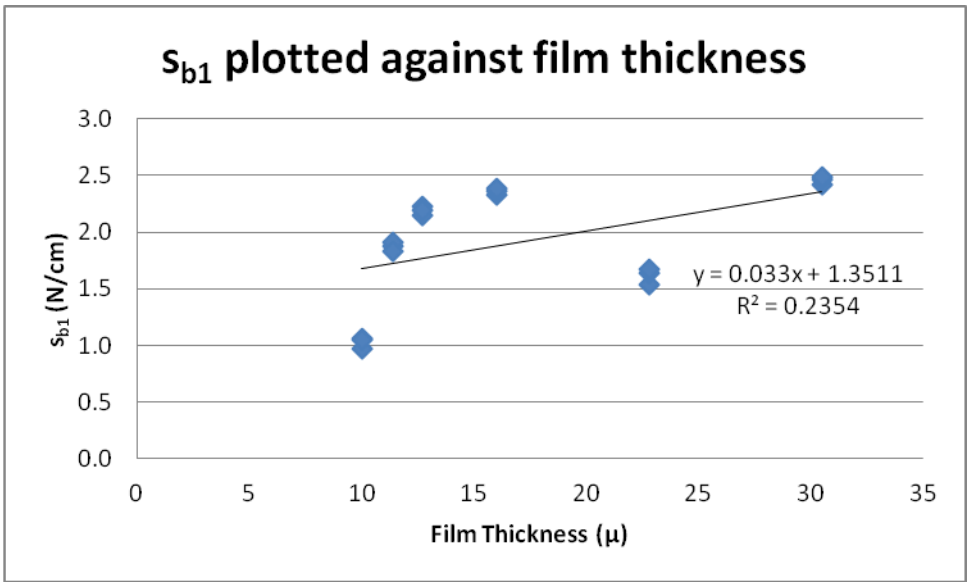

Figure 29 The s_{b1} results are plotted against the original material thickness

The COV of the s_{b1} results are shown in Table 6. The AEP 22.8µ film had the highest COV which was 11.6% and the Paragon 10µ had the lowest COV at 5.1%. A Tukey's HSD analysis was conducted on the s_{b1} COV results and it was determined that none were found to be statistically different at a CI of 95%.

The S_{b20} results in Table 6 have an average of 54.59 N/cm and a standard deviation of 16.42 N/cm. They have a range of 45.53 N/cm with a maximum s_{b20} of 69.89 N/cm from the AEP 30.5µ film and a minimum s_{b20} of 27.36 N/cm from the Paragon 10µ film. The two Intertape films allowed for higher than expected s_{b20} values and the Paragon 10µ allowed for a lower than expected s_{b20} value providing significant variation from anticipated linear trend of s_{b20} vs. µ.

A least squares regression was conducted to determine if there was a relationship between the s_{b20} and the µ. The R^2 of the line was low at .29 indicating that very little of the variation of the data set was captured by the linear model. A graph with the results and the respective least squares fit is shown in Figure 30. The fit of the regression is poor due to the lower s_{b20} results of the Paragon 10µ and the AEP 22.8µ and the high Intertape 12.7µ results. However, there is a statistically significant positive slope indicating a higher s_{b20} as the thickness of the material increases.

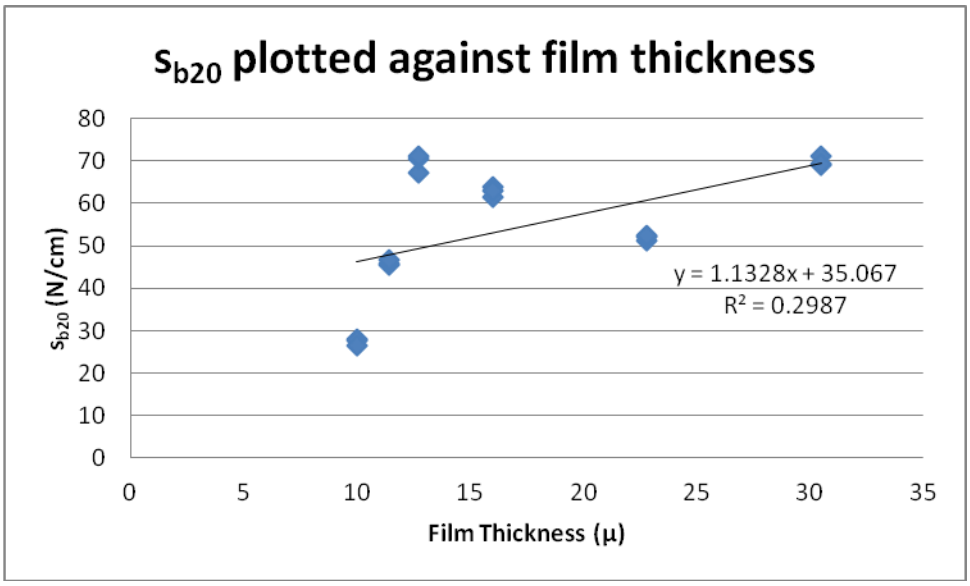

Figure 30 The s_{b20} results are plotted against the original material thickness

The COV of the s_{b20} results are shown in Table 6. The Intertape 12.7μ had the largest COV of 3.2% and the AEP 22.8μ film had the lowest COV of 1.2%. All of the COV's for the s_{b20} sample set were under 3.2%. A Tukey's HSD analysis was conducted on the s_{b20} COV results and it was determined that none were found to be statistically different at a CI of 95%. The COV of the s_{b1} samples was higher than the s_{b20} samples due to the large error associated with evaluating the smaller sample size. See section 3.1.3 for details.

A least squares linear correlation was used to determine if there is significant correlation between the s_{b20} values from the s_{b1} values. The form of the correlation model is shown in Equation 3-2. The R^2 of the prediction was 0.86 and the ANOVA conducted on the prediction found that it was significant [F=1775.502(1,17), Prob>F=<0.0001]. These results indicate that the prediction fit the data relatively well and was significant.

$$s_{b20} = (s_{b1} * 28.4374) + Error \qquad \textbf{Equation 3-2}$$

The s_{b20}/s_{b1} results are shown in Table 6. Even though the s_{b20} samples are 20 times wider than the s_{b1} samples, the s_{b20} results are on average 28 times higher than the s_{b1} results. This higher than expected average is due to the larger strain hardening area compared to the necking area in the larger sample size as discussed in Section 2.3.2 and Figure 3. For an alternative comparison between the s_{b1} and the s_{b20} samples, the force measured in the s_{b1} samples was transformed by multiplying the data times 20 (s_{b1}`). A graphical comparison of the $s_{b1}$` and s_{b20} per the thickness is shown in Figure 31. A graphical comparison of the s_b responses versus the least square means is shown in Figure 32. Note that the s_{b1}` is consistently lower than the s_{b20}.

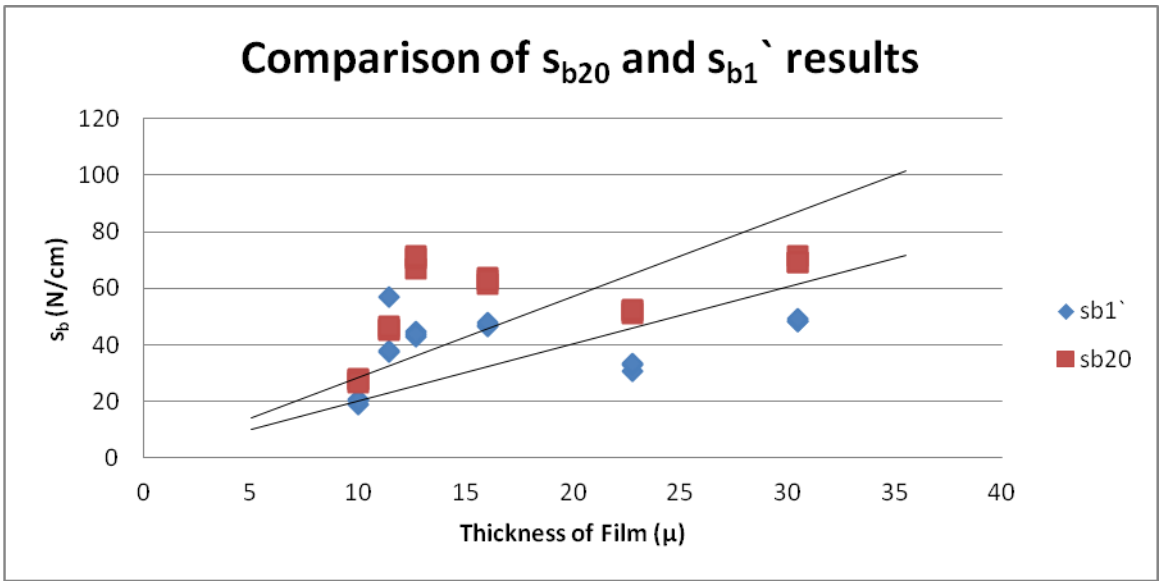

Figure 31 The force from the s_{b1} test was multiplied times 20 to calculate s_{b1}`. This figure shows a comparison between the $s_{b1}$` and the s_{b20} results where the trend lines are forced through the origin.

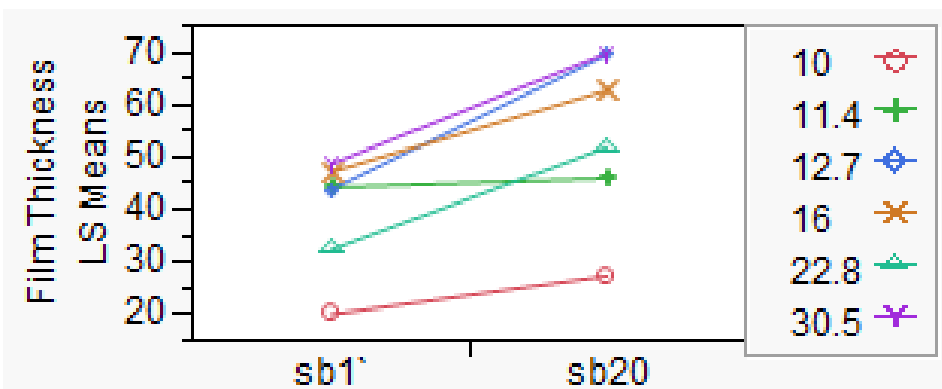

Figure 32 Graphical comparisons of how the means from the sb1`(N/cm) and the sb20(N/cm) compare

The statistical multivariate comparison shown in Figure 33 is an analysis of covariance (ANCOVA). The test determined whether or not the s_b test results were statistically different when compared against the original thickness of the film. Note that the origins were not forced in the ANCOVA so a more strict comparison could be conducted. The t ratio results from the ANCOVA are shown in Table 7. The results show that there is a significant difference between the interaction between the s_{b1} and the s_{b20}, but there is no proof of a significant difference between the s_{b1}` and the s_{b20} and, therefore, it cannot be concluded that one of the tests is a more appropriate method to measure film stiffness.

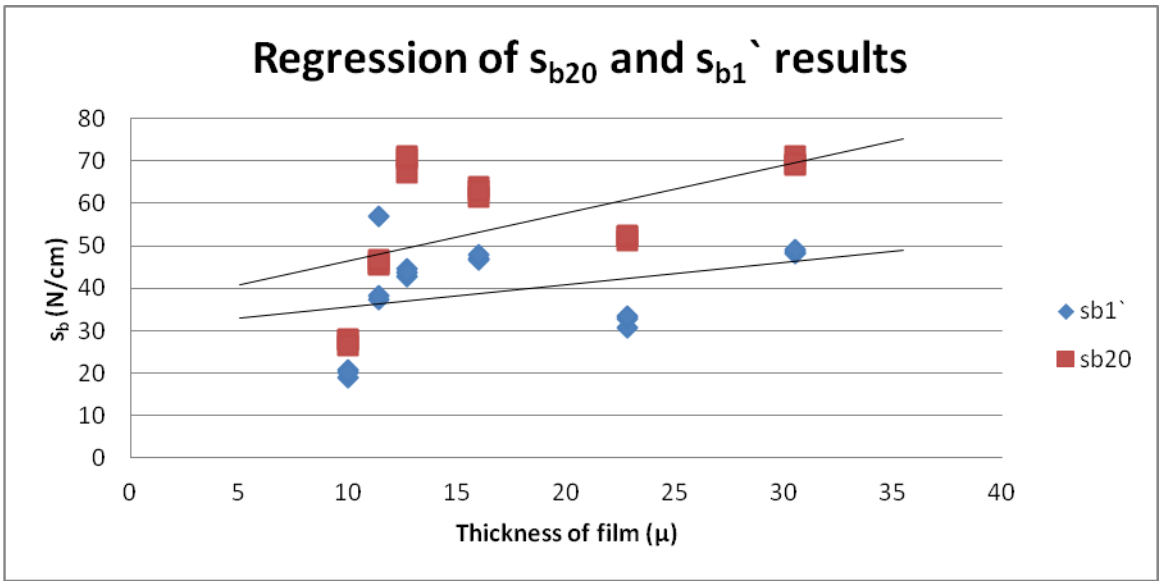

Figure 33 Slopes compared using the ANCOVA analysis. Note that the origin was not forced so an ANCOVA could be conducted.

Table 7 ANCOVA t-ratio results for all interactions concerning s_b

	Estimate	Std Error	t ratio	Prob>ItI
s_{b1} vs s_{b20}	-0.5499	0.2171	-2.53	0.0164
S_{b1}` vs s_{b20}	-0.0301	0.2781	-1.09	0.2839

The results of the ANCOVA indicate that there is significant difference between the slopes of the s_{b1} and the s_{b20} regressions, however, there is no evidence of a significant difference between the s_{b1}` and the s_{b20} regressions. Because of this, there is no statistically conclusive evidence that the full width test results (s_{b20}) and the s_{b1} test results are different. Therefore, the s_{b1} data was deemed an appropriate test to measure film stiffness and was used in further comparisons in Section 6.

Table 8 Average and COV results for f_i in s_b evaluation during tensile testing

	Thickness (μ)	f_{i1}(N)	f_{i20} (N)	f_{i20}/f_{i1}	f_{i1} COV	f_{i20} COV
Paragon	10	1.16	35.52	30.75	59.0%	1.6%
Berry	11.4	2.01	46.75	23.24	4.3%	1.9%
Intertape	12.7	2.42	81.95	33.90	21.3%	2.6%
Intertape	16	3.45	81.48	23.60	2.7%	0.3%
AEP	22.8	3.31	81.30	24.53	2.4%	1.2%
AEP	30.5	4.56	110.83	24.32	7.8%	1.4%

The initial tensile force f_{i1} results in Table 8 have an average of 2.82 N and a standard deviation of 1.2 N. They have a range of 3.4 N with a maximum f_{i1} of 4.55 N from the AEP 30.5μ film and a minimum f_{i1} of

1.15 N from the Paragon 10µ film. The Intertape 16µ film allowed for higher than expected f_{i1} value providing a slight variation from anticipated linear trend of f_{i1} vs. thickness (µ).

A least squares regression was conducted to determine if there was a relationship between the f_{i1} and the µ. The R^2 of the line was 0.76 indicating that much of the variation of the data set has been captured by the linear model. A graph with the results and the f_{i1} vs. µ least squares fit is shown in Figure 34. The fit of the regression line was lessened by the effect of the large cov of the Paragon 10µ film and the results of the Intertape 16µ film.

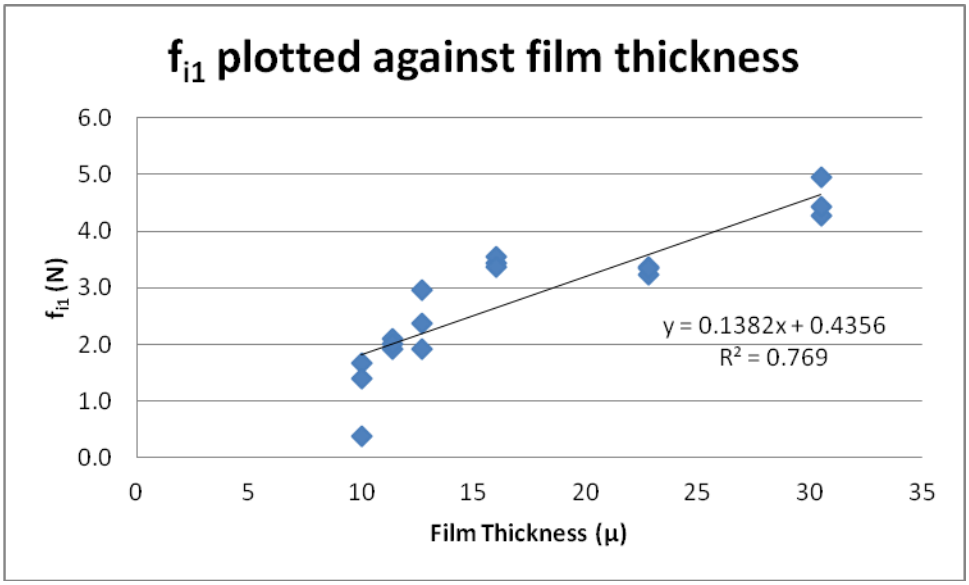

Figure 34 The f_{i1} results are plotted against the original material thickness

The COV of the f_{i1} results are shown in Table 8. There were unacceptably large variations in the f_{i1} data for the Paragon 10µ and the Intertape 12.7µ. These data variations were statistically different than the other variations and were most likely due to the large error associated with evaluating a smaller sample size.

The f_{i20} results in Table 8 have an average of 72.97 N and a standard deviation of 27.37 N. They have a range of 75.31 N with a maximum f_{i20} of 110.83 N from the AEP 30.5µ film and a minimum f_{i20} of 35.52 N from the Paragon 10µ film. The Intertape 12.7µ film allowed for higher than expected f_{i20} value while the Paragon 10µ film allowed for a lower than expected f_{i20} value from anticipated linear trend of f_{i20} vs. µ.

A least squares fit was conducted to determine if there was a relationship between the fi20 and the µ. The R^2 of the line was 0.71 indicating that the linear correlation between measured f_{i20} and film thickness is relatively high. A graph of the results and the respective least squares fit is shown in Figure 35. The fit of the least squares line was reduced by the Paragon 10µ and the Intertape 12.7µ results.

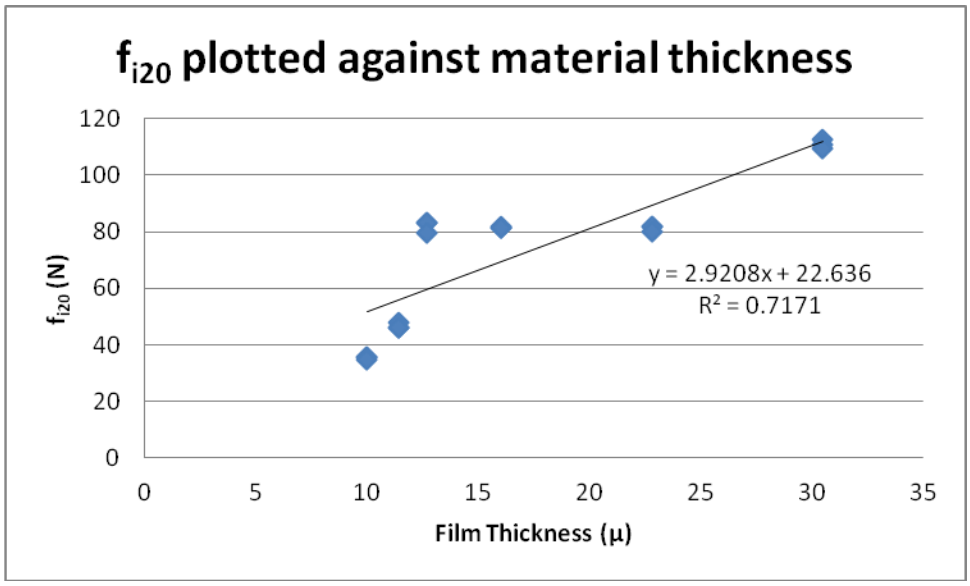

Figure 35 The f_{i20} results are plotted against the original material thickness

The COV of the f_{i20} results are shown in Table 8. There was no significant trend between µ and COV of the samples. The Intertape 12.7µ film had the largest COV of 2.6% and the Intertape 16µ had the smallest COV of 0.3%. The COV of the f_{i1} results are significantly higher than the f_{i20} results due to the large error associated with evaluating the smaller sample size. See section 3.1.3 for details.

A least squares linear correlation was used to calculate the correlation of the f_{i20} values from the f_{i1} values. The form of the correlation model is shown in Equation 3-2. The R^2 of the prediction was 0.75 and the ANOVA conducted on the production found that it was significant [F=643.6814(1,17) Prob>F=<0.0001]. The means that the prediction fit the data relatively well and was significant.

$$\mathbf{f_{i20}} = (\mathbf{f_{i1}} * \mathbf{25.0373}) + \mathit{Error} \qquad \textbf{Equation 3-2}$$

The f_{i20}/f_{i1} results are shown in Table 8. The f_{i20} results are 27 times higher than the f_{i1} results. This is due to the larger strain hardening area compared to the necking area in the larger sample sizes as discussed in Section 2.3.2 and Figure 3. For a proper comparison between the f_{i1} and the f_{i20} samples, the f_{i1} was multiplied by 20. (f_{i1}`). A graphical comparison of the $f_{i1}$` and f_{i20} per the thickness of the film is shown in Figure 36. A graphical comparison of the f_i responses versus the leas square means is shown in Figure 37.

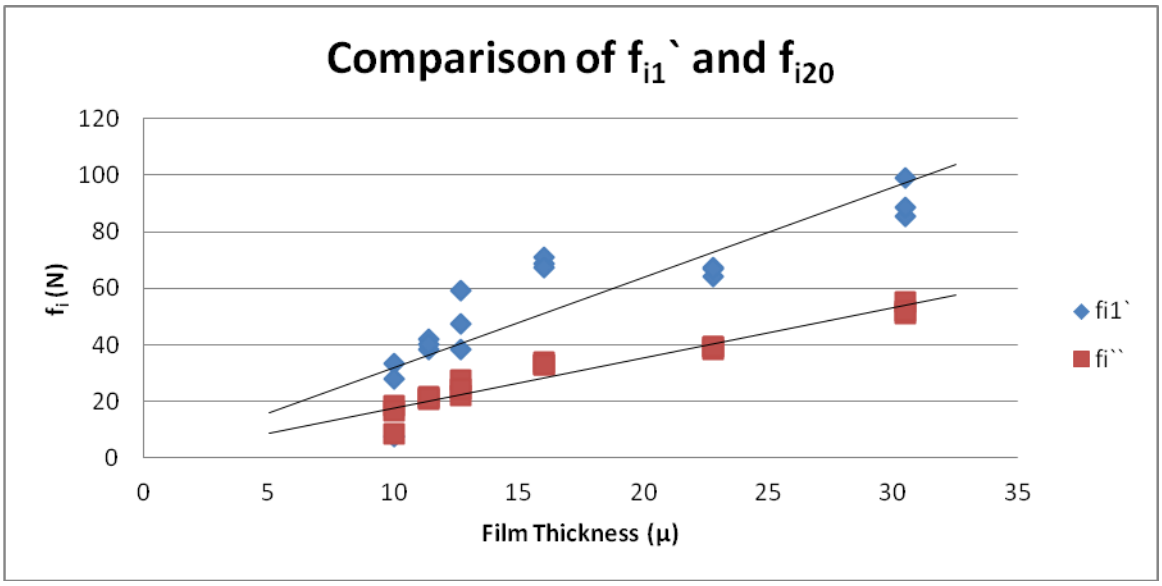

Figure 36 The f_{i1} was multiplied by 20 to calculate the f_{i1}`. This figure shows a comparison between the $s_{b1}$` and the s_{b20} results.

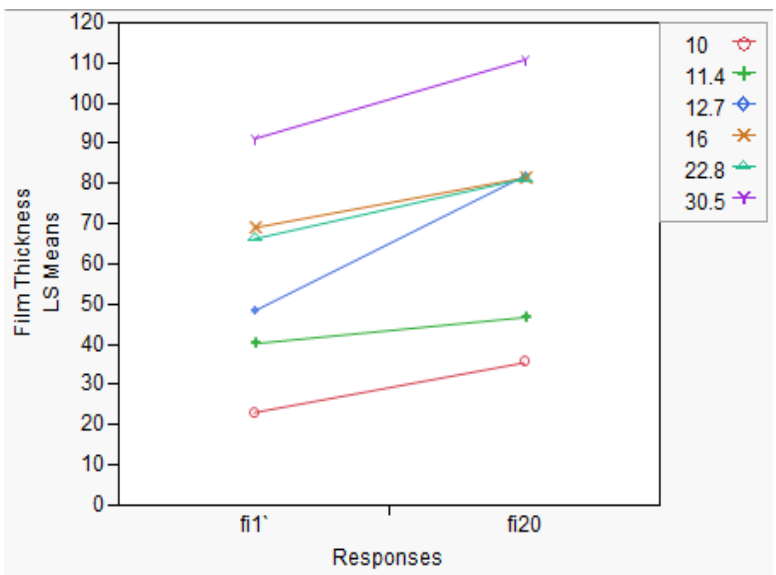

Figure 37 Graphical comparisons of how the means from the f_{i1}`(N) and the f_{i20} (N)compare

A statistical test that allows the multivariate comparison shown in Figure 36 is an ANCOVA. The test determined if the f_i test results were statistically different when compared against the original thickness of the film. Note that the origins were not forced in the ANCOVA, so a more strict comparison could be conducted. The t test results from the ANCOVA are shown in Table 9 ANCOVA t ratio results for all interactions concerning f_i. The results show that there is significant difference between the interaction between the f_{i1} and the f_{i20}, but there is no proof of a significant difference between the f_{i1}` and the f_{i20}.

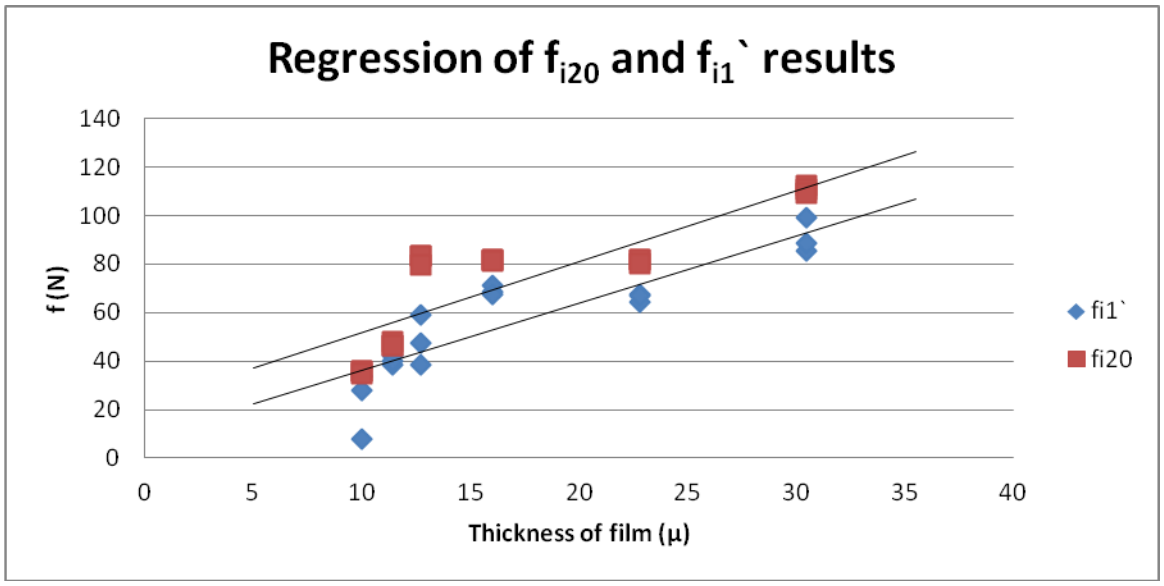

Figure 38 Slopes compared using the ANCOVA analysis. Note that the origin was not forced so an ANCOVA could be conducted.

Table 9 ANCOVA t ratio results for all interactions concerning f_i

	Estimate	Std Error	t ratio	Prob>ltl
f_{i1} vs f_{i20}	-1.3913	0.2295	-6.06	<0.0001
fi_1` vs f_{i20}	-0.0779	0.2974	-0.26	0.7674

The results of the ANCOVA indicate that there is significant difference between the slopes of the f_{i1} and the f_{i20} regressions, however, there is no evidence of a significant difference between the f_{i1}` and the f_{i20} regressions. Because the f_{i1} properly represents the f_{i20} data and the f_{i1} sample preparation method emulates a current ASTM standard (ASTM, 2007), the f_{i1} data set should be used in future comparisons.

In summary, the ANCOVA between the 2.54cm samples and the 50.8cm samples yielded significantly different results. When the results from the 2.54cm samples were adjusted for a common width (x20) to reflect the 50.8cm samples, the ANCOVA found that there was no significant evidence that they were different in terms of overall trends and response. This finding implies that either sample preparation method can be used to compare relative differences in film properties of stiffness and initial force.

The bias ratio between the 50.8cm samples and the 2.54cm samples was relatively consistent at 27 times. This implies that both tests offer the same bias when evaluating either test sample preparation method. This was unexpected as the 2.54cm samples are 1/20 the size of the 50.8cm samples. The larger bias implies that there is a fundamental relationship that is occurring within all the test samples. Further research will have to be conducted to properly understand these relationships.

The COV of the 50.8cm (20”) was consistently lower than the 2.54cm (1”) film, implying that the 50.8cm (20”) test is a more stable and consistent test than the 2.54cm (1”) test. This was expected per the

discussion in Section 3.1.3. The construction of the grips did not allow for a consistent test setup, allowing for variation in initial tension to sample alignment.

The significant correlation between the s_b and f_i and film thickness imply that higher film thickness allows for higher results of the respective test methods. As discussed in Section 2.1 the base material for most stretch film is the same which further justifies the general increase in material properties. Note that surrounding this general increase are other production variables that are able to produce varying s_b and f_i results.

Both the 50.8cm (20") and the 2.54cm (1") sample width test methods seem to be valid for measuring relative differences in film stiffness (s_b) and initial tension force (f_i) after one hour of holding an applied prestretch. However, the 50.8cm film sample is not currently based on an ASTM standard and produced a higher than expected correlation over the 2.54cm film results in the f_i evaluation. This is because of the complicated strain hardening versus necking system which allows for additional error induced into the system. Therefore, the 2.54cm sample size is recommended for use in predicting stretch film behavior as applied to the unit load. Determining which film correlates better to the applied stiffness (s_a) is determined in Section 6. Note that a direct correlation between s_b & f_i and s_a & f_c is not expected per the necking function and the differentiation of stress and strain between the two evaluation methods therefore some functional adjustment may be required.

4.1.4 Conclusion & Summary

The first objective of this research was to evaluate the tensile stiffness of stretch film in a method that simulates the application of stretch film to a unit load. The research in this section satisfied the objective by creating the Bisha Stiffness evaluation method and using two different sample preparation methods to quantify the Bisha Stiffness of multiple films. The Bisha Stiffness method emulated actual film application by initially stretching the film (simulating prestretch), holding the film for a period of time (simulating the amount of time between the application of the film and the evaluation of the film) and then re-extending the film (simulating the evaluation of applied film). The two sample preparation methods used in determining the Bisha Stiffness of a stretch film were a 2.5cm wide sample (s_{b1}) and a 50.8cm wide sample (s_{b20}). It was theorized that the initial force of the Bisha Stiffness would remain constant across sample widths (after normalizing for the sample widths). Therefore, the initial force of the s_{b1} was denoted as the f_{i1} and the initial force of the s_{b20} was denoted as the f_{i20}.

The ANCOVA between the 2.54cm samples and the 50.8cm samples yielded significantly different results. Per the 20x relationship between the 2.54cm and the 50.8cm samples, the results from the 2.54cm samples were multiplied by 20 determine if the smaller samples were representative of the larger samples. After this multiplication, the ANCOVA found that there was no significant evidence they were different. This finding implies that the data from the 2.54cm samples can be used to compare the relative differences against the 50.8cm samples.

A determination of which test method (2.54cm or 50.8cm) accurately represents the material profile that correlates to the applied stiffness of stretch film cannot be made at this time. However, due to the precedent of the 2.54cm sample being established in ASTM D 5459 (ASTM, 2007), the 2.54cm test

method is preferred. Because there are no relative differences between the stiffness and initial force of the two different sample methods, the 2.54cm data sets will be used in comparison with applied film in Section 6.

The differences between the 2.54cm and 50.8cm results were attributed to the discussion surrounding Figure 3 in Section 2.3.2. The s_{b20} samples allowed for proportionally less necking and more strain hardening area compared to the s_{b1} samples. The larger strain hardening area meant that more of the polymer chains were perpendicular with the jaws, leaving the chains in the strongest orientation possible, whereas the s_{b1} samples were mostly consumed by necking, not allowing for the proper proportion of necking to strain hardening and therefore producing smaller s_b values.

In comparing the results of the s_b and f_i test, make note of Table 5 showing the variability of the prestretching imparted on the film. While the prestretch of the different films was evaluated using the same machine settings and techniques, the stretch film/stretch wrapper interaction cannot produce a consistent amount of stretch. This creates a difficult scenario to compare the performance of the films directly without knowing how they behave in the field. In the future, film specifications could offer a suggested prestretch range and comparative tensile testing results on the extremes of the suggested range.

The s_b and f_i results in this section were plotted against the original material thickness. The non-linearity of the results may provide evidence that there are other significant material additives or treatments that can be used to enhance or degrade film performance. Note that these same processes may cause the different films to behave significantly different when under tensile load with regard to necking, material thinning and stress and strain focusing within the sample.

The testing profile developed in this section deviates significantly from the suggested material tensile testing profile identified in ASTM D 5459 (ASTM, 2007). The ASTM test requires the film be stretched and relaxed back to zero between individual extensions (see Section 2.4.2). The testing profile utilized to evaluate the s_b and f_i assumed that the film was never relaxed back to zero. Allowing for the evaluation of the film to be conducted as the film is applied to a unit load. Therefore the past calculations of permanent deformation, elastic recovery and stress retention via ASTM D4649 may not be comparable to calculations using the new testing method. This limitation in the existing standard could also imply that companies who are depending on that testing standard may be misled in developing their stretch films.

5 Evaluating the stiffness of applied film, containment force and the layering effect

The results and conclusions found from the work in this section satisfied the second objective, to evaluate stretch film properties with regard to their stiffness and containment force performance behavior when applied to a unit load. Recall that the base material of stretch film is LLDPE with each film converter mixing in their own concoction of additives, slightly changing the molecular make up of the film, allowing each converter to claim that their film is superior. After the film is extruded, the film is typically stretched during the MDO (machine direction orientation) process beyond its yield stress to align the molecules in the same direction. Note that stretching in the transverse direction is also possible.

When the stretch film is stretched by the prestretch carriage on the stretch wrap machine it further stretches the film beyond its yield stress, further aligning the molecules. According to preliminary research in section 8.2, there can be significant variation in percent stretch imparted on the film by the prestretch carriage. This variation, while large, has not been quantified to determine if there are statistical differences in the performance of the film at the different extensions.

The methods used in applying stretch film and the associated challenges are identified in Section 2.2. There are three general methods used to apply stretch film with hundreds of variations depending on the manufacturer's intellectual property that is associated with that machine (Section 2.2). The simplest method to wrap a unit load with stretch film is the manual wrapping process. The manual process involves having a worker hold the stretch film and physically walk around the unit load applying film in the desired pattern. The next level of complexity with regard to stretch wrapping a unit load involves a semi-automatic wrapping machine, where the unit load is placed in a designated location for wrapping and a machine is manually started that wraps the unit load. For high capacity facilities there is a fully automatic solution in which the unit load is delivered on conveyors and wrapped automatically. The stretch wrapper to be used in this experiment is described in detail in Section 3.2.3.

Recall that the definition of containment force in this research is the force applied by the film on the corner of the test frame (see section 3.2.1). This definition is in contrast to the common market definition of the force required to pull the film out four inches in a specific location on the unit load.

Most unit loads are designed as either square or rectangular shapes that are efficient in terms of storage and packaging design considerations. Such a design means that if the unit load is placed upon a turn table to be wrapped, the outside corners of the unit load move faster than the faces of the unit load. This discrepancy leads to an inconsistent wrapping rate depending on the geometry of the unit load as shown in **Error! Reference source not found.** and discussed in Section 2.2.3. Because of these inconsistencies, the average speed of the turn table was used as an averaging factor when calculating the rotation speed of a unit load, as shown in Figure 18 and discussed in Section 3.2.3.

As stated in Section 2.4.2, the current ASTM standard (ASTM, 2007) requires film to be evaluated over either 60 second or 24 hour intervals. However, in the introduction of Section 3.4, preliminary research using the Bisha Stiffness technique (Section 3.1) determined that the film stabilizes within the first hour

of evaluation. Therefore, in preliminary testing for this experiment, the s_a (applied stiffness) and f_t (tension force) were evaluated on three different films with three different layering variants, using the f_{af} method described in Section 3.2. Each test was replicated a minimum of four times. The resultant f_{af} data was used to calculate the s_a and the f_t per Equation 3-26. Examples of the results are shown in Figure 39 and Figure 40. Note that during this experiment the rotational speed of the unit load was neglected.

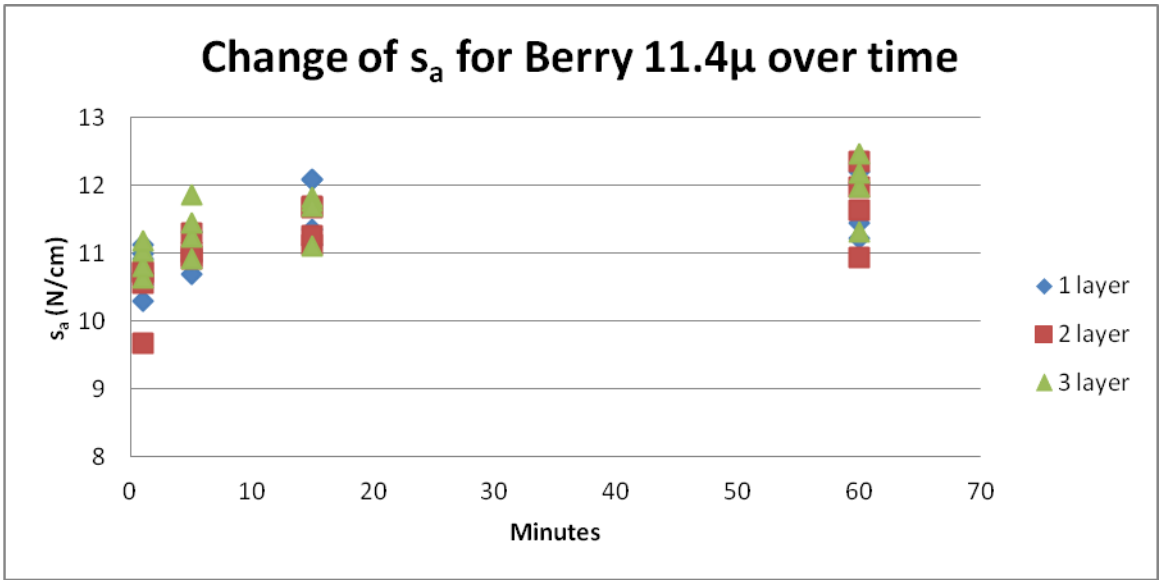

Figure 39 The change in s_a of Berry Plastics 11.4µ over an hour. While there was no discernible layer effect of the film, in every test the s_a increased over time and eventually leveled off in one hour.

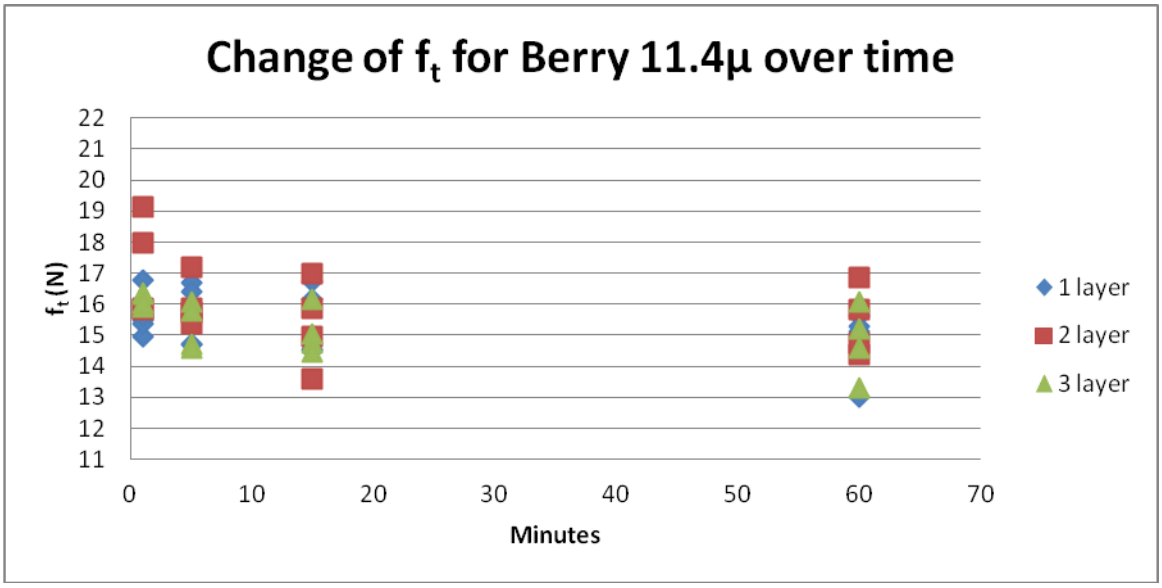

Figure 40 The change in f_t of Berry Plastics 11.4µ over an hour. While there was no discernible layering effect of the film, in every test the f_t decreased over time and eventually leveled off in one hour.

As shown in Figure 39 and Figure 40 the results, in both cases, resulted in a stabilization of the material before the end of the hour long tests which is in line with the preliminary research outlined in the introduction of Section 3.4. In addition, the trend of the s_a is inverse to the trend of the f_t. This is in line with findings in Section 2.3 that state that the stretch film increases in stiffness over time while reducing the amount of tension force required to sustain a given deflection. For a complete explanation of the experiment conducted see Section 8.4 (Appendix).

Preliminary evaluations and the research outlined above indicate the need for a precise method to evaluate the s_a (applied stiffness) and f_c (containment force) of stretch film as applied to a unit load. As previously discussed and identified in the introduction to Section 3.4, stretch film will stabilize an hour after application, therefore, the force required to pull the film off the unit load was evaluated after an hour using two different methods described in Sections 3.2.4 and 3.2.6. The force required to pull the film off the test frame with the pull plate was denoted as the f_{af} and the force required to pull the film off the unit load with the corner method was denoted as the f_{ac}. From the f_a (force of applied film) and extension values (x_a), the s_a (applied stiffness) and f_c (containment force) of film applied to a test frame was calculated and compared.

5.1 Evaluating the applied stiffness and containment force of applied stretch film

This experiment helped to satisfy the second objective of this research. The applied stiffness (s_a) and the containment force (f_c) of the film applied to a test frame are calculated from two different methods that evaluate the f_{ac} (applied corner force) and the f_{af} (applied face force) as identified in Section 3.2. The f_{af} method emulates the current ASTM standard for evaluating containment force (different definition than used in this paper) ASTM D 4649 as discussed in Section 3.2.4. The method used to evaluate f_{ac} on the test frame is a new measurement technique developed for this research which involves wrapping a unit load configured with a bar under the stretch film that is on the corner of the test frame and pulling out on that bar, see section 3.2.6 for details. For definitions of the functions to be explored and the different testing methods used see Materials and Methods Section 3.2.

5.1.1 Experimental Design

Six films were applied to the test frame as outlined in Section 3.2. There were five replicates for the pull plate method and three replicates for the corner method for a total of 48 samples evaluated. The stiffness of the applied film (s_a) and the containment force (f_c) that the film applies to the corner of the unit load was calculated from the force / displacement (Pull plate: f_{af}, x_{af}. Corner: f_{ac}, x_{ac}) data collected during this experiment. The parameter estimation procedure for the experimental design was to allow for the more variable evaluation (f_{af}) to have more repetitions for more accurate results. A visual representation of the experimental design is shown in Table 10.

Table 10 Experimental design for evaluating the s_a and f_c of the applied stretch film

Test Evaluation Method➔	Face of test frame	Corner of test frame
Load Deflection Data Measured➔	f_{af}, x_{af}	f_{ac}, x_{ac}
Parameters Estimated➔	s_{af1},f_{cf1} & s_{af2},f_{cf2}	s_{ac}, f_{cc}
Film Thickness:	Number of test replicates	
10 µ	5	3
11.4 µ	5	3
12.7 µ	5	3
16 µ	5	3
22.8 µ	5	3
30.5 µ	5	3

5.1.2 Materials and Methods

The 6 films used in this section were Paragon 10µ UF 100500, Berry Plastics 11.4µ Stratos, Intertape 12.7µ Stretch Flex, Intertape 16µ Super Flex, AEP 22.8µ A1 and AEP 30.5µ A1 (see Table 11). There was a wide range of material thickness used in this experiment to help determine if there was any correlation between gauge and applied material stiffness.

Each film was loaded into the stretch wrapper and wrapped with the same machine settings allowing for an output prestretch roller speed and turn table speed of 75.692cm/sec (29.8”/Second). For more details on machine operation, see Section 3.2.3. The movement of the prestretch carriage was restricted of movement and only one layer of film was placed on the outside of the test frame. The films were evaluated using the f_{ac} and the f_{af} methods.

As discussed in the introduction each film interacts with the stretch wrapper and test frame differently; therefore, each film was evaluated for its own percent prestretch. The different extensions are shown in Table 11. Note that because the rotational speeds of the stretch wrap turn table and prestretch output rollers are similar, the corners of the test frame traveled faster than the output prestretch rollers while the faces of the test frame moved slower than the output rollers causing the tension to load to stretch the film. For more details see Section 3.1.4.

Table 11 Films and their respective prestretched used in evaluating the f_{af} and f_{ac}

Film Type	% Stretch when Applied to the Test Frame
Paragon 10µ UF 100500	305%
Berry Plastics 11.4µ Stratos	310%
Intertape 12.7µ Stretch Flex	319%
Intertape 16µ Super Flex	300%
AEP 22.8µ A1	297%
AEP 30.5µ A1	297%

In Section 3.2.1, the relationships between the measured loads (f_{ac} and f_{af}) for the two different test methods and the containment force properties (f_a and the s_a, f_t and f_c)were derived and the equation relationships are summarized here in Equations 5-1 and 5-2.

$$\mathbf{f_{ac} = (s_{ac} * x_{ac} + f_{cc}) + error}$$ **Equation 5-1**

$$\frac{\mathbf{f_{af}}}{\mathbf{2} * \sin(\boldsymbol{\beta})} = (\mathbf{s_{af}} * \Delta\ell + \mathbf{f_t}) + \mathbf{error}$$ **Equation 5-2**

Where:

f_{ac} = Force resisted by the applied film measured on the Corner (N). Describes the resistance force of the film applied to a unit load or test frame that has been measured using the bar method (See Section 3.2.6 for methods)

s_{ac} = Stiffness of Applied film (N/cm). Describes the spring stiffness of any single layer of film applied to a unit load or test frame, calculated by dividing the f_{ac} by the x_{ac}

x_{ac} = Distance (cm)the applied film was pulled during the s_{ac} test method

f_{cc} = Containment Force on corner(N). Describes the amount of inward force that a film applies to a corner of a unit load or test frame as evaluated by the bar on the corner

f_{af} = Force resisted by the applied film measured on the Face (N). Describes the resistance force of the film applied to a unit load or test frame that has been measured using the Pull Plate method described ASTM D 4649 and in Section 2.4.1

s_{ac} = Stiffness of Applied film (N/cm). Describes the spring stiffness of any single layer of film applied to a unit load or test frame, calculated by dividing the f_{ac} by the x_{ac}

β = the inside angle between the face of the test frame and the film during f_{af} evaluation

$\Delta\ell$= (cm) Change in length of the film during stretch film evaluation where the initial length (x_i) is subtracted from the finial length (x_f) in the face evaluation. The equation is shown in Equation 5-3.

$$\Delta\ell = \mathbf{x_i} - \mathbf{x_f}$$ **Equation 5-3**

f_t = Tension Force (N). Describes the amount of tension in the film on a given side of the unit load or test frame. Note that by using Pythagorean's theorem, the f_{cf} can be calculated from the f_t of the individual faces of the test frame. The conversion is shown in Equation 5-8.

$$\mathbf{f_{cf}} = \sqrt{\mathbf{f_{t1}^2} + \mathbf{f_{t2}^2}}$$ **Equation 5-4**

f_{cf} = Containment Force on Face (N). Describes the calculated amount of inward force that a film applies to a corner of a unit load or test frame as evaluated by the pull plate on the face of the test frame

The s_a and fc results were visually and statistically compared by forming a regression of the results against the original material thickness and using an ANCOVA to compare the results. The standard form of an ANCOVA is shown in Equation 5-5.

$$y_{ij} = \ddot{\mathrm{U}} + \tau_i + \beta(x_{ij} - \bar{x}) + e_{ij} \qquad \textbf{Equation 5-5}$$

The individual test conducted were

$$\mathbf{s_{ac}} = \ddot{\mathrm{U}} + \tau_i + \beta(\mathbf{s_{af}} - \overline{\mathbf{s_{af}}}) + e_{ij} \qquad \textbf{Equation 5-6}$$

$$\mathbf{f_{cc}} = \ddot{\mathrm{U}} + \tau_i + \beta(\mathbf{f_{cf}} - \overline{\mathbf{f_{cf}}}) + e_{ij} \qquad \textbf{Equation 5-7}$$

Where:

$\ddot{\mathrm{U}}$ = Average of all data analyzed

τ_i = Treatment effect

β = Covariate effect

e_{ij} = error for data set

5.1.3 Results & Discussion

Using the load deflection data collected from the f_{af} and f_{ac} methods, s_{af} and s_{ac} were estimated using Equation 3-20 and Equation 3-26. The results are shown in Figure 41 and the average results are shown in Table 12. The s_{af2} was consistently higher than the s_{af1} by ~15% and higher than the s_{ac} by ~52%.

A linear correlation analyses was used to determine if there are independent relationships between the s_{af1}, s_{af2}, s_{ac} and the μ. Note that analysis forced the trend line through the origin because there is no stiffness when there is no thickness. The R^2 of the respective pairings was 0.94, 0.64 and 0.85 implying that the regression of the s_{ac} fit just as well as either s_{af} value. The regressions are shown below in Figure 41. How the means from each test method, per the film thickness, compare to each other is shown in Figure 42. As previously discussed, the s_{ac} is consistently lower than either s_{af} evaluation.

Table 12 Average results for s_{af} and s_{ac}

	Thickness (μ)	s_{af1} (N/cm)	s_{af2} (N/cm)	s_{ac} (N/cm)
Paragon	10	6.32	6.79	4.01
Berry	11.4	7.74	9.64	6.73
Intertape	12.7	7.99	10.20	5.72
Intertape	16	10.49	13.47	9.01
AEP	22.8	13.01	13.24	9.69
AEP	30.5	17.07	17.81	13.05

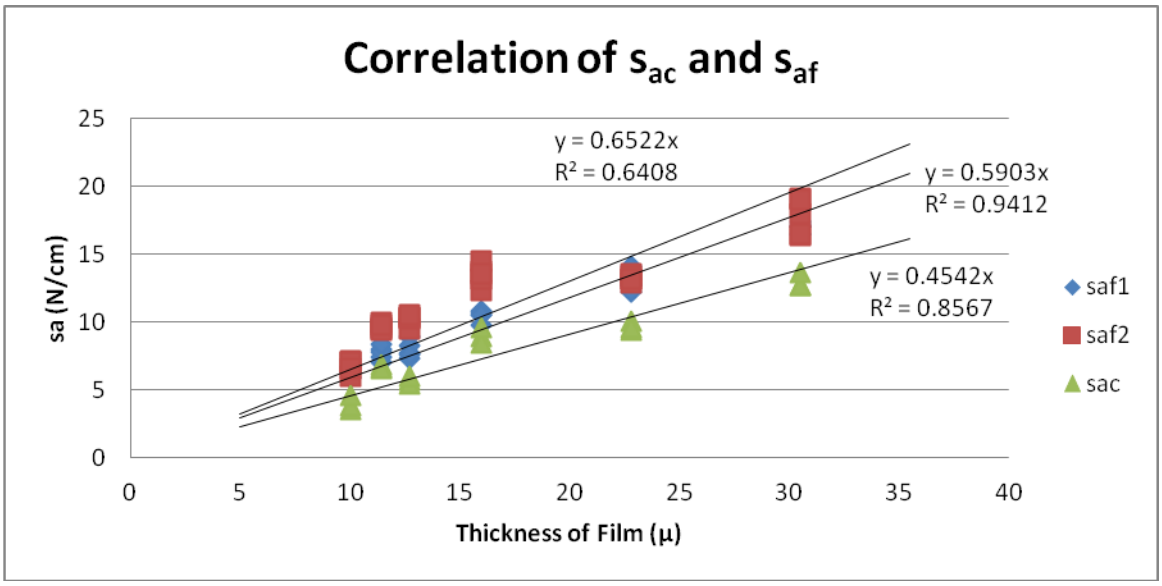

Figure 41 Correlation of s_{ac} and s_{af} results, note that s_{ac} is consistently lower than either s_{af}. The s_{ac} is the stiffness of the film measured via the corner test while the s_{af} is the stiffness of the film measured with the face test. Note that the trend lines are forced to fit the origin.

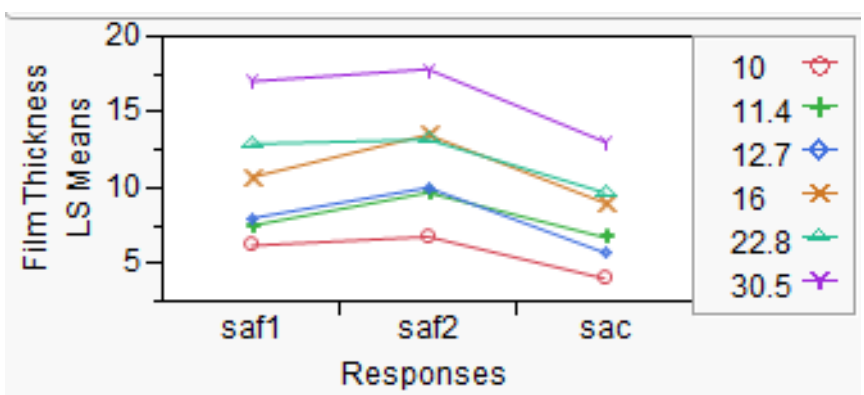

Figure 42 Graphical comparisons of how the means from the s_a (N/cm) testing compare

The COV of the average s_a results are shown in Table 13. All of the COV's were within the same range except the s_{ac} for the Paragon 10µ film.

Table 13 COV of s_a results.

	Thickness (μ)	s_{af1}	s_{af2}	s_{ac}
Paragon	10	4.3%	6.9%	13.4%
Berry	11.4	6.3%	2.5%	2.5%
Intertape	12.7	7.9%	4.1%	5.1%
Intertape	16	3.7%	6.0%	6.6%
AEP	22.8	5.4%	1.9%	3.3%
AEP	30.5	2.1%	7.5%	4.2%

The statistical analysis that was used to test if the regressions of the s_{af1}, s_{af2} and s_{ac} per the thickness of the film were different (as shown in Figure 43) is an analysis of covariance (ANCOVA). The t-ratio results from the interactions of the ANCOVA are shown in Table 14. The high probability results indicate that there is no statistically significant proof that the s_{ac} & s_{af2} and the s_{af1} & s_{af2} are different.

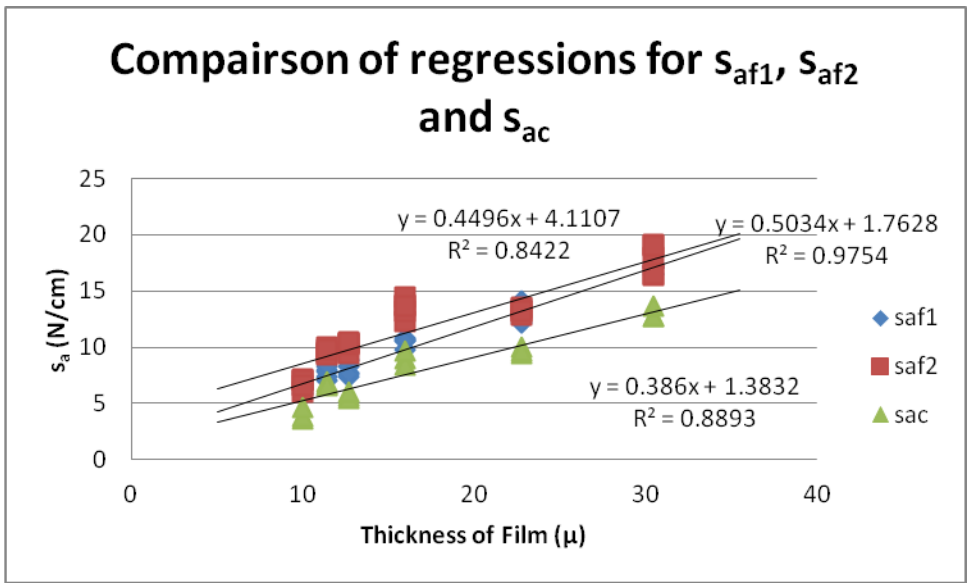

Figure 43 Comparison of regressions for s_{af1}, s_{af2} and s_{ac}. Note that the origin in not forced within the ANCOVA analysis.

Table 14 ANCOVA t ratio results for all interactions concerning s_a

	Estimate	Std Error	t ratio	Prob>ltl
s_{ac} vs s_{af1}	-0.0586	0.0162	-3.6	0.0008
s_{ac} vs s_{af2}	0.0317	0.0272	-1.17	0.249
s_{af1} vs s_{af2}	0.0269	0.0198	1.35	0.181

The proven significant difference between the s_{ac} and the s_{af1} implies that it would be redundant to further test the s_{af2} in Section 6, which was found as not different as either. Therefore, the s_{ac} will be

used because it is a direct test method used in collecting unit load containment data and the s_{af2} will not be used because there is no statistical evidence that it is different from the s_{af1}.

Using the load deflection data collected from the f_{af} and f_{ac} methods, f_{cf} and f_{cc} were estimated using Equation 3-20 and Equation 3-26. The results are shown in Figure 44 and the average results are shown in Table 15. The f_{cf} was mostly higher than the f_{cc} and the f_{cf} was much more uniform and linear than the f_{cc}.

A linear correlation analyses was used to determine if there are independent relationships between the f_{cf}, f_{cc} and the µ. Note that analysis forced the trend line through the origin because at no thickness of film there should be no stiffness. The R^2 of the respective pairings was 0.97 and 0.58 implying that the regression of the f_{cf} was a much better fit than the f_{cc}. The correlations are shown below in Figure 44. Note that the f_{cc} AEP 22.8µ analysis did not follow the anticipated trend and therefore skewed the analysis. How the means from each test method, per the film thickness, compare to each other is shown in Figure 45. As previously discussed, except the AEP 22.8µ film, the containment forces are relatively consistent.

Table 15 Average f_c results

	Thickness (µ)	f_{cf} (N)	f_{cc} (N)
Paragon	10	21.26	22.92
Berry	11.4	23.16	16.62
Intertape	12.7	26.41	27.71
Intertape	16	30.77	24.39
AEP	22.8	41.91	20.53
AEP	30.5	60.20	59.14

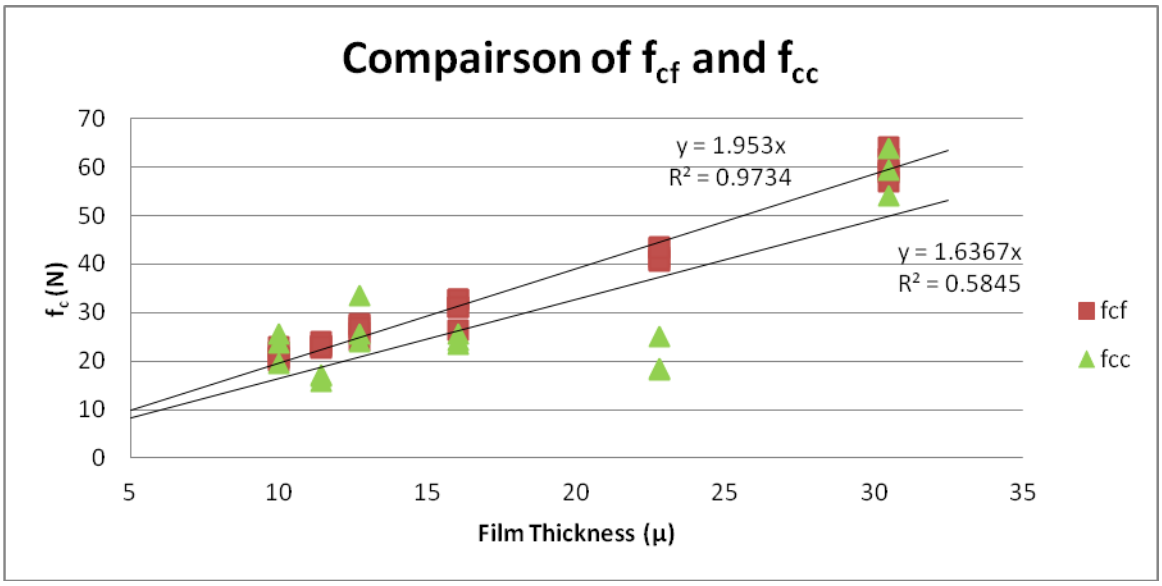

Figure 44 Correlation of f_{cf} and f_{cc} results. The f_{cf} is much more linear than the f_{cc} results due to the AEP 22.8µ film producing lower than anticipated results. Note that the trend lines are forced to fit the origin.

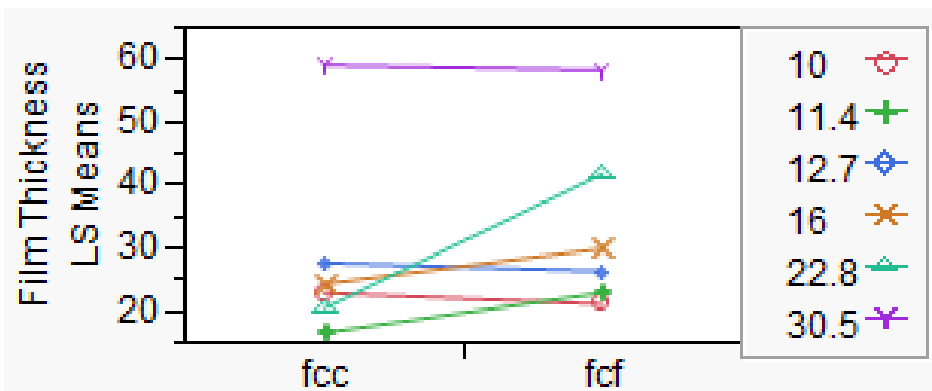

Figure 45 Graphical comparisons of how the means from the f_c (N) testing compare

The COV of the average f_c results are shown in Table 16. Half of the COV's of the f_{cc} test are within the same range as the f_{cf} test. The outliers with higher COV's are the Paragon 10µ, Intertape 12.7µ and the AEP 22.8µ films.

Table 16 COV of f_c results

	Thickness (μ)	f_{cf}	f_{cc}
Paragon	10	5.3%	13.7%
Berry	11.4	2.0%	4.4%
Intertape	12.7	5.2%	18.4%
Intertape	16	8.4%	4.5%
AEP	22.8	3.2%	19.3%
AEP	30.5	4.7%	8.3%

The statistical analysis that was used to test if the regressions of the f_{cf} and f_{cc} per the thickness of the film, as shown in Figure 46, was an ANCOVA. The t ratio results from the ANCOVA are shown in Table 17. The high probability results interaction indicate that there is no statistically significant proof that the f_{cc} and the f_{cf} are different

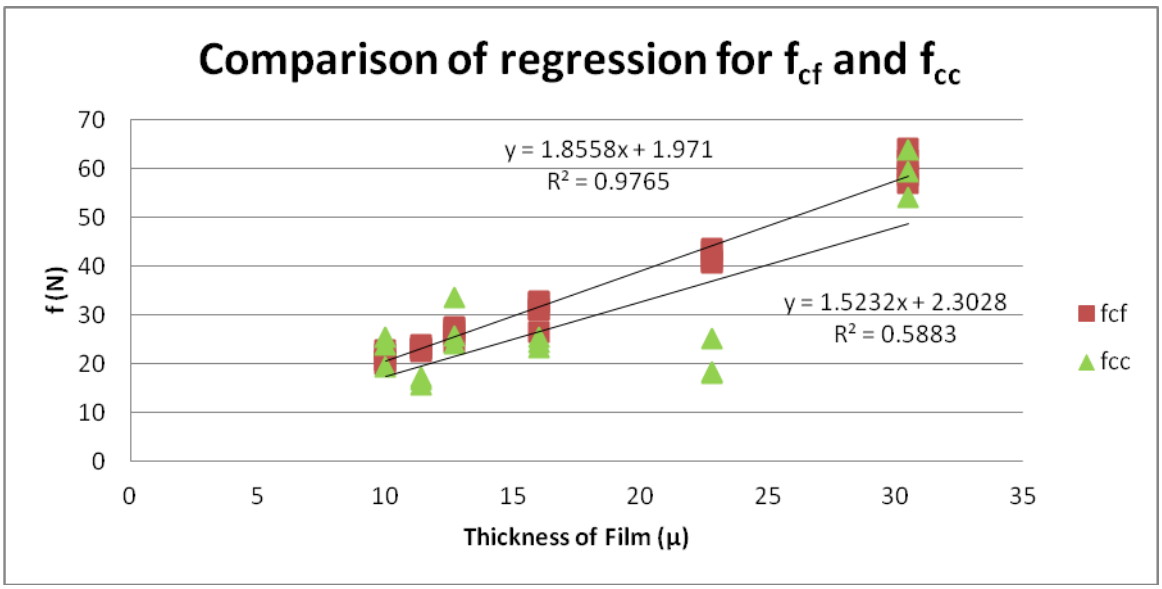

Figure 46 Comparison of regressions for f_{cf} and f_{cc}. Note that the origin is not forced within the ANCOVA analysis

Table 17 ANCOVA t ratio results for the interaction between f_{cc} and f_{cf}

	Estimate	Std Error	t ratio	Prob ltl
f_{cc} vs f_{cf}	-0.1663	0.1265	-1.31	0.195

The insignificant difference between the results of the two test methods mean that either the f_{cc} or the f_{cf} can be used to predict the f_c applied to the test frame. During comparison of f_c to the f_i in Section 6 either data set can be used. The f_{cc} is a direct measurement of the containment force and therefore a better choice for such a comparison. However, because of the low AEP 22.8μ f_{cc} data series and the high COV associated with the f_{cc}, both the f_{cc} and the f_{cf} will be used to compare to the f_i data set.

In summary, the ANCOVAs provided statistical evidence that when the s_a data is plotted against the original material thickness, the s_{ac} and s_{af2} and the s_{af2} and s_{af1} are not significantly different but the s_{ac} and s_{af1} are significantly different. Therefore, the s_{ac} and s_{af1} will be used in comparing against the Bisha Stiffness in Section 6. The results also provided that there was no difference between the f_{cc} and the f_{cf}, but due to the large COV and lack of trend line of the f_{cc} data, both the f_{cc} and the f_{cf} data sets will be used in future comparisons.

The COV's of the different data sets imply that the method for evaluating the s_a of a given film will produce approximately the same error set while evaluating the f_c with the corner method (f_{cc}) will produce slightly higher error within the data. The higher COV of the f_{cc} data set is related to the evaluation bar falling off the corner of the test frame during the f_{ac} evaluation. To reduce this error, either a lighter bar could be used or the bar could be attached to a track system that would prevent the drop of the bar and ensure that the bar is pulled in the same direction during each evaluation.

The variability of evaluating the f_{af} with the pull plate includes precision errors associated with ASTM test configuration of manually pulling the plate out from the unit load at a angle that was not perfectly perpendicular with the face of the test frame. An additional and more likely significant error is associated with the supplementary force vectors acting on the pull plate, as described in Figure 22. How the force vectors change as the plate is pulled from the test frame is beyond the scope of this study.

The variability of evaluating the f_{ac} with the bar on the corner of the test frame includes the potential for the film to slowly creep off the bar during the evaluation as was happening during the evaluation of the Bisha Stiffness – Tube (s_{bt}) in Section 8.4 (Appendix). Another possible cause of error could have been the angle at which the film was pulled off the corner of the test frame was chosen by wrapping the test frame and pulling with the bar until the test frame rotated (on the turn table) and until both sides of the test frame were exerting equal force allowing the test frame to remain still during the f_{ac} evaluation. If the fixed position changed during the evaluation of the f_{ac}, the values would be lower than the actual values. This changing position was not observed during any of the tests. Similar phenomena could occur if the test frame was able to slowly slide along the turn table during the f_{ac} evaluation. This sliding was not observed, but would result in lower than anticipated values.

5.1.4 Conclusions & Summary

The second objective of this research was to evaluate stretch film properties with regard to their performance behavior when applied to a unit load. This section satisfied this objective by quantifying the stiffness of the applied film (s_a) and the containment force (f_c).

Due to the ANCOVA results, the s_{ac} & s_{af1} and the f_{cc} & f_{cf} should be used in comparison against the Bisha Stiffness and initial force in Section 6. The s_{af2} data set will not be used in this research because the s_{af1} and the s_{af2} were determined to have no statistical difference. Both f_c data sets will be used despite there being no difference between the two because the f_{cc}, although more erroneous, is a more direct evaluation of the direct force on the corner.

The results in this section are only relevant for this stretch wrapper at these settings. If the machine settings were to change, the results would change in a proportional manner depending on the ratio of

speed differential between the turn table and the output prestretch roller (slack). How the slack affects the applied stiffness and containment force is the next step in determining how to predict stiffness and containment force. It is anticipated that there is a minimum slack level of effective application, a point where the films no longer act as a single layer of film, allowing too much slippage between films and slippage around the corners of the unit load. Note that slack will change stiffness and containment force readings, but the relationship between the face evaluation and the corner evaluation should remain the same.

When applying the Intertape 12.7µ and the AEP 22.8µ films to the test frame both films did not lay flat on the roll as seen in Figure 47 and Figure 48. These flaws could lead to a lower than desired stiffness or containment force when applying the film. Note that at least 15.2m (50 ft.) of unstretched film was taken off the rolls before films samples were taken and the more film was on the roll the more the errors in the film were observed.

Figure 47 Roll of AEP 22.8µ film used in testing with irregular profile

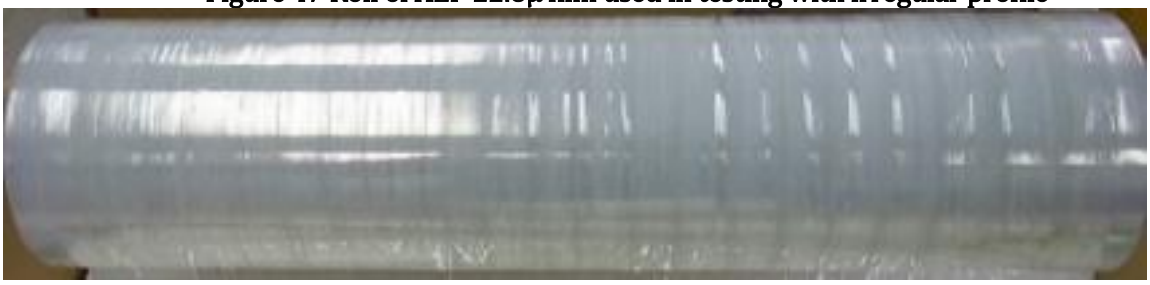

Figure 48 Roll of Intertape 12.7µ film used with irregular profile

The f_{ac} test was developed for this research and has application within the stretch film market place. The testing method could be used on actual unit loads to calculate the average force to damage the corners of the unit load in question. Stretch film applies the most force to the corners of the unit load during the application of the film; therefore, if the film is applied and immediately evaluated for f_c, the maximum force applied to a unit load without damage can be quantified.

5.2 Evaluating the layering effect on the applied stiffness and containment force of the film

The layering process is an essential part of almost all wrap patterns as outlined in Section 2.2.5. The ability to layer film allows the users to place more film on areas within a unit load that need more stabilization. There is one base wrap pattern on top of which many variations of the same pattern are applied. The base pattern is a double spiral wrap of film over the entire exterior of the unit load. One layer will be a spirally wrapped up and the other will be spirally wrapped down. To build upon this base wrap pattern, there are parallel wrapped layers applied to the top and bottom of the unit load depending on user specification. The results of this section are the final piece to theoretically calculating the wrap patterns stiffness and containment force.

As discussed in the literature review in Section 2 and the introductions to Sections 3.4, 5, and 5.1, the base material of stretch film is LLDPE with each film converter mixing in their own concoction of additives, slightly changing the molecular make up of the film, allowing each converter to claim that their film is superior. After the film is extruded, the film is typically stretched during the MDO (machine direction orientation) process beyond its yield stress to align the molecules in the same direction. Note that stretching in the transverse direction is also possible.

When the stretch film is stretched by the prestretch carriage on the stretch wrap machine it further stretches the film beyond its yield stress, further aligning the molecules. According to preliminary research, there can be significant variation in percent stretch imparted on the film. This variation, while large, has not been quantified to determine if there are statistical differences in the performance of the film at the different extensions.

The methods used in applying stretch film and the associated challenges are identified in Section 2.2. There are three general methods used to apply stretch film with hundreds of variations depending on the manufacturer's intellectual property that is associated with that machine (Section 2.2). The simplest method to wrap a unit load with stretch film is the manual wrapping process. The manual process involves having a worker hold the stretch film and physically walk around the unit load applying film in the desired pattern. The next level of complexity with regard to stretch wrapping a unit load involves a semi-automatic wrapping machine. This is typically where the unit load is placed in a designated location for wrapping and a machine is manually started that wraps the unit load. For high capacity facilities there is a fully automatic solution where the unit load is delivered on conveyors and wrapped automatically. The stretch wrapper to be used in this experiment is described in detail in Section 3.2.3.

Most unit loads that are wrapped are either square or rectangular. This means that if the unit load is placed upon a turn table to be wrapped, the outside corners of the unit load move faster than the faces of the unit load. This discrepancy leads to an inconsistent wrapping rate depending on the geometry of the unit load as shown in Figure 18 and discussed in Section 2.2.3. Because of these inconsistencies, the average speed of the turn table was used as an averaging factor when calculating the rotation speed of a unit load, as shown in Figure 18 and discussed in Section 3.2.3.

Preliminary research in tensile testing in Section 3.4 and film application in Section 5 indicated that stretch film will stabilize an hour after application, meaning that over the first hour, the stiffness of the film is increasing as the containment force of the film is decreasing. After that hour has passed, the

stiffness and containment force continue to change in their respective directions, however, at a very low rate.

The following experiment used three films and similar methods from Section 5.1 to understand how layering affects the stiffness and containment force of applied stretch film. This experiment will further satisfy the second objective in evaluating stretch film properties with regard to their performance behavior when applied to a unit load.

5.2.1 Experimental Design

Three films were applied to the test frame as outlined in Section 3.2. Each film was wrapped in one, two and three layer variants with three replications per test for a total of 27 samples evaluated. The stiffness of the applied film (s_{ac}) and the containment force (f_{cc}) that the film applies to the corner of the unit load was calculated from the force / displacement data (f_{ac}, x_{ac}) collected during this experiment. The purpose of this design was to allow the film properties to be measured over the three most typical layering variants as discussed in Section 2.2.5.

Table 18 Experimental design for evaluating the s_{ac} and the f_{cc} of the different layers of applied film

Test Evaluation Method➔	Corner of test frame		
Load Deflection Data Measured➔	f_{ac}, x_{ac}		
Parameters Estimated➔	s_{ac}, f_{cc}		
Film Thickness:	1 Layer	2 Layers	3 Layers
10 µ	3	3	3
12.7 µ	3	3	3
22.8 µ	3	3	3

5.2.2 Materials and Methods

The three film used were Paragon's 10µ, Intertape's 12.7µ and AEP's 22.8µ. Each film was applied to the test frame and wrapped with the machine settings allowing for a turn table and output prestretch roller speed of 75.692cm/sec (29.8"/sec) which was the same setting as used in Section 5.1 and discussed in Section 3.2. The film was evaluated using the f_{ac} evaluation method outlined in Section 3.2.6.

The f_{ac} and f_{cc} data was used to calculate the s_a and f_c of the different layers using Equation 5-8. The results were analyzed using a Tukey's HSD with a CI of 95% to compare groups of means.

$$f_{ac} = (s_a * x_{ac} + f_c) + error \qquad \text{Equation 5-8}$$

Where:

f_{ac} = Force resisted by the applied film measured on the Corner (N). Describes the resistance force of the film applied to a unit load or test frame that has been measured using the bar method (See Section 3.2.6 for methods)

s_a = Stiffness of Applied film (N/cm). Describes the spring stiffness of any single layer of film applied to a unit load or test frame, calculated by dividing the f_{ac} by the x_{ac}

x_{ac} = Distance (cm)the applied film was pulled during the s_{ac} test method

f_c = Containment Force (N). Describes the amount of inward force that a film applies to a corner of a unit load or test frame

5.2.3 Results & Discussion

The average results of the s_{ac} calculations are shown in Table 19. The s_{ac} initially applied to the test frame increased with the thickness of the applied film. Each additional layer resulted in incrementally greater s_a depending on material thickness.

Table 19 Average results of s_{ac} for layer evaluation

	Thickness (µ)	1 Layer (N/cm)	2 Layer (N/cm)	3 Layer (N/cm)
Paragon	10	4.01	10.99	16.46
Intertape	12.7	5.72	14.16	23.24
AEP	22.8	9.69	22.35	34.13

The COV's of the results for the s_a evaluation of the layering test are shown in Table 20. The Paragon 10µ COV was notably higher at 13% however, using a Tukey's analysis on the entire data set the COV's were determined to be statistically the same.

Table 20 COV of the s_{ac} results for layer evaluation

	Thickness (µ)	1 Layer	2 Layer	3 Layer
Paragon	10	13.4%	2.7%	3.9%
Intertape	12.7	5.1%	2.1%	3.9%
AEP	22.8	3.3%	8.5%	4.7%

The two pieces of information that are critical to determining how to build a wrap pattern are the amount of s_{ac} that is added per layer and when that amount becomes a diminishing return in performance when considering marginal costs due to application and thicker film materials. The amount of s_{ac} that was added per layer was determined by plotting the s_{ac} against the number of layers applied. The raw results with projections are shown in Figure 49. The general trend of each plot was upward (as expected), with the amount of s_{ac} per layer increasing more as the thickness of the original material increases. This trend allowed for the comparison of the increase in the s_{ac}/layer per the original thickness of the material in Figure 50. With only three data points, the averaging s_{ac}/layer per thickness of film is not robust enough to be used as an industry wide averaging guide for all films.

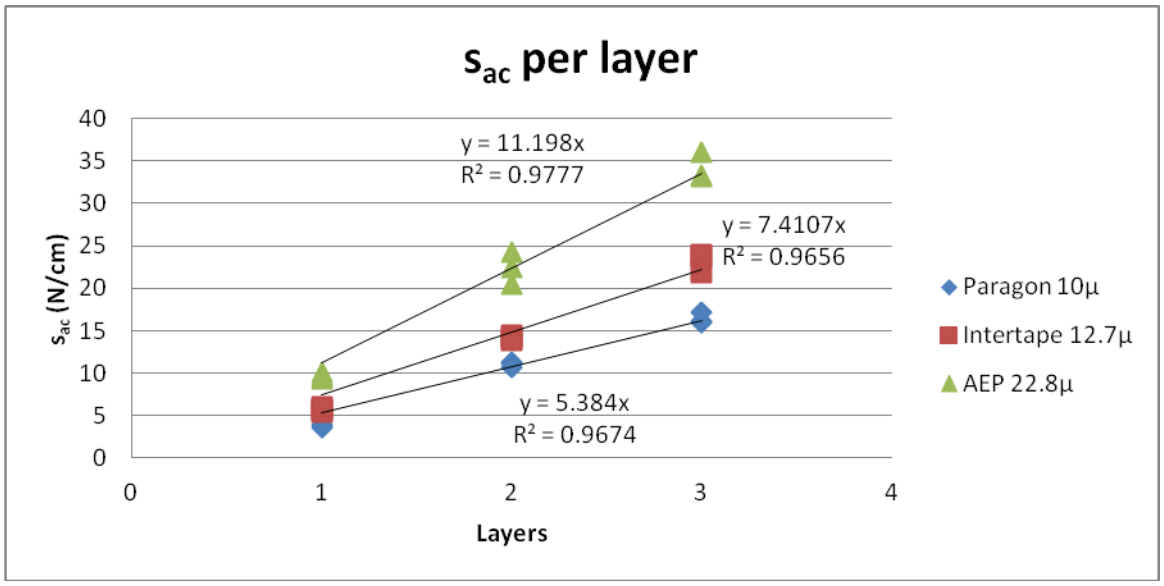

Figure 49 s_{ac} per layer of film applied to the test frame.

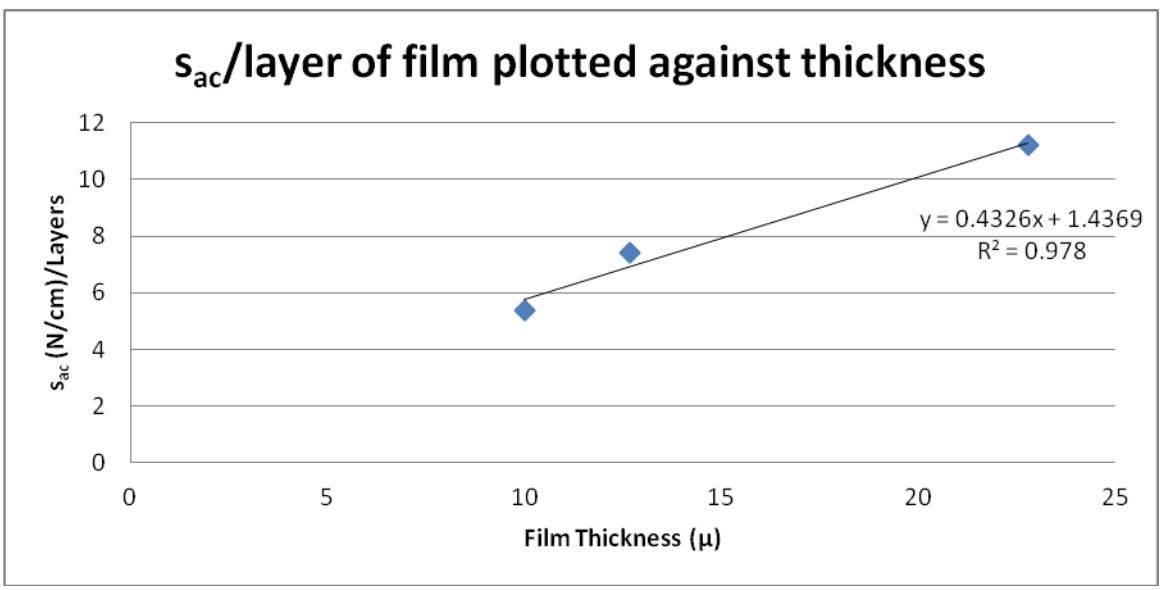

Figure 50 Plot of the increase in s_{ac}/layer applied to the test frame per thickness of film.

In Table 19, the doubling of the s_{ac} from the first layer equals less than the s_{ac} from the second layer, therefore, there is an additive effect that is occurring when film is applied on top of itself. This was called the applied stiffness affect (s_{aa}). The s_{aa} each film per layer applied is shown in Figure 51. The effect was calculated by Equation 5-9. If a thinner film has a larger additive effect than a thicker film, the thinner film may be able to surpass the performance of the thicker film in the s_{ac} test. Note that two layers of Paragon 10µ is a total thickness of 20µ and that there are so few data points a statistical comparison is unpractical.

$$\text{Additive } s_{ac} = s_{ac} - 1 \text{ layer } s_{ac} * l_n$$ Equation 5-9

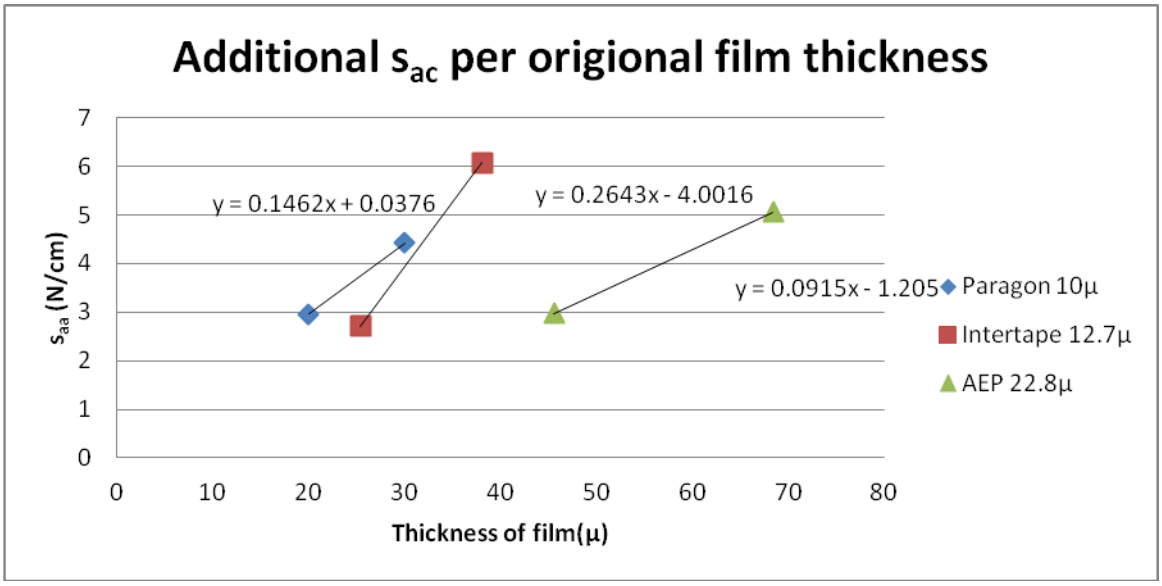

Figure 51 The additive s_{ac} effect of each film is shown. This is a very powerful comparison which may prove that thinner films can behave like thicker films.

The average results of the f_{cc} calculations are shown in Table 21. The force that was initially applied on the corner of the test frame was relatively consistent at approximately 24N. But when layers of film were added to the system, the amount of force that each additional layer added depended on the thickness of the film. The consistency of the initial force applied to the unit load should correspond to the respective machine settings. If the ratio between the turn table and the output prestretch roller would change, this value would change. Then, depending on the initial machine settings, the initial force should stay consistent across all films as they are applied to the unit load as this value is solely determined by the machine settings. More testing will have to be conducted to determine the true relationship.

Table 21 Average results of f_{cc} for layer evaluation

	Thickness (µ)	1 Layer (N)	2 Layer (N)	3 Layer (N)
Paragon	10	22.92	33.93	52.98
Intertape	12.7	27.71	66.47	75.10
AEP	22.8	20.53	67.13	129.60

The COV's of the results for the f_{cc} evaluation of the layering test are shown in Table 22. The COV's of the f_{cc} are much higher than any other data set within this research. This variability can be attributed to the inherent inconsistency of the stretch wrap machine and the wrapping process outlined in Section 2.2. A Tukey's HSD test indicated that none of the COV's were found to be statistically different for any film.

Table 22 COV of the f_{cc} results for layer evaluation

	Thickness(μ)	1 Layer	2 Layer	3 Layer
Paragon	10	13.7%	4.2%	9.1%
Intertape	12.7	18.4%	12.5%	7.4%
AEP	22.8	19.3%	18.2%	39.5%

The raw results of the f_{cc} calculations and the projections for additional layers are shown in Figure 52. Note that one of the AEP 22.8μ data points was excluded from the graph due to its extreme value (3 layers, 187.5N). The general trend of each plot was upward as expected, the amount of f_{cc} per layer increasing more as the thickness of material increases. The relationship between the thickness of the material applied and the slope of the f_{cc} per layer is shown in Figure 53.

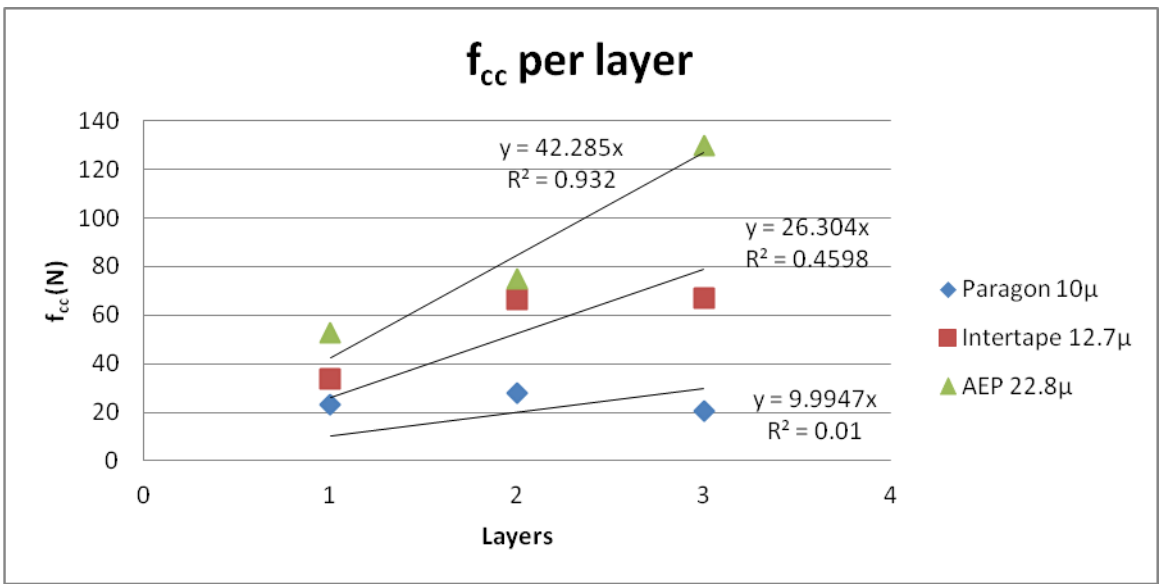

Figure 52 f_{cc} per layer of film applied to the test frame

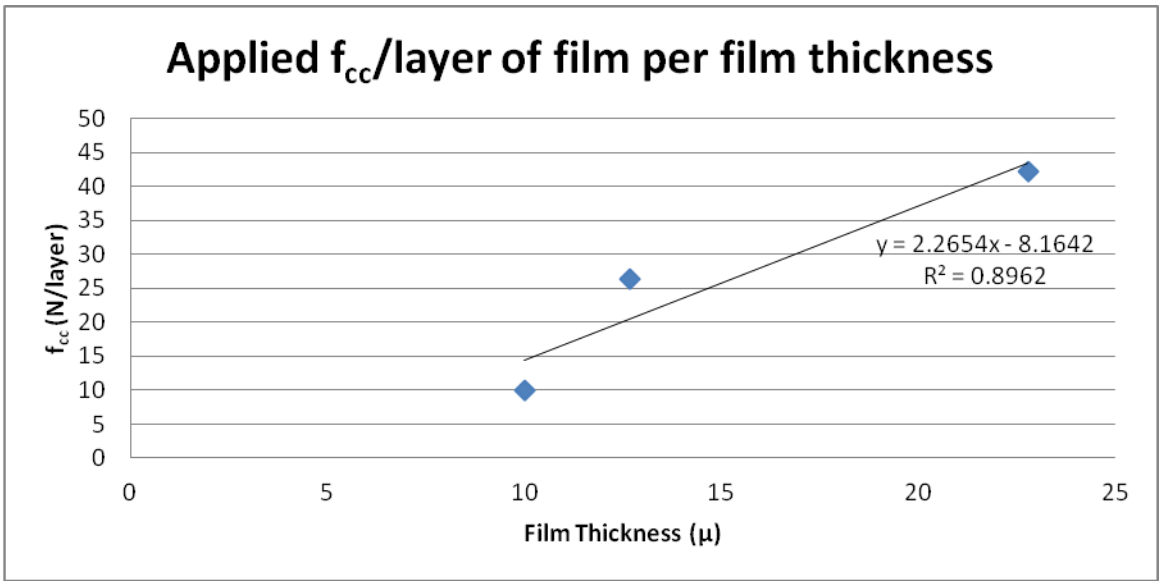

Figure 53 Plot of the increase in f_{cc}/layer applied to the test frame per thickness of film.

In Table 19, the doubling of the f_{cc} from the first layer equals less than the f_{cc} from the second layer in two cases, therefore, there is an effect that is occurring when film is applied on top of its self. This was denoted as the containment force effect (f_{ca}). The f_{ca} of each film per layer applied is shown in Figure 54. The effect was calculated by Equation 5-10. Knowing how the f_{cc} changes when it is applied to a unit load will allow users to be more precise when applying their film. The results indicate that the Paragon 10µ and the Intertape 12.7µ film did not produce any additional f_{cc} effect when layering the film. In contrast to the AEP 22.8µ film, the amount of f_{cc} applied per layer was reduced. This result may be because of the chemical formulation of the film or the amount of prestretch that was imparted on the thin film. Either way, more testing should be conducted to confirm these results. Note that two layers of Paragon 10µ is a total thickness of 20µ and that there are so few data points a statistical comparison is unpractical.

$$\textbf{Additive } f_{cc} = f_{cc} - 1 \textbf{ layer } f_{cc} * l_n$$

Equation 5-10

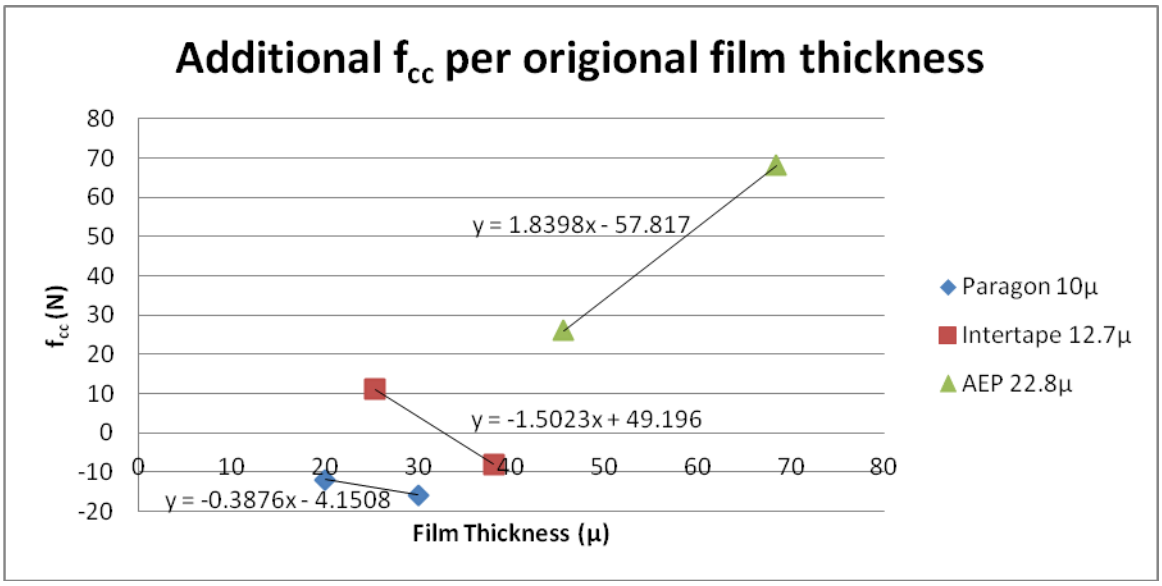

Figure 54 The f_{cc} effect of each film is shown. This comparison provides knowledge as to the layering forces the film applies to the corner of the test frame.

The potential for the sources of errors within the f_{ac} evaluation discussed in Section 5.1, still hold true for the results of this section. The variability of evaluating the f_{ac} with the bar on the corner of the test frame includes the potential for the film to slowly creep off the bar during the evaluation as was happening during the evaluation of the Bisha Stiffness – Tube (s_{bt}) in Section 8.4 (Appendix). Another possible cause of error could have been the angle at which the film was pulled off the corner of the test frame was chosen by wrapping the test frame and pulling with the bar until the test frame rotated (on the turn table) until both sides of the test frame were exerting equal force allowing the test frame to not rotate during the f_{ac} evaluation. If the fixed position changed during the evaluation of the f_{ac}, the values would be lower than the actual values. This was not observed during any of the tests, but for future testing the turn table should be fixed. Similar phenomena could occur if the test frame was able to slowly slide along the turn table during the f_{ac} evaluation. This was not observed, but would result in lower than anticipated values.

5.2.4 Conclusion & Summary

This section satisfied the second objective of understanding how the layering of stretch film affects the applied stiffness and force the film applies to the test frame. Layering of the film when applied is a critical component of any wrap pattern as it allows the user to select where more protection for the unit load is needed. The projection of the additional s_{ac} and f_{cc} per thickness of the original film was an appropriate predictor of performance and will be used in Section 5.3 to determine the s_w (stiffness of wrap pattern) and the f_{cwp} (containment force of wrap pattern).

Recall that the films were applied with consistent tension between the output prestretch rollers and the unit load. As the machine settings are reverted back to more real world application, film slack will be introduced into the system. Slack occurs in the application process when the output prestretch rotates

faster than the turn table. Future research should focus on how slack effects applied material properties. A minimum slack effect is anticipated where there is not enough film to film contact to allow all the layers to act as a single layer and will allow for too much slippage around the corner of the unit load during evaluation. For this reason, the relationship between the additive layering effects of stiffness and containment force are unknown and should be further studied in detail.

This comparison between films that are significantly different in thickness is not relevant, as an end user would not likely be in a position to choose between film thicknesses that are so drastically different. An end user is more likely to require a comparison of two films which have similar thicknesses. Such a comparison would provide the user information as to which film will provide superior stiffness and containment force values assuming that the wrap pattern is consistent.

The results for the f_c evaluation, while similar to the stiffness evaluation, offer a different application utilization by the end user. For example, if a high containment force, medium stiffness film was applied to a fragile unit load, the film may cause damage to the unit load due to the high containment force. However, if a low containment force, medium stiffness film was applied to the same unit load, the film has a much lower potential for damaging the unit load.

In general, the thicker the film applied to a unit load, the more likely the wrap pattern possesses the desired characteristics. Conversely, when applying thinner film, a more precise utilization of the film can be applied, leading to cost savings but potentially more damage if application is not precisely controlled. Note that more layers is more time spent wrapping, more roll changes, more equipment wear, etc. adding to the overall cost of the system. The correct cost/performance analysis should be independently determined for each facility. The information provided by this study can be used to establish a standard method from which to perform such analyses.

5.3 Summary of stiffness and containment force of applied film

This section addressed the second objective, to evaluate stretch film properties with regard to their performance behavior when applied to a unit load. These objectives were achieved by creating a framework of applying one layer of stretch film to a test frame 121.9 x 101.6cm (48x40”) and evaluating that film using two different measurement methods. The pull plate method (f_{af}) emulated the current ASTM standard for film evaluation and was conducted on either side of test frame. The second method involved wrapping stretch film over a unit load test frame configured with a bar on the corner (f_{ac}) and then pulling the bar at a consistent rate. The f_{ac} method estimated applied film stiffness values (s_a) that were lower than those from the f_{af} method and the f_{af} measured on the longer side of the test frame was lower than the f_{af} measured on the shorter side.

The difference in the f_{af} methods were easily explained by the lengths of the different sides of the test frame in conjunction with the changing rotation speed of the test frame. The shorter side is wrapped more quickly than the longer side allowing for less material to be applied at a higher extension then on the long side of the test frame. The lower s_{ac} value has two potential justifications. Either during testing the film it was able to slip off the bar, producing lower than anticipated results or there were extraneous forces acting on the plate during the f_{af} test as identified in Figure 22. The latter justification is much

more likely as the changing geometric effect caused by the rotation during the f_{af} test were evident during the evaluations. During the f_{af} test, the film initially pulled evenly on all edges of the pull plate, but as the plate was pulled out from the face of the test frame, the force on the plate became more focused on the sides of the plate that were parallel with the sides of the test frame.

An ANCOVA was used to compare the regressions of the applied stiffness and containment forces measured with the different methods and plotted against the original material stiffness. The results indicated that there was no significant difference between the slope of the corner stiffness and the stiffness on the short side of the test frame. When the corner stiffness was compared to the stiffness on the long side of the test frame there was a significant difference in the slopes. There was no significant difference in the measured force on the corner of the test frame and the theoretical force from the face evaluation. However, the results of the f_{cc} did not follow the anticipated trend (AEP 22.8µ produced results that were much lower than anticipated), therefore both data sets were used in the upcoming comparisons. All comparisons were conducted with a 95% confidence interval. Due to these results, the corner stiffness (s_{ac}) and the long face stiffness (s_{af1}) and both the containment forces (f_{cf} and f_{cc}) were compared to the Bisha Stiffness and initial force values in Section 6.

The benefit of the pull plate test is that it can be conducted in the field at any time for approximate results. However, the film will most likely slip around the corner of the unit load when conducting this evaluation which can significantly influence the results. This slipping can be limited by applying tape to the corners of the unit load. The tape will provide the stretch film with a surface to adhere to, reducing the amount of slip around the corners. If the tape does not prevent slippage, it will at least cause the film to “jump” as the stretch film is pulled across it, letting the operator know that an error is occurring.

The corner test is more difficult to conduct in the field. Unless the unit load is perfectly centered on the turn table and the unit load is square, the film stiffness on either side of the unit load will be different. This means that during the f_{ac} evaluation, the bar will naturally drift towards the side of the unit load with a higher stiffness making the corner test very difficult to replicate with consistent results.

In both cases, the face and the corner appear to be stable predictors of applied film properties. This result implies that the face test, despite the unknown geometry effects leading to a higher bias, could be used to estimate stiffness and containment force of film applied to a unit load.

Note that in both cases, when evaluating different unit loads, the unit load and machine interaction changes when the size of the unit load is changed (smaller unit loads will rotate faster). This change means that if several different size unit loads are used on one stretch wrapper, machine settings may need to change per the unit load to maintain consistent containment and performance. It may be of interest in high flow facilities with consistently sized unit loads to purchase/make a test frame of their own and use it to calibrate their stretch wrapper. Calibrating stretch film on multiple unit load configurations is difficult as the individual units within the unit load can affect the specific containment force applied to one load. This calibration does not have to include a complex test frame. An angle iron frame with a back stop for the pull plate in the desired locations is recommended for an adequate test configuration (see Section 3.2.2 for details).

The results in this research were plotted against the original material thickness. As noted with evaluating the s_b, the lack of linear results may be evidence of other chemical additives, treatments, or other factors not considered affecting the film's performance. This conclusion is consistent with the findings in Section 4.

The layering effect of the film was measured using the f_{ac} method and with one, two and three layer variants. The results showed there is a strong and predictable correlation between the layering of the film and the measured stiffness and containment force, although there were too few results to conduct a thorough statistical analysis. Beyond the regression of the s_{ac} and f_{cc} of the individual films, the additive effect of each value was calculated. The additive effect is how much the stiffness or containment forces increase or decrease with layering beyond an additive function. Note that these additive functions are based on the assumption that the stretch films had enough tackifier to bond one layer to another. When combined with the lack of applied slack in the wrapping sequence, multiple layers acted as a single entity.

In general, the application of a thicker film to a unit load will mean an increased stiffness and containment force, insuring that the unit load will stay intact during transport. In contrast, the application of a thinner film allows for a more precise cost control while potentially increasing the risk for damage. Additional knowledge surrounding the additive forces with multiple layered films, either s_a or f_c, are attributes that allow for the user to fine tune the stretch film as applied to their unit loads.

The data from the layer testing methods was not conclusive enough to create a standard model of film behavior when layering film. Note that such a tool would be powerful for companies, allowing them to compare new film to the existing film market (or their own in house films) to optimize wrapping and layers.

All of the application settings in this section are not representative of real world application and are very specific to the machine settings on the stretch wrapper used. A slight change in a setting would yield different results. However, the relationship between the face evaluations and the corner evaluations should remain constant, even as slack is introduced into the application process. Slack is the speed differential between the output prestretch roller and the turn table of the stretch wrapper. The effect of slack on layering effects should be more significant. The more slack that is introduced into the system, the less film contact there is between layers and the less likely the film is to not slip around the corners during the evaluation.

6 Predicting applied stretch film stiffness and load containment using modified ASTM tensile testing.

This Section addresses the third objective of this research to investigate the relationship between the applied material properties and the film properties as evaluated in a tensile test. The applied material properties were identified as the applied film stiffness (s_a) and the containment force (f_c) that a film can apply to a unit load. The tensile properties of interest were the Bisha Stiffness (s_b) and the initial force of the Bisha Stiffness (f_i). To satisfy the third objective, the s_{ac} and s_{af1} were compared to the s_b and the f_{cf} and f_{cc} were compared to the f_i.

The Bisha Stiffness (s_b) was described in Section 3.1 and was derived and measured in Section 3.4. In summary, the s_b is the stiffness of the film as the film is extended, held and extended on a tensile testing machine as shown in Figure 55. This sample testing profile was chosen because it simulated the prestretch and application of stretch film to a unit load. The final stretch of the film during the s_b test emulates the stretch of the film during the physical evaluation of the film.

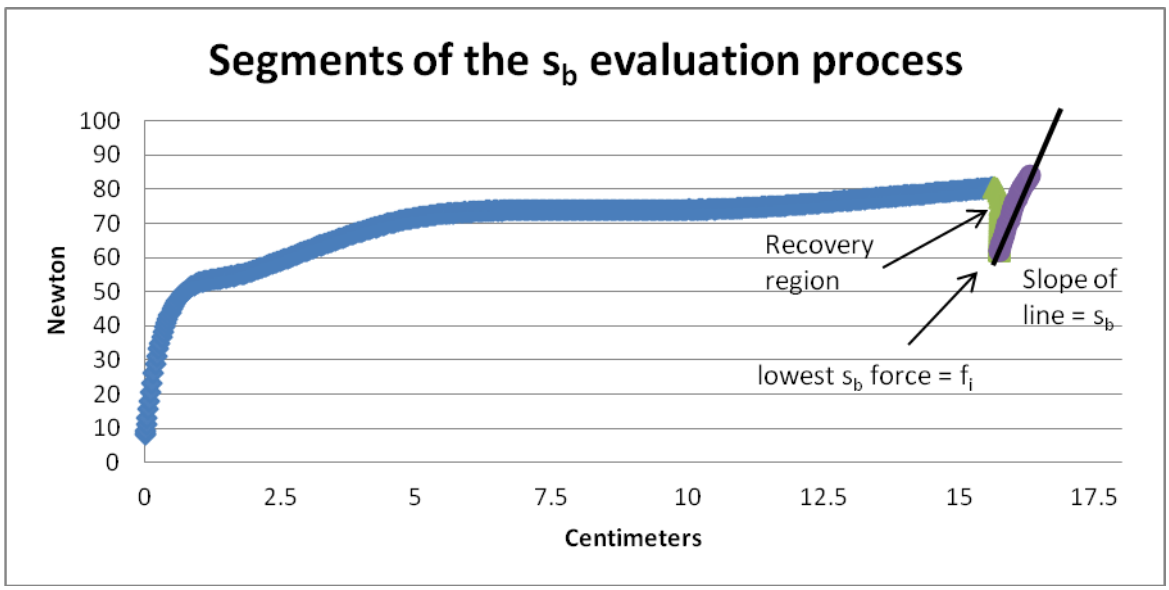

Figure 55 Different segments of the proposed tensile test profile identified

There were two sample preparation methods used in evaluating the s_b, the first emulated the current ASTM D 5459 (ASTM, 2007) standard allowing for a 2.54cm (1”) wide sample that was 12.7cm (5”) long (s_{b1}). The second sample preparation method used a 50.8cm (20”) wide sample that was 12.7cm (5”) long (s_{b20}). This sample preparation alternative was chosen to ensure that a 2.54cm wide sample properly represented a 50.8cm wide sample. Note that the Initial force (f_i) of the s_b evaluation was recorded to determine if it would correlate to the containment force of an applied film.

The tests were conducted at the same speed on the same machine. The s_{b1} samples where held with grips that were purchased from MTS (shown in Figure 8). The s_{b20} samples were held with modified grips made out of wood, wrapped in hand stretch film and secured with 4 bolts shown in Figure 7.

As expected, the results from the two data sets were significantly different. The expected 20:1 ratio between the two sets of results did not occur. The s_{b20} and f_{i20} results were 27 times higher for the s_b and f_{i1} results. This was due to the much larger strain hardening area in the s_{b20} samples as shown in Figure 56.

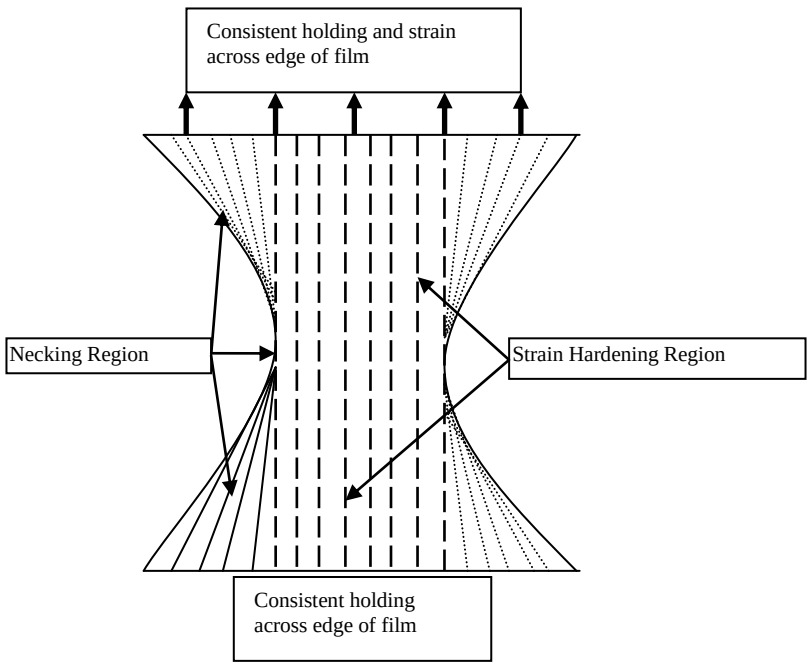

Figure 56 Crystalline alignment with a film under strain

An ANCOVA was used in comparing the effect of material thickness (μ), test method and thickness and test method interaction. For this comparison the force from the s_{b1} data was multiplied by 20 (s_{b1}`) to compare against the 50.8cm (20”) data. Note that this also included the $f_{i1}$ data set ($f_{i1}$`). The results indicated that there was no significant difference between the s_{b20} & s_{b1}` and the $f_{i20}$ & $f_{i1}$` meaning the s_{b1} and the f_{i1} results represent the larger s_{b20} and f_{i20} results. Therefore the comparisons in this section were conducted with the smaller (2.54cm) sample evaluation methods.

In addition to the ANCOVA results, the larger ratio of necking to strain hardening in the s_{b20} samples, the imperfect grip setup and the lack of ASTM standard that calls for the evaluation of wider films to the utilization of the s_{b1} samples when comparing stiffness between the s_b samples and the applied stiffness of the films. Note that the necking phenomena may be cause for some functional adjustments when comparing the s_b data to the applied stiffness data.

The stiffness (s_a) and containment force (f_c) of stretch film applied to a test frame were derived in Section 5. The s_a and f_c were estimated using two different methods, the pull plate (s_{af} and f_{cf}) and the bar (s_{ac} and f_{cc}). The pull plate emulates the current ASTM standard with a few slight modifications found in Section 3.2.4. The pull plate was placed under the film and pulled out allowing for force per unit displacement measurements. The bar test allowed for a bar to be wrapped under the film on the corner of the test frame and then pulled out using a MTS machine, allowing for force per unit displacement measurements.

A comparison of the results indicated that the s_{af1}, measured on the longer side, was lower than the saf2. Both s_{af} values were higher than the s_{ac}. The f_{cf} was in general agreement with the f_{cc} except for a series of low data points by one film. All of the results increased as the original thickness of film increased. The differentiation between the s_{af} values occurred because the different lengths of the sides of the test frame caused a different amount of material prestretch to be applied to each side. See Section 2.2.3 for details. The ANCOVA results indicated that there was no statistical difference between the slope of the s_{ac} and s_{af2} when plotted against the original thickness of the film. The results of a different ANCOVA indicated that there was no significant difference between the f_{cc} and f_{cf}.

With these results in mind, the location of the measurement of the s_a is more desirable on the individual faces of the test frame, especially if the unit load is a rectangle, which may allow for different stiffness readings on either face. However, because of the potential error associated with the force vectors of the film changing during the s_{af} evaluation and general errors associated with conducting the ASTM standard, the s_{ac} was determined to be a more reliable test for s_a. The evaluation of the f_c is more desirable on the corner of the unit load as the four corners are the only locations in which the stretch film is applying actual force to the unit load. Both of these phenomena are shown in Figure 57.

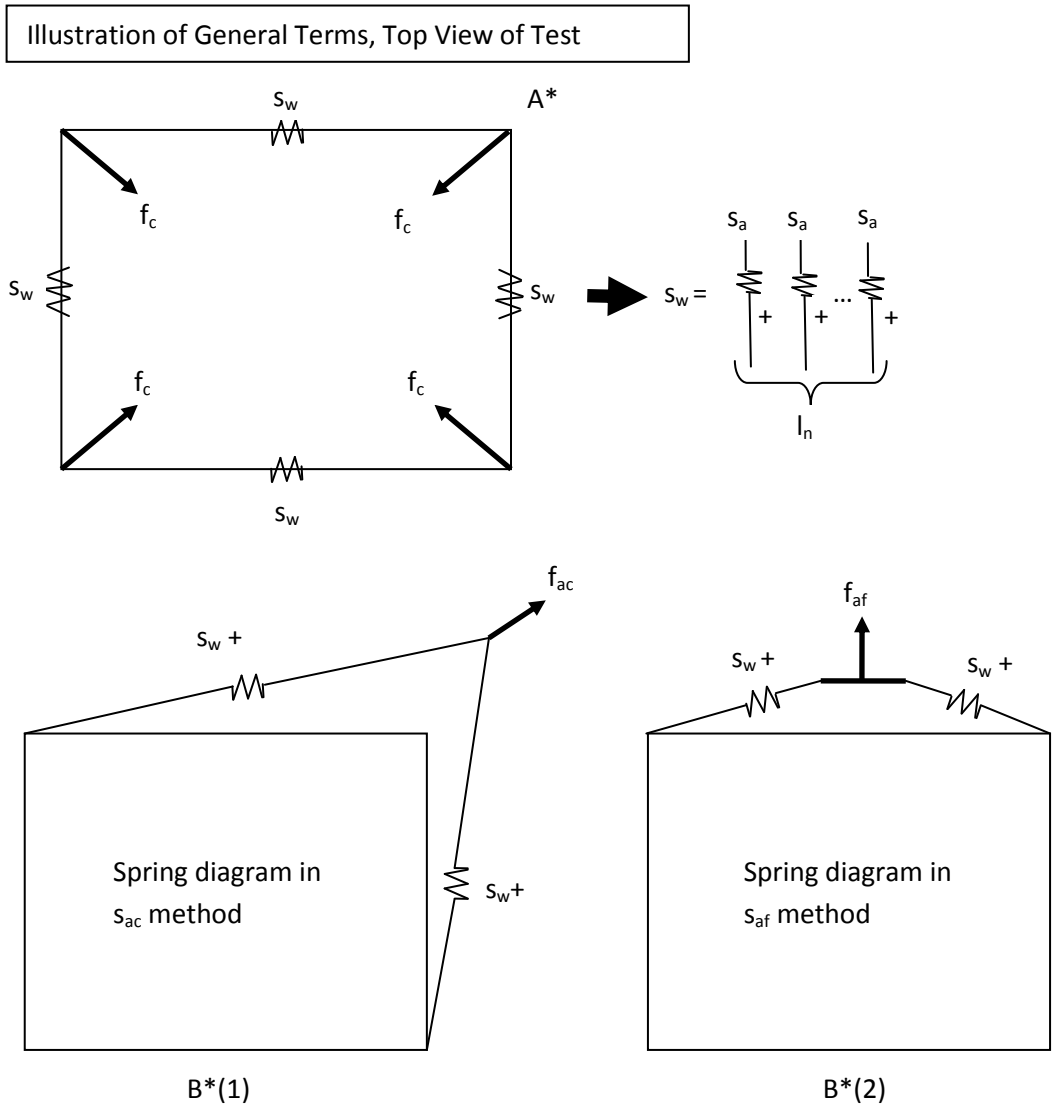

Figure 57 Spring diagrams identifying the general theory of evaluating the film stiffness of a given wrap pattern (sw)

6.1 Using Bisha Stiffness to predict the applied stiffness of stretch film

Per the ANCOVA results in Sections 3.4 and 5, the Bisha Stiffness 2.54cm (s_{b1}) data was compared to the Applied Stiffness on the Corner (s_{ac}) and the Applied Stiffness on the long Face (s_{af1}). A data table of averages is shown in Table 23, graphical comparisons are shown in Figure 58.

Table 23 Average results of s_{af1}, s_{ac} and s_{b1}

	Thickness (μ)	s_{af1} (N/cm)	s_{ac} (N/cm)	s_{b1} (N/cm)
Paragon	10	6.32	4.01	1.03
Berry	11.4	7.74	6.73	1.87
Intertape	12.7	7.99	5.72	2.19
Intertape	16	10.49	9.01	2.36
AEP	22.8	13.01	9.69	1.62
AEP	30.5	17.07	13.05	2.46

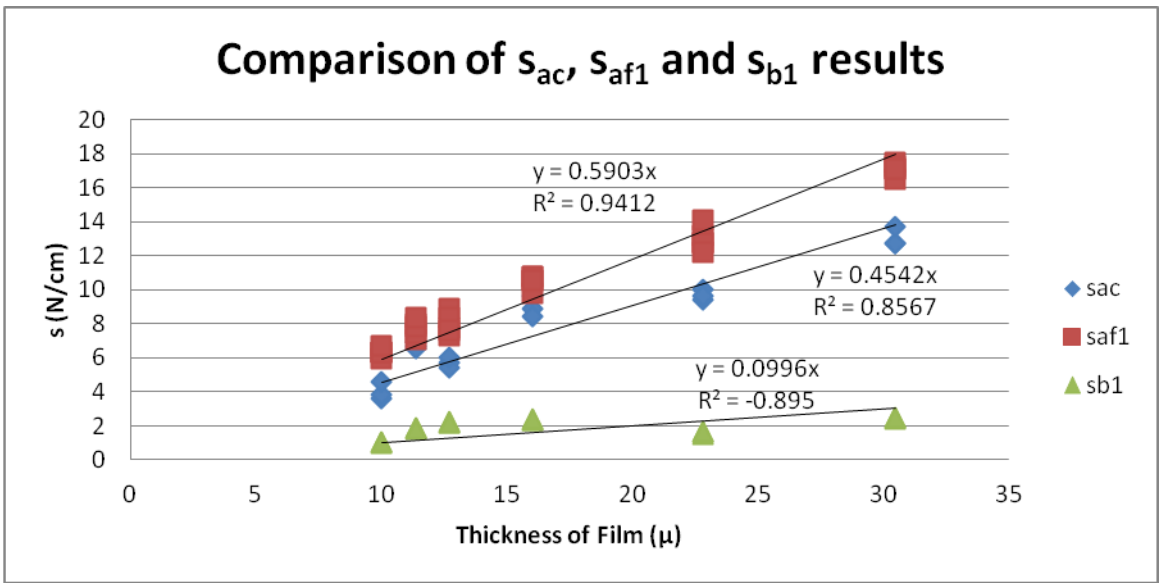

Figure 58 Comparison of s_{b1}, s_{ac} and s_{af1} results plotted against original material thickness.

The s_{b1} data was used to predict the s_{af1} and the s_{ac} using a standard least squares regression and an ANOVA to determine the significance of the regression. The results are shown in Table 24. While both of the regressions are significant, the coefficient of determination (R^2) for both models are substantially less than 0.5 indicating that a majority of the variation is not explained with a simple linear model. A graphical comparison of the predictions is shown in Figure 59.

Table 24 Results of least squares regression using the s_{b1} results to predict the s_{af1} and s_{ac}

Interaction	Slope	Intercept	R^2	F Ratio	DF	Prob>F
s_{b1} Predicting s_{ac}	3.9079	0.535	0.42	11.61	1,16	0.0036
s_{b1} Predicting s_{af1}	4.2476	2.2395	0.31	7.375	1,16	0.0153

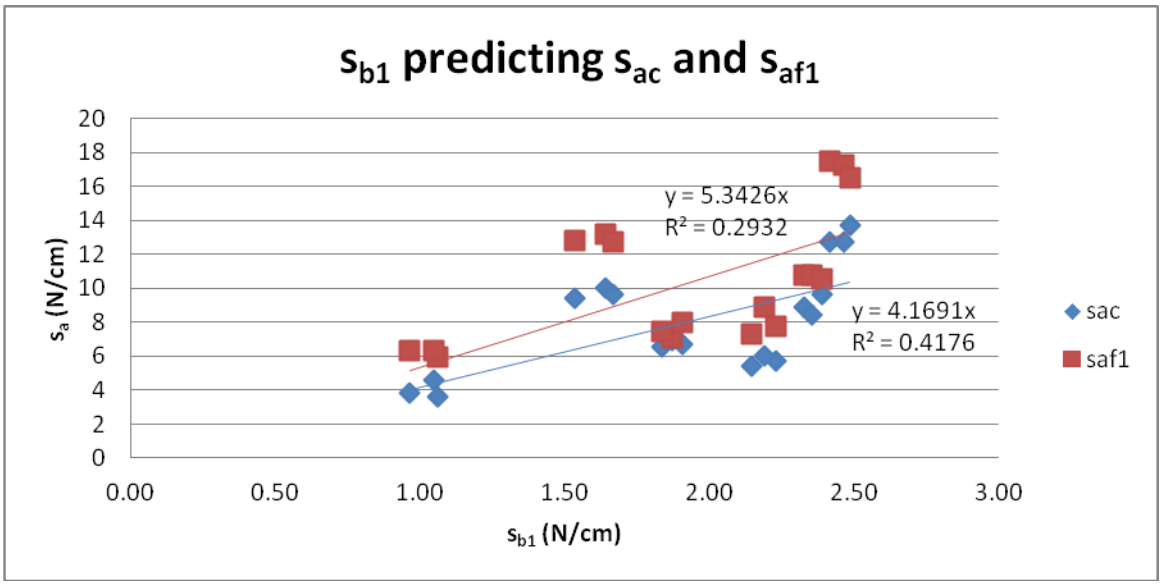

Figure 59 The s_{b1} data was used to predict the s_{ac} and the s_{af1} data. Note that the overall trend was consistent but not very linear and that the s_{ac} prediction was consistently lower than the s_{af1} prediction.

6.2 Using the initial force from the Bisha Stiffness to predict the applied containment force of stretch film

Per the ANCOVA results and the justification in Sections 4.1.3 and 5.1.3, the initial force of the Bisha Stiffness of the 2.54cm sample (f_{i1}) was compared to the containment force measured with the bar method on the corner of the test frame (f_{cc}) and the theoretical containment force calculated using a composite of the film tension values on either side of the test frame (f_{cf}). A data table of averages is shown in Table 25.

Table 25 Average results of f_{cf}, f_{cc} and f_{i1}

	Thickness (μ)	f_{cf} (N)	f_{cc} (N)	f_i (N)
Paragon	10	21.26	22.92	1.15
Berry	11.4	23.16	16.62	2.01
Intertape	12.7	26.41	27.71	2.41
Intertape	16	30.77	24.39	3.31
AEP	22.8	41.91	20.53	3.45
AEP	30.5	60.20	59.14	4.55

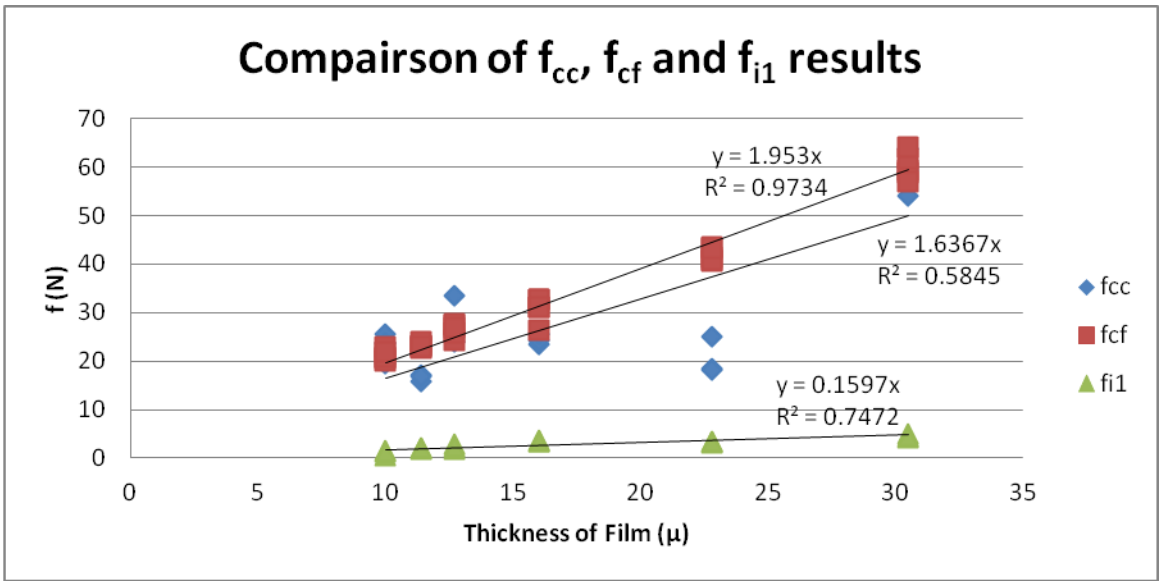

Figure 60 Comparison of f_{i1}, f_{cc} and f_{cf} results plotted against original material thickness.

The f_{i1} data was used to predict the f_{cc} and the f_{cf} using a standard least squares regression and an ANOVA to determine the significance of the regression. The results are shown in Table 26. While both of the regressions are significant, the coefficient of determination for the f_{cf} prediction was significantly higher than the f_{cc} prediction. Because range of the R^2 values and the inconsistency of the predictions shown in Figure 61, the majority of the variation is not explained with a simple linear model.

Table 26 Results of least squares regression using the f_{i1} results to predict the f_{cc} and f_{cf}

Interaction	Slope	Intercept	R^2	F Ratio	DF	Prob>F
f_{i1} Predicting f_{cc}	8.3447	5.0351	0.43	12.502	1,16	0.0027
f_{i1} Predicting f_{cf}	9.8576	5.681	0.74	45.971	1,16	<0.0001

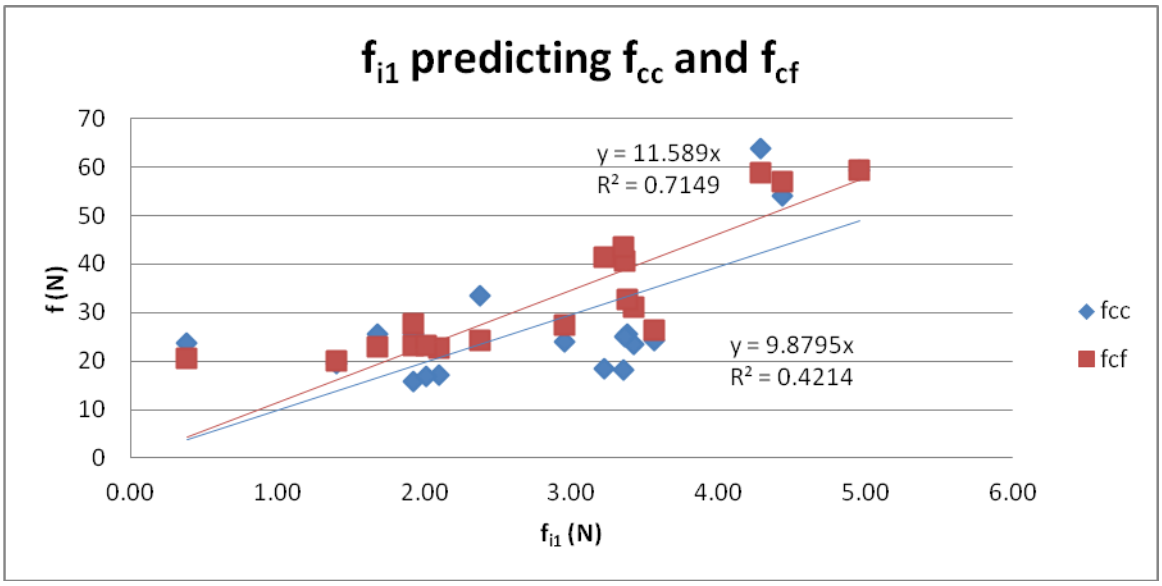

Figure 61 The f_{i1} data was used to predict the f_{cc} and the f_{cf} data. Note that the overall trend was inconsistent.

6.3 Summary

This section fulfilled the third objective, to investigate the relationship between the applied material properties as applied to a unit load and the measured tensile stretch film properties. The tensile properties evaluated were the Bisha Stiffness and the initial force from the Bisha stiffness evaluation. For more on the Bisha Stiffness see section 3.1. The applied stretch film evaluation was conducted using two different methods. The s_{ac} was measured by wrapping a bar on the corner of the test frame underneath the applied stretch film and pulling out on the bar. For more details regarding s_{ac} see section 3.2.6. The s_{af} was measured by placing a pull plate under the applied stretch film and pulling out on the film. For more on the s_{af} see section 3.2.4.

The results indicate that the ability to predict the applied material behavior is significant, whether stiffness or containment force. However, the amount of the stiffness (s_{ac}) and containment force (f_{cc}) variation explained by the Bisha Stiffness evaluation was a respective 41% and 42%, indicating that other variables, such as film formulation, manufacturing, testing procedures and other factors may have an influence. Note that these comparisons were conducted using the 2.54cm wide data set. If the 50.8cm wide data set or the s_{b1} ' (s_{b1} multiplied by 20 for the entire film width) measurements were used, the Bisha Stiffness results were 80% higher than the s_a results. In either case, the results were significantly different from the applied stiffness and containment force results.

While the stiffness trends were consistently predicted when plotted against original material thickness in both cases, the lack of samples evaluated do not allow for complete conclusions to be made as there may be other factors affecting the results.

The containment force prediction was more inconsistent than the stiffness prediction implying that there may be additional factors beyond material properties that affect a film containment force, such as

tension to load. On more advanced stretch wrappers, an output variable of tension to load is available. Future research should be conducted using the methods in Section 5.1 attempting to correlate containment force and tension to load.

The settings used in the application of the film are machine specific, any change in these settings will change the stiffness and containment force values of the applied film and will therefore change the relationship with the s_{b1}. Until the effect of slack (change in rotation speed between the output prestretch roller and the turn table) has been quantified, the relationship with the Bisha Stiffness cannot be determined.

7 Conclusions

The purpose of this research was to create a method of predicting the applied behavior (stiffness and containment force) of stretch film from laboratory testing of stretch film. This was achieved by developing a new tensile testing method that simulated the application and evaluation of applied stretch film. In evaluating applied film, the current definition of containment force was broken into two separate values of film stiffness and containment force. Finally, the results from the tensile test were compared to the applied film values. The objectives of the research were:

- Characterize elastic properties of stretch film through tensile testing.
- Evaluate film behavior in terms of stiffness and containment force performance when applied to a unit load.
- Investigate the correlation between the elastic tensile properties and the applied stiffness and containment force of stretch film.

The conclusions from each objective are listed below:

7.1.1 Characterize elastic properties of stretch film through tensile testing.

- The Bisha Stiffness method was created in an attempt to emulate actual film application by initially stretching the film (simulating prestretch), holding the film for a period of time (simulating the amount of time between the application of the film and the evaluation of the film) and then re-extending the film (simulating the action of a film applied to a unit load).
- The two sample preparation methods (2.54cm versus 50.8cm) used to evaluate the film measured the Bisha Stiffness (s_b) and initial force of the Bisha Stiffness (f_i) produced results with no statistically significant difference when normalized for sample width and plotted against original material thickness
- The 2.54cm results were consistently 27 times less than 50.8cm results despite their 20 times difference in film width.
- The bias in the results between the 2.54cm and the 50.8cm results are due to the differences in geometrical and material effects (thickness, necking, strain hardening, necking, percent stretch) during tensile testing and needs further studied to determine the precise influence of these effects.
- The 2.54cm sample procedure was established as the most appropriate tensile test method for determining Bisha Stiffness, s_b, because its sample preparation method was closer to the current standard evaluation method because there was no difference in results when the data was normalized and plotted against original sample thickness
- Preliminary research indicated that stretch film will significantly increase in stiffness, s_b and decrease in tension, f_i, during the first hour after stretch, after which the values begin to stabilize. More research should be conducted to determine if this trend will continue across multiple film types, thicknesses and times.

7.1.2 Evaluate film behavior in terms of stiffness and containment force performance when applied to a unit load.

- The current ASTM D 4649 definition of containment force was expanded to include two film properties, film stiffness (N/cm), measured on the face of the unit load and containment force (N), measured on the corner of the unit load. ASTM D 4649 should be updated to reflect this definition.
- A new stretch film evaluation method was created by modifying the current pull plate method outlined in the ASTM D 4649 standard. The film was evaluated in the middle of the face of the unit load to ensure equal forces were applied to the evaluation plate and multiple force readings were recorded at multiple distances to allow for a film stiffness and film tension calculation.
- An additional new stretch film evaluation method created to allow for the direct measurement of force on the corner of the unit load. A bar was wrapped under the film and pulled out at a constant rate. This method allowed for the direct measurement and calculation of film stiffness and film containment force.
- Data collection methods were established and formulas were derived to calculate the normalized stiffness and containment force for each evaluation method.
- The corner method and the pull plate method produced values that were not found to be statistically different when evaluating film stiffness and containment force values.
- Stiffness and containment force results are machine setting specific, however, the relationships found between the pull plate method and the corner method should hold true as machine settings change. More research should be conducted to confirm this.
- When layering applied stretch film, the additive values of stiffness and containment force were evaluated. The results were inconclusive, but identified that the layering of films may be more complex than a simple additive relationship.
- The correct balance of additive (or subtractive) stiffness and containment force will be different for each unit load
- Thicker films are generally more costly and allow for a higher insurance against damage during shipment while thinner films allow for a reduction in cost but a lower insurance rate against damage. It is up to the individual end user to determine the balance.
- Preliminary research found that after stretch film was applied the stiffness increased and the containment force decreased significantly within the first hour.

7.1.3 Investigate the correlation between the elastic tensile properties and the applied stiffness and containment force of stretch film.

- The correlation of the Bisha Stiffness and applied stiffness and containment force yielded statistically significant results. However, the simple linear model that was hypothesized explained less that 50% of total variation observed indicating that other factors not studied in this research should be considered in future research.
- The geometrical effects of the Bisha Stiffness evaluation and how stretch wrapper settings effect applied film properties need to be better understood and modeled to better predict the applied stiffness and containment forces in a unit load using elastic film tensile properties.

- The initial force of the Bisha Stiffness may be better suited as part of a data set used to predict the behavior of the film over time rather the containment force.

7.2 Limitations of Research

The methodological approach for this research was to investigate the physical properties of applied stretch film and attempt to correlate the results to the film properties as evaluated on a tensile testing machine. The purpose of using this approach was to take a step back from the chemical properties and marketing literature and determine if it was possible to create a methodology to predict applied film behavior in unit loads using standard laboratory film testing techniques. The results indicate that the predictions are possible but the interacting mechanisms that can influence these predictions are more complex than originally hypothesized in this research. Therefore, more research is required to better quantify the deformation of the samples during tensile testing and how other differences, like slack effects, applied stiffness and containment force may interact together.

The Bisha Stiffness evaluation method was created to represent the prestretching and application of stretch film in application. The results of this research indicate that a one to one prestretch comparison between the Bisha Stiffness and the applied stiffness (s_a) may not be the correct method of stretch film evaluation.

The test frame used was built out of wood in the shape of a typical unit load (rectangle). Although properly representative, this caused a differentiation of properties on either side of the unit load which may have affected the corner evaluation results.

The stretch wrapper used in the research is an industrial machine, not a scientific research device. Many of the errors within this research could have been caused by the uncontrollable stretch film and prestretch roller interaction or the electronic inconsistencies of the stretch wrap machine.

7.3 Future Research

Based on the observations and conclusions of this research the following suggestions for future research can be made:

7.3.1 Improvement of corner evaluation method

In evaluating the film stiffness and containment force on the corner of the test frame, a bar wrapped under the stretch film and was extended from the corner of the test frame. Once the friction between the bar and the corner of the test frame was reduced enough, the bar would slip off the corner causing a small, temporary increase in the amount of force the film exerted on the bar. This temporary increase could have an effect on the measured film stiffness and containment force. Future research should use a track system for the bar to ensure the dropping of the bar does not affect material properties.

7.3.2 Quantification of slack in application of films

In contrast to the application of stretch film in this research, the output prestretch rollers typically move significantly faster than the turn table. This causes excess film to be output from the prestretcher which is taken up by the flat sides of the unit load. The effect of slack on applied stiffness and containment force has to be quantified before the Bisha Stiffness can be used to predict applied film behavior.

An experimental design would consist of multiple films across multiple thicknesses and layers to ensure that all film types and wrap patterns are addressed. The speed of the prestretching process would remain consistent but the speed of the turn table would be variable. Starting with a matching rotational speed, an evaluation should be conducted at 25cm/sec intervals allowing for a minimum of 10 increments. This model would allow for the effect of slack to be quantified on multiple films and compared. A proposed experimental design should include multiple film thicknesses, replicates, layer variants and evaluation speeds.

The methods for this experiment would emulate those found in the primary experiment, allowing for a test frame to be wrapped with parallel wraps to be evaluated with both the pull plate test in the center of a face and the bar test on the corner of the test frame. Both methods should continue to be used in case the relationship between the face values and the corner values start to diverge when slack is introduced into the system.

7.3.3 Comparison between s_a and s_b of a single film.

Once the effect of slack has been determined, a broad based experiment should be conducted to determine if with the slack factored into the model, the Bisha stiffness (s_b) can be used to better predict the applied stiffness (s_a) and containment force (f_c) of a given film. The same methods from the primary research should be used, allowing for a test frame to be wrapped with settings that represent actual use with a parallel film in a number of layer and evaluated with both the face and corner methods. Note that if there is no statistically significant difference in the results between the corner and the face in this comparison, the face method should become the primary method of evaluation due to its ease of use in the field and laboratory. The experimental design should be extended to also include multiple layer variants and evaluation speeds.

7.3.4 Evaluating how corner slippage effects stiffness and containment force

Once the stiffness and containment force have been evaluated and understood on specific faces of the unit load considering the effect of slack, a study should be conducted to determine how the stiffness and containment force change when the film is able to slip around the corner of the unit load, as in real world application. The same experimental design should be conducted as in Section 7.3.2 but the sticky tape on the corners of the test frame would be removed, though only the face evaluation method would be necessary (if they continue to produce results that have no difference).

7.3.5 Evaluating prestretch, length, thickness and width interactions

During tensile testing, it was expected that the values of the 2.54cm film would be 1/20 the 50.8cm film. Per the results in Section 4.1.4, this was not the case, therefore, the prestretch, length, thickness, width, and grip mechanism interactions that occurred in tensile testing were not as expected and should be carefully studied in future research to develop a more accurate and precise testing method.

7.3.6 Extrapolation of layering data with regard to wrap pattern

As indicated, the stiffness and containment force of a wrap pattern is not simply the addition of layers, but possibly a more complex function depending on the film's properties. When these properties are identified, a simplex view of calculating the stiffness and containment force of a wrap pattern is shown in Equation 7-1 and Equation 7-2. Note that depending on the vertical speed of the prestretch carriage,

the rotation speed of the unit load and the size of the unit load, the angle at which the film is applied may significantly change the applied length of the film on the side of the unit load. An additional consideration may also include the relationship between the applied film angle and the evaluation method. With the force vectors no transferring directly to the side of the unit load, there is a possibility for the introduction of additional error.

$$s_w = s_a * l_n + s_{aa} \qquad \text{Equation 7-1}$$

$$f_w = f_c * l_n + f_{ca} \qquad \text{Equation 7-2}$$

Where:

s_w = stiffness of wrap pattern

s_a = applied stiffness of film

l_n = number of layers

s_{aa} = additional effect on stiffness when layering film

f_w = containment force of wrap pattern

f_c = containment force

f_{ca} = additional effect on stiffness when layering film

7.3.7 Extrapolation of layering data with regard to stretch roping

The layering data can also be used to predict how the film will behave in the application of stretch roping with regard to the stiffness and containment force of the applied rope. Stretch roping is the rolling of the film into a "rope" as it is applied to a unit load for extra stability. The process of roping the film is essentially the same as applying many layers of film within a thin band, therefore, if the number of complete rolls (or layers) is known (l_n), then the applied stiffness (s_a) and containment force (f_c) of the roll can be calculated by the following series of equations. Note that more research will have to be conducted to determine the accuracy of these equations.

The circumference of a circle is Equation 7-3.

$$C = 2 * \pi * r \qquad \text{Equation 7-3}$$

The term radius (*r*) term in Equation 7-3 is replaced with a term that allows for the calculation of the circumference of a rope given the number of layers within the rope shown in Equation 7-4.

$$C = 2 * \pi * \left(\frac{\mu + l_n * 2\mu}{2}\right) \qquad \text{Equation 7-4}$$

Where

C = circumference of a rope given the number of layers and the film thickness

μ = Thickness of film

l_n = number of layers

Using Equation 7-4, the circumference of each additional layer is summed until it equals the transverse direction width.

$$td_w = C_1 + C_2 + C_3 \dots\dots C_x \qquad \textbf{Equation 7-5}$$

Where:

td_w = transverse direction web width of film

C_x = the circumference of a given rope given the original film thickness and the number of layers

The maximum number of layers that allows for the td_w can be used in conjunction with the s_a and f_c and their respective additive forces, to calculate the stiffness and containment force of an applied rope.

7.3.8 Observed functional adjustments to Bisha Stiffness data

The following empirical functional adjustments were observed to reduce unexplained variation in the simple linear model correlating the Bisha Stiffness to applied film stiffness. However, this empirical adjustment was not able to be theoretically justified within the time frame and data collection methods for this study. Nevertheless the empirical adjustment is reported here to perhaps shed some insights into future research.

The Bisha Stiffness was used to predict the stiffness on the corner of the test frame using Equation 7-6. A graph comparing the s_{b1}`` data and the stiffness on the corner (s_{ac}) and the long face of the test frame (s_{af1}) is shown in Figure 62.

$$s_{b1}`` = \sqrt{\mu} * s_{b1} \qquad \textbf{Equation 7-6}$$

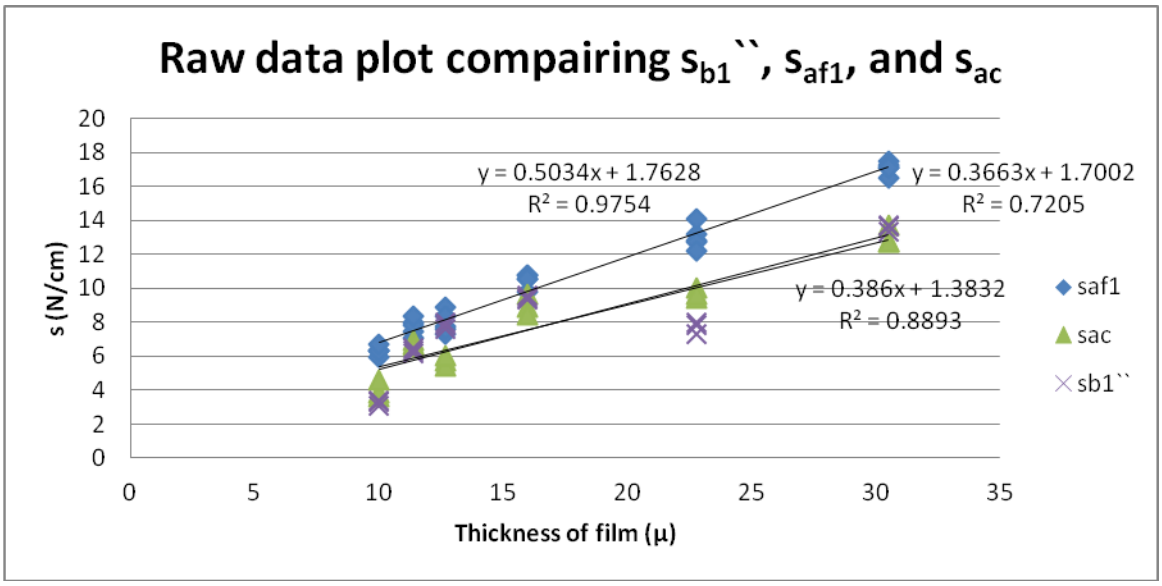

Figure 62 Raw data plot comparing s_{b1}``, s_{af1}, and s_{ac} across original µ

An ANCOVA was conducted to determine if the s_{b1}`` was significantly different than the $s_{ac}$ or the $s_{af1}$ if they were all plotted against the original material thickness. The t-raio results from the interactions of the ANCOVA are shown in Table 27. The results indicate that there is no difference between the $s_{b1}$`` and the s_{ac} but there is a significant difference between the s_{ac} and the s_{af1} implying that the s_{b1}`` can be used to predict the s_{ac}.

Table 27 Results of the ANCOVA comparing the s_{b1}`` and the s_a test

	Estimate	Std Error	t ratio	Prob>ltl
s_{b1}`` vs s_{ac}	0.0098	0.0332	0.3	0.7682
s_{b1}`` vs s_{af1}	0.0685	0.0238	2.87	0.0063

A similar functional adjustment, Equation 7-7, was attempted to allow for the comparison of the initial force (f_{i1}``) of the Bisha Stiffness and the applied containment force results. This functional adjustment did not provide a significant prediction of the applied containment force values.

$$f_{i1}`` = \sqrt{\mu * f_{i1} * 20} \qquad \text{Equation 7-7}$$

Note that how the percent stretch and machine settings affects the functional adjustment should be involved with the investigation.

7.3.9 Use of actual stress and strain in evaluating the Bisha Stiffness

The primary research used the engineering stress and strain to evaluate the Bisha Stiffness. The use of the actual stress and strain may significantly reduce the error associated with the necking, thickness and length interactions. The ability to measure the width and thickness deformations dynamically with a sufficient level of accuracy and precision was not available at the time of this research.

7.3.10 Investigation of potential errors with evaluating applied stretch film properties

With regard to the pull plate evaluation used in this research and outlined by ASTM 5459 (ASTM, 2007), the evolution of the force vectors as the pull plate is extended from the side of the unit load, as identified in Figure 22, should be modeled to allow for appropriate adjustments when calculating the stiffness and containment force of a applied film. Finite element analysis technique may be required to model pull plate and force vector relationships depending on the complexity or dynamic interactions that are revealed.

The bar used to evaluate the stiffness and containment force on the corner of the test frame should have been covered in a polymeric material that would prevent the stretch film from potentially slipping of the bar. This potential slippage could have caused lower than anticipated results. Future research should ensure that the bar and film interaction is not compromised by their interaction.

7.3.11 Improvement of the test frame

The test frame used in this research was not studied to quantify the amount error due to frame deflection. In future research the maximum allowable error tolerances due to any frame deflection should be calculated from which a containment force test frame should be assessed. The containment force test frame should be engineered and constructed with an appropriate level of stiffness and stability to satisfy any deflection tolerance requirements (i.e angle iron, channel, i-beams, trusses, etc.) and be 121.9cm (48”) square to minimize errors due to geometric asymmetry. ASTM D 4649 calls for the evaluation of containment force on the 121.9cm (48”) side of a unit load only. In making the test frame 121.9cm (48”) square, containment force evaluation can be done on all sides. The test frame cannot utilize solid sided construction. When evaluating stretch film that has been stretched over a flat surface (such as a real unit load) and the film is pulled from the unit load to measure s_a, a vacuum can occur behind the film enabling significantly higher containment force readings. In addition, the test frame should be fixed to the turn table and the turn table should be fixed in place during all applied film evaluations to ensure that the test frame is unable to move during the stiffness and containment force evaluations.

7.3.12 Energy absorbed by stretch wrap

The extrapolation of the stiffness of the applied film to the amount of potential energy stored in the film would give an end user a tool that allows for the direct analysis of load density versus the energy required to resist a certain amount of movement. Once the slack and edge effects have been quantified, an extrapolation to the amount of energy the stretch film can absorb is possible.

7.3.13 Prestretch roller surface and stretch film interaction

The prestretching of the film within the preliminary research for this paper was inconsistent at best. A further investigation to the optimum material to use on the prestretch rollers to achieve a more consistent stretch would be advantageous.

7.3.14 Improved application of ASTM D 5459

The hysteresis test as described in ASTM D 5459 is not representative of how stretch film is used in application. To make the test more relevant, an initial elongation should be made (250%), after which a hysteresis test should be conducted using the 250% elongation as a base line.

Another similar improvement would allow the film stretch an additional 25% each time and come back to at additional 25% recovery point. For example, an initial stretch of 250% is imparted on the film. After a given time, the film is stretched to 300%, immediately after the film is then relaxed to 275% and held for a given time. During the next cycle the film would be pulled to 325% and then relaxed to 275% and so on.

7.3.15 Other research options not directly related to this dissertation

How does vertical containment force affect the stability of a unit load? Meaning, if the wrapping layers are set to a steep angle, will the downward force vector be enough to decrease the motion within the unit load?

White identified that stretch wrapping over the pallet can increase unit load stability and that was reiterated in the preliminary research for this study. A complete investigation, of this interaction that includes stretch roping and that quantifies an amount of increased stability should be completed (White, 2008).

Stretch films, like all plastics, are temperature and humidity sensitive. Any models that are created should be adjusted per the average temperature within the given supply chain.

Literature Cited

ASTM D 4169 “Performance Testing of Shipping Containers and Systems” ASTM 100 BARR Harbor Drive, West Conhohocken, PA 19428

ASTM D 4649 “Standard Guide for Selection of Stretch Wrap Films” ASTM 100 BARR Harbor Drive, West Conhohocken, PA 19428

ASTM D 4649 “A1. Test Method or General Evaluation of Stretch Wrap Materials Under Non-Laboratory Conditions” ASTM 100 BARR Harbor Drive, West Conhohocken, PA 19428

ASTM D 5414 -95 “Evaluation of Horizontal Impact Performance of Load Unitizing Stretch Wrap Films” ASTM 100 BARR Harbor Drive, West Conhohocken, PA 19428

ASTM D 5415 -95 “Evaluating Load Containment Performance of Stretch Wrap Films by Vibration Testing” ASTM 100 BARR Harbor Drive, West Conhohocken, PA 19428

ASTM 5459 -95 (2007) “ Machine Direction Elastic Recovery and Permanent Deformation and Stress Retention of Stretch Wrap Film” ASTM 100 BARR Harbor Drive, West Conhohocken, PA 19428

Forest Products Laboratory. 1986. “Unitizing Goods on Pallets and Slipsheets” General Technical Report FPL-GTR-52. pg. 2-11

ASTM. (2003a). Standard Guide for Selection and Use of Stretch Wrap Films (Vol. ASTM D 5459). West Conshohocken, PA.

ASTM. (2003b). Standard Guide for Selection and Use of Stretch Wrap Films (Vol. ASTM D 4649 - 03). West Conshohocken, PA.

ASTM. (2007). Standard Test Method for Machine Direction Elstic Recovery and Permanent Deformation and Stress Rentention of Stretch Wrap Film (Vol. ASTM D 5459 - 95). West Conshohocken, PA.

ASTM. (2009). Standard Test Method for Tensile Properties of Thin Plastic Sheeting (Vol. ASTM D 882 - 09). West Conshohocken, PA.

Billham, M., Clark, A. H., Garrett, G., McNally, G. M., & Murphy, W. R. (2001, May 6-10). *Comparison of the Mechanical Performace of Extruded Blown and Cast Polyolefin Thin Film.* Paper presented at the Antec 2001: plastics, the loan star, Dallas, Texas.

Bisha. (2008). *THE EFFECT OF LOAD STABILIZER SELECTION ON LOAD SHIFT WITHIN UNIT LOADS* Masters of Wood Science and Forest Products, Virginia Polytechnic Institute and State University, Blacksburg, VA.

Brown, R. (1999). *Handbook of Polymer Testing* (Vol. 10). New York, New York: Marcel Dekker, Inc.

BTS, B. o. T. S. (2002). *Table 1 - Commercial Freight Activity in the United States by Mode of Transportation: 2002*. Retrieved from http://www.bts.gov/publications/freight_in_america/html/table_01.html.

Campbell, I. m. (2004). *Introduction to Synthetic Polymers* (Second Edition ed.). New York City, NY: Oxford University Press.

Collins, M. *Specifying the Ideal Stretch-Wrap Machine for the Application* Orion Packaging. Collierville, TN.

Crain. (2011). Companies serving the end market - stretch film *North american film & sheet manufactures* Retrieved 3-6, 2012, from http://www.plasticsnews.com/rankings/listrank.html?mode=fs&inpmkt=Stretch%2Bfilm

Downey, J. S., & Climenhage, D. (2001). The Effects of Pre-Stretching on the Physical Properties of LLDPE Stretch Films. Retrieved from

elasticity (n.d.). (Ed.) Dictionary.com.

G. Panagopoulos, J., W.A. Khan, S.E. Pirtle. (1991). *The effect of fabrication on cling and stretch properties of LLDPE film*. Paper presented at the Polymers, Laminations & Coatings Conference, Montreal.

Gardner-Publications. (2003). Solid growth ahead for stretch & shrink film Retrieved 11/20/2011, 2011, from http://www.thefreelibrary.com/Solid+growth+ahead+for+stretch+%26+shrink+film.-a0111648865

German, P. M. (1998). *Stretch Films: Background and Basics*. Paper presented at the TAPPI Polymers Lamination and Coatings Conference, San Francisco, CA.

GMA-Wipro, G. M. A. a. W. (2010). The impact of Sales and Procurement on Reverse Logistics Managment. In J. i. u. l. team (Ed.). Washington DC.

GroupO. (2012) Retrieved 3-6, 2012, from http://www.groupo.com/

Hernandez, R. J., Selke, S. E. M., & Culter, J. D. (2000). *Plastics Packaging: Properties, Processing, Applications and Regulations*. Cincinnati, OH: Hanser Gardner Publishers.

ITW Mima Packaging Systems. (2009). Stretch Wrapping Glossary from http://www.stretch-wrap-machines.co.uk/?page=StretchWrapGlossary

Jackson, W. (2006-2007). Inside Scoop Archive E-book. In N. P. S. inc (Ed.). Atlanta GA.

Jozef Bodig, B. A. J. (1993). *Mechanics of wood and wood composites* Malabar, FL: Krieger publishing company.

Lantech. (2011). CRT-5 Containment Force Tool Instruction Guide. Louisville, KY.

Mal, A. K., & Singh, S. J. (1991). *Deformation of Elastic Solids*. Englewood Cliffs, NJ: Prentice-Hall Inc.

McNally, G. M., Small, C. M., Murphy, W. R., & Garrett, G. (2005). The effect of polymer properties on the mechanical behavior and morphological characteristics of cast polyethylene film for stretch and cling film applications. *Journal of Plastic Film and Sheeting, 21*(Compendex), 39-54.

Osborn, K. R., & Jenkins, W. A. (1992). *Plastic Films: Technology and Packaging Applications*. Lancaster, PA: Technomic.

Patrick Lancaster, R. w. (1993). *Containing & Protecting Pallet Loads*. Paper presented at the Perspectives on Material Handling Practive.

Peacock, A. J. (2000). *Handbook of Polyethylene* (10 ed.). New York, NY: Marcel Dekker, Inc.

Provincial Paper & Packaging Ltd. (2008). Stretch Wrap Terms Retrieved June 1, 2010, from http://www.provincialpaper.com/stretchfilm/terms.asp

Riemenschneider, K. (2011). *Stretch Film Testing Methods :In the Film and In the Lab*. Presentation. AMI Stretch & Shrink Conference. Vienna, Austria.

Rotondo, C. (2006). Secondary Investigation of Stretch WRap Performace on Unit Load Stability. 19.

Schwind, G. F. (1996, October). Stretch Wrappers: One for Every Job. *Material Handling Engineering, 51*.

Smith, R. D. (2010). *New Devlopments in Stretch Film Winding to Improve Productivity*. Davis-Standard Converting Systems. Fulton, NY.

Soroka, W. (1999). *Fundamentals of Packaging Technology* (Second ed.): Richard Washington.

U.S.-Census-Bureau. (2009). Transportation and Warehousing - NAICS 48/49 - Estimated Revenues, Sources of Resenue, and Expenses for Employer Firms. In A. Q. Services (Ed.). Washington DC: Us Goverment.

U.S., U. S. C.-B. (2012). *669 - Gross Domestic Product in Current and Chained (2005) Dollars by Type of Product and Sector*. Washington D.C.

UNCTAD, U. N. C. o. T. a. D.-. (2011). Review of Maritime Transport 2011.
UPS. (2005). Air Freight Packaging Pointers. In U. P. Service (Ed.). Atlanta, GA.
Wainer, M. V. (2002). Stretch film properties - Effects of equipment and process variables. *Journal of Plastic Film and Sheeting, 18*(Compendex), 279-286.
White, B. (2008). *A Preliminary Study of Unit Load/ Stretch Wrap Stability*. Undergraduate Research. Virginia Polytechnic Institute and State University. Blacksburg, VA.

8 Appendix A

8.1 Appendix A1: Thesaurus of Stretch film terms

Containment force: lay-on force, load containment, retainment force, film tension, film force, film force to load, retained tension

Elasticity: elastic elongation, elastic recovery, resilience, film memory, memory, creep, restretch resistance, recovery

Tear resistance: zippering, tear value

Yield Stress: elastic limit, yield point

Necking: neckdown

Breaking Point: point of rupture, ultimate elongation force, ultimate strength, ultimate stress

Tensile Strength: holding force

Tension-to-load: post-stretch, tension stretch

Cling: tack, film tack

8.2 Appendix A2: Determining prestretch variability of the stretch wrap machine

The objective of this preliminary experiment was to understand the variability of the prestretching process of the stretch wrap machine. This experiment was a portion of the second objective which is to evaluate film behavior in terms of stiffness and containment force performance when applied to a unit load. The results would also have implications on the methods of evaluating the first objective which is to characterize elastic properties of stretch film through tensile testing.

Recall that the prestretching process occurs within the prestretching carriage on the stretch wrap machine. As the film moves through the carriage, the film comes in contact with many different rollers; however, only the two rubberized rollers are of importance for this research. The first rubberized roller is smaller in diameter and has a dual purpose of pulling the stretch film off the stock roll on one side and regulating film flow through the other side. The second rubberized roller is larger in diameter and the surface travels faster than the smaller roller. The differential in surface speed of the two rubberized rollers causes a prescribed amount of stretch to be imparted on the film.

The critical interface of the previously described process is the interactions between the prestretch rollers and the stretch film. Achieving a steady film/roller interaction allows for predictable prestretched film properties. The interaction can be affected by the alignment of the rubberized rollers. If the two rubberized rollers are not perfectly aligned the film may “walk” back and forth during the prestretch process causing sections of the film to be prestretched more than others. The interaction may also be affected by the relationship between the film tack, the force to stretch the film and the

surface friction of the rollers. If the coefficient of friction between the film and the rollers is not high enough during the stretching process, the film may slip, causing inconsistent stretch. Note that this relationship is a moving target among films. A higher force required to stretch the film requires more tack to ensure adequate roller contact. In addition, if the rubberized rollers were to degrade over time or become dusty, the amount of tack would perhaps have to be even higher to overcome such degradation.

The precision error of the prestretching process was measured and quantified so that the film stiffness and containment force properties at the different extremes of the range could be compared in subsequent research findings. If there was no significant difference in film performance within the range then the prestretch precision error can be ignored. However, if there is evidence of a significant precision error that might influence subsequent experiments, the prestretching process should be improved before actual stiffness and containment force values are measured.

8.2.1 Experimental Design

Eleven films were evaluated for consistency of prestretch. Each film required four length measurements (cm), initial top length (l_{it}), initial bottom length (l_{ib}), final top length (l_{ft}) and final bottom length (l_{fb}) for a total of 440 measurements taken. The parameter estimation procedure for the experimental design was to allow for a wide range in film thickness and manufacturers. A visual representation of the experimental design is shown in Table 28.

Table 28 Films used in evaluating prestretch by the stretch wrapper

Data Measured→	l_{it}, l_{ib}, l_{ft}, l_{fb} (cm)		Replicates	
Manufacture	Thickness (μ)	Marketing Name	Top	Bottom
Berry Plastics	11.4	Stratos	10	10
Paragon	11.9	F5	10	10
Intertape	12.7	Stretch Flex	10	10
Paragon	13	Ultimate Force	10	10
Berry Plastics	14.5	Revolution	10	10
AEP	15.2	A1	10	10
Berry Plastics	16	Revolution	10	10
AEP	16	XR	10	10
Intertape	16	Super Flex	10	10
AEP	16.5	ADU	10	10
Berry Plastics	23.1	Revolution	10	10

8.2.2 Materials and Methods

The films used were identified in Table 28. Each film was loaded into the stretch wrapper (Section 3.2.3) and was used to partially wrap the test frame specified in Section 3.2.2. During the cycle, the machine was stopped and four markings were placed on the unstretched film, two at the top of the roll and two at the bottom of the roll. Each set of markings were 12.7cm (5”) apart and were placed far enough back on the roll so that the machine was able to reach full speed by the time that the marks entered the prestretching rolls.

The wrapping cycle was then initiated, allowing for the film to be prestretched. Once through the prestretch rollers and over the tension bar but before being applied to the unit load, measurements were taken, center mark to center mark, of the observed distance between the marks. Data collection procedure alternated top and bottom with respect to which was taken first. This alternating collection procedure was done as a precaution in case the film was prone to retracting enough to effect results during the time taken to take the first measurement. Average, minimum and maximum values were calculated and before and after stretching were compared.

The stretch wrap machine setting was set at dot 5 for rotation speed and at dot 7.5 for film tension although the exact speeds of the output prestretch roller and the turn table were not recorded. Note

that this combination allowed for substantial film slack between the tension bar and the test frame ensuring that there was no tension to load stretch occurring. The movement of the prestretch carriage was restricted as described in Section 3.

The final length of the top (l_{ft}) was subtracted from the initial length of the top (l_{it}) and was divided by the l_{it} to calculate the total percent stretch (Equation 8-1). The same calculations were conducted on the lower data set (l_{ib}, l_{fb}). The results were plotted in order of film thickness.

$$\% \textbf{ Stretch} = \frac{l_{ft} - l_{it}}{l_{it}} \qquad \textbf{Equation 8-1}$$

8.2.3 Results & Discussion

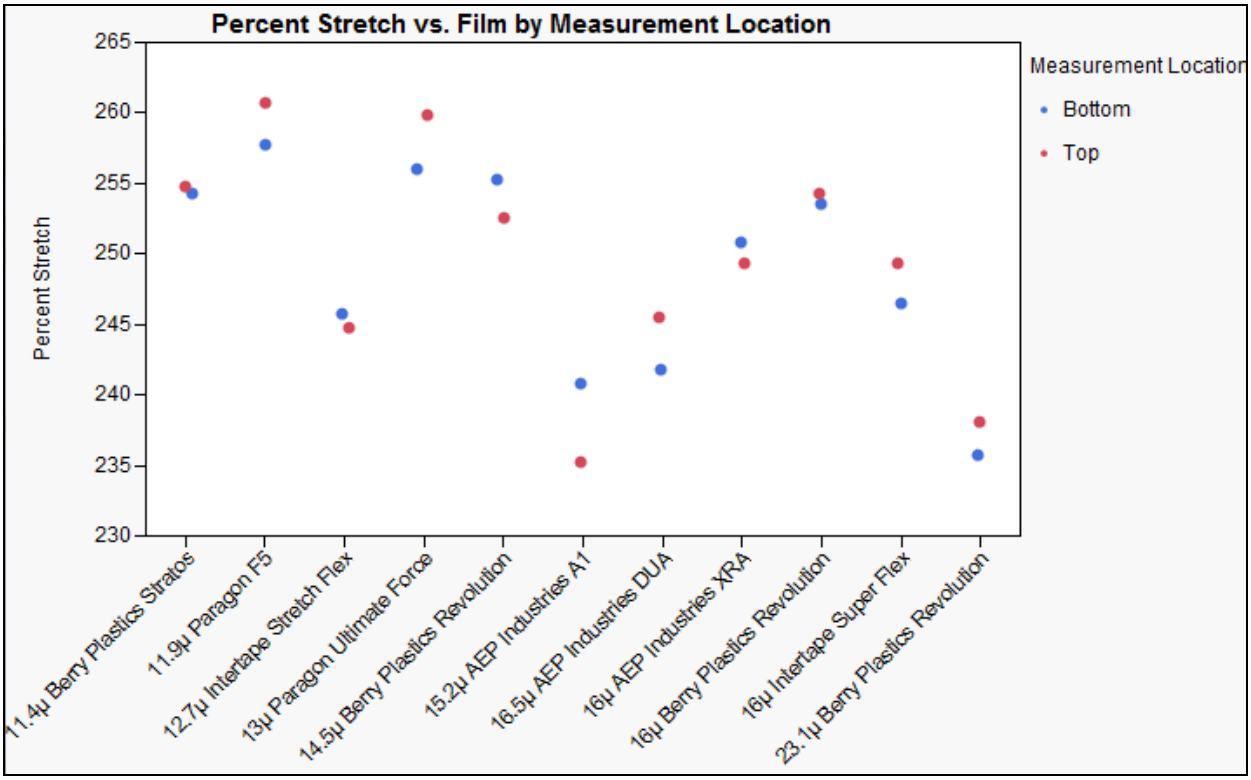

Figure 63 Results of comparing the percent stretch of different films on the stretch wrapper

The results are shown in Figure 63. The percentage in stretch differentiation between top and bottom was the most in AEP's 15.2µ film and the least in Berry Plastics 11.4 µ film. Paragon's 11.9 µ film stretched the most and Berry Plastics 23.1µ film stretched the least. There is a small trend of film variation vs. manufacture. Intertape had the lowest variation followed by Berry Plastics, AEP and, finally, Paragon had the highest prestretch variation.

The average prestretch stretch imparted on the films was 249.18% with a standard deviation of 15.05%. This large variation could be for a variety of issues, a more in-depth investigation into the interaction

between the film used and the rubberized prestretch rollers would have to be conducted to understand why the variation occurred.

There was a general downward trend with regard to percent stretch versus film thickness. The exact reasoning for this trend is not known and more research will have to be conducted to confirm and explain this trend. Note that investigating the trend from a volume of material standpoint, the more material in the sample (thicker) the more force is required to stretch the film.

8.2.4 Conclusion & Summary

The objective of this preliminary experiment was to quantify the prestretching variability of the machine that was to be used in measuring the stiffness and containment force of applied film in Section 5. The advertised percent prestretch of the machine was 200%, however, the actual stretching imparted on the films was 249.18% with a standard deviation of 15.05%.

The reasoning for the variation in percent stretch between the top and bottom of the web width, the general downward trend in percent stretch as the original material thickness increased and whether the results have a significant effect on applied material properties will have to be investigated in future research. As previously mentioned, these behaviors may be explained by, but not limited to, the alignment of the prestretch rollers, the condition of the prestretch rollers (clean or dirty), the force required to stretch the films, the tack of the films and the coefficient of friction between the prestretch rollers and the stretch film.

It was observed during testing that the prestretch action starts before the film leaves the initial prestretch roller and continues after it comes in contact with the second prestretch roller. The amount of additional stretching distance will change per film depending on the variable interactions described in the previous paragraph.

In future testing, the average percent stretch imparted on a film by the stretch wrapper should be used in tensile testing of the film. The stretch should be reduced to a minimum when evaluating the applied containment force of a film. In addition, the item being wrapped for this test should be round, such as the roll of paper in Figure 64. This will allow the tension bar to stay at a consistent placement allowing for a consistent speed of the prestretch rollers. Preliminary testing did not show that the speed of the rollers affected the amount of prestretch, however, further investigation should be conducted to verify these test results.

Figure 64 Round unit load recommended for wrapping during prestretching evaluation

8.3 Appendix A3: Comparing the Bisha Stiffness of films using different sample preparations methods

Recall that the Bisha Stiffness (s_b) simulates the pulling, or extension, of the film off the unit load as the film is being evaluated for s_a per ASTM D 4649. The tensile testing profile that was used is shown in Figure 65. The initial extension was calculated from the actual prestretch of the film as applied to the test frame. Prestretch is blue in Figure 65. The film was then held for an hour (green) allowing for the film to recover and stiffen. The film was then extended again at the same speed (purple) to simulate the evaluation of s_a. The slope of this line is within the first centimeter was called the Bisha Stiffness (s_b), while the initial force of the s_b test is called the f_i. Note that the longer the green line recovers (falls), the less containment force (f_c) is theoretically applied on to the unit load. The s_b value does not capture the diminishing nature of f_c, only the film stiffness.

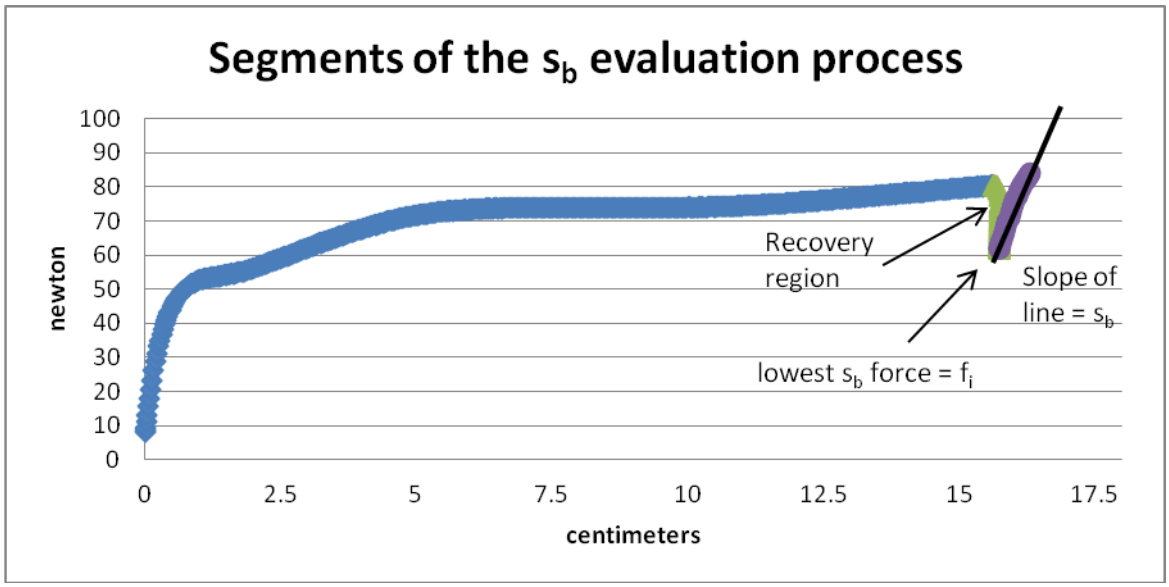

Figure 65 Different segments of the proposed tensile test profile identified

In determining if the applied stiffness and containment force could be predicted from a tensile test, there were many different sample preparation methods investigated using the testing profile identified in Figure 65. As previously discussed in Section 3.1.2, the current ASTM D 5459-95 testing method calls for a 2.5cm (1") wide sample that is 12.7cm (5") inches long. In not knowing if this was the optimum sample preparation method, two other methods were created to estimate the same parameters.

The goal was to create a sample and testing method that allowed for an accurate representation of what was occurring as the film was applied to the unit load. Recall that the stretch film used in this research was 50.8cm (20") wide and could be considered infinitely long as applied to a unit load. The infinite length could not be simulated so the methods developed were created to try and simulate the appropriate width of the film.

Recall the breakdown of forces when evaluating the force of applied film on the face (f_{af}) originally shown in Section 3.2.1 and shown in Figure 67. The initial distance of the film is labeled ℓ' and the finial distance is labeled ℓ''. The change in distance for one side was turned into a percent change in distance via Equation 8-2. A proportional amount of percent extension was used in calculating the Bisha Stiffness in tensile testing during this research.

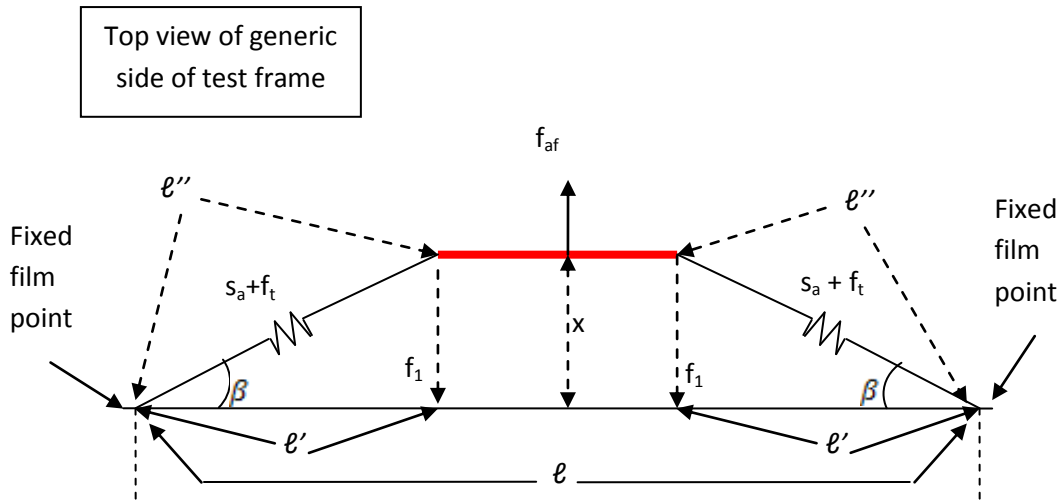

Figure 66 Top view of the component break down with forces associated with modeling f_{af}

$$e_{\%} = \frac{\sqrt{\ell'^2 + x^2} - \ell'}{\ell'} * 100$$ **Equation 8-2**

8.3.1 Experimental Design

Four films were tested and each film was prepared using one of two methods as described below. Each experiment was replicated three times resulting in 36 tensile tests. This experiment investigated the influence of testing method and film gauge on desirable material properties (s_b +f_i) of film 1 hour after being stretched to the target prestretch. The purpose of this experimental design was to investigate if the ASTM D 5459 (ASTM, 2007) standard 2.54 cm (1") sample testing procedure produced similar results to the new sample preparation methods. A visual representation of the experimental design is shown in Table 29 Visual representation of the experimental design.

Table 29 Visual representation of the experimental design for comparing s_b preparation methods

Test Sample preparation➔	ASTM 2.54 cm	Tube	Roll
Parameter Estimated➔	s_{b1}	s_{bt}	s_{br}
Film Thickness:	Number of test replicates		
11.4 µ	3	3	3
12.7 µ	3	3	3
16 µ	3	3	3
16 µ	3	3	3

8.3.2 Materials & Methods

The four films and their respective extensions are shown in Table 30. Each percent extension was estimated by loading the roll of film onto the stretch wrap machine described in Section 3.2.3 and evaluating the prestretch imparted in the film by the prestretch carriage using the ruler method defined

in Section 2.2.4. This percent extension was used when conducting the initial pull of the Bisha Stiffness test.

Table 30 Description of materials and respective extensions used

Make and Model of Stretch Film	Thickness (μ)	% Extension
Berry Plastics Stratos	11.4	245
Intertape Stretch Flex	12.7	245
Berry Plastics Revolution	16	253
Intertape Super Flex	16	247

During the secondary pull of the Bisha Stiffness test multiple force/distance measurements were recorded to calculate how the stiffness of the material changed over the initial 2 cm. Being that all the samples in this experiment were 12.7cm (5”) in length, the Bisha Stiffness of the sample was calculated at the extensions shown in Table 31. This was done so that the stiffness of an applied film could be correlated to a given Bisha Stiffness extensions (the applied stiffness part of the experiment was never completed).

Table 31 Range of Bisha Stiffness evaluations

Evaluation Distance (cm)	% Extension	COV
0.78	6.69	14.0%
0.99	8.38	11.0%
1.20	10.08	9.0%
1.42	11.78	8.0%
1.63	13.48	7.0%

There were three sample preparation methods used. The first was the s_{b1} as described in Section 3.1. The evaluated material length was 12.7cm (5”) long and was 2.54cm (1”) wide sample. The sample width was cut with a razorblade sample cutter. This method is the same that is described in ASTM D 5459. It was evaluated in the same method Section 3.1.2. The limitations associated with the s_{b1} samples and the MTS grips the samples were evaluated with are outlined in Section 3.1.3.

The second sample preparation method was the Roll (s_{br}). The film was cut off the stock roll of film and laid flat on a table with no wrinkles. A 1.905cm (.75”) diameter bar was used to roll up the film. This size bar was used because its circumference was 5.985cm and when the film was taken off the bar and pressed flat the sample was 2.99cm wide. This was as close 2.54cm that was available to the author at the time. A picture of the sample preparation process is seen in Figure 67. This process was created to evaluate the same sample length 12.7cm (5”) of the s_{b1} preparation methods but modified to include the volume of film that would be used in a full width test 50.8cm (20”). The s_{br} samples were evaluated using the same methods as the s_{b1} samples as described in Section 3.1.2, including the same grips, tensile testing machine and load cell.

Figure 67 Visual representation of creating the s_{br} samples

The limitations of the s_{br} preparation method include the difficultly to get the samples to lay flat during the rolling process of sample creation. This difficulty would lead to uncontrollable bubbles and wrinkles in the sample. The layering of the film during the sample creation process could have additive effects that are not representative of film behavior in non layered form. More research should be conducted to determine the layering effects as described in Section 5.2.3. The limitations of the testing method are the same as the s_{b1} samples as outlined in Section 3.1.3.

The third sample preparation technique was the Pipe (s_{bp}). The tube sample was created to try to evaluate the full width of the film including multiple layers. Sample preparation started with a film rewind station that was created to apply the film uniformly and consistently to the same substrate. A photograph is shown in Figure 68.

Figure 68 s_{bp} Stretch film rewind station

The full roll of stretch film was suspended on a 2.54cm dowel rod. Perpendicular to the initial dowel rod, 60.96cm (24”) away (center dowel rod to center dowel rod), a 10.16cm (4”) PVC pipe was cut to

60.96cm and suspended on a similar 2.54cm dowel rod. A starting edge line was drawn on the pipe parallel to the dowel rod and the pipe was wrapped in .15875cm (1/16") polyethylene foam. A photograph is shown in Figure 69. The foam wrap had a taped butted joint to prevent unevenness in the film and was tight enough on the pipe to prevent buckling when wrapped with stretch film but loose enough to allow for removal.

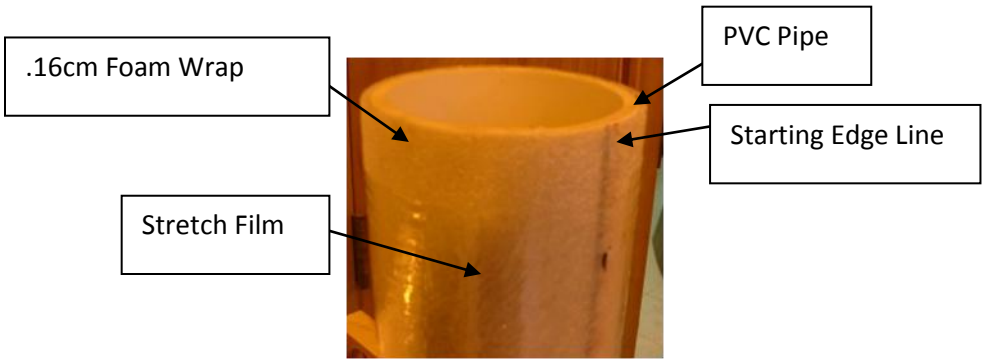

Figure 69 Layers of the rewind pipe when creating S_{BP} samples

The stretch film was pulled off the roll and the front edge was aligned with the straight edge line drawn on the pipe. Then the film was rolled around the pipe, completing as many rotations (layers) as required. Once complete, two ink marks were placed on the edge of film in line with the starting edge line and in a location that would allow for a .635cm (.25") overlap between the starting and ending layers. The film was then pulled off the pipe far enough so that the film could be laid flat on the bottom of the rewind apparatus. A straight edge connected the two ink marks and a razor was used to cut the film in line with the straight edge. The left over film was then applied back on the rewind pipe as uniformly as possible. The stretch film and the foam wrap were then slid off the end of the pipe and the foam was removed by folding it in on its self. A photograph is shown in Figure 70.

This process made it difficult to create a single layer sample. After the foam was removed from the stretch wrap it was reapplied to the PVC pipe for the next sample.

Figure 70 The separation of stretch wrap and foam

A horizontal fixed pipe system was used for evaluating the s_{bp} samples. Both the upper and lower pipes were 2.54cm in diameter and were bolted to the upper and lower pipe bracing. The upper pipe was put through the tube sample with the sample seam up. It was then bolted to the upper pipe bracings. The lower pipe was then run through the bottom of the tube sample and bolted to the lower pipe bracing. The seam of the tube sample was aligned with the center line of the top pipe.

A 3.81cm (1.5”) PVC pipe was cut horizontally (1.27cm (.5”) tall) and lined with the same .15875cm (1/16”) foam material as mentioned previously. This top cap was placed on the top pipe (on the stretch film seam) upon which a 60.96cm x 2.54cm x .635cm (24” x 1” x .25”) piece of metal was placed on top of the PVC top cap and finger tightened to the upper pipe bracing. This top cap was used to keep the seam of the stretch film in contact with itself during testing. Without the cap some of the films were prone to peeling themselves off the top pipe. The test was conducted at 12.7cm/minute (5”) per ASTM 4649.

The circumference of the rewind PVC pipe plus the foam was 32.893cm (12.95”). The circumference of the pipes in which the stretch film was stretched was 7.9796cm (3.14”). This configuration allows for a total sample length of 12.446cm (4.9”) which is close to the 12.7cm (5”) as required in ASTM 4649. The testing setup is pictured in Figure 71. A picture of the entire testing machine and setup can be found in Figure 72.

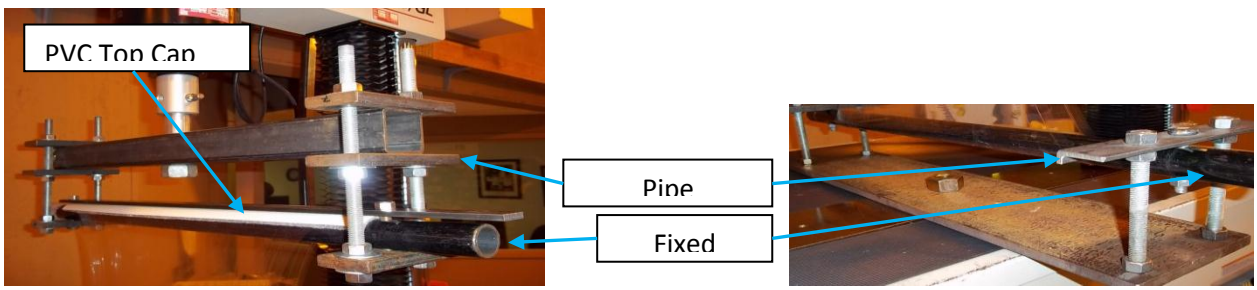

Figure 71 s_{bp} tensile testing setup

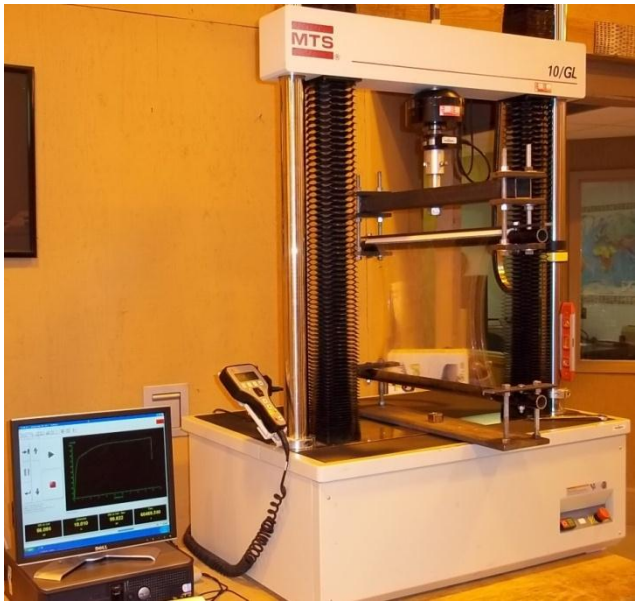

Figure 72 Complete view of s_{bp} tensile testing setup

The creation of the s_{bp} samples offered similar limitations as the s_{br} samples. It was hard to align the layers as the PVC pipe was wrapped and the wrapping action caused many bubbles and wrinkles. The film may be able to slip around pipe during testing or creep, providing artificially low stiffness readings and longer than normal recovery times and the layering effect of the film is not known.

All results were either multiplied up to or divided down to single film width 50.7cm (20”). The s_{bp} data was divided by six (2 sides and 3 layers), the s_{br} data was kept the same and the s_{b1} data was multiplied 20.

8.3.3 Results & Discussion

The s_b results of the different sample preparation methods are shown in Table 32. Per the materials and methods, the force measured when evaluating the s_{b1} was multiplied by 20, the s_{bp} was divided by 6 for and the s_{br} data was left alone. With the exception of the Barry Plastics 16µ, the measured stiffness of the s_{b1} samples was the highest, followed by the s_{br} and lastly the s_{bp}. In every case the Berry Plastics 16µ film was the stiffest film while the other films were not consistent in their rankings.

Table 32 Bisha Stiffness results for of s_{b1}, s_{br}, s_{bt}

s_{b1}			s_{br}			s_{bp}		
Berry Plastics 11.4µ								
% Stretch	s_{b1} (n/cm)	COV	% Stretch	s_{br} (n/cm)	COV	% Stretch	s_{bp} (n/cm)	COV
5.52	43.38	5.88%	7.18	39.69	3.76%	7.20	32.39	0.85%
7.20	40.62	6.52%	8.85	37.38	3.91%	8.87	30.25	0.74%
8.86	37.53	6.14%	10.52	34.69	3.85%	10.54	27.90	0.59%
10.54	34.57	7.09%	12.19	31.81	3.62%	12.21	25.55	0.61%
12.21	31.37	7.60%	13.86	28.94	3.44%	13.88	23.34	0.70%
Berry Plastics 16µ								
6.15	51.06	0.76%	6.15	52.25	1.37%	7.84	38.70	0.65%
7.82	47.95	1.15%	7.82	48.91	1.48%	9.51	35.82	0.84%
9.49	44.31	1.00%	9.49	45.05	1.65%	11.19	32.75	1.02%
11.17	40.41	1.30%	11.17	40.99	1.78%	12.86	29.81	1.18%
12.84	36.72	1.17%	12.84	37.15	1.82%	14.53	27.15	1.27%
Intertape 12.7µ								
6.63	43.56	2.00%	6.65	41.56	1.96%	8.40	34.84	1.47%
8.37	41.15	2.08%	8.38	39.15	1.98%	10.13	32.30	1.85%
10.10	37.66	1.75%	10.11	36.03	2.15%	11.86	29.42	2.42%
11.83	33.86	1.35%	11.84	32.56	2.36%	13.59	26.56	2.85%
13.56	30.23	0.94%	13.58	29.09	2.22%	15.33	23.96	3.13%
Intertape 16µ								
5.62	43.71	2.52%	5.58	43.54	2.09%	7.32	33.76	0.97%
7.33	42.31	3.38%	7.30	41.56	1.93%	9.04	31.93	0.82%
9.05	39.52	3.41%	9.01	38.78	1.80%	10.75	29.75	0.68%
10.76	36.45	3.59%	10.73	35.53	1.70%	12.46	27.47	0.73%
12.48	33.22	3.40%	12.44	32.32	1.68%	14.18	25.29	0.84%

In comparing the different evaluation methods, the s_{br} and the s_{bt} produced results that were not statistically different using a Tukey's HSD with a 95% CI while the s_{bp} consistently produced lower results that were statistically different. The s_{bp} produced lower results because the film creped off the pipe during testing, causing a lower Bisha Stiffness value. The COV of the s_{bp} data was the lowest because there was so much martial used in the test. Note that the COV of the s_{b1} 11.4µ Berry Plastics was much higher than any of the other films.

Dual necking was observed when evaluating the s_{br} samples. After the initial elongation and 1 hour wait time the samples became so stiff that the sample was slipping out of the jaws instead of evaluating the material property. For a visual example of this phenomena see Figure 73. If this sample preparation

and testing method is repeated a different testing jaw should be used that would not allow slippage of the film.

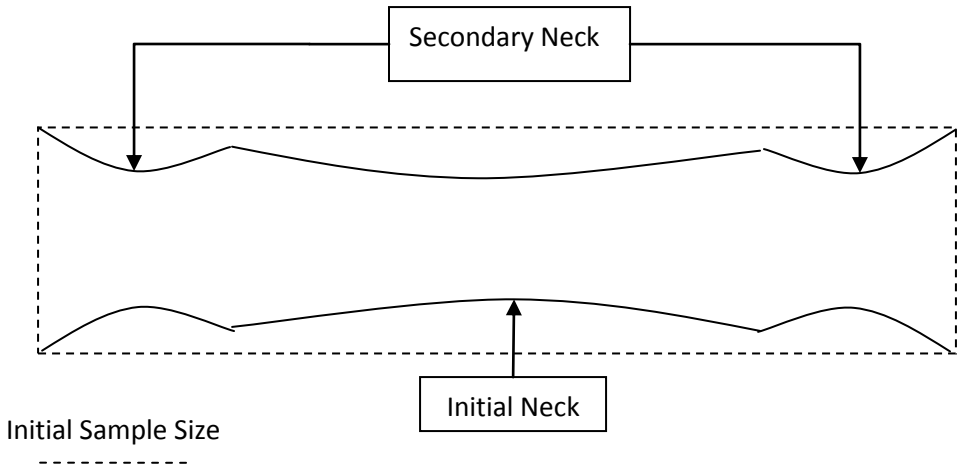

Figure 73 Dual necking phenomena when evaluating the S_{BR} samples

8.3.4 Conclusions & Discussion

The objective of this test was to compare different sample preparation methods for evaluating the Bisha Stiffness. Each of the data set was adjusted to allow for equal comparisons. The s_{b1} samples acted as the control sample of the experimental design. The s_{b1} results were not statistically significantly different than the s_{br} results however; the s_{bp} results were significantly lower than either the s_{b1} o the s_{br}.

The s_{bp} samples demonstrated stiffness's that were unusually low compared to the other two simple preparations. This occurred because when the film was being extended and held, it was able to slowly creep off the pipe during the test allowing lower Bisha Stiffness values. Unless the interface between the pipe and the film can be quantified, this testing procedure appears to be inadequate for evaluating s_b.

Even though the s_{br} samples produced results that were no different from the s_{b1} results, the dual necking observation gives cause to believe that the results were not truly representative of the Bisha Stiffness for the sample preparation method. This test method should be revaluated with jaws that would not allow sample slippage.

8.4 Appendix A4: Comparing the time dependent elastic properties of stretch film using the s_{af} and the s_{br} methods

This was the first experiment in attempting to correlate the Bisha Stiffness and initial force (s_b, f_i) and the applied stiffness and film tension (s_a, f_t) of a stretch film. This research was designed to answer the fourth objective. The research was halted before completion due to the lack of desirable results and was moved to the Appendix because of the valuable lessons learned that may be relevant to future research.

Recall in 3.2 Section that as test frame was built to simulate a unit load. The frame was made out of SPF 2x4 material and was assembled with drywall screws. The frame was attached to a pallet and was loaded with weight to keep it from moving during application and evaluation of the stretch film.

The stretch wrapper used was a semi-automatic Wulftec brand stretch wrapper. The average prestretch of the applied film was 249.18% with a standard deviation of 15.05% as found in Section 8.2.

The stretch wrapper applied the film to the test frame and the film was evaluated using the pull plate method identified in Section 3.2.4. The method of evaluating applied film properties was based on ASTM D 4649 where the pull plate was used to pull out on the film to evaluate the containment force. The pull plate method used in this research varied the location of the evaluation and called for multiple force evaluations (f_{af}) over five different extensions (x). The f_{af} was then turned into applied stiffness (s_a) and tension force (f_t) values by Equation 8-3.

$$\frac{\mathbf{f_{af}}}{\mathbf{2} * \sin(\boldsymbol{\beta})} = (\mathbf{s_a} * \Delta\ell + \mathbf{f_t}) + \mathbf{error}$$

Equation 8-3

Recall that the Bisha Stiffness was evaluated using a tensile testing machine and testing profile outlined in Section 3.1. Recall that the Bisha Stiffness (s_b) simulates the pulling, or extension, of the film off the unit load as the film is being evaluated for s_a per ASTM D 4649. The tensile testing profile that was used is shown in Figure 74. The initial extension was calculated from the actual prestretch of the film as applied to the test frame. Prestretch is blue in Figure 74. The film was then held for an hour (green) allowing for the film to recover and stiffen. The film was then extended again at the same speed (purple) to simulate the evaluation of s_a. The slope of this line is within the first centimeter was called the Bisha Stiffness (s_b), while the initial force of the s_b test is called the f_i. Note that the longer the green line recovers (falls), the less f_t is theoretically applied on to the unit load. The s_b value does not capture the diminishing nature of f_t, only the film stiffness.

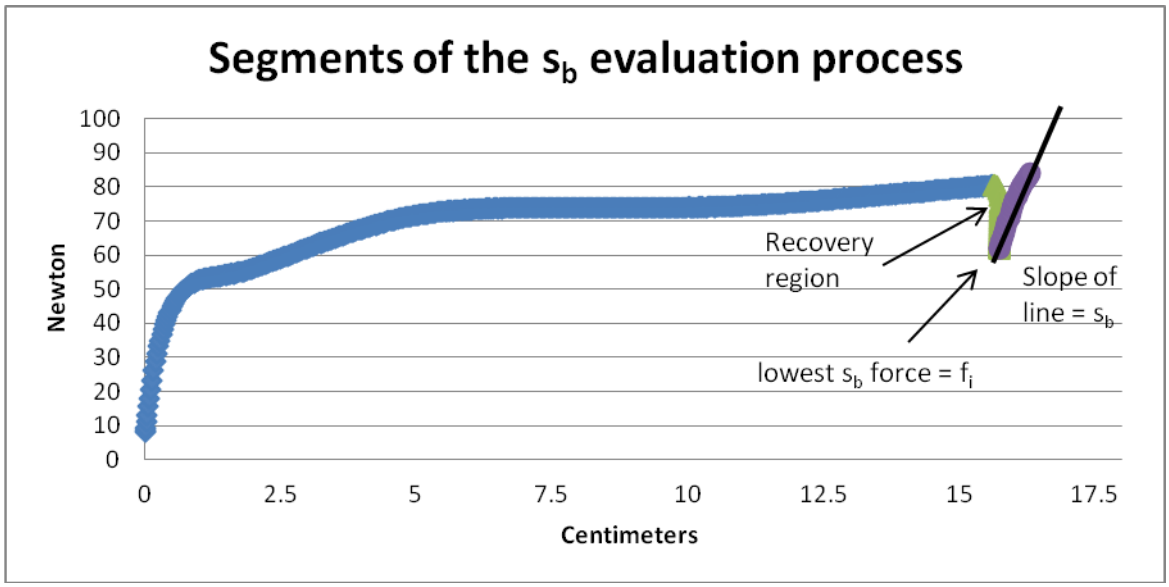

Figure 74 Different segments of the proposed tensile test profile identified

The sample preparation method for the tensile test utilized was the Roll Method (s_{br}) outlined in section Section 8.3.2. Recall that this involved rolling the film over a bar, slipping the film off the bar, laying the tube flat and testing the sample.

Note that this testing was cut short due to the lack of desirable results. However, it is included here because of its valuable information with regard to stretch film application and behavior as required in the second objective.

8.4.1 Measuring how s_{br} changes over time

The s_{br} sample preparation and evaluation method outlined in Section 8.3.2 was used to determine material stiffness changes over time. The films were evaluated using the Bisha Stiffness method. The results were compared to the applied stiffness evaluated with the pull plate (s_{af}) results (Section 8.4.2) in Section 8.4.3

Experimental Design

Two films were used in 8 time increments (1, 15, 30, 45, 60, 90 and 120 minutes) for up to 5 replications per test. The Bisha Stiffness was calculated and the f_i was recorded for each sample. This experiment investigated the influence of time on the Bisha Stiffness. A visual representation of the experimental design is shown in Table 33.

Table 33 Visual representation of the experimental design for Section 8.4.1

Test Sample preparation➔	Roll
Parameters Estimated➔	S_{br} and F_{i1}
Film Thickness➔	11.4 µ, 16 µ
Time Increments (min):	Number of test replicates
1,30, 60	5
15, 45, 90, 120	3

Materials and Methods

Berry Plastics 16µ and 11.4µ films were used. The samples were created using the Roll method outlined in Section 8.3.2. They were evaluated using the Bisha stiffness technique outlined in Section 3.1. Each sample was pulled at 50.8cm/min (20”/min) with an initial sample length of 6.6cm (2.6”). Note that the short sample size was used because this is the distance between the two prestretch rollers on the machine that was used to apply the film to the test frame in evaluating the s_{af} (Section 8.4.2). The time increments of interest were 1, 15, 30, 45, 60, 90 and 120 minutes. Five replicates were completed of ever other time increment while the intermediate only had three. The samples were pulled to 250% and the initial force of the Bisha stiffness (f_i) and the Bisha stiffness (s_{br}) were calculated at an additional 8% elongation from the original sample.

Results

The results for the Bisha Stiffness (s_{br}) calculation are shown in Figure 75 & Figure 76 and the results of the initial force (f_i) of the Bisha Stiffness are shown in Figure 77 & Figure 78.

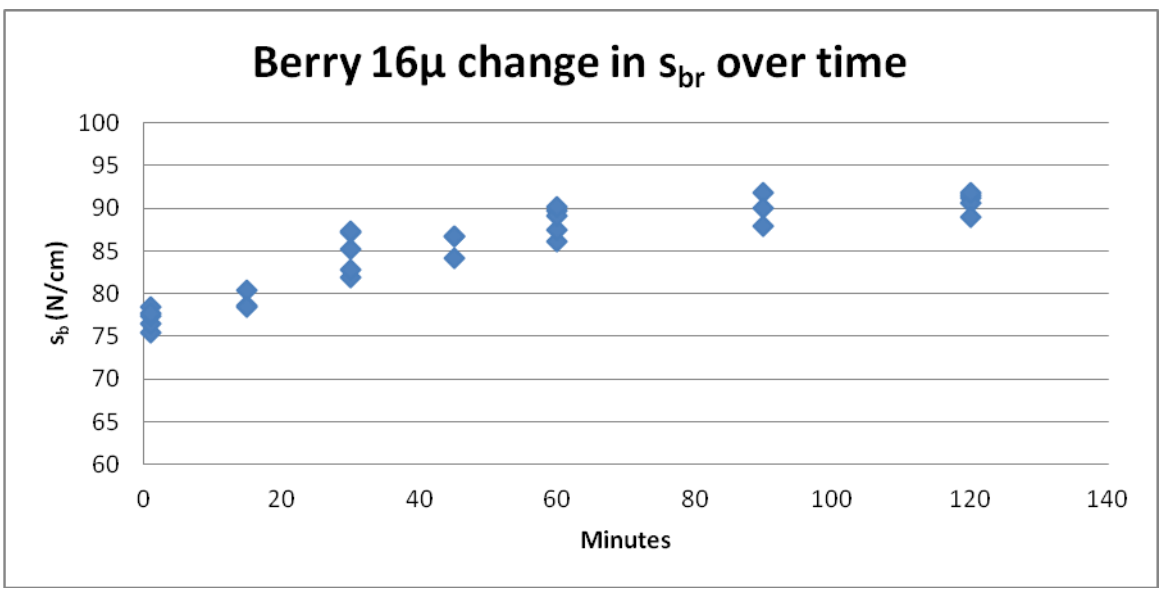

Figure 75 Berry 16µ s_{br} results over time

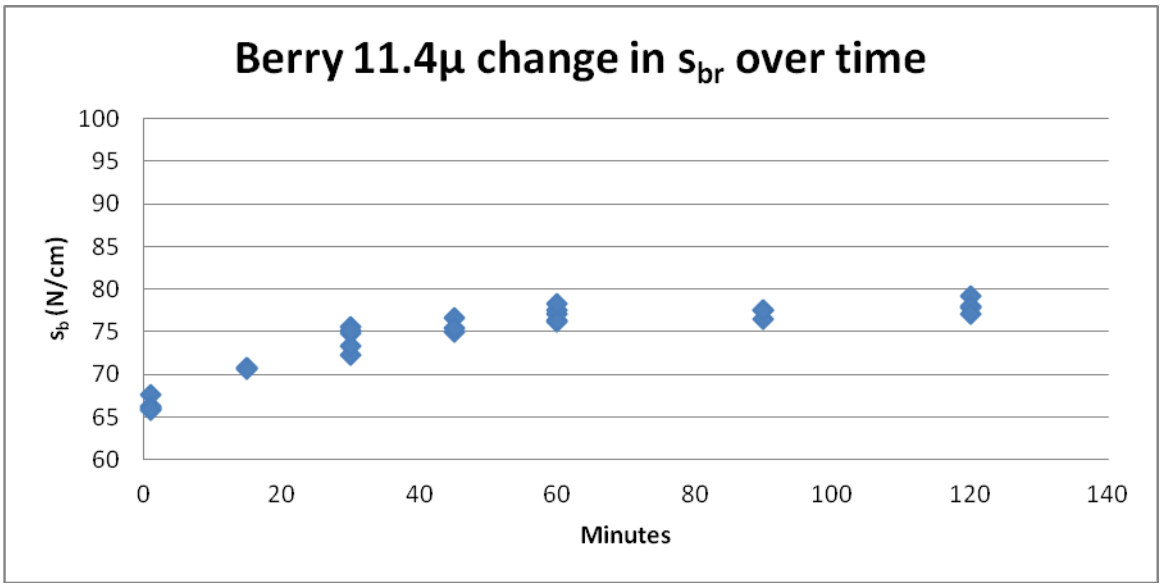

Figure 76 Berry 11.4µ s_{br} results over time

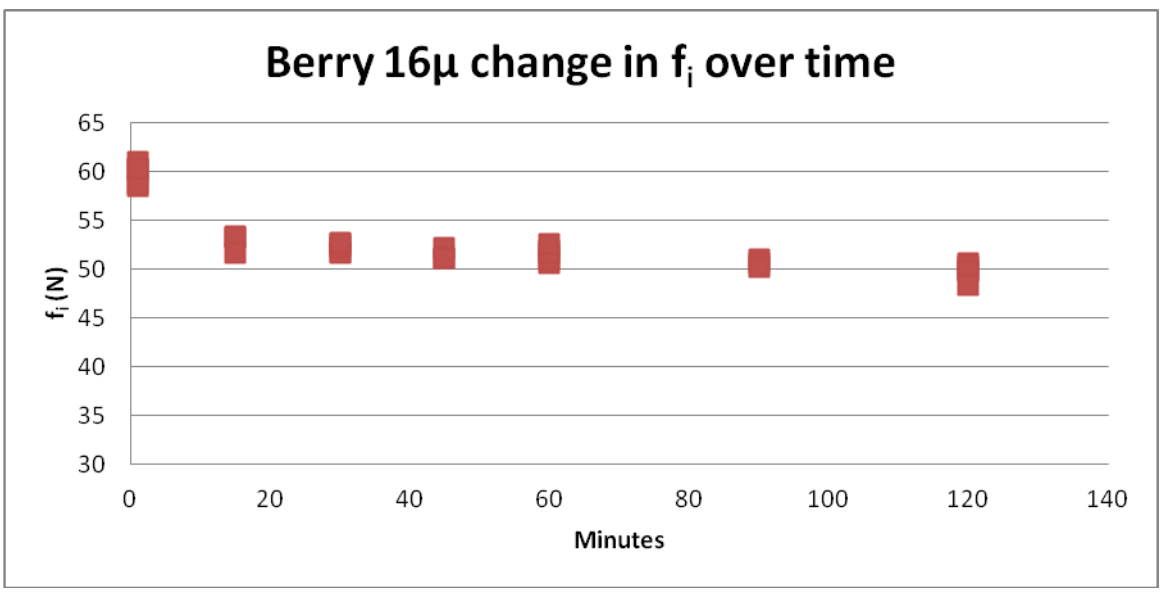

Figure 77 Berry 16µ f_i results over time

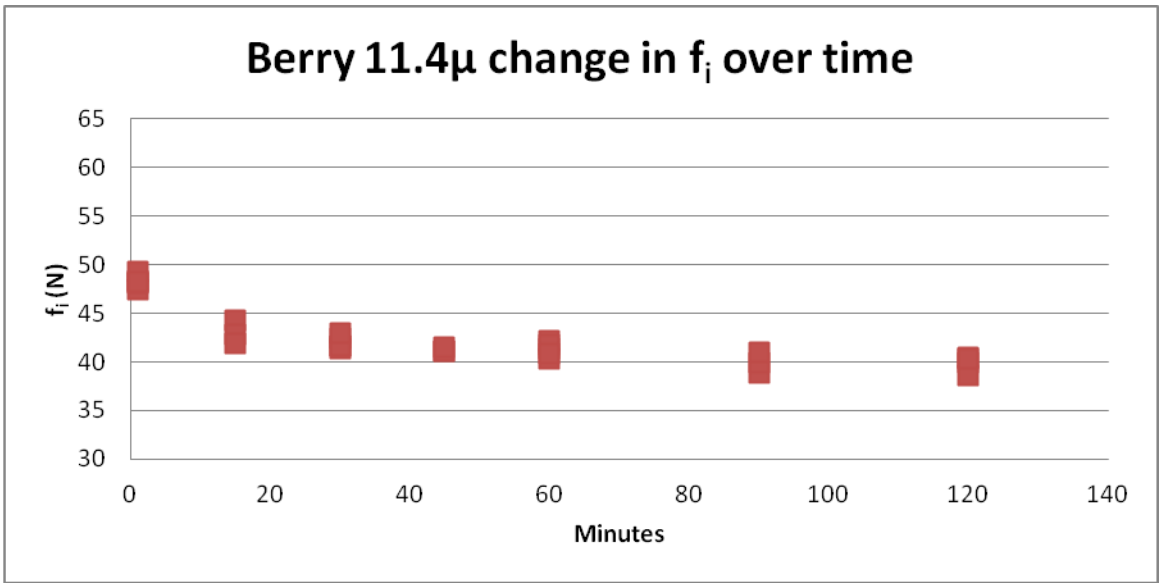

Figure 78 Berry 11.4µ f_i results over time

The calculated s_{br} results provided show that there was a 12% increase in stiffness over the first hour for the 11.4µ film and an 18% increase in stiffness for the 16µ film. These results were expected as the film molecules are realigning during the relaxation period, allowing for the film to become stiffer over time. Note that the relationship between increases in stiffness is very close to the relationship in original material thickness. While there were identifiable trends in the films behavior, much more research needs to be conducted concerning the behavior of materials over time with regard to material stiffness.

The observed f_i results provided an inverse trend to the s_{br} results. This was expected as the film is relaxing over time causing the initial force of the Bisha stiffness to fall in line with the increasing stiffness. Note that the relationship between the reductions in f_i is similar to the ratio of the original thickness of the material just as with the material Bisha Stiffness.

The trends in Bisha Stiffness and initial force will continue for many days but it appears that a significant amount of change occurs in the first 60 minutes. While there were identifiable trends in the films behavior, there needs to be much more research conducted on how materials behave over time with regard to material stiffness and initial force.

Conclusion & Discussion

The Roll sample preparation method was used evaluate the Bisha Stiffness over multiple time increments. The results indicated that during the first hour the amount of stiffness increased as the amount of initial force decreased. This was expected as the polymers are aligning during the recovery period, becoming stiffer and providing less force to hold the sample during the test. More testing on a wider range of films will have to be conducted to determine if the one hour time frame is the appropriate time frame.

This experiment was halted after two films because it was not correlating to actual stiffness readings found in Section 8.4.2.

After this test was completed, it was noted in Section 8.3 that the s_{br} samples formed a double neck in evaluating the Bisha Stiffness. This occurred because the films became so stiff during the timed evaluation that the grips used to hold the samples were not strong enough to prevent the samples from pulling out. A graphic of the double necking phenomena is shown in Figure 79. This error that occurred may have affected the results; therefore, future testing should not use this sample preparation method unless grips that prevent slippage can be found.

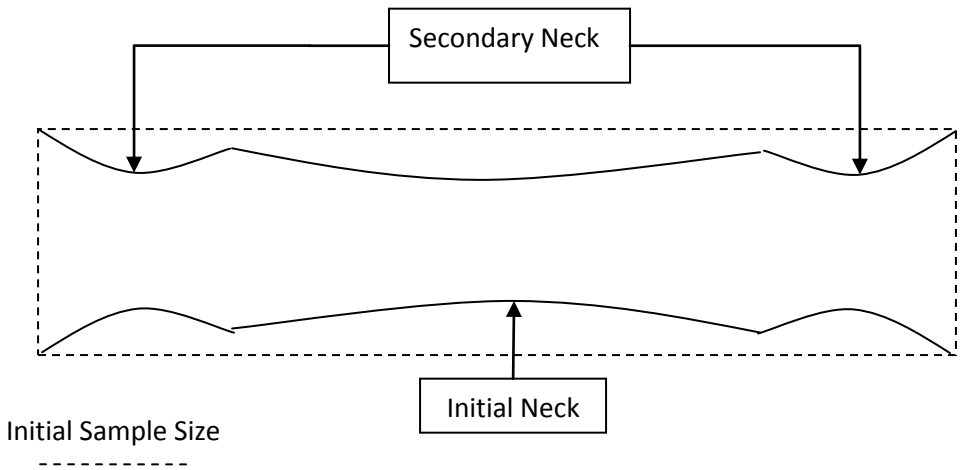

Figure 79 Dual necking phenomena when evaluating the s_{br} samples

8.4.2 Measuring how s_{af} changes over time

Stretch film was applied to the test frame and the f_{af} was evaluated at many different extensions and time increments. The s_{af} and f_t were calculated for each set of f_{af} data. How the s_{af} and f_t changed over time was plotted and compared to the results of how the s_{br} and initial force of the s_{br} (f_{ir}) changed over time in Section 8.4.1 in Section 8.4.3.

Experimental Design

Two films were used. There were three different levels of layering tested at four different time increments. There were 5 repetitions per film per layer. This experiment investigated the influence of time on the applied stiffness of a stretch film. A visual representation of the experimental design is shown in Table 36.

Table 34 Visual representation of the experimental design for Section 8.4.1

Parameters Estimated➔	s_{af}, f_t
Film Thickness➔	11.4 µ, 16 µ
Layer Increments➔	1, 2 & 3
Time Increments (min):	Number of test replicates
1, 5, 15, 60	5

Materials & methods

The films used were Berry Plastics 16µ and 11.4µ. The film was applied with the stretch wrap machine outlined in Section 3.2.3. The film tension of the machine was set at the 5 dot while the turn table was set at the 7.5 dot on the setting panel of the machine. Note that the exact speed of the output prestretch rollers and the turn table were not recorded. The prestretch carriage movement was restricted and was applied to the test frame outlined in Section 3.2.3. The films were applied in 1, 2 and 3 layer variants and evaluated at 1,5,15 and 60 minutes. The applied stretch film was evaluated using the pull plate method outlined in Section 3.2.4. The f_{af} results were turned into s_{af} and f_t via Equation 8-4 which was derived in Section 3.2.1. After the stiffness and tension force results were calculated, they were averaged down to force per layer for ease of comparison.

$$\overline{\frac{\mathbf{f_{af}}}{\mathbf{2} * \sin(\boldsymbol{\beta})}} = (\mathbf{s_a} * \Delta\ell + \mathbf{f_t}) + \mathbf{error}$$

Equation 8-4

Results

The s_{af} and f_t results for the Berry 16µ film are shown in Figure 80 & Figure 81 and the Berry 11.4µ results are shown in Figure 82 & Figure 83. Note that the second layer of the Berry 16µ was not completed due to lack of film resources.

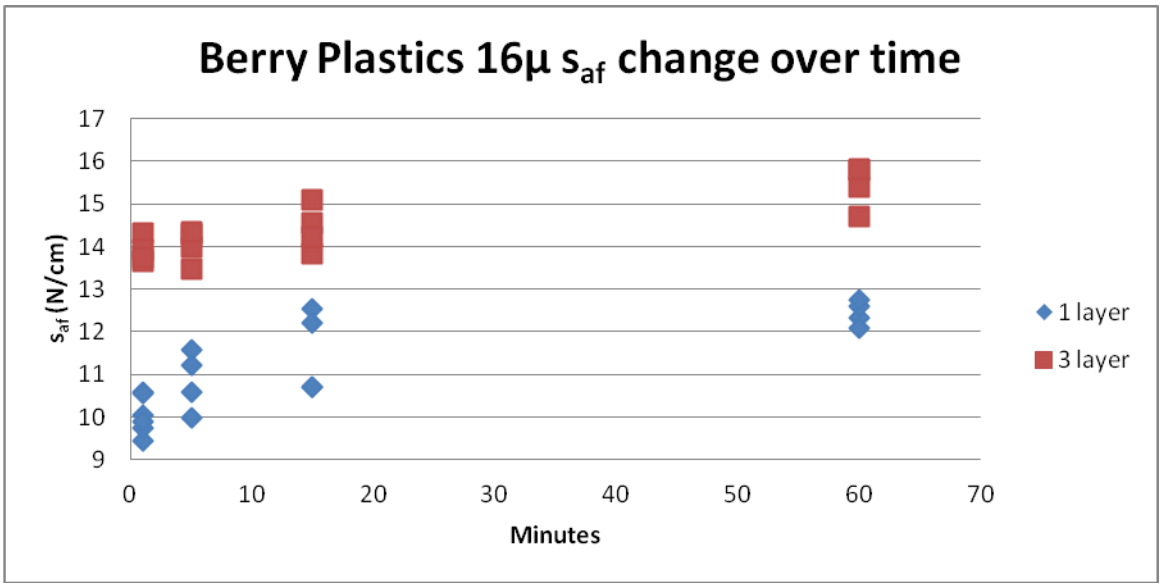

Figure 80 Berry Plastics 16µ s_{af} change over time. Note that the second layer variant was not completed due to lack of film resources.

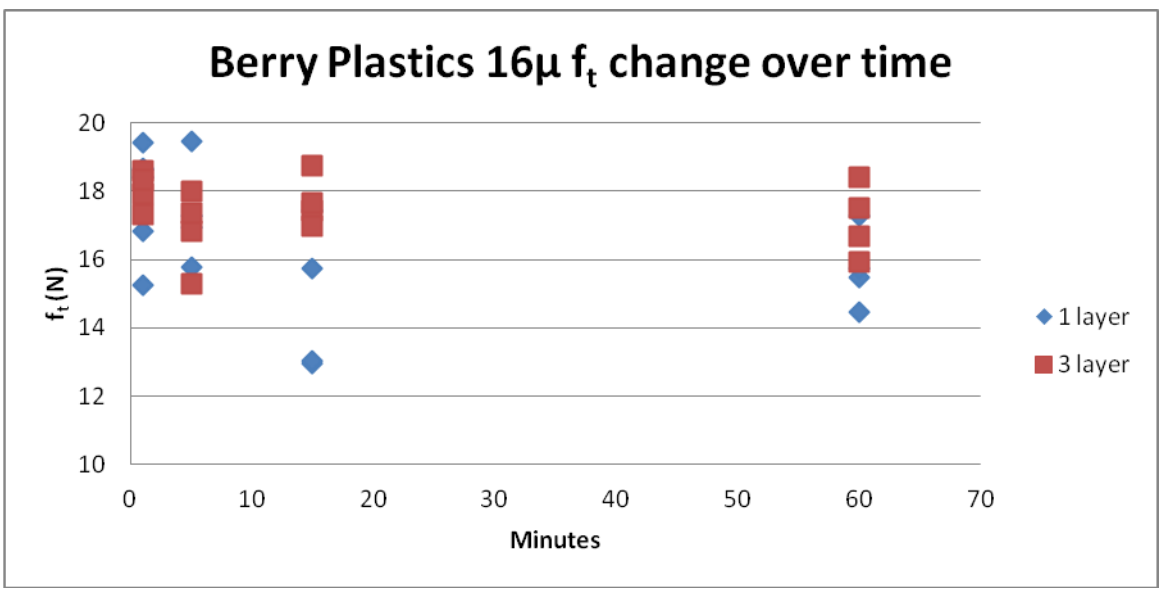

Figure 81 Berry Plastics 16µ f_t change over time. Note that the second layer variant was not completed due to lack of film resources.

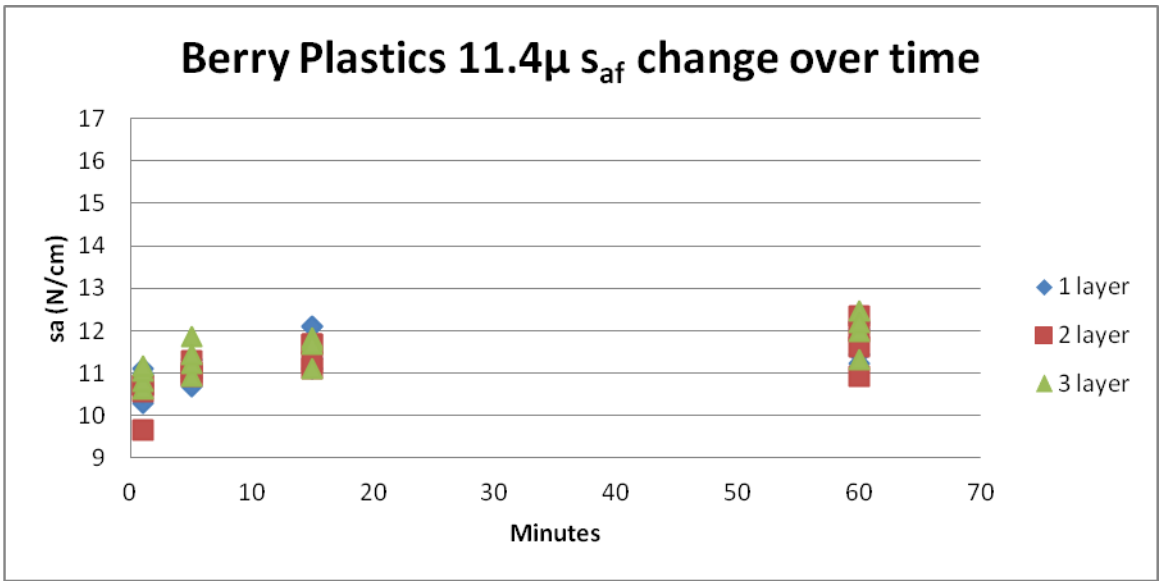

Figure 82 Berry Plastics 11.4µ s_{af} change over time.

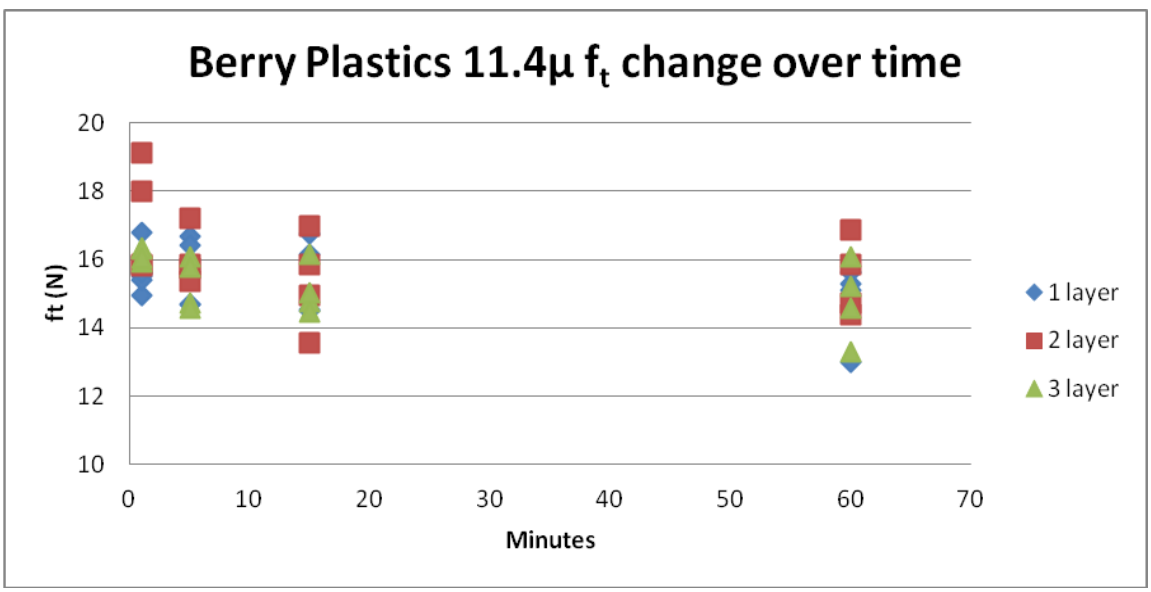

Figure 83 Berry Plastics 11.4µ f_t change over time.

The results of the s_{af} for each of the films were very similar, changing fewer than 10% within the hour allotted. The layering did not affect the 11.4µ film but did seem to affect the 16µ film. The f_t results for the 11.4µ film provided a visible inverse pattern to the s_{af} whereas there was not much of a pattern for the f_t of the 16µ film. The COV's for each data series was fewer than 3%. There were not enough films tested to draw any major statistical conclusions. Note that the film was applied to the test frame with slack in the film; how this affected the testing results is currently unknown.

Conclusions & Discussion

The objective of this experiment was to evaluate how different applied films behaved over time in different layer increments. This was done to determine if there was an additive effect in layering film and to determine how the s_{af} and f_t changed over time. There was an observable pattern between the rising s_{af} and the falling f_t in both cases, however there was no observable layering affect. Note that this research did not contain enough films or replicates to conduct an appropriate statistical analysis or draw any conclusions. This research was stopped short due to its lack of correlation with the results of Section 8.4.1.

A major limitation of this experiment was the lack of control of the stretch wrap machine settings. The rotation speeds of the stretch wrapper turn table and the output prestretch roller were not quantified. That means that not only can this experiment can't be replicated, but also the amount of slack imparted onto the system by the speed differential (-PP) (Equation 3-31) can't be quantified.

8.4.3 Predicting applied stiffness and film tension from the Bisha Stiffness

The applied stiffness of stretch film was measured by applying the stretch film with a semi-automatic stretch wrapper to a test frame in one, two and three layer variants in perfectly horizontal wraps. The film was then evaluated with the pull plate method. The force of the applied film data (f_{af}) was then turned into the stiffness of the applied film measured on the face (s_{af}) and the film tension (f_t) via Equation 8-5. For more details on the application and evaluation of the film or the derivation of Equation 8-5 see Section 3.2. Note that the speeds of the turn table and the output prestretch rollers were not recorded for this experiment.

$$\overline{\frac{\mathbf{f_{af}}}{\mathbf{2} * \sin(\boldsymbol{\beta})}} = (\mathbf{s_a} * \Delta\ell + \mathbf{f_t}) + \mathbf{error} \qquad \text{Equation 8-5}$$

The Bisha Stiffness of a stretch film is found by extending a specimen on a tensile testing device, holding it for a given period of time and then extending it again. The slope of the secondary force/deflection curve is defined as the Bisha Stiffness. For more on the Bisha Stiffness see Section 3.1. The test sample creation method Section 8.4.1 was the Roll creation process defined in Section 8.3.2. The Roll creation process involved laying the stretch film flat on a table and rolling the film up with a bar, removing the bar from the center of the roll, flattening the sample and cutting it to a desired length. Note that the Bisha Stiffness from this sample creation method was called the s_{br} and the initial force from the s_{br} is denoted as f_i.

Comparison of stiffness and force results

The results for the 16µ and the 11.4µ films are shown in Table 35 and Table 36. In both cases the Bisha Stiffness and the Initial force from the Bisha stiffness are significantly higher than the applied stiffness and the film tension. This occurred because of the poor control of the stretch film application process and the unique film sample preparation method used to evaluate the Bisha Stiffness. Note that the layering data has been averaged together for the comparison because of its indifference.

Table 35 Average results of the 16µ Bisha Stiffness, applied stiffness, tension force and initial force of Bisha Stiffness

Minutes	s_{br}(N/cm)	s_a (N/cm)	f_i (N)	f_t (N)
1	77.05	11.59	59.78	17.93
5	N/A	12.43	N/A	17.12
15	79.17	12.98	52.77	16.25
30	84.86	N/A	52.09	N/A
60	88.53	13.94	51.56	16.44

Table 36 Average results of the 11.4µ Bisha Stiffness, applied stiffness, tension force and initial force of Bisha Stiffness

Minutes	s_{br} (N/cm)	sa (N/cm)	fi (N)	ft(N)
1	66.34	10.71	48.29	16.23
5	N/A	11.13	N/A	15.65
15	70.75	11.57	43.00	15.31
30	74.24	N/A	41.93	N/A
60	77.06	11.81	41.29	15.00

8.4.4 Conclusions & Summary

This section was the initial attempt to correlate the applied stiffness of stretch film and the film tension with the Bisha Stiffness and the initial force of the Bisha Stiffness. The results were significantly different. The Bisha Stiffness and initial force were consistently higher than the applied stiffness and tension force. This was because of the speed of the turn table and the output prestretch roller was not correlated allowing slack in the applied stretch film.

The Bisha Stiffness and respective forces and the applied stiffness and film tensions all appeared to undergo noteworthy changes within the first hour of testing. More testing should be conducted to ensure that this is consistent across a wide variety of products. In addition, long term decay of films should be evaluated for modeling purposes. Knowledge of how a film behaves over time and whether or not it still can offer significant stabilizing power would be beneficial for manufacturing facilities that require long term storage before shipment.

How slack affects the application of stretch film has not been quantified and should be in future research. In addition, the Roll sample preparation method used when evaluating the Bisha Stiffness produced a sample with many different layers. As found in Section 5.2, there may be an additive effect within the layering of the sample. This layering effect should be quantified for this film before a proper comparison between data sets can be conducted.

This test was halted because of the inconsistencies between the testing methods. There were not enough replicates or enough film used to make any kind of far reaching conclusions from the data.

8.5 Appendix A5: The Effect of Stretch Wrap Containment Force on Unit Load Stability

The purpose of this research was to identify and isolate a characteristic of a unit load and determine how that characteristic affects unit load stability. Greater load stability will help to prevent damage to a unit load, ease the material handling process and increase worker safety in the material handling environment. The objective of this research was to determine if increasing the level of containment force applied by 20.3µ stretch film affects unit load stability in vibration and impact testing. Note that for this research, containment force is defined as it is in ASTM D 4649, being the amount of force required to pull out on the face of the unit load 10.1cm (4") which is inconsistent with the rest of the research within this document. Therefore, the containment force was called the standard containment force (f_{c-s}) within this section.

8.5.1 Experimental Design

The 20.3µ stretch film was applied to a standard test unit at one of three desired containment forces (high, medium and low). Testing on a given level of standard containment force was repeated three times. Each unit load was then exposed to one of two ASTM tests for a total of 18 unit load tested. Nine of the test units were used in vibration testing and nine were used in impact testing. Table 37 shows the experimental design.

Table 37 Experimental Design for measuring the effect of standard containment force on load stability

Test Unit Used	Number of Load Stabilizers	Number of ASTM Tests	Test Replications	Load Tensions	Total Unit Loads Tested
1	1	2	3	3	18

8.5.2 Materials & Methods

The test unit used consisted of forty-five corrugated boxes (test containers) were used to construct the load for each test unit. The 69-23-69 C flute RSC containers had inside dimensions of 40.6cm long x 31.7cm wide x 25.4cm deep (16" x 12.5" x 10"). Each test container was packed with 16 2x4s (Lumber Grade SPF) that were cut to 39.3cm (15.5") in length and stacked in two layers. Stacking pattern of a single layer is shown in Figure 84.

Figure 84 Stacking Pattern of One Layer of 2x4's in Test Containers

Each test container weighed 120.1 Newtons (27#). The test containers were placed on a 121.9cm long x 101.6cm wide (48" x 40"), three stringer pallet (test pallet) that weighed 186.8 Newtons (42#). A specification of the test pallet is found at the end of Section 8.5. The dimensions of the test unit measured 125.7cm long x 97.7cm wide x 109.22cm (49.5"x 38.5"x 43"). Each test unit incorporated nine (9) columns of boxes with five (5) boxes per layer for a total of 45 test containers. The test unit weighed 5591.41 Newtons (1,257#). A photograph of the standard test unit is shown in Figure 85.

Figure 85 Photograph of the Standard Test Unit

The stretch film selected for this experiment was AEP's Alpha Series (A12) 20.3µ cast film on a 50.8cm (20") wide roll. It was applied by a Wulftech Smart Series stretch wrap machine model number WSML-150_B. A photograph of the stretch wrapper is shown in Figure 86.

Figure 86 Photograph of the Wulftech Stretch Wrap Machine used to Apply

The wrap pattern of each test unit consisted of three layers of overlap on the top and three and one-half layers on the bottom, which is a common commercial wrapping pattern (see Section 2.2.2). Each test unit was wrapped and sat in a resting position for 3 hrs.

A Shimpo digital force gauge was used to measure the $f_{c\text{-}s}$ of each load stabilizer. It was measured by referencing ASTM D 4649 Annex A1.10.1, the 10.1cm (4") pull method. A 10.1cm incision, parallel to the pallet, was cut into the stabilizer in the middle of layers 1, 3 and 5 on each side of the test unit after testing. A 10.1cm rod attached to the force gauge was placed in the incision and turned perpendicular to the direction of cut. The rod was then pulled 10.1 from the corrugated container and the force recorded. This procedure was conducted on each face of the test unit in the middle of layers 1, 3 and 5. Average containment forces were calculated by taking the average force across all faces and layer per standard containment force sample grouping of three test units. The procedure used was a destructive procedure that would affect the stabilizer performance therefore the standard containment force was measured after each test.

Three potential stretch films $f_{c\text{-}s}$ were used, high, medium and low. Settings on the stretch wrapper were estimated and tested on a dummy test loads. Once initial the standard containment force and stretch wrap machine settings were correlated, the three containment forces/machine settings were tested to ensure statistical independence. Three repetitions were conducted on each of the three settings and $f_{c\text{-}s}$ readings were taken. The results are shown in Table 38. Note that the rotational speeds of the turn table and the output prestretch rollers were not recorded during this test.

Table 38 $f_{c\text{-}s}$ pretest

	Average	COV
High	163.0	15.9%
Medium	112.9	27.5%
Low	74.3	35.5%

Standard containment force readings were collected from every test unit after testing using the same data collection methods. The results are shown in Table 39.

Table 39 f_{c-s} for actual testing

	Average	COV
High	35.7	16.3%
Medium	23.7	30.7%
Low	12.6	30.3%

In both cases the three setting were statistically different from each other using a 95% confidence interval. This allowed the comparison of container displacements of the three wrap intensities as three independent variables.

The vibration tests were conducted according to ASTM D 5415 - Evaluating Load Containment Performance of Stretch Wrap Films by Vibration Testing. A LAB Instruments vibration table using Signal Calc 350 Vibration Controller Software was used. A photograph of the vibration table is shown in Figure 87. For the test parameters ASTM D 4169 – Performance Testing of Shipping Containers and Systems, Section 12 Schedule D was referenced. A random tractor trailer simulation was run at Assurance level 2 with an overall g_{RMS} of 0.53. For all vibration tests the RMS was taken from the Signal Calc software output. The RMS was then divided by the g_{RMS} to calculate the average transmissibility.

Assurance level 2 was selected because it would ensure quantitative values for all test samples. A higher assurance level could result in failure of a load stabilizer, allowing for non-quantitative values. In addition, the amount of displacement that occurs at level 2 would be proportional to the amount that would occur at level 1. While the numeric values would change, the differences between the numbers should stay the same.

Stanchions were placed on the outside edges of the vibration table to prevent the test units from walking off the table during vibration. The stanchions were placed in line with the middle columns of the corrugated boxes, within the test units, so they would not interfere with any displacement of the boxes during testing. A minimum of two inches was left in between the test unit and the stanchions.

Figure 87 Photograph of the LAB vibration tale used. The stanchions used are seen on the table.

The impact tests were conducted according to ASTM D 5414 - Evaluation of Horizontal Impact Performance. The incline impact tester was manufactured by Gaynes Engineering Co. The angle of the track was 10 degrees from the floor and the trolley rode parallel to the track. To simulate a standard horizontal impact test, the incline impact tester was modified by retrofitting the impact trolley with a steel leveling table. The test units were placed on the steel leveling table with the deck boards parallel to the impact surface or perpendicular to the direction of the stringers. A “pallet stop” fabricated into the steel leveling table ensured the pallet stopped when the sled impacted the bumper, allowing the test load to move freely. There was a 16.5cm (6.5”) bumper between the end of the track and the backstop intersect. This allowed a maximum displacement distance of 17.7cm (7”) at the bottom of the test unit and 36.1cm (14.25) at the top. Photographs of the testing apparatus are shown in Figure 88 and Figure 89.

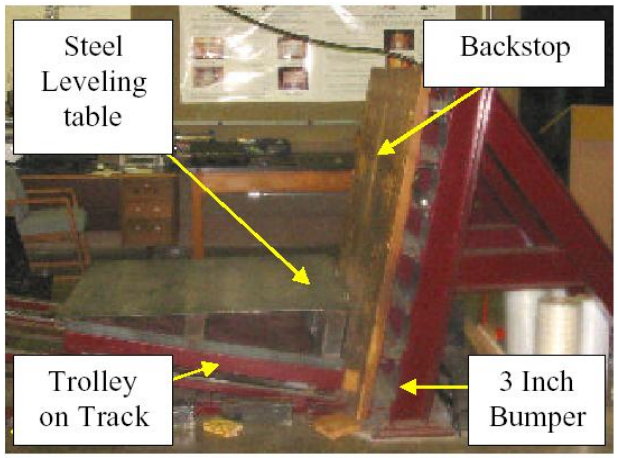

Figure 88 Photograph of the Incline impact tester used in testing with the steel leveling table in place

Figure 89 Photograph of the Pallet Stop fabricated into the steel leveling table

Each unit received one impact from a distance of 91.4cm (36”), measured from the front of the sled to front of the bumper. According to a Shear accelerometer by PCB Piezotronics coupled with Lansmont TP3 Lite software and Test Partner, the test units experienced G forces in the 10g range. The G force results are shown in Table 40.

Table 40 Impact Testing Forces

Horizontal G’s	Vertical G’s
10.36	10.07

Displacement of the containers that comprised the test unit was utilized as the indicator of load stability. Container displacement is defined as the displacement of one test container layer relative to another. To measure the container displacement, eight vertical masking tape lines 1.9cm (3/4”), two per face, were placed approximately 15.2cm (6”) in from the four outside corners of the test unit directly onto the corrugated boxes. The location of the lines is shown in Figure 90.

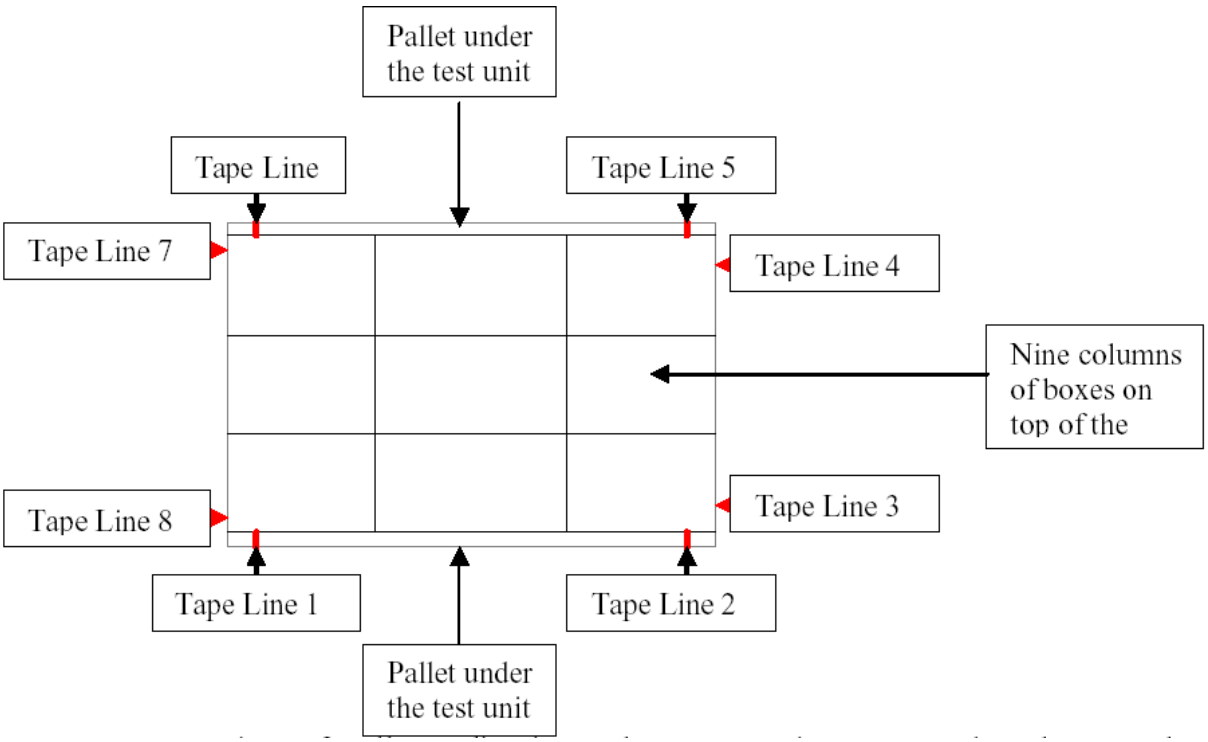

Figure 90 Top View of Pallet Indicating Where Tape Lines Were Placed On

Each vertical box intersection was labeled along the tape line. The tape was then cut with a razor blade to allow natural displacement during testing. The locations of the intersections are shown in Figure 91.

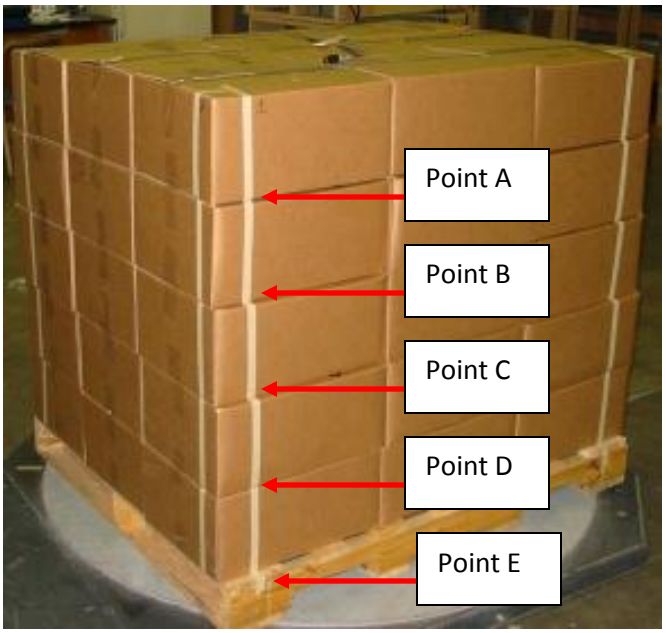

Figure 91 Photograph of the Side View of the Pallet Indicating Where the 5 Measurements were taken

After the appropriate stabilization method was applied to the load, any shifting along the tape lines, on all faces of the test unit, was measured with a ruler to the nearest .05 cm before testing. Displacement to the right was positive and displacement to the left was negative. Once a test was performed, the displacement of each tape intersection on every face was measured again in the same manner. This method was used on all test units.

Displacement data was collected on each face of the test unit to ensure the entire movement of the unit load was captured. Displacement to the right was recorded as positive and displacement left was recorded as negative. First, the total displacement due to testing was determined for each layer on each face (final container displacement minus initial container displacement). The cumulative displacement of the layers (a through c) from the pallet up was calculated. Before the displacement of each face could be accurately compared, the sign notation of the displacements had to be corrected. When viewing the test unit from above and attempting to average all displacement into two directions (X and Y), displacement to the right in direction X was positive on one face and negative on the opposite face. The same was true for direction Y.

To correct for this, the signs on two sides of the test units were inverted, allowing all displacement to the right to be positive and all displacement to the left to be negative for both directions. A visual interpretation is shown in Figure 92. To eliminate the directionality of the displacement data, the absolute value of the cumulative displacement was used as a measure of displacement.

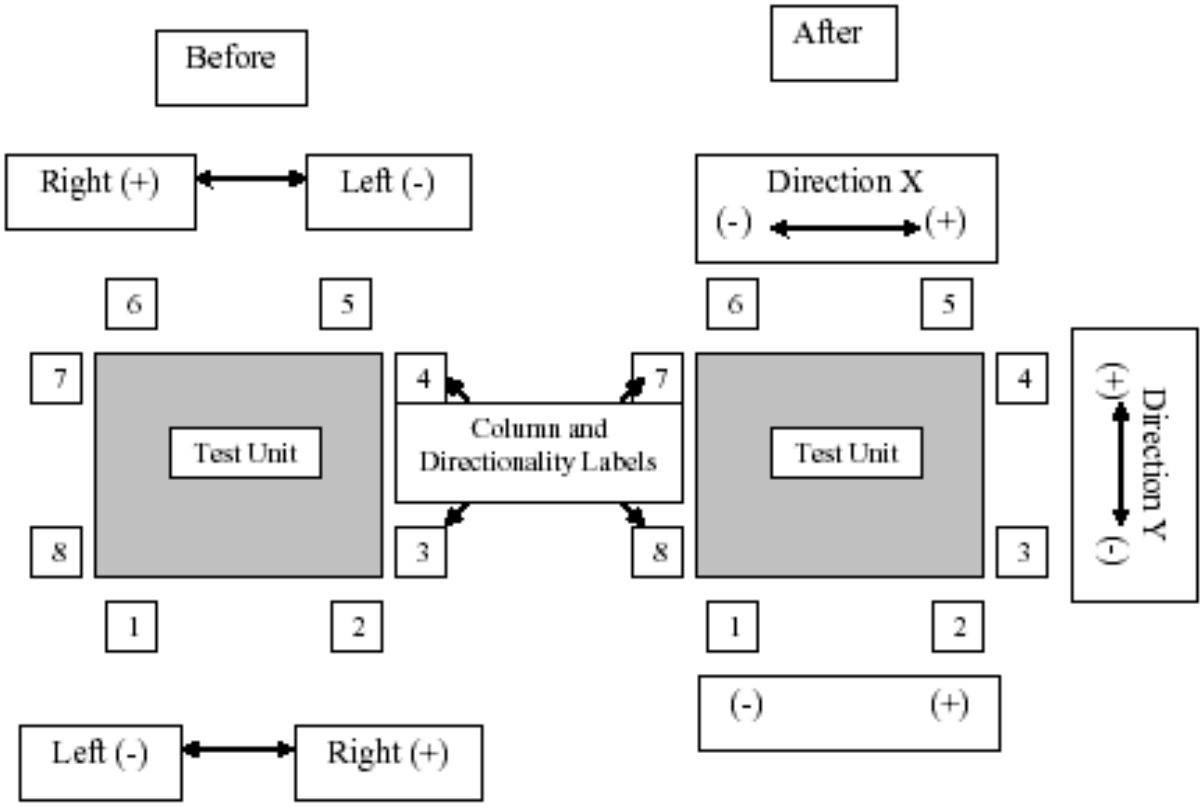

Figure 92 Visual Column Sign Inversion Explanation

It is not clear whether average load displacement or maximum load displacement is the most appropriate measure of load shift. The maximum displacement experienced could be statistically insignificant, but the average displacement may not correctly identify when failure occurs. Therefore, both measures were used. First, the Cumulative Average Displacement (CAD) was calculated by using the average container displacements by direction, per column, by layer and across the five test units. Then, the Cumulative Average Maximum Displacement (CAMD) was calculated as the maximum displacement by direction, per column, by layer and across the three test units.

8.5.3 Results & Discussion

Research was conducted in the order of high, then medium and lastly low containment force. The experimental design and testing setup were previously described in Materials and Methods.

Results - Vibration Testing

One desirable characteristic of an effective stabilizer is an ability to minimize transmissibility. Table 41 shows the average transmissibility for the three standard containment force levels. The higher standard containment force allowed for a higher transmissibility, and the lower standard containment force allowed for a lower transmissibility. This was expected as a higher standard containment force would hold the test unit tighter allowing it to act simultaneously as one mass.

Table 41 Average Transmisibility

High	5.64
Medium	3.69
Low	2.11

The comparison of the average container displacement that occurred in vibration testing for the three standard containment force levels through Cumulative Average Displacement (CAD) and Cumulative Average Maximum Displacement (CAMD) are shown in Figure 93 & Figure 94 below. Using both calculation methods, the least amount of displacement occurred in the high standard containment force test units, while the most amount of displacement occurred in the low standard containment force test units.

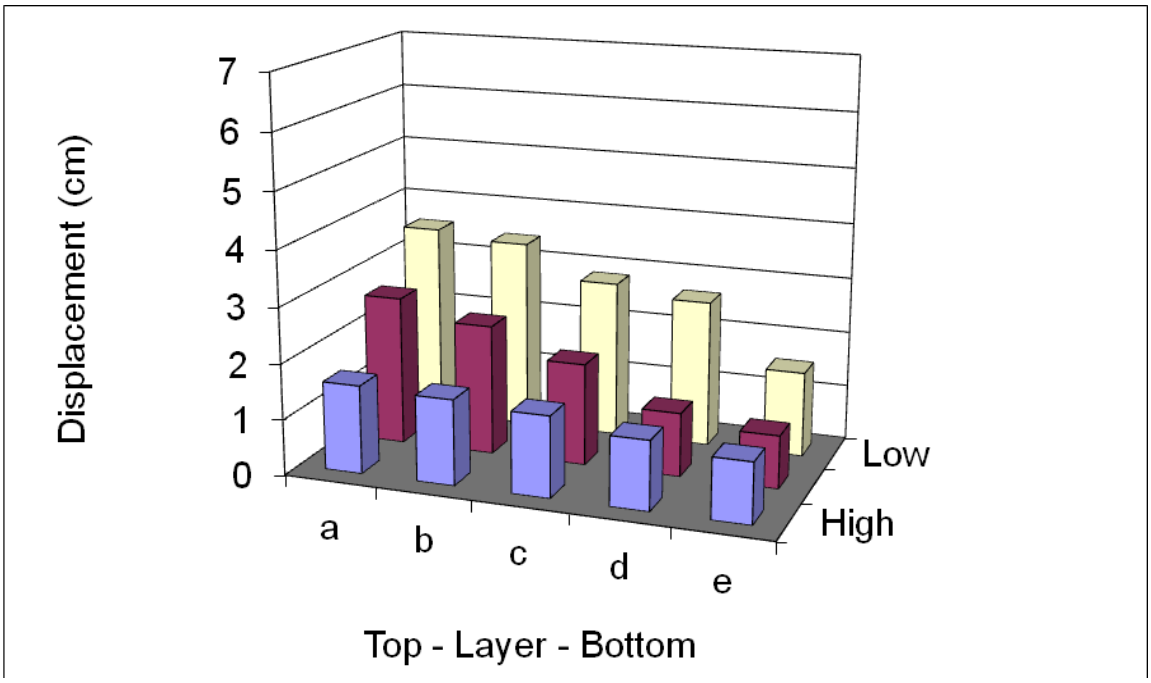

Figure 93 CAD in Vibration Testing

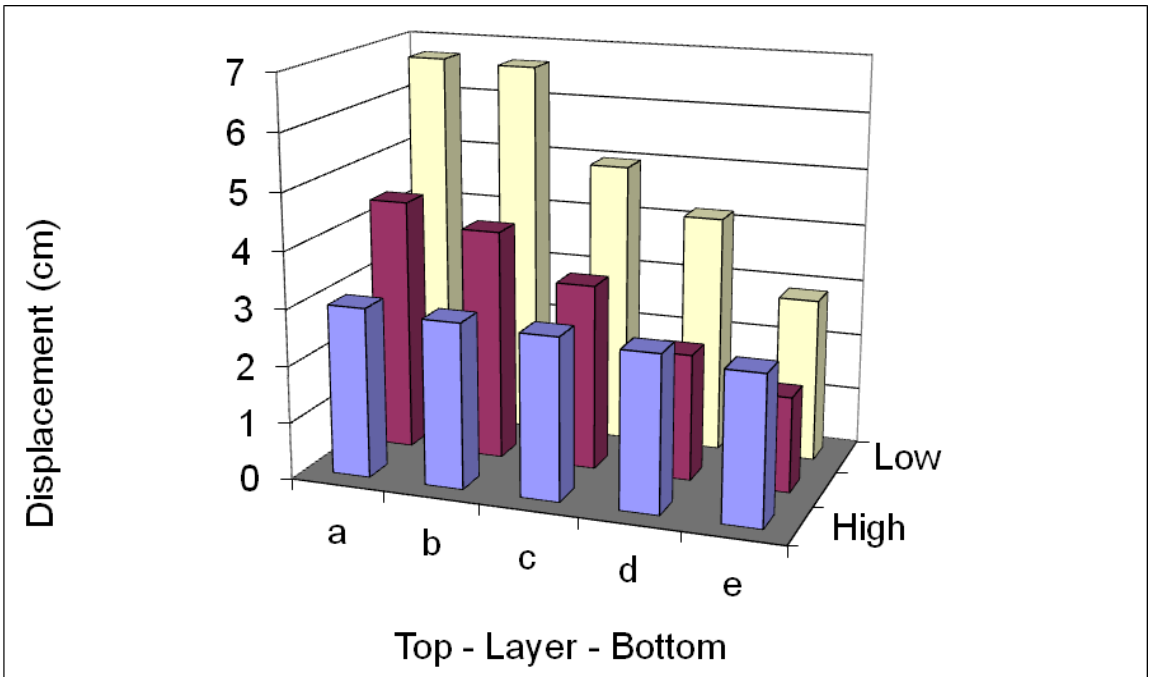

Figure 94 CAMD in vibration testing

Results - Impact Testing

Comparison of the average container displacement that occurred in impact testing for the three standard containment force levels through Cumulative Average Displacement (CAD) and Cumulative Average Maximum Displacement (CAMD) is shown in Figure 95 & Figure 96 below. Using both calculation methods, the least amount of displacement occurred in the low standard containment force test units, while the most amount of displacement occurred in the high standard containment force test units.

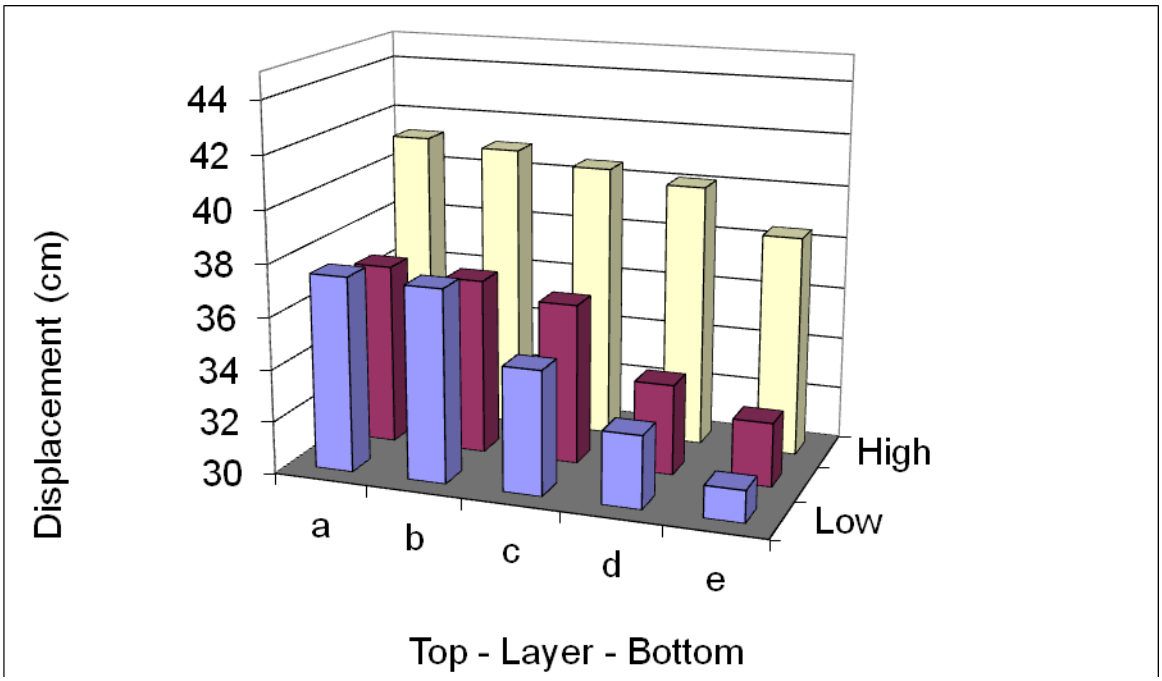

Figure 95 CAD in impact testing

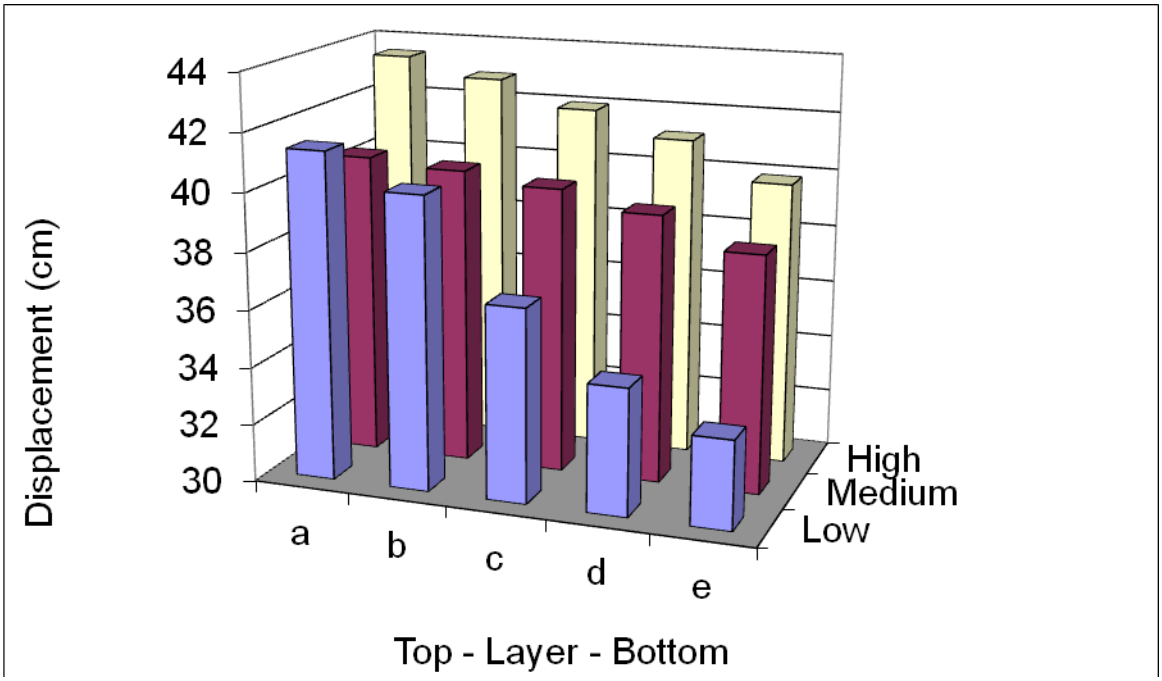

Figure 96 CMAD in impact testing

The results above were unanticipated and in searching for reasoning why higher standard containment force allowed larger displacements, the bottom layer of container displacement was removed from the data set. The outcome is shown below in Figure 97 & Figure 98.

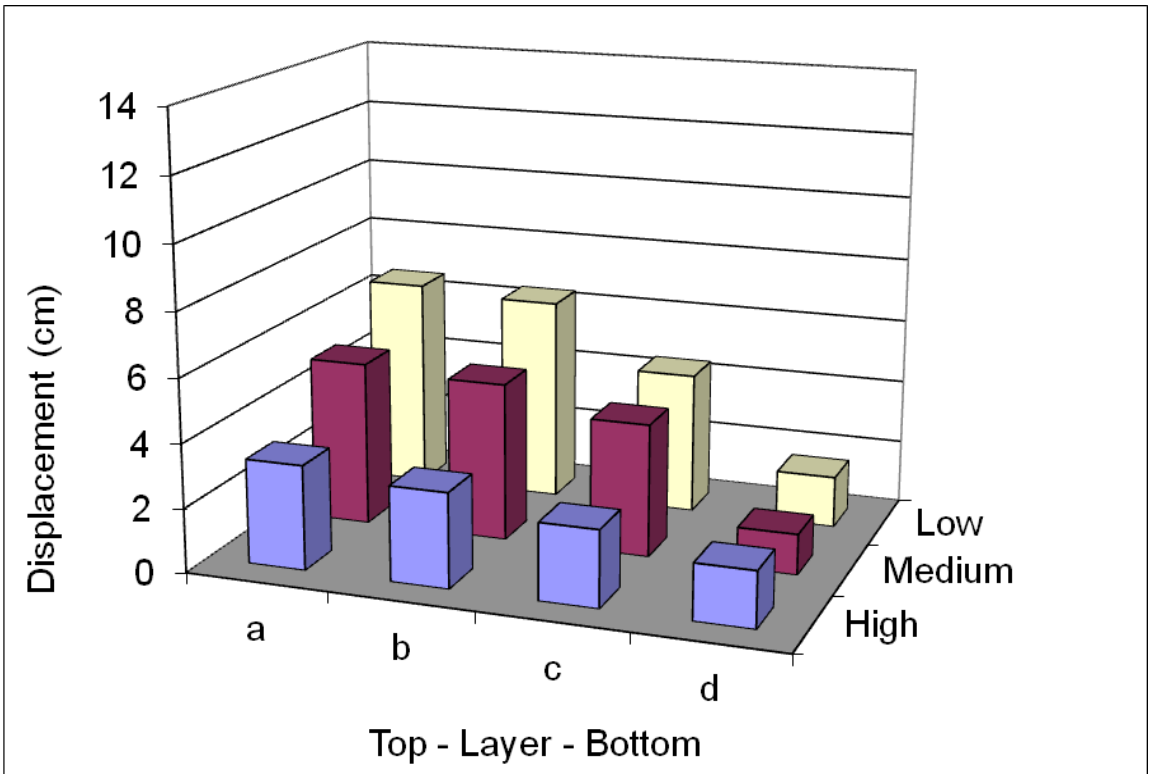

Figure 97 CAD for impact testing without bottom layer data

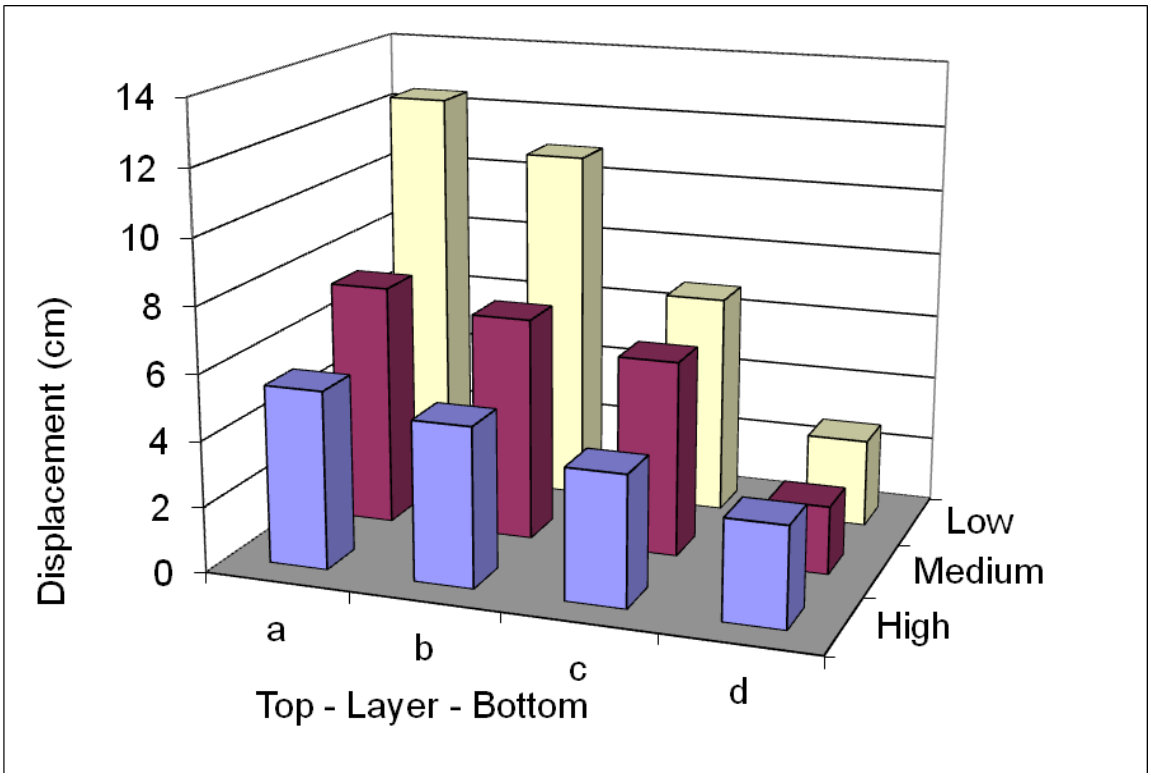

Figure 98 CMAD for impact testing without bottom layer data

Per Figure 97 and Figure 98 above, the lower standard containment force stretch film allowed for the greatest amount of movement and the high standard containment force stretch film allowed for the least. These results are more consistent with common industry knowledge, anticipated results, and the vibration data set.

The results of vibration testing were as expected. The results of impact testing were not as expected. If the bottom layer data was removed from the data set, the results were as expected. This unusual behavior of the impact test units can be attributed to necking of the film during the application process. The 20.3µ film had an initial width of 50.8cm (20”) but due to tension to load in the application process, that width was reduced to 30.4cm (12”). This 20.3cm (8”) necking reduction (10.1cm (4”) from each side), was enough to prevent stretch film coverage over the pallet at the bottom of the unit load. This lack of coverage was found to have an effect on unit load stability by White (White, 2006).

8.5.4 Conclusion & Summary

The objective of this research was to determine if increasing the level of standard containment force applied by 20.3µ stretch film affects unit load stability in vibration and impact testing.

- Increasing the standard containment force of stretch film did increase load stability during vibration testing
- Increasing the standard containment force of stretch film did increase load stability during impact testing

Stretch film coverage over the pallet can affect the stability of a unit load during impact testing

Pallet Specification (Used under fair use, 2012)

PALLET DESIGN SYSTEM Version 4.0

Pallet Specification Sheet

All dimensions in inches

Customer:

Prepared by:
The Pallet Alliance Inc.
100 Europa Dr., Suite 450
Chapel Hill, NC, 27517
PDS License: 321 Date: March 15, 2007

Pallet ID: Sofwood GMA
Classification: 48.00 x 40.00, Stringer-Class, Double-Face Non-Reversible, Partial 4-Way, Multiple-Use, New Manufacture

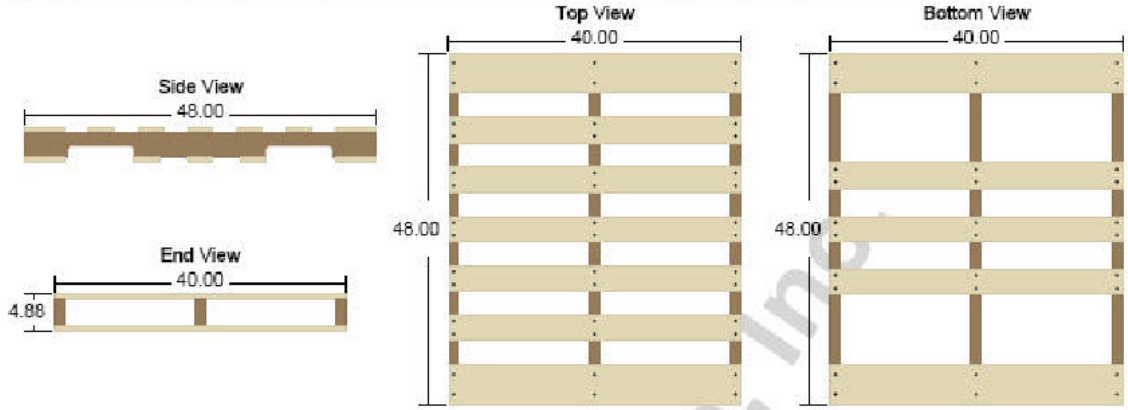

Components

Top Deck:
Style: Deckboard Type: New Lumber

Number	Thickness	Width	Length
5	0.688	3.500	40.00
2	0.688	5.500	40.00

Volume: 5.4 bd ft

Bottom Deck:
Style: Deckboard Type: New Lumber

Number	Thickness	Width	Length
3	0.688	3.500	40.00
2	0.688	5.500	40.00

Volume: 4.1 bd ft

Stringers:
Type: New Lumber

Number	Width	Height	Length
3	1.500	3.500	48.00

Partial 4-way Entry Notch:
Depth: 1.500 Length: 9.00 Location: 6.00 Radius: 0.75
Volume: 5.3 bd ft

Materials

Fasteners:

Fastener ID:	2.0 x .113
Fastener Type:	Helically Threaded Nail
Fastener Length:	2.00
Thread Length:	1.25
Thread Diameter:	0.126
Wire Diameter:	0.113
Head Diameter:	0.280
Helixes:	9.0
Flutes:	5
Thread Angle:	60
MIBANT Angle:	36
FWI:	89
FSI:	68
Total Number:	72

New Lumber:
Lumber ID: Southern Softwood

Species Class	Grade
Southern Yellow Pine	Utility &BTR

Moisture Content (at manufacture and assembly): Green

Total New Lumber Volume: 14.8 bd ft

Custom Notes and Information:

Property of: The Pallet Alliance, Inc. PDS License: 321

PALLET DESIGN SYSTEM Version 4.0
Pallet Structural Analysis

Customer:

Prepared by:
The Pallet Alliance Inc.
PDS License: 321 Date: March 15, 2007

Pallet ID: Sofwood GMA
Classification: 48.00 x 40.00, Stringer-Class, Double-Face Non-Reversible, Partial 4-Way, Multiple-Use, New Manufacture

Unit Load Type: Uniformly Distributed - Full Pallet Coverage
Unit Load Weight Variability: Low
Service Environment: Dry Environment (EMC <= 19%)

Support Condition	Safe Maximum Load	Deflection at Maximum Load	User Specified Deflection Limit	Maximum Load for Deflection Limit	Critical Member
Stacked 1 Unit Load High 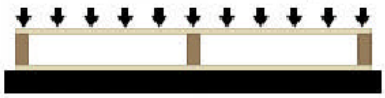	5060 lbs.	0.18 in.	----	----	Top Deckboard
Stacked 2 Unit Loads High 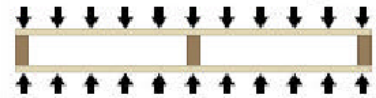	3163 lbs. (each pallet)	0.18 in.	----	----	Top Deckboard

Lateral Collapse Resistance

PALLET DESIGN SYSTEM Version 4.0
Pallet Physical Property Analysis

Customer:

Prepared by:
The Pallet Alliance Inc.
PDS License: 321 Date: March 15, 2007

Pallet ID: Sofwood GMA
Classification: 48.00 x 40.00, Stringer-Class, Double-Face Non-Reversible, Partial 4-Way, Multiple-Use, New Manufacture

	At Manufacture	At 25% MC	At 19% MC	At 15% MC	At 12% MC
Average Pallet Weight	49 lbs.	41 lbs.	39 lbs.	38 lbs.	37 lbs.

Dimensional Change due to Wood Drying

Component	Original Dimension	Shrinkage from Manufacture to 19% MC	Shrinkage from Manufacture to 15% MC
Top Deckboards	0.688 in. Thickness 3.500 in. Width 5.500 in. Width	0.014 in. (+/- 0.003 in.) 0.069 in. (+/- 0.015 in.) 0.109 in. (+/- 0.024 in.)	0.020 in. (+/- 0.004 in.) 0.100 in. (+/- 0.022 in.) 0.157 in. (+/- 0.034 in.)
Stringers	3.500 in. Height 1.500 in. Width	0.069 in. (+/- 0.015 in.) 0.030 in. (+/- 0.007 in.)	0.100 in. (+/- 0.022 in.) 0.043 in. (+/- 0.009 in.)
Bottom Deckboards	0.688 in. Thickness 3.500 in. Width 5.500 in. Width	0.014 in. (+/- 0.003 in.) 0.069 in. (+/- 0.015 in.) 0.109 in. (+/- 0.024 in.)	0.020 in. (+/- 0.004 in.) 0.100 in. (+/- 0.022 in.) 0.157 in. (+/- 0.034 in.)

PALLET DESIGN SYSTEM Version 4.0

2-D Pallet Drawings

All dimensions in inches

Pallet ID: Sofwood GMA
Classification: 48.00 x 40.00, Stringer-Class, Double-Face Non-Reversible, Partial 4-Way, Multiple-Use, New Manufacture

Side View

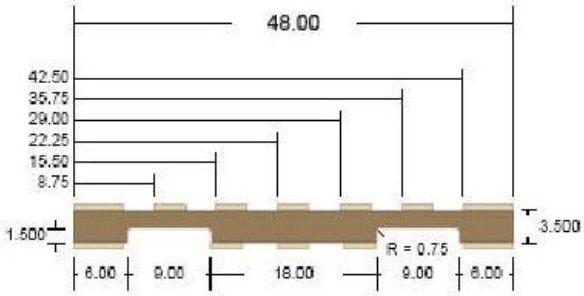

End View

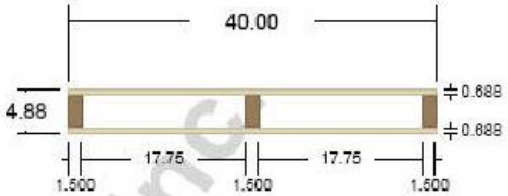

Top View

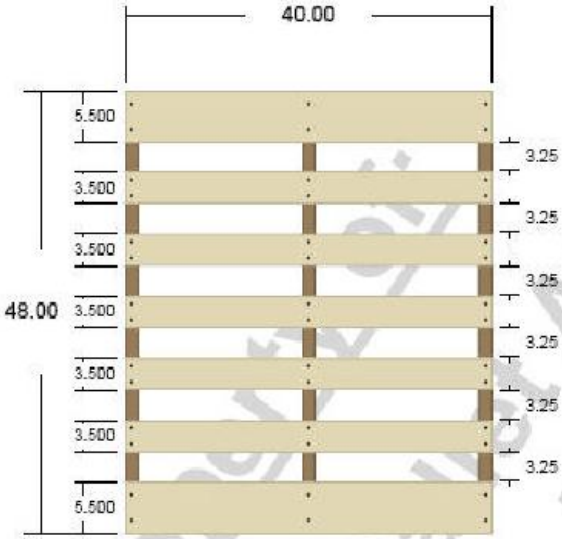

Bottom View

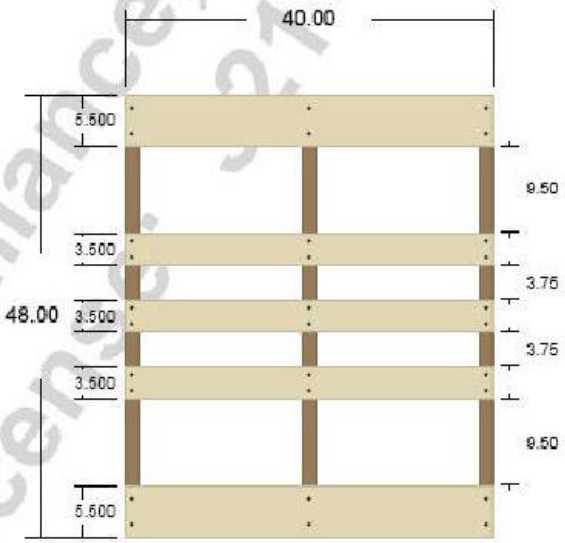

All materials generated from the PDS software (including without limitation specification sheets, drawings, analyses and all other output) (PDS Materials) are protected by copyright and other intellectual property laws. The direct pallet user/ customer may not copy the PDS materials without the express written permission of the PDS licensee that provided the customer with the PDS materials.

Customer:

Prepared by:
The Pallet Alliance Inc.
100 Europa Dr., Suite 450
Chapel Hill, NC, 27517

Property of The Pallet Alliance, Inc. PDS License: 321

PALLET DESIGN SYSTEM Version 4.0

Pallet Drawing - Side and End View

All dimensions in inches

Pallet ID: Sofwood GMA

Classification: 48.00 x 40.00, Stringer-Class, Double-Face Non-Reversible, Partial 4-Way, Multiple-Use, New Manufacture

Side View

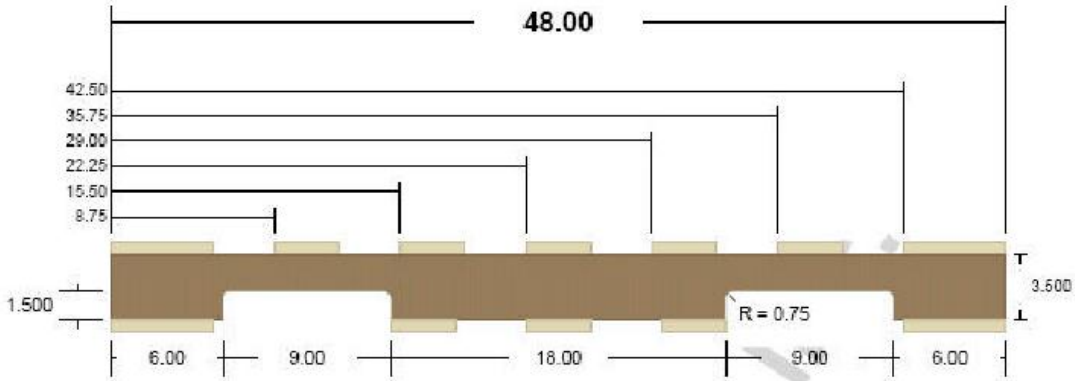

End View

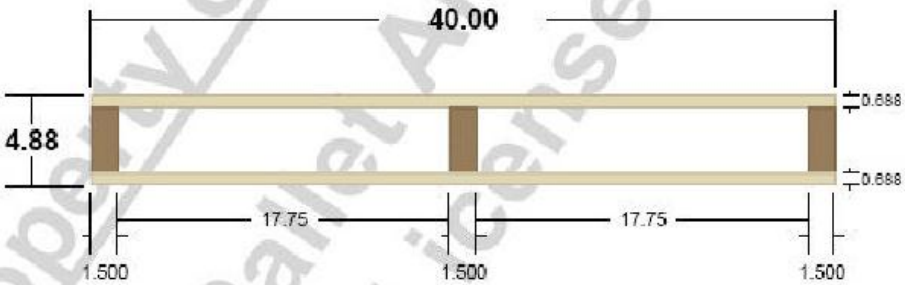

Property of: The Pallet Alliance, Inc. PDS License: 321

All materials generated from the PDS software (including without limitation specification sheets, drawings, analyses and all other output) (PDS Materials) are protected by copyright and other intellectual property laws. The direct pallet user customer may not copy the PDS materials, without the express written permission of the PDS licensee that provided the customer with the PDS materials.

Customer:

Prepared by:
The Pallet Alliance Inc.
100 Europa Dr., Suite 450
Chapel Hill, NC, 27517

PALLET DESIGN SYSTEM Version 4.0

Pallet Drawing - Top View

All dimensions in inches

Pallet ID: Sofwood GMA

Classification: 48.00 x 40.00, Stringer-Class, Double-Face Non-Reversible, Partial 4-Way, Multiple-Use, New Manufacture

Top View

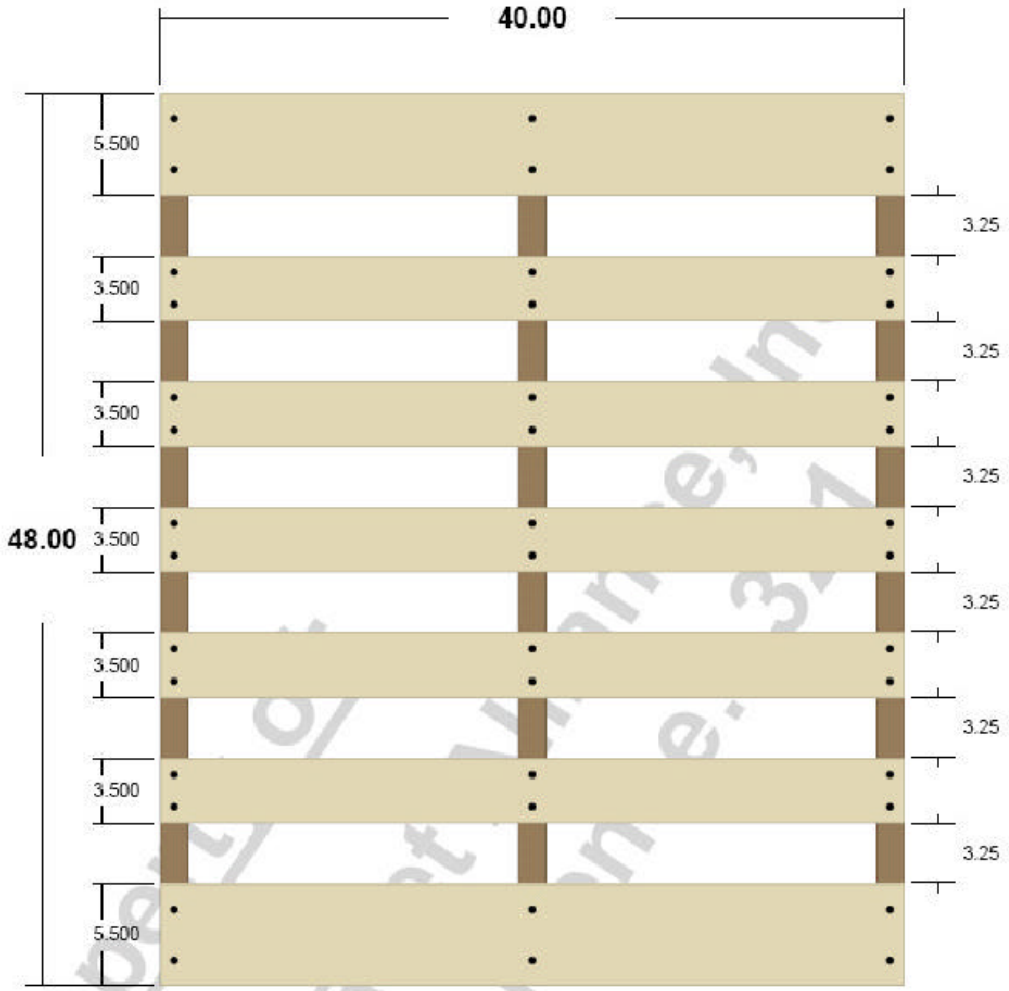

Customer:

Prepared by:
The Pallet Alliance Inc.
100 Europa Dr., Suite 450
Chapel Hill, NC, 27517

PALLET DESIGN SYSTEM Version 4.0

Pallet Drawing - Bottom View

All dimensions in inches

Pallet ID: Sofwood GMA

Classification: 48.00 x 40.00, Stringer-Class, Double-Face Non-Reversible, Partial 4-Way, Multiple-Use, New Manufacture

Bottom View

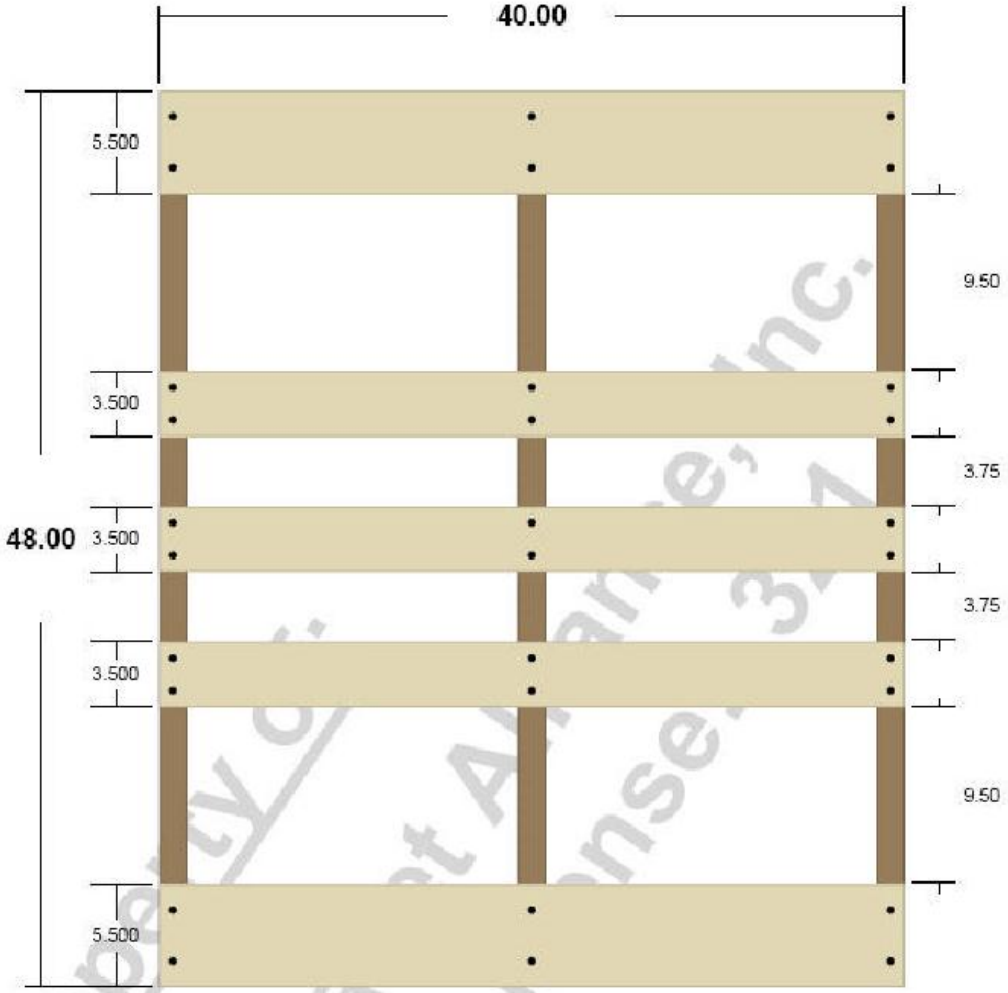

Property of The Pallet Alliance, Inc. PDS License: 3.4

Customer:

Prepared by:

The Pallet Alliance Inc.
100 Europa Dr., Suite 450
Chapel Hill, NC, 27517

9 Appendix B1: Raw Data Tables

Table 42 Data table of Stiffness

Manufacture	Thickness (µ)	s_{af1}	s_{af2}	s_{ac}	s_{b1}	$s_{b1`}$	s_{b20}
Paragon	10	5.94244	6.05078	3.5781	1.06162	20.701	27.8877
	10	6.30525	7.07059	3.84913	0.96571	19.0774	27.7262
	10	6.31715	7.19343	4.61149	1.04815	20.3295	26.4786
	10	6.32015	7.02836				
	10	6.71788	6.59694				
Berry	11.4	7.09601	9.59996	6.89635	1.8707	37.4141	45.4223
	11.4	7.98834	9.96353	6.72476	1.90906	38.1811	45.8035
	11.4	7.43975	9.4761	6.56214	1.83645	57.0368	46.688
	11.4	7.82749	9.37401				
	11.4	8.3563	9.78548				
Intertape	12.7	7.73849	9.4647	5.72778	2.23256	44.6513	67.0981
	12.7	7.33969	10.2774	5.42917	2.14465	42.893	70.4387
	12.7	8.92488	10.3379	6.01051	2.19175	43.835	71.2392
	12.7	8.33036	10.4044				
	12.7	7.63451	10.5147				
Intertape	16	10.8004	13.7475	8.92787	2.32895	46.5791	61.5862
	16	10.7418	14.5006	8.46325	2.35709	47.1418	63.7678
	16	10.5622	12.299	9.63823	2.38913	47.7825	63.0156
	16	9.82441	13.2053				
	16	10.5451	13.6016				
AEP	22.8	12.8138	13.1951	9.40311	1.53386	30.6772	51.2269
	22.8	13.1984	13.5472	10.0305	1.64159	32.8317	52.1946
	22.8	12.7186	12.8609	9.64108	1.67044	33.4089	52.3581
	22.8	14.0919	13.3728				
	22.8	12.222	13.2319				
AEP	30.5	17.4518	16.381	12.7289	2.41559	48.17	71.2875
	30.5	17.2236	18.0258	12.7353	2.46432	48.5757	68.9965
	30.5	16.4728	19.1544	13.687	2.4873	49.2722	69.4012
	30.5	17.0864	19.0332				
	30.5	17.0977	16.454				

Table 43 Data table of initial force and containment force

Manufacture	Thickness (μ)	f_{t1}	f_{t2}	f_{cf}	f_{cc}	f_{i1}	f_{i1}`	f_{i20}
Paragon	10	16.6502	15.6269	22.8349	25.5281	1.676	33.52	35.791
	10	13.1687	15.9575	20.6895	23.7896	0.384	7.68	35.888
	10	12.8525	15.3366	20.01	19.4378	1.405	28.1	34.874
	10	13.0636	16.2198	20.8264				
	10	12.6007	17.9749	21.9517				
Berry	11.4	13.8721	18.614	23.2146	15.8217	1.925	38.5	47.783
	11.4	12.5361	18.8035	22.5993	17.2392	2.098	41.96	46.244
	11.4	13.6809	18.6235	23.1085	16.7972	2.01	40.2	46.21
	11.4	13.0645	19.9646	23.8593				
	11.4	11.8765	19.7387	23.0363				
Intertape	12.7	15.6439	22.4063	27.3272	24.0294	2.954	59.08	83.232
	12.7	16.8041	21.9324	27.6298	25.5695	1.925	38.5	83.149
	12.7	11.6352	21.2815	24.2545	33.5458	2.373	47.46	79.482
	12.7	14.2781	21.662	25.9443				
	12.7	15.7404	21.7841	26.8758				
Intertape	16	18.1623	25.1334	31.009	23.3815	3.425	68.5	81.538
	16	17.7107	19.5186	26.3561	24.2482	3.559	71.18	81.714
	16	17.5592	27.4884	32.6181	25.5437	3.376	67.52	81.198
	16	20.7262	25.3167	32.7186				
	16	18.2201	25.2823	31.1636				
AEP	22.8	23.2684	34.3518	41.4905	18.3682	3.221	64.42	81.922
	22.8	23.0407	33.4209	40.5935	25.0948	3.364	67.28	81.821
	22.8	23.7232	36.4796	43.5149	18.1143	3.356	67.12	80.147
	22.8	22.4461	34.1147	40.8368				
	22.8	25.0053	35.1415	43.13				
AEP	30.5	30.9837	50.6426	59.3688	59.4233	4.959	99.18	112.445
	30.5	31.9121	49.2612	58.6945	63.8976	4.283	85.66	110.687
	30.5	30.1451	48.3818	57.0046	54.1034	4.43	88.6	109.353
	30.5	34.0111	51.4874	61.7066				
	30.5	35.1093	53.7587	64.2079				

Table 44 Data table of layering results

Manufacture	Thickness (μ)	Layers	s_{ac}	f_{cc}
Paragon	10	1	3.58	25.53
	10	1	3.85	23.79
	10	1	4.61	19.44
	20	2	11.09	33.19
	20	2	11.22	33.04
	20	2	10.65	35.57
	30	3	16.03	53.56
	30	3	16.15	57.50
	30	3	17.21	47.87
Intertape	12.7	1	5.73	24.03
	12.7	1	5.43	25.57
	12.7	1	6.01	33.55
	25.4	2	14.44	58.22
	25.4	2	14.17	74.87
	25.4	2	13.86	66.31
	38.1	3	23.79	74.42
	38.1	3	21.91	80.96
	38.1	3	24.01	69.92
AEP	22.8	1	9.40	18.37
	22.8	1	10.03	25.09
	22.8	1	9.64	18.11
	45.6	2	20.43	81.14
	45.6	2	24.22	58.47
	45.6	2	22.40	61.77
	68.4	3	35.98	90.88
	68.4	3	33.27	110.36
	68.4	3	33.13	187.57